Structure/Property Relationships of Commercial Propylene/1-Pentene Random Copolymers

by

Marietjie Lutz

Dissertation presented for the degree of

Doctor of Philosophy (Polymer Science)

at the

University of Stellenbosch

Promotor: Dr. A.J. van Reenen April 2006

DECLARATION

I, the undersigned, hereby declare that the work contained in this dissertation is my own original work and has not previously, in its entirety or in part, been submitted at any university for a degree.

_____ _____

Signature Date

ABSTRACT

Propylene/1-pentene random copolymers are a relatively new family of random copolymers being prepared by Sasol Polymers and reveals high impact strength, good tensile properties, excellent optical properties, good rheological properties and a large pool of processing possibilities. These commercial copolymers are being prepared with stereospecific heterogeneous Ziegler-Natta catalytic systems containing multiple active sites and therefore producing copolymers with a varying degree of stereoregularity. Two different groups of propylene/1-pentene random copolymers were received by Sasol Polymers and investigated in this project.

The first group (Group 1, Polymers A - F) consisted of six totally different batches of commercial propylene/1-pentene copolymers which were produced by different catalyst systems. All had different melt flow indices (MFIs) and different 1-pentene contents and all of the copolymers, except for one, were nucleated. The second group (Group 2, Polymers G - J) were produced by the same catalyst, but with varying donor:catalyst ratios and also differing in their 1-pentene content. Investigation of the Group 1 copolymers was used in order to construct a “molecular toolbox” which was then used to study the Group 2 copolymers.

The original commercial copolymers were all studied by various analytical techniques: high-temperature carbon thirteen nuclear magnetic resonance spectroscopy (^{13}C-NMR), high-temperature gel permeation chromatoghraphy (HT-GPC), crystallization analysis fractionation (CRYSTAF), differential scanning calorimetry (DSC), wide angle X-ray diffraction (WAXD) and positron annihilation lifetime spectroscopy (PALS).

The random copolymers were all fractionated by preparative TREF and the fractions analyzed utilizing the following analytical techniques: ^{13}C-NMR, HT-GPC, CRYSTAF and DSC. The results of these analyses were used to investigate *inter alia* the distribution of 1-pentene in the copolymers.

In order to investigate the low molecular weight material of the copolymers, which were part of the room temperature fraction during TREF, solvent extractions were carried out using different solvents and different

extraction techniques. A complete structural analysis study was carried out on the extracts. The percentages of xylene-solubles were also determined during the quantitative xylene extraction study of the copolymers. Characterization of the xylene non-soluble material was carried out using ^{13}C-NMR, HT-GPC, CRYSTAF, DSC and WAXD in order to compare the properties of the unextracted copolymers with the material after removal of the xylene soluble fraction. Positron annihilation lifetime spectroscopy (PALS) was used as an alternative investigation method for the Group 1 copolymers and their XNS fractions in order to determine what type of information this novel analytical method could generate and how the results compared with those of previous PALS studies on poly-olefins.

A new fractionation technique, preparative solution fractionation (SF), was developed and evaluated. The commercial propylene/1-pentene copolymers were fractionated using this novel technique, the fractions were analyzed by ^{13}C-NMR, HT-GPC, CRYSTAF and DSC and the results were compared with previously existing fractionation methods, namely TREF and CRYSTAF.

A final study was done on the random copolymers by blending one of the commercial Ziegler-Natta catalyzed propylene/1-pentene copolymers with a tailored, low 1-pentene content, metallocene propylene/1-pentene copolymer in different ratios. The blends were analyzed by molecular weight, thermal and crystal phase analysis in order to investigate the effect of the tailored, highly isotactic propylene/1-pentene copolymer on the properties the commercial random copolymers.

Throughout the project the influence of the 1-pentene as well as the donor:catalyst ratio on the copolymers was investigated. This study, in its entirety, therefore allow a better understanding of the effects that the commercial, heterogeneous, transition metal catalysts have on the make up of the copolymers and, by extension, the ultimate properties of the materials.

OPSOMMING

Propileen/1-penteen statistiese kopolimere is ‘n relatief nuwe familie van kopolimere wat deur Sasol Polimere vervaardig word en vertoon hoë impaksterkte, goeie treksterkte, uitstekende optiese eienskappe, goeie reologiese eienskappe en ‘n groot verskeidenheid van vervaardigingsmoontlikhede. Hierdie kommersiële kopolimere word vervaardig met stereospesifieke heterogene Ziegler-Natta katalis sisteme wat meervoudige aktiewe setels bevat en dus kopolimere produseer met variasies in stereochemie. Twee verskillende groepe propileen/1-penteen kopolimere is vanaf Sasol Polimere ontvang en ondersoek in hierdie projek.

Die eerste groep (Groep 1, Polimere A - F) het uit ses heeltemal verskillende monsters kommersiële propileen/1-penteen kopolimere bestaan wat deur verskillende katalis sisteme vervaardig is. Almal het verskillende smelt-vloei indekse (MFIs) gehad en verskillende 1-penteen inhoude en al die kopolimere, behalwe een, het kristallisasie hulpmiddels bevat. Die tweede groep (Groep 2, Polimere G - J) is vervaardig deur dieselfde katalisator, maar met wisselende donor:katalis verhoudings en die polimere het ook verskil t.o.v. die 1-penteen inhoud. Die ondersoek van die Groep 1 kopolimere was gebruik om ‘n “molekulêre gereedskapskis” saam te stel wat gebruik was om die Groep 2 kopolimere mee te bestudeer.

Die oorspronklike kommersiële kopolimere is almal met behulp van ‘n verskeidenheid analitiese tegnieke bestudeer: hoë temperatuur koolstof dertien kern magnetiese resonans spektroskopie (^{13}C-NMR), hoë temperatuur gel deurlatings chromatografie (HT-GPC), kristallisasie analise fraksionering (CRYSTAF), differensiële skandering kalorimetrie (DSC), wye hoek X-straal diffraksie (WAXD) en positron uitwissings leeftyd spektroskopie (PALS).

Die kopolimere is almal gefraksioneer deur middel van voorbereidende TREF en die fraksies ge-analiseer deur gebruik te maak van die volgende analitiese tegnieke: ^{13}C-NMR, HT-GPC, CRYSTAF en DSC. Die resultate van hierdie analises is gebruik om onder andere die verspreiding van 1-penteen in die kopolimere te ondersoek.

Oplosmiddel ekstraksies met verskillende oplosmiddels en verskillende ekstraksie tegnieke is gebruik om die lae molekulêre massa materiaal, wat deel was van die kamertemperatuur fraksie tydens TREF, van die kopolimere te ondersoek. 'n Volledige strukturele analise studie is uitgevoer op die ekstrakte. Die persentasies van xileen-oplosbare materiaal is ook vasgestel tydens die kwantitatiewe xileen ekstraksie studie van die kopolimere. Karakterisering van die xileen nie-oplosbare materiaal is uitgevoer d.m.v. ^{13}C-NMR, HT-GPC, CRYSTAF, DSC en WAXD om sodoende die eienskappe van die oorspronklike kopolimere met die materiaal te vergelyk na die verwydering van die xileen oplosbare fraksie. Positron uitwissings leeftyd spektroskopie (PALS) is gebruik as 'n alternatiewe ondersoek metode vir die Groep 1 kopolimere en hul xileen nie-oplosbare fraksies om sodoende te bepaal watter tipe inligting beskikbaar gestel word deur hierdie relatief nuwe analitiese metode en te sien hoe die resultate vergelyk met die van vorige PALS studies op poli-olefiene.

'n Nuwe fraksioneringsmetode, voorbereidende oplossing fraksionering (SF), is ontwikkel en ge-evalueer. Die kommersiële propileen/1-penteen kopolimere is gefraksioneer d.m.v. hierdie nuwe tegniek, die fraksies is ge-analiseer deur middel van ^{13}C-NMR, HT-GPC, CRYSTAF en DSC en die resultate is vergelyk met vorige bestaande fraksioneringsmetodes, naamlik TREF en CRYSTAF.

'n Finale ondersoek is gedoen op die kopolimere deur die samesmelting van een van die kommersiële Ziegler-Natta gekataliseerde propileen/1-penteen kopolimere met 'n laboratorium gesintetiseerde, lae 1-penteen inhoud, metalloseen propileen/1-penteen kopolimeer in verskillende verhoudings. Die samesmeltings is ge-analiseer t.o.v. molekulêre massa, termiese en kristalfase analises om sodoende die invloed van die metalloseen propileen/1-penteen kopolimeer op die eienskappe van die kommersiële kopolimere te bepaal.

Die invloed van die 1-penteen sowel as van die donor:katalis verhouding op die kopolimere is deurgaans tydens die projek ondersoek. Hierdie studie, in sy geheel, lewer dus 'n beter begrip vir die effek wat die kommersiële, heterogene, oorgangsmetaal kataliste het op die samestelling van die kopolimere en dus op die finale eienskappe van die materiale.

This thesis is dedicated to Daniël, Ben and Jan for their unwavering love and support.

And to my parents and Danie for always believing in me.

ACKNOWLEDGEMENTS

I would like to thank the following people and institutions for their contributions:

Dr. A.J. van Reenen, my study leader, for his guidance, advice, financial support and most of all for his belief in me throughout my post graduate years.

Jean McKenzie and **Elsa Malherbe,** for the many hours they've spent in order to achieve the best NMR results possible.

Derek McCauley, for all the CRYSTAF analyses, which sometimes landed in heaps on his desk.

Valerie Grummel and **Nyambeni Luruli,** for the HT-GPC work.

Dr. Peter Mallon for the PALS analyses and help on the interpretation of the results.

Elias Thole, from Sasol for the DSC and DMA analyses.

Monja Geldenhuys, my true friend and mentor from Sasol, for her input and support through fruitful discussions. Also for providing us with samples from Sasol for the project.

Heidi Assumption, Principle Scientist from Sasol Technology R&D, for her help and valuable guidance with NMR analysis.

Remy Buchner from Ithemba labs, carrying out the WAXD analysis for the project.

Margaretha Brand and **Carlien Bester**, my two assistants, for doing more than the expected sometimes.

Sasol, for the financial support of the project.

The **Olefins group** for their support and help.

Dr. M.J. Hurndall, for her advice on the writing of this publication and the proofreading thereof.

The financial assistance of the **National Research Foundation (NRF)** towards this research is hereby acknowledged. Opinions expressed and conclusions arrived at, are those of the author and are not necessarily to be attributed to the NRF.

LIST OF CONTENTS

LIST OF FIGURES

LIST OF TABLES

LIST OF ABBREVIATIONS

α-CN	α-Chloronaphtalene
^{13}C-NMR	Carbon thirteen nuclear magnetic resonance spectroscopy
CRYSTAF	Crystallization analysis fractionation
d_2-TCE	Deuterated tetrachloroethane
DSC	Differential scanning calorimetry
EVA	Ethylene-vinylacetate copolymer
GC	Gas chromatography
GPC	Gel permeation chromatography
HDPE	High density polyethylene
HT-GPC	High temperature gel permeation chromatography
iPP	Isotactic polypropylene
IR	Infrared spectroscopy
IV	Intrinsic viscosity
LDPE	Low density polyethylene
LLDPE	Linear low density polyethylene
M1	Mass of pellets
M2	Empty round bottom flask
M3	Round bottom flask with sample
MFI	Melt flow index
M_n	Number average molecular mass
M_w	Weight average molecular mass
MWD	Molecular weight distribution
o-DCB	Ortho-dichlorobenzene
PALS	Positron annihilation lifetime spectroscopy
PP	Polypropylene
Ref.	Reference
RT	Room temperature
SEC	Size exclusion chromatography
SF	Solution fractionation
T_c	Crystallization temperature
TCB	1,2,4-Trichlorobenzene

T_f	Fractionation temperature
T_m	Melting temperature
TREF	Temperature rising elution fractionation
ULDPE	Ultra low density polyethylene
V	Aliquot part of sample
VLDPE	Very low density polyethylene
WAXD	Wide angle X-ray diffraction
$\Sigma W_i\%$	Accumulative weight fraction
$W_i\%/\Delta T$	Differential weight fraction to temperature
XI	Xylene index
XNS	Xylene non-soluble
XS	Xylene soluble
ZN	Ziegler-Natta

CHAPTER 1

Introduction and Objectives

1.1 GENERAL INTRODUCTION

Polypropylene (PP) homopolymers are extremely versatile materials. Isotactic polypropylene (iPP) has many useful applications, such as in fibers, films, pipes, tapes, non-woven materials, blow moulded and thermoformed containers, and many different injection moulded items. The high melting point of iPP (166°C) also contributes to its application over a wide temperature range. These homopolymers are however very brittle below their glass transition temperature (0°C) and also exhibit poor transparency.

The introduction of comonomers into these extremely crystalline polymers has resulted in even more versatile commercial polymers. The introduction of small quantities of ethylene or 1-butene as comonomers has been shown to lower the melting point and improve flexibility. It also improves the transparency and gloss of the polymers. Furthermore, the welding and heat sealing temperatures of these copolymers are lower than for the homopolymers [1, 2].

With the correct catalyst, comonomer and production system it is even possible to tailor-make a propylene copolymer with the specific required mechanical, physical, thermal and optical properties. Polypropylene copolymers have therefore received much attention over the past few years due to the excellent properties that have been obtained by the introduction of comonomers [1, 3].

The role of the α-olefins with uneven carbon numbers as comonomers has been largely ignored, presumably due to their limited availability. The Sasol Fischer-Tropsch process, however, yields a wide spectrum of hydrocarbons in the C1 - C20 range [4] and has the significant cost advantage that high-value by-products are produced simultaneously with synthetic oil. Propylene/1-pentene copolymers were only recently commercialized by Sasol

Polymers. To date, there are only a few publications in the open literature [1, 2, 5-8] which focus on these novel and very versatile commercial copolymers.

This study specifically addresses this need for a detailed investigation, on a molecular level, into the commercially produced, random propylene/1-pentene copolymers.

1.2 OBJECTIVES

Propylene/1-pentene copolymers have some unique properties. The overall objective of this project is to understand these properties on molecular level by investigating the relationship between the chemical structure and properties of these materials.

Six totally different batches of commercial propylene/1-pentene copolymers (hereafter referred to as Group 1, or Polymers A - F) were originally received from Sasol Polymers, produced by different catalyst systems. All had different melt flow indices (MFIs) and different 1-pentene contents. A further four batches of these commercial copolymers (hereafter referred to as Group 2, or Polymers G - J) produced by the same catalyst, but with varying donor:catalyst ratios and also differing in their 1-pentene content, were received at a later stage. Group 1 copolymers were used in order to construct a “molecular toolbox” which was then used to investigate Group 2 copolymers. This should allow a better understanding of the effects that the commercial, heterogeneous, transition metal catalysts have on the make up of the copolymers and, by extension, the ultimate properties of the materials

The individual objectives of this study were the following:

1. A complete analysis of the original commercial copolymers utilizing the following analytical techniques: high-temperature carbon thirteen nuclear magnetic resonance spectroscopy (^{13}C-NMR), high-temperature gel permeation chromatoghraphy (HT-GPC), crystallization analysis fractionation (CRYSTAF), differential scanning calorimetry (DSC), wide

angle X-ray diffraction (WAXD) and positron annihilation lifetime spectroscopy (PALS).

2. Extraction of the low molecular weight fraction in the original propylene/1-pentene copolymers. (Different extraction methods were to be used: the standard soxhlet extraction technique, solvent extractions and a refined successive extraction process.)
3. The complete structural analysis of the low molecular weight extracts of the propylene/1-pentene copolymers.
4. Determination of the percentage of xylene-solubles (XL) of Polymers A - J and characterization of the xylene non-soluble (XNS) samples, in order to compare the analysis results with the results of the original copolymers (Polymers A - J). (This was to be done by carrying out quantitative xylene extractions.)
5. Use of positron annihilation lifetime spectroscopy (PALS) as an alternative investigation method for the propylene/1-pentene copolymers (Group 1) and their XNS fractions in order to determine what type of information this novel analytical method could generate and how the results correlated with those of previous PALS studies on poly-olefins.
6. Fractionation of the copolymers using TREF in order to investigate the weight percentage distribution of Polymers A - J.
7. Analysis of the various TREF fractions in order to determine the comonomer distribution in the polymers and the effect of the 1-pentene incorporation in the various fractions.
8. Development and evaluation of a new fractionation technique, preparative solution fractionation (SF). (It was to be evaluated by comparison with previously existing fractionation methods, namely TREF and CRYSTAF.)
9. Blending of a metallocene-catalyst-produced propylene/1-pentene copolymer with one of the commercial copolymers (Polymer J) in different ratios.
10. Analysis of the blends in order to investigate the effect of the tailored, highly isotactic propylene/1-pentene copolymer on the thermal properties and crystal phase of the commercial random copolymers.

1.3 REFERENCES

1. Potgieter, A.H., *Propylene/1-pentene random copolymers: preparation, characterisation and commercialisation*, *PhD dissertation*. 2002, University of Stellenbosch: Stellenbosch.
2. Juhász, P., Belina, K., J. Reinf. Plast. and Comp., 2001. **20**: p. 2.
3. Hosier, I.L., Alamo, R.G., Esteso, J.R., Isasi, J.R., Mandelkern, L., Macromolecules, 2003. **36**: p. 5623.
4. *www.sasol.co.za*.
5. Halász, L., Vorster, O.C., Belina, K., Tincul, I., Potgieter, A.H. in *XIIIth International Congress on Rheology*. 2000. Cambridge, UK.
6. Juhász, P., Varga, J., Belina, K., Belina G., J. Macromol. Sci., Part B - Physics, 2002. **B41**: p. 1173.
7. Tincul, I., Potgieter, A.H. in *Polypropylene 96, 5th Annual World Congress*. 1996. Zürich.
8. Tincul, I., Joubert, D.J., Potgieter, A.H. in *Polypropylene 99, 8th Annual World Congress*. 1999. Zürich.

CHAPTER 2

Historical Overview of Propylene Polymers

2.1 TRANSITION METAL CATALYSTS

2.1.1 Background

A Ziegler-Natta (ZN) catalyst can be defined as a transition metal compound having a metal-carbon or metal-hydride bond able to carry out repeated insertions of olefin units. Usually, though not necessarily, the catalyst consists of two components:

- a transition metal salt, most frequently a halide, and
- a main-group metal alkyl which serves the purpose of generating the active metal-carbon bond.

These types of catalysts can be heterogeneous, with the active metal centre occupying a position on the surface of the crystal. Polymerization at the active site is influenced by the electronic and steric environment of the crystal lattice sites. These catalysts tend to produce polymers with broad molecular weight distribution (MWD) and also non-homogeneous comonomer distribution in olefin copolymers [1].

Important steps in the development of the Ziegler-Natta catalyst family and new catalyst and process generations are discussed in Sections 2.1.2 - 2.1.6. The assignment of numbers for the catalyst generations is somewhat arbitrary because of the large number of innovative catalyst systems. The generation numbers are therefore used to characterize quantum-leap progress in catalyst and process technology, instead of measuring significant advances within one specific catalyst family. Literature reviews of the advances in ZN catalysts have been published by Brintzinger [2] , Pino [3], Tait *et al.* [4-6], and Corradini *et al.* [7].

2.1.2 First generation catalysts

In 1954 Natta and co-workers developed a catalyst system composed of δ-$TiCl_3$ activated with $AlEt_2Cl$, which was a modified Ziegler catalyst [8]. Although the stereoselectivity of iPP was improved from 40 to 90% with this catalyst compared to Ziegler's $TiCl_4/AlR_3$ catalyst system, extensive purification was still needed in order to produce commercial iPP. Natta and his group subsequently discovered that the different diastereoisomers of iPP could be separated by extractions with boiling solvents [9].

2.1.3 Second generation catalysts

It was soon recognized that catalyst performance could be enhanced by improving the surface area and by the presence of anhydrous $AlCl_3$, which can substitute inactive bulk $TiCl_3$, as well as by the presence of weak electron donors, such as sterically hindered dialkylethers, during catalyst preparation. Nielsen [10] was the first to investigate this new and improved catalyst system, the 'Solvay'-type δ-$TiCl_3/AlCl_3$/isoamylether/$AlEt_2Cl$ catalyst system which had a tenfold catalyst activity increase and resulted in stereoselectivity exceeding 95%.

2.1.4 Third generation catalysts

During the late 1980s, third generation supported catalysts were introduced. These exhibited significantly improved stereoselectivities without sacrificing high catalyst activities. At Montedison and Shell it was discovered that highly active catalysts were obtained when $TiCl_4$ was supported on anhydrous high-surface-area magnesium chloride in the presence of electron-donating Lewis bases [11-15]. The use of Lewis bases to enhance catalytic activity was first proposed by Razuvaev and co-workers [16]. Coover and co-workers, however, were the first to prepare active catalyst systems from $TiCl_3$, $AlEt_2Cl$ and a Lewis base [17].

2.1.5 Fourth generation catalysts

Based upon the insight gained from the correlation between catalyst structure and morphology development, Galli and co-workers developed the reactor granule technology [18, 19]. This technology is able to produce both dense and microporous PP granules.

2.1.6 Fifth generation catalysts

Metallocene catalysts result from the reaction of group 4 (titanium, zirconium or hafnium) metallocenes and an organoaluminium cocatalyst. Next to titanium, zirconium is the most active metallocene of the three metals [20]. These catalyst systems are able to produce highly stereoregular isotactic or syndiotactic polypropylene, in extremely high yields, with narrow molecular weight distributions and homogeneous comonomer distribution along the polymer chains [21, 22].

Breslow and Natta [23, 24] discovered metallocene catalysts for olefin polymerization soon after the original discovery of Ziegler-Natta catalysts. The chronological development of metallocene catalyst structures for olefin polymerization up to 1984 is summarized in Table 2.1 [25].

Table 2.1 Timetable of the historical developments in the metallocene catalyst research field (1952 – 1984) [25]

Year	Development	Ref.
1952	Development of the structure of metallocenes (ferrocene) by Fischer and Wilkinson.	[26]
1955	Metallocene as component of Ziegler-Natta catalysts, low activity with common aluminium alkyls.	[24]
1973	Addition of small amount of water to increase the activity ($Al:H_2O$ = 1:0.05, up to 1:0.3).	[27, 28]
1975	Unusual increase in activity by adding water at the ratio $Al:H_2O$ = 1:2.	[29]
1977	Using separately prepared methylaluminoxane (MAO) as cocatalyst for olefin polymerization.	[30]
1982	Synthesis of ansa metallocenes with C_2 symmetry.	[31]
1984	Polymerization of propylene using a rac/meso mixture of ansa titanocenes leads to partially isotactic polypropylene.	[32]
1984	Chiral ansa zirconocenes produce highly isotactic polypropylene.	[29]

2.1.7 Lewis donors in Ziegler-Natta catalysis

Soon after the discovery of $MgCl_2$-supported catalysts it was realized that some Lewis bases (donors) must be used in order to improve their stereospecificity [13, 33]. The evolution of the research and the main results obtained can be summarized as follows:

Table 2.2 Improvements in the Ziegler-Natta catalyst system using donors

Internal donor	External donor	Catalyst	Isotactic index
None	None	$MgCl_2$-$TiCl_4$/AlR_3	40%
Aromatic monoesters	None	$MgCl_2$-$TiCl_4$-ethylbenzoate/AlR_3	60%
Aromatic monoesters	Aromatic monoesters	$MgCl_2$-$TiCl_4$-ethylbenzoate/AlR_3-methyl-*p*-toluate	95%
Aromatic diesters	Silanes	$MgCl_2$-$TiCl_4$-phthalate/AlR_3-alkoxy silane	97-99%
Diethers	None	$MgCl_2$-$TiCl_4$-1,3-diether/AlR_3	97-99%

Before the use of silanes as external donors, Lewis bases left very strong odours in the final product as they consisted of aromatic esters. The catalyst systems were also relatively unstable above 70°C. This led to the development of silane compounds as external donors. This improved catalyst system comprised a diester (e.g. dibutyl phthalate) as an internal weak Lewis base and a silane (e.g. triethoxy-phenylsilane) as an external Lewis base (donor) [34-39]. Most modern industrial processes make use of this catalyst system for the production of PP because of the following advantages it offers [40]:

- high isotacticity obtained with low ratios of aluminium to Lewis base,
- stereospecificity stable at the production temperature,
- high sensitivity towards hydrogen in the polymerization sytem, and
- the activity of the growing chains is greatly enhanced by hydrogen, which acts as transfer agent.

During the late 1980s and early 1990s, hindered 1,3-diethers were introduced as a new class of electron-donating Lewis bases [41]. This class of Lewis bases results in high catalyst activities as well as stereoselectivities, and no additional external Lewis base is needed. In fact, the aluminum alkyl activator does not appear to be able to remove the diether from the solid

catalyst component [42]. The reaction between the activator and other external donors are problematic in most catalyst systems.

The role of the Lewis bases in improving the stereospecificity of ZN catalysts is summarized (according to Galli *et al*. [43]) as follows:

- the more exposed and less stereospecific active catalyst centres are selectively poisoned,
- poisonous substances are removed from the catalyst surface through a complexing process,
- the structure of the active centre and the chirality are stabilized, and
- the reducing power of $TiCl_3$ is decreased.

In the literature, several papers deal with the functions carried out by donors. Even if their main function is to control the catalyst stereospecificity, it is well known that they strongly affect the catalyst activity, the first insertion and the propagation stereoregularity, and the molecular mass and the molecular mass distribution of the polymers produced [44].

2.2 POLYPROPYLENE (PP)

2.2.1 PP homopolymers

Today polyolefins are among the most important commodity polymers. More precisely, polyethylenes and polypropylenes are, in terms of tonnage, the major plastic materials produced worldwide [40]. The reason why these two polymers have attracted so much interest is mainly the diversity of structural variety that one can obtain by the use of ethylene and propylene monomers through the use of Ziegler-Natta catalysts. The recent advances in catalyst technology have especially revolutionized the production of PP, allowing substantial simplification of production processes, which has subsequently had a huge impact on economics. It is therefore no surprise that PP has the highest production volume of all olefin polymers in the current world market [40].

Polypropylene is a very versatile polymer due to its excellent thermal and chemical resistance, good mechanical properties and excellent physical

properties, such as high stiffness and tensile strength. The main structural factors influencing these important properties of PP are the tacticity, molecular weight and molecular weight distribution [45]. The different types of stereoisomers of PP are illustrated in Figure 2.1.

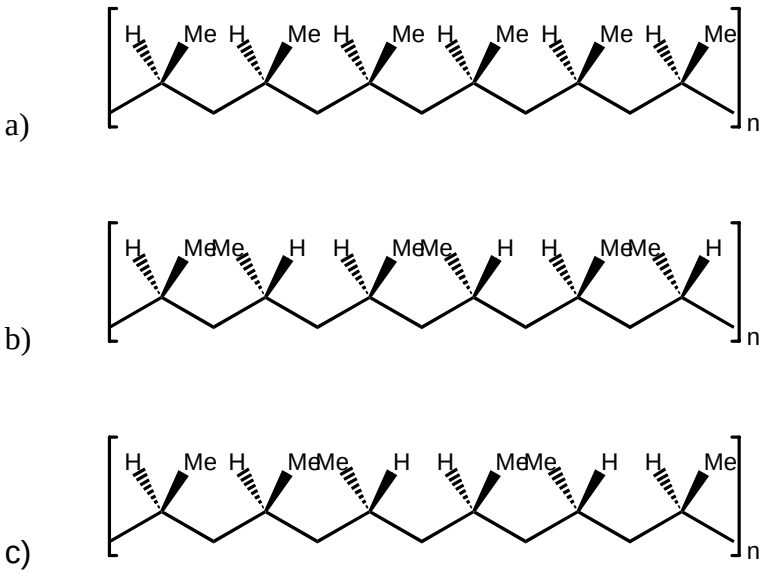

Figure 2.1 PP stereoisomers: a) isotactic, b) syndiotactic and c) atactic

2.2.2 PP copolymers

The brittleness and poor impact strength of PP homopolymers at low temperatures limit their applications. Extensive research has been carried out in order to tailor PP properties to meet specific requirements. To improve the low impact performance of the homopolymer the trend is to use reactor-produced “block” copolymers and blends with high rubber content or extruded compounds of PP polymers with elastomers. The brittleness of the PP homopolymer changes to more ductile behaviour when the elastomer content in PP is increased. Unfortunately, impact resistance then increases at the expense of other properties. The other option is then to produce random copolymers of propylene with ethylene or 1-butene, which have moderate impact strength and stiffness and good optical properties. Another interesting random copolymer contains 1-hexene as comonomer, which exhibits higher

impact strength, clarity and modulus than do the ethylene random copolymers [46].

The properties of the PP random copolymers are largely dependent on the amount of comonomer included as well as the distribution of the comonomer throughout the polymer chain [19]. It was found that upon inclusion of a comonomer the crystallization rate generally decreased and the degree of crystallinity and melting point were reduced [47]. The crystals produced in these random copolymers are not as perfect as those of the homopolymer and therefore the difference in refractive index between the crystalline and amorphous areas is less, leading to lower haze and higher clarity [45].

2.2.2.1 Propylene/1-pentene copolymers

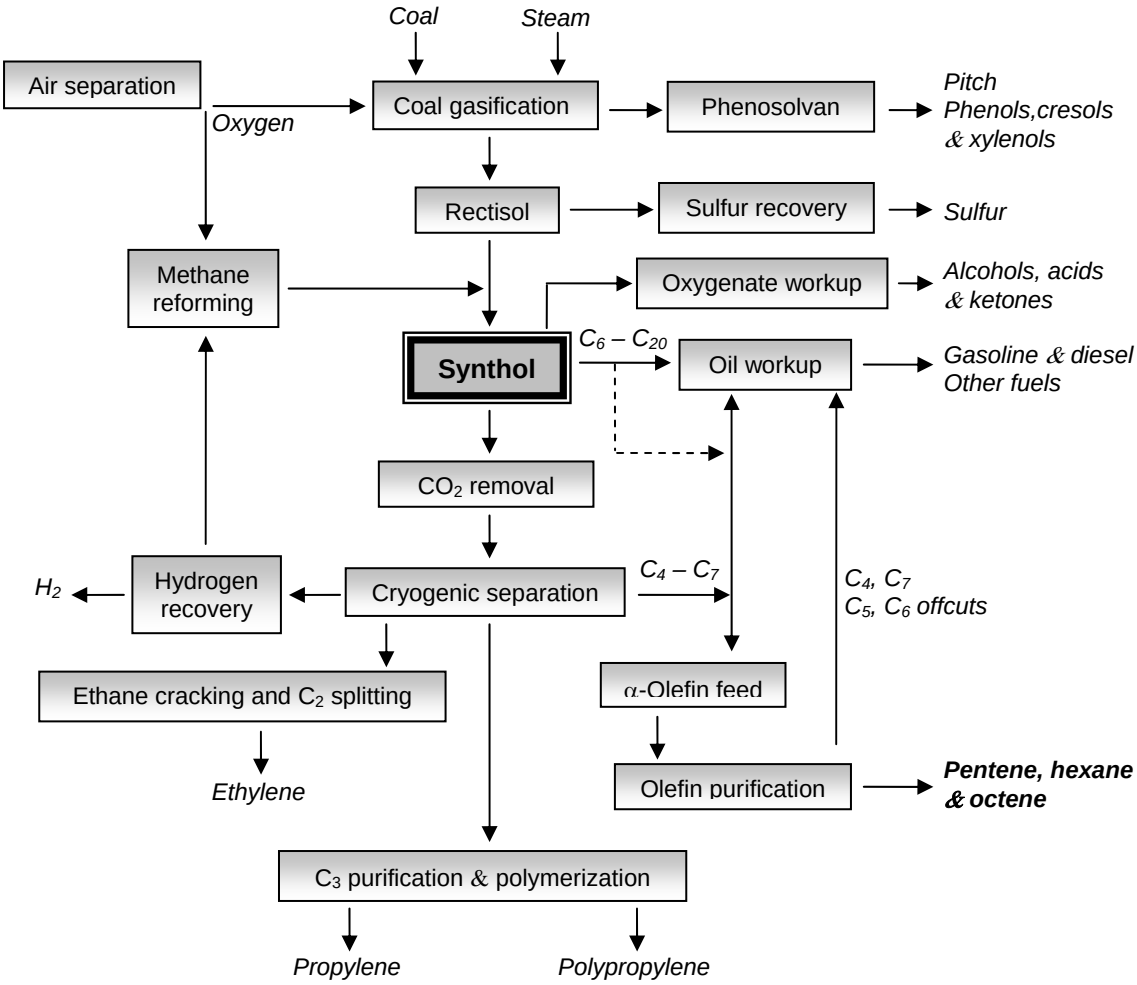

Figure 2.2 Variety of products from Sasol's industrial Synthol process [40]

From the Sasol Synthol process (Figure 2.2), during which coal is converted to ethylene, propylene and higher olefins, a wide variety of different α-olefins are formed as byproducts. This means that there is a large pool of odd-carbon-number α-olefins and branched α-olefins available, in addition to the classical even-carbon-number α-olefins. The use of odd-carbon-number α-olefins has long been totally neglected. However, through research into the use of many of these byproducts from the Sasol oil-from-coal conversion process together with polypropylene and polyethylene, a new family of random propylene/1-pentene copolymers was born [48, 49]. These commercial propylene/1-pentene copolymers are prepared with stereospecific

heterogeneous ZN catalytic systems containing multiple active sites which yield copolymers with varying degrees of stereoregularity. Propylene/1-pentene random copolymers have high impact strength, good tensile properties, good rheological properties, excellent optical properties and a large processing window [50].

Typical application areas for commercial propylene/1-pentene random copolymers include the following [51]:

1. Blow moulding (extrusion and injection): Packaging of shampoo, cosmetics.
2. Thermoforming: Packaging of dairy products, food trays, vegetable trays.
3. Films: Garment packaging, vegetable packaging, flower pockets.
4. Coatings: Coating of woven cloth.
5. Injection moulding: Domestic ware.
6. Injection stretch blow moulding (ISBM): Cosmetic packaging, and various other packaging.

2.3 SOLVENT EXTRACTION OF POLYMERS

Polymers may be extracted by solvents. The removal of extractable material from polymers is dependent on the solvating power of the solvent used in the process. The more powerful the solvent, the more material will therefore be extracted [52].

Natta and co-workers [53] investigated the differential solubility of atactic and isotactic polypropylene during the initial characterization of PP. They introduced the term ‘isotactic index’, which is an indication of the amount of polymer material insoluble in boiling *n*-heptane. Natta also showed that polypropylene can be divided into several fractions with different melting points (106 – 175°C) and crystallinities (15 – 66%) by successive extractions, using *n*-alkanes with increasing boiling points [54].

Heptane extraction is easy to accomplish and reproducible and therefore still widely used as a standard method for isotacticity determination instead of ^{13}C-NMR, which provides the most detailed information of the

microstructure of PP [55]. It is known that the heptane-soluble fraction not only consists of atactic polymer, but also contains low-molecular-weight isotactic material [56-58]. It has been proposed that this fraction contains so-called stereoblock polymer with alternating structures of blocky isotactic and atactic sequences [59]. Paukkeri and Lehtinen [55] found that low molecular weight isotactic material dissolves in heptane, whereas non-isotactic material located as blocks in the same chains with long isotactic sequences remains in the heptane-insoluble fraction. They also concluded that successive soxhlet extraction of PP with solvents of increasing boiling points separates mainly according to tacticity, with only a slight molecular-weight dependence.

Nakajima *et al.* [60] fractionated polypropylene by extraction with boiling hydrocarbons with different boiling points and confirmed that the respective polymer fractions had different molecular weights and isotacticities. They suggested that tacticity and molecular weight fractionations occurred during the *n*-alkane extraction.

It has been confirmed experimentally [61-63] that the respective fractions obtained through the successive extraction of polypropylene with n-alkanes have different pentad tacticities. This gives a definite indication of the occurrence of tacticity fractionation.

2.4 POLYMER FRACTIONATION METHODS

TREF and CRYSTAF are two widely used techniques used for the qualitative estimation of chemical composition distribution of semi-crystalline copolymers. TREF is carried out in two steps, namely precipitation and elution [64, 65]. In the first step dissolved polymer chains are crystallized and precipitated onto a support in a column, at a constant rate. The second step involves the elution of the precipitated polymer into various fractions, at increased temperatures. TREF provides a technique for polymer separation on the basis of crystallizability.

CRYSTAF [66-69] is based on a single polymer solution crystallization step at a constant cooling rate and is a powerful analytical technique for the determination of the chemical composition distribution (CCD) of a polymer

sample. A cumulative concentration profile is drawn up by monitoring the change in concentration of the polymer solution as the temperature of the solution is reduced at a constant rate. The first derivative of the data is then calculated in order to obtain an indication of the fraction of crystallized polymer at constant temperature intervals.

2.4.1 TREF

2.4.1.1 Background

Shirayama *et al.* [70] were the first to use the term “temperature rising elution fractionation” (TREF) in order to describe the method used to fractionate low density polyethylene according to the degree of short-chain branching. The technique was, however, described earlier by Desreux and Spiegels [71] when they recognized the potential to achieve crystallization separation by elution at different temperatures. It must be clearly noted that the elution of amorphous polymers under rising temperature conditions will cause fractionation on the basis of molecular weight and not crystallinity. Size exclusion chromatography (SEC) is known to be used for the purpose of fractionation on the basis of molecular weight [72]. There is, therefore, little interest shown for the fractionation of amorphous polymer when using the TREF technique. TREF is a technique used for analyzing semi-crystalline polymers by separation of the molecular species according to their crystallizabilities.

After the experimental introduction of TREF by Desreux and Spiegels [71] a need for a more practical and efficient system became clear. This led to the development of a system in which a polymer is crystallized onto a support in packed columns [73].

There are two kinds of experimental TREF methods: analytical and preparative TREF. These two methods are discussed in Sections 2.4.1.2 and 2.4.1.3.

2.4.1.2 Analytical TREF

Analytical TREF is generally automated and connected with analytical instruments such as IR and GPC. The molecular structure of polymer fractions can therefore be determined on-line. The fractionation system requires smaller columns and smaller samples than in the case of preparative TREF. It is also a faster process than preparative TREF, but generates less information about the polymer microstructure.

Table 2.2 contains a detailed list of various analytical TREF systems and their corresponding variables that have been utilized recently.

Table 2.3 Recent experimental work carried out in the field of analytical TREF

Polymer	Sample size (mg)	Solvent	Support	Heating rate (°C/h)	Cooling rate (°C/h)	Ref.
LDPE	200	TCB	Chromosorb-P	8	1.5	[74]
LDPE, LLDPE, EVA	100	TCB	Chromosorb-P	20	1.5	[75]
LDPE, LLDPE	20	o-DCB	Chromosorb-P	-	1.5	[76]
LLDPE	2	o-DCB	Glass beads	Stepwise	Slow	[77]
LDPE, HDPE, LLDPE, EVA	10	α-CN	Silanated silica gel	10 - 40	0.5	[78]
LLDPE	15	TCB	Steel shot	50	10	[79]
VLDPE	-	TCB	Chromosorb-P	25	1.5	[80]
LLDPE, HDPE, EVA	-	o-DCB	-	240	5	[81]
PP-co-PE	2 -5	Xylene	Diatomaceous earth	240	5	[82]
LLDPE	-	TCB		6 - 60	0.2	[83]
LLDPE, HDPE	-	Xylene	Diatomaceous earth	240	6	[84]
LLDPE	2	TCB	Diatomaceous earth	240	5.6	[85]
PE, $C_{104}H_{210}$	-	TCB	Glass beads	20	1	[86]
LLDPE	-	o-DCB	Glass beads	1	1.5	[87]
LDPE	-	o-DCB	Chromosorb-P	20	1.5	[88]

2.4.1.3 Preparative TREF

Preparative TREF is used to obtain larger quantities of polymer fractions. The respective polymer fractions can then be characterized off-line by various analytical methods, such as NMR, DSC, WAXD, GPC, CRYSTAF, and FTIR. The fractions are collected at predetermined temperature intervals. Preparative TREF is a time consuming fractionation process, but the large amount of information that can subsequently be obtained makes the process well worth the time. The system requires larger columns and larger sample

sizes than in the case of analytical TREF. Table 2.3 summarizes some preparative TREF systems recently described in literature and their corresponding variables.

Table 2.4 Experimental work carried out in the field of preparative TREF

Polymer	Sample size (mg)	Solvent	Support	Heating rate (°C/h)	Cooling rate (°C/h)	Analy-tical method	Ref.
LDPE	4	Xylene	Chromosorb-P	8	1.5	IR	[74]
LDPE	3	Xylene	-	9.6	1	IV, IR, SEC, DSC, NMR	[89]
PP	1	Kerosene	Firebrick	Stepwise	Natural	IV, Density	[90]
PP	7 - 10	Xylene	Sand	Stepwise	Slow	IV, NMR	[91]
LDPE	4	Xylene	Sand	Stepwise	Slow	IR, IV	[70]
LLDPE, LDPE, HDPE, PP, VLDPE	8	Xylene	Chromosorb-P		5	-	[92]
PP-co-PE	4	Xylene	Diatomaceous earth		5	NMR, GPC	[82]
LLDPE	2.5	o-DCB	-		-	NMR, DSC, FTIR	[77]
PP-co-PE	2	Xylene	Sea sand		1.5	DSC	[93]
PP-co-PE, PP	15	TMB	Glass beads		± 1.7	CRYS-TAF, NMR, FTIR, GPC, DSC	[94]
PP	1	Xylene	Sea sand		1.5	NMR	[95]
PP-co-PE	1	Xylene	Sea sand			NMR, FTIR, DSC	[96]
PP-co-PE/B	15	TMB	Glass beads		± 1.15	NMR, GPC, CRYS-TAF, DSC	[97]
LLDPE	4	Xylene	Chromosorb-P		1.5	SEC	[75]
LDPE	4	Xylene	Chromosorb-P	4	1	IR, DSC	[98]
LDPE, HDPE	3.5	o-DCB	Glass beads	Stepwise	100	GPC	[99]
LLDPE, LDPE, HDPE	-	TCB	Chromosorb-P		1.5	IR, NMR, GPC, DSC	[100]
LLDPE	-	o-DCB	Glass beads		1.5	GPC, DSC, IR	[87]
ULDPE	-	TCB	Chromosorb-P		1.5	NMR, DSC	[101]
PP-co-EPR	-	Xylene	Ballotini		5	DSC, GPC, FTIR	[102]

PP	10	Xylene	Sea sand		-	NMR, DSC	[103]
PP-co-PE	-	Xylene	Sea sand		1.5	NMR, DSC	[104]
LLDPE	-	TCB	Chromosorb-P	20	1.5	DSC, SEC, IR, NMR	[100]
LLDPE	0.27	TCB	Steel shot	12	2.5	SEC, IR	[79]
LLDPE	0.75	α-CN	Silanated silica gel	Stepwise	Slow	DSC, IR, SEC, NMR	[78]
VLDPE	-	TCB	Chromosorb-P	Stepwise	1.5	DSC, DMA	[80]
PP-co-PE	3 - 5	Xylene	Sea sand		6.5	NMR, FTIR, WAXD, DSC	[105]
LLDPE	2.5	o-DCB	Glass beads	Stepwise	Slow	DSC, SEC, IR, NMR	[77]

2.4.1.4 TREF of polypropylene

High-pressure low-density polyethylene (HP-LDPE) was the first polyolefin to be studied by a TREF related technique by Desreux and Spiegels [71] in 1950. Hawkins and Smith [106] applied the same technique in 1958 to the, at that time, new HDPE produced by heterogeneous ZN catalysts. The first attempt to fractionate isotactic polypropylene was only reported in 1960 by Wijga *et al.* [90]. Their method was compared to the fractionation of polypropylene by the elution gradient method, whereby fractionation is carried out by increasing the fraction of solvent in a solvent/non-solvent mixture, at constant temperature. Their work demonstrated that an elution gradient fractionation operates on the basis of molecular weight whereas TREF separates according to crystallinity or stereoregularity.

Although this early work demonstrated the successful use of TREF for polypropylene fractionation, the value of the technique does not seem to have been as well recognized as in the polyethylene area. Most studies involving stereoregularity separation of PP have been conducted using successive solvent extraction with n-alkane solvents [61, 107].

The first insight into the mechanism regulating the fractionation efficiency of TREF was reported by Kamatah and Wild [108]. They found that the fractional crystallization of polypropylene from a dilute solution is mainly dependent on stereoregularity and almost independent of molecular weight.

Recently Kioka *et al.* [109] fractionated mainly isotactic polypropylene produced by a $TiCl_4/MgCl_2$ catalyst, with and without electron donors. The fractionation was carried out over a wide temperature range (-65 to 140°C) and the samples produced with electron donors used as part of the catalyst system showed much narrower distributions of molecular weight and isotacticity. The average molecular weight of the various fractions increased with an increase in fractionation temperature, but not to such an extent as to conclude that the molecular weight influenced the fractionation. The study also showed that the melting point and isotacticity indexes increased with elution temperature, which indicates that the fractionation mechanism is controlled by stereoregularity.

A fractionation study of PP prepared with $MgCl_2$-supported catalysts [110] showed four different types of structures obtained at various fractionation temperatures:

1. Room temperature: atactic PP containing some stereoblock structures.
2. 80°C: PP of low isotacticity with *rr* and long *r* sequences.
3. 103°C: PP with small amounts of *rr* defects.
4. 115°C: highly isotactic PP with no stereodefects.

It was believed that these fractions were produced by different types of active sites during polymerization. Further studies [111] were carried out by the same group, showing that the addition of electron donors to $MgCl_2$-supported Ziegler-Natta catalysts can increase the overall isotacticity of PP. Electron donors reduced the weight percentage of the fractions that eluted at lower temperature and increased the weight percentage of fractions having high isotacticity.

Albizzati *et al.* [112, 113] observed that electron donors also changed the elution temperature range of PP fractions. They reported that all fractions were eluted before 110°C in the case of the PP produced by catalysts containing no electron donor, whereas PP produced with catalysts containing an electron donor showed a maximum value of differential weight fraction to

temperature ($W_i\%/\Delta T$), at 112°C. This implies that highly isospecific active sites are only formed after addition of electron donors. Xu *et al.* [114] later found that electron donors can convert aspecific sites into different isospecific active sites and that the conversion is related to the structrure of internal electron donors.

Analytical TREF does not seem to have been applied to any extent to polypropylene analysis, possibly because of the need to then have to subject the fractions to further analysis. ^{13}C-NMR analysis of the fractions, for example, can yield much information about the active sites of the catalysts from the microstructure, because various active sites in ZN catalysts lead to differences in polymer stereoselectivity. Kakugo *et al.* [91] did show that analytical TREF with a calibration based on pentads might be useful for some polypropylene studies.

2.4.1.5 TREF of propylene copolymers

There are significantly fewer reports on the TREF of propylene copolymers compared to the TREF of PP homopolymers and LLDPE. The fractionation of propylene copolymers is a bit more complicated than that of PP homopolymers. The reason for this is that the crystallinity of propylene copolymers is affected by more factors than PP homopolymers are. Composition distribution and sequence distribution must be taken into account, besides tacticity distribution.

Kakugo *et al.* [91] investigated propylene/1-butene copolymers prepared with a $TiCl_3$-$AlEt_3$ catalyst. The isotacticity of the fractions increased and the 1-butene content decreased with increasing elution temperature. The $MgCl_2/TiCl_4$-$AlEt_3$ catalyst system showed similar results [115]. The role of electron donors in supported catalysts, however, showed a different tendency in the fractionation of propylene/1-butene copolymers [115, 116]. The overall isotacticity of the copolymers was enhanced by electron donors and the isotacticity of copolymer fractions also increased with elution temperature. Electron donors also reduced the 1-butene content of the copolymer as well as the 1-butene content of all the fractions. The difference in the extent of

decrease in 1-butene content of various fractions indicated that the influence of electron donors were different on various active sites, and that the electron donors had a greater influence on the most aspecific and most isospecific active sites than on other active sites.

Kakugo *et al.* [110] also fractionated random ethylene-propylene copolymers using preparative TREF and solvent extraction. ^{13}C-NMR spectroscopy indicated that the eluted fractions were a mixture of polyethylene, random copolymer and copolymer containing long sequences of ethylene.

Cheng and Kakugo [117] found that catalytic sites yielding random ethylene-propylene copolymers of lower tacticity were more active toward ethylene. They also used multiple-site-type statistical models to investigate the compositional heterogeneity of the ethylene-propylene catalysts. They concluded that the catalyst comprised three to four types of active sites, in agreement with the Bernoullian model.

High-impact copolymers of propylene and ethylene have also been studied by TREF. Mirabella [118, 119] was the first to fractionate this type of copolymer using TREF and he identified the following different zones in the polymer, namely:

- the rubbery propylene/ethylene copolymer fractions soluble at room temperature,
- the fractions of crystallizable ethylene propylene copolymer present at higher temperatures (room temperature to ~ 70°C),
- a fraction of ethylene-rich copolymer eluted at even higher temperatures (~ 70°C to ~ 102°C), and
- a final fraction of iPP which was recovered at the end of the fractionation (~ 102°C to ~110°C).

Usami *et al.* [120] reported similar results.

2.4.2 CRYSTAF

2.4.2.1 Analytical CRYSTAF

CRYSTAF involves a single-step solution crystallization process, during which semicrystalline polymer molecules precipitate at different temperatures according to their crystallizabilities [121]. The results from CRYSTAF indicate the quantity of polymer remaining in solution at each crystallization temperature, and can be converted to chemical composition distribution (CCD) using a calibration curve that relates crystallization temperature and comonomer content. This technique was developed by Monrabal [67] and has been shown to provide similar results to analytical TREF, but in a shorter time and with a simpler apparatus [67, 68, 121]. The technique has therefore become a standard means of analysis in many laboratories and an indispensable tool for product development and product quality monitoring in the polyolefin industry worldwide.

LLDPE is a type of polymer that has been extensively analyzed by CRYSTAF. The chain crystallizability of LLDPE is mainly controlled by the longest crystallizable ethylene sequence in the polymer chain. In the case of stereoregular polymers, such as isotactic and syndiotactic PP, microstructure and symmetry are the main factors affecting crystallizability. CRYSTAF can therefore be used to measure the distribution of polymer tacticity in these stereoregular polymers.

In order to investigate the structure-property relationships of polymers, polymerization kinetics and mechanisms, and polymer reaction engineering, it is very important to have adequate knowledge about the polymers' CCD. There are many factors contributing to CCD heterogeneity [122]. The most important one is the statistical nature of polymerization which forces the composition of any synthetic copolymer to be distributed around a certain average value. In addition to this, in the case of using the ZN catalyst system, each site type makes a polymer with different average microstructures as demonstrated in Figure 2.3. The temporal and spatial variations in the

monomer concentration and temperature during polymerization may also be responsible for CCD heterogeneity.

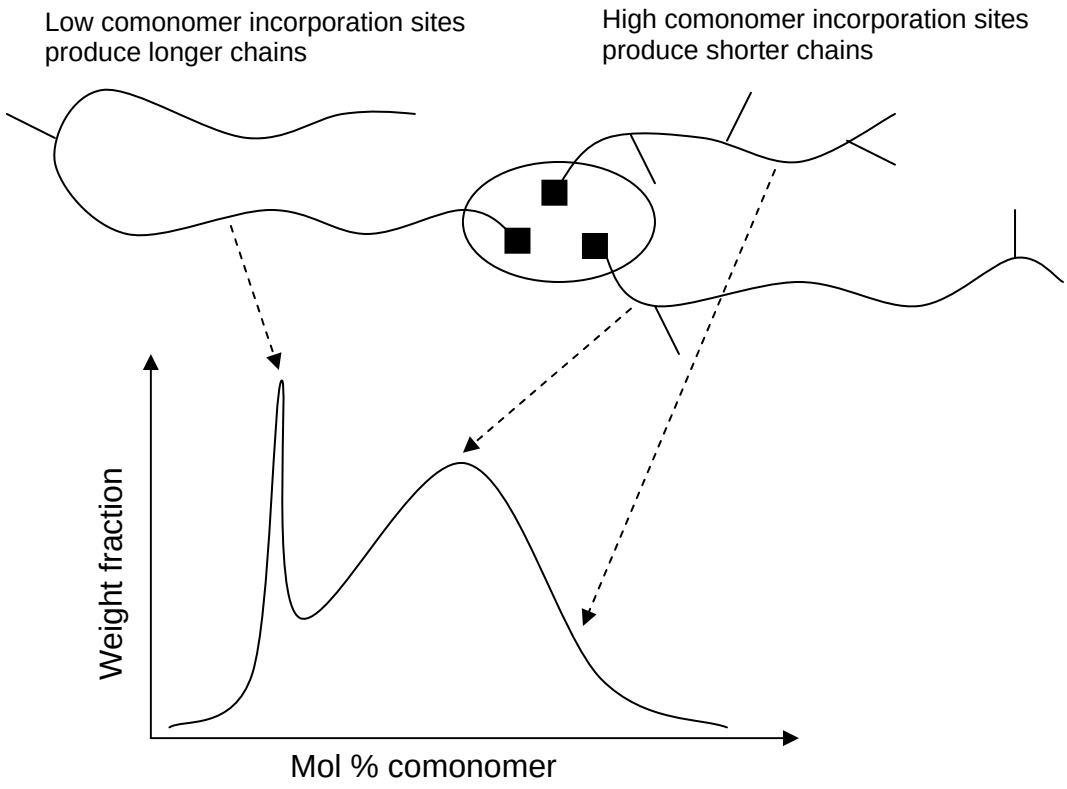

Figure 2.3 Copolymers produced by Ziegler-Natta catalysts exhibiting broad CCDs [65]

Nieto *et al.* [123] investigated the influence of molecular weight on CRYSTAF by using a series of ethylene homopolymers with different molecular weights. They concluded that the crystallization temperature obtained by CRYSTAF depends on the molecular weight only below a threshold value of approximately 5 000 $g.mol^{-1}$. They also showed that as the molecular weight increases, the CRYSTAF profiles become narrower.

Anantawaraskul *et al.* [124] concluded that samples with a number-average molecular weight higher than 28 000 $g.mol^{-1}$ showed approximately the same crystallization peak temperature. They also showed that for samples with lower molecular weight averages, the CRYSTAF profiles became broader because the crystallization temperatures of the shorter

chains in the sample are affected by their length. These CRYSTAF profiles may therefore show a low-crystallization-temperature tail.

Sarzotti *et al*. [125] studied the effect of comonomer content on CRYSTAF profiles. They used ethylene/1-hexene copolymers with different 1-hexene contents but approximately the same molecular weights. The CRYSTAF peak temperatures were significantly influenced by the comonomer content and the CRYSTAF profiles became broader with an increase in the 1-hexene content.

Brüll *et al*. [126] investigated the effect of comonomer type in propylene/α-olefin copolymers. They used several comonomers (1-octene, 1-decene, 1-tetradecene and 1-octadecene) and reported that both the peak T_c measured by CRYSTAF and the T_m and T_c measured by DSC were independent of the comonomer type, but strongly dependent on the comonomer content.

2.4.2.2 Preparative CRYSTAF

A preparative CRYSTAF system was recently reported by Bruaseth *et al.* [127]. The instrument is equipped with two separate stainless steel crystallization vessels. Each vessel is again connected to eight glass vessels. Up to eight fractions can therefore be separated. The temperature program comprises:

- a constant high temperature (130°C) stage for 90 min, during which the polymer is dissolved in xylene,
- an equilibration stage at 105°C for 90 min,
- a cooling stage at a rate of 0.10°C/min to 30°C,
- a heating stage to the first predetermined fractionation temperature, and
- a repeat of the previous step for any further predetermined fractionation temperatures.

The temperature is kept constant for 30 min at a certain fractionation temperature and the dissolved polymer is transferred to connected vessel number 1. After the cleaning step xylene is again added and the temperature

increased in order to repeat the process and collect the next fraction in vessel number 2, and so forth.

The abovementioned fractionation method however seems to be better described as solution TREF [128].

Another preparative CRYSTAF method has also recently been reported [129]. It involves a solvent/non-solvent method which allows for the fractionation of polymers based on molecular weight. The fractionation is therefore achieved by adding an increasing volume of a non-solvent into the polymer solution, which leads to a controlled precipitation of the initial polymer in different fractions of increasing molecular weight [130]. This preparative method has to be used together with suitable analytical techniques in order to characterize the chemical and structural properties of the polymer fractions.

2.5 REFERENCES

1. Mamielec, A.E., Soares, J.B.P., *Polypropylene: An A-Z reference*, Ed. J. Karger-Kocsis. 1999, Dordrecht: Kluwer Academic Publishers. p. 447.
2. Brintzinger, H.H., Fischer, D., Mülhaupt, R., Rieger, B, Waymouth, R.M., Angew. Chem. Int. Ed. Engl., 1995. **34**: p. 1143.
3. Pino. P., M., R., Angew. Chem. Int. Ed. Engl., 1980. **19**: p. 857.
4. Tait, P.J.T., *Comprehensive Polymer Science*, Eds. G. Allen, Bevington, J.C., Eastmond, G.C., Ledwith, A., Russo, S., Sigwalt, P. Vol. 7. 1989, Oxford: Permagon. p. 1.
5. ibid: p. 533.
6. ibid: p. 575.
7. ibid: p. 29.
8. Mülhaupt, R., *Polypropylene: An A-Z reference*, Ed. J. Karger-Kocsis. 1999, Dordrecht: Kluwer Academic Publishers. p. 910.
9. ibid: p. 901.
10. Nielsen, R.P., *Transition Metal Catalyzed Polymerization*, Ed. R.P. Quirk. 1983, New York: Harwood. p. 47.

11. Chadwick, J.C., *Ziegler Catalysts*, Eds. G. Fink, Mülhaupt, R., Brintzinger, H.H. 1995, Berlin: Springer-Verlag. p. 428.
12. Galli, P., Barbe, P.C., Noristi, L., Angew. Makromol. Chem., 1984. **120**: p. 73.
13. Barbé, P.C., Cecchin, G., Noristi, L., Adv. Polym. Sci., 1987. **81**: p. 1.
14. Goodall, B.L., *Transition Metal Catalyzed Polymerizations*, Ed. R.P. Quirk. Vol. Part A. 1983, New York: Harwood. p. 355.
15. Tait, P.J.T., Zohuri, G.H., Kells, A.M., McKenzie, I.D., *Ziegler Catalysts*, Eds. G. Fink, Mülhaupt, R., Brintzinger, H.H. 1987, Berlin: Springer-Verlag. p. 344.
16. Razuvaev, G.A., Minsker, K.S., Fedoseeva, G.T., Bykhovskii, V.K., Polym. Sci. USSR, 1961. **2**: p. 299.
17. McConnel, R.L., McCall, M.A., Cash, G.O., Jr., Joyner, F.B., Coover, H.W., Jr., J. Polym. Sci., 1965. **3**: p. 2135.
18. Galli, P., Haylock, J.C., Macromol. Symp., 1992. **63**: p. 19.
19. Galli, P., Haylock, J.C., Simonazzi, T., *Polypropylene, Structure, Blends and Composites*, Ed. J. Karger-Kocsis. Vol. 2. 1995, London: Chapman and Hall. p. 1.
20. Albizzati, E., Giannini, U., Collina, G., Noristi, L., Resconi, L., *Polypropylene Handbook*, Ed. E.P. Moore, Jr. 1996, Munich: Hanser Publishers. p. 46.
21. Ewen, J.A., J. Am. Chem. Soc., 1984. **106**: p. 6355.
22. Kaminsky, W., Külper, K., Brintzinger, H.H., Wild, F.R.W.P., Angew. Chem. Int. Ed. Engl., 1985. **24**: p. 507.
23. Natta, G., Pino, P., Mazzanti, G., Giannini, U., J. Am. Chem. Soc., 1957. **79**: p. 2957.
24. Breslow, D.S., Newburg, N.R., J. Am. Chem. Soc., 1957. **79**: p. 5072.
25. Mashima, K., Nakayama, Y., Nkamura, A., Adv. Polym. Sci., 1997. **133**: p. 1.
26. Wilkinson, G., Birmingham, I.M., J. Am. Chem. Soc., 1954. **76**: p. 4281.
27. Long, W.P., Breslow, D.S., Justus Liebigs Ann. Chem., 1975: p. 463.
28. Reichart, K.M., Meyer, K.R., Makromol. Chem., 1973. **169**: p. 163.

29. Andresen, A., Cordes, H.G., Herwig, J., Kaminsky, K. Merck, A., Mottweiler, R., Pein, J., Sinn, H., Vollmer, H.J., Angew. Chem. Int. Ed. Engl., 1976. **15**: p. 630.
30. Sinn, H., Kaminsky, W., Adv. Organomet. Chem., 1980. **18**: p. 99.
31. Wild, F.R.W.P., Zsolani, L., Huttner, G., Brintzinger, H.H., J. Organomet. Chem., 1982. **232**: p. 233.
32. Ewen, J.A., Jones, R.L., Razavi, A., Ferrara, J.P., J. Am. Chem. Soc., 1988. **110**: p. 6255.
33. Sacchi, M.C., Tritto, I., Locatelli, P., Prog. Polym. Sci., 1991. **16**: p. 331.
34. Seppälä, J.V., Härkönen, M., Luciani, L., Makromol. Chem., 1989. **190**: p. 2535.
35. Hu, Y., Chien, J.C.W., Polymer Sci. Polymer Chem., 1988. **26**: p. 2003.
36. Spitz, R., Bobichon, C., Gugot, A., Makromol. Chem., 1989. **190**: p. 707.
37. Soga, K., Shiono, T., Doi, Y., Makromol. Chem., 1988. **189**: p. 1531.
38. Ushida, Y., Kashiwa, N., in *Eur. Patent 86 288*. 1983, Mitsui Petrochemical Industries.
39. Parodi, S., Nocci, R., Giannini, V., Barbé, P.C., Scata, V., in *Eur. Patent 45 977*. 1981, Montedison.
40. Potgieter, A.H., *Propylene/1-pentene Random Copolymers: Preparation, Characterisation and Commercialisation*, *Polymer Science*. 2002, University of Stellenbosch: Stellenbosch.
41. Albizzati, E., Giannini, U., Morini, G., Smith, C.A., *Ziegler Catalysts*, Eds. G. Fink, Mülhaupt, R., Brintzinger, H.H. 1995, Berlin: Springer-Verlag. p. 413.
42. Iiskola, E., Pelkonen, A., Kakkonen, H.J., Pursiainen, J., Pakkanen, T.A., Makromol. Chem. Rapid Commun., 1993. **14**: p. 133.
43. Galli, P., Luciani, L., Cecchin, G., Aangew. Makromol. Chem., 1981. **94**: p. 66.
44. Sacchi, M.c., Albizzati, E., Balbontin, G., Mingozzi, I, Macromolecules, 1996. **29**: p. 5770.
45. Del Duca, D., Moore, E.P., Jr, *Polypropylene Handbook*, Ed. E.P. Moore, Jr. 2002, Munich: Hanser. p. 237.

46. Burdett, I. in *Hydrocarbon Processing*. 1986.
47. Del Duca, D., Moore, E.P., Jr, *Polypropylene Handbook*, Ed. E.P. Moore, Jr. 2002, Munich: Hanser. p. 237-254.
48. Tincul, I., Joubert, D.J., Potgieter, A.H. in *Polypropylene 99, 8th Annual World Congress*. 1999. Zürich.
49. Tincul, I., Potgieter, A.H. in *Polypropylene 96, 5th Annual World Congress*. 1996. Zürich.
50. Vorster, O., Halasz, L., Tincul, I., Potgieter, T. in *Plastex*. 2000.
51. Geldenhuys, M. 2004.
52. Virkkunen, V., Laari, P., Pitkanen, P., Sundholm, F., Polymer, 2004. **45**: p. 3091.
53. Natta, G., Mazzanti, G., Crespi, G., Moraglio, G., Chim. Ind., 1957. **39**: p. 275.
54. Natta, G., J. Polym. Sci., 1959. **34**: p. 531.
55. Paukkeri, R., Lehtinen, A., Polymer, 1994. **35**: p. 1673.
56. Firsov, A.P., Yeremina, I.V., Chirkov, N.M., Vysokomol. Soyed., 1964. **6**: p. 377.
57. Porter, R.S., Cantow, M.J.R., Johnson, J.F., Makromol. Chem., 1966. **94**: p. 143.
58. Quynn, R.G., Riley, J.L., Young, D.A., Noether, H.D., J. Appl. Polym. Sci., 1959. **2**: p. 166.
59. Russel, C.A., J. Appl. Polym. Sci., 1960. **4**: p. 219.
60. Nakajima, A., Fujiwara, H., Bull. Chem. Soc. Jpn., 1964. **34**: p. 909.
61. Doi, Y., Suzuki, E., Keili, T., Makromol. Chem., Rapid Commun., 1981. **2**: p. 293.
62. Pavan, A., Provassoli, A., Moraglio, G., Zambelli, A., Makromol. Chem., 1977. **178**: p. 1099.
63. Wolfsgruber, C., Zannoni, G., Rigamonti, E., Zambelli, A., Makromol. Chem., 1975. **176**: p. 2765.
64. Wild, L., Adv. Polym. Sci., 1990. **98**: p. 1.
65. Soares, J.B.P., Hamielec, A.E., Polymer, 1995. **36**: p. 1639.
66. Britto, L.J.D., Soares, J.B.P., Penlidis, A., Monrabal, B., J. Polym. Sci. Part B: Polym. Phys., 1999. **37**: p. 539.
67. Monrabal, B., J. Appl. Polym. Sci., 1994. **52**: p. 491.

68. Monrabal, B., Macromol. Symp., 1996. **110**: p. 81.
69. Monrabal, B., Blanco, J., Nieto, J., Soares, J.B.P., J. Polym. Sci. Part A: Polym. Chem., 1999. **37**: p. 89.
70. Shirayama, K., Okada, T., Kita, S., J. Polym. Sci. A-2, 1965. **3**: p. 907.
71. Desreux, V., Spiegels, M.C., Bull. Soc. Chim. Belg., 1950. **59**: p. 476.
72. Moore, J.C., J. Appl. Polym. Sci. A, 1964. **2**: p. 835.
73. Schneider, N.S., J. Polym. Sci. C, 1965. **8**: p. 179.
74. Wild, L., Ryle, T., Polym. Preprint Am. Chem. Soc., 1977. **18**: p. 182.
75. Wild, L., Ryle, T.R., Knobeloch, D.C., Peat, I.R., J. Polym. Sci.: Pol. Phys. Ed., 1982. **20**: p. 441.
76. Knobeloch, D.C., Wild, L. *Prepr. 427*. in *SPE Polyolefins IV*. 1984.
77. Usami, T., Gotoh, Y., Takayama, S., Macromolecules, 1986. **19**: p. 2722.
78. Keluski, E.C., Elston, C.T., Murray, R.E., Polym. Eng. Sci., 1987. **27**: p. 1562.
79. Hazlitt, L.A., Moldovan, D.G., *US Patent 4 798 081*. 1989.
80. Karoglanian, S.A., Harrison, I.R., Am. Chem. Soc. Proceedings Pol. Mat. Sci. and Eng., 1989. **61**: p. 748.
81. Wild, L., Blatz, C., Polymeric Materials: Science and Engineering, 1992. **67**: p. 153.
82. Mirabella, F.M., Jr., Journal of Liquid Chromatography, 1994. **17**: p. 3201.
83. Anantawaraskul, S., Soares, J.B.P., Wood-Adams, P.M., J. Polym. Sci., Part B: Polym. Phys., 2003. **41**: p. 1762.
84. Mirabella, F.M., Jr., J. Polym. Sci., Part B: Polym. Phys., 2001. **39**: p. 2800.
85. Mirabella, F.M., Jr., J. Polym. Sci., Part B: Polym. Phys., 2001. **39**: p. 2819.
86. Bonner, J.G., Frye, C.J., Capaccio, G., Polymer, 1993. **34**: p. 3532.
87. Zhang, M., Lynch, D.T., Wanke, S.E., J. Appl. Polym. Sci., 2000. **75**: p. 960.
88. Starck, P., Polym. Int., 1996. **40**: p. 111.
89. Kulin, L.I., Meijerink, N.L., Starck, P., Pure and Appl. Chem., 1988. **609**: p. 1403.

90. Wijga, P.W.O., Van Schooten, J., Boerma, J., J. Makromol. Chem., 1960. **36**: p. 115.
91. Kakugo, M., Miyatake, T., Mizunuma, K., Kawai, Y., Macromolecules, 1988. **21**: p. 2309.
92. Wild., L., Knobeloch, D.C., in *United States Patent 5 030 713*. 1991: New York.
93. Xu, J., Fu, Z., Fan, Z., Feng, L., Eur. Pol. Jnl., 2002. **38**: p. 1739.
94. Zhang, Y.-D., Wu, C.-J., Zhu, S.-N., Polym. Jnl., 2002. **34**: p. 700.
95. Xu, J., Feng, L., Yang, Y., Kong, X., Eur. Pol. Jnl., 1998. **34**: p. 431.
96. Feng, Y., Hay, J.N., Polymer, 1998. **39**: p. 6589.
97. Zhang, Y.-D., Gou, Q.-Q., Wang, J., Wu, C.J., Polym. Jnl., 2003. **35**: p. 551.
98. Bergström, C., Avela, E., J. Appl. Polym. Sci., 1979. **23**: p. 163.
99. Nakano, S., Goto, Y., J. Appl. Polym. Sci., 1981. **26**: p. 4217.
100. Mirabella, F.M., Jr., Ford, E.A., J. Polym. Sci., Part B: Polym. Phys., 1987. **25**: p. 777.
101. Karoglanian, S.A., Harrison, I.R., Thermochimica Acta, 1996. **288**: p. 239.
102. Mierau, U., Voigt, D., Bohme, F., Brauer, E., J. Appl. Polym. Sci., 1997. **63**: p. 283.
103. Kukago, M., Miyatake, T., Naito, Y., Mizunuma, K., Macromolecules, 1988. **21**: p. 314.
104. Xu, J., Feng, L., Yang, S., Wu, Y., Yang, Y., Kong, X., Polymer, 1997. **38**: p. 4381.
105. Feng, Y., Hay, J.N., Polymer, 1998. **39**: p. 6723.
106. Hawkins, S.W., Smith, H., J. Polym. Sci., 1958. **28**: p. 341.
107. Kawamura, H., Hayashi, T., Inoue, Y. Chujo, R., Macromolecules, 1989. **22**: p. 2181.
108. Kamatah, P.M., Wild, L., Polym. Eng. Sci., 1966. **6**: p. 213.
109. Kioka, M., Makio, H., Mizuno, A., Kashiwa, N., Polymer, 1994. **35**: p. 580.
110. Kakugo, M., Natio, Y., Miyatake, T., Mizunuma, K., Makromol. Chem., 1989. **190**: p. 849.
111. Xu, J.T., Feng, L.X., Yang. S.L., J. Chin. Univ., 1997. **18**: p. 1734.

112. Morini, G., Albizzati, E., Balbontin, G., Mingozzi, I. Sacchi, M.C., Forlini, F., Tritto, I., Macromolecules, 1996. **29**: p. 5770.
113. Albizzati, E., Giannini, U., Mori, G., Galimberti, M. in *STEPOL '94*. 1994. Milano.
114. Xu, J., Feng, L., Eur. Pol. Jnl., 2000. **36**: p. 867.
115. Xu, J.T., Feng, L.X., Yang. S.L., Yang, Y.Q., Kong, X.M., Macromolecules, 1997. **30**: p. 7655.
116. Xu, J.T., Feng, L.X., Yang. S.L., Acta. Polym. Sin., 1997. **4**: p. 508.
117. Cheng, H.N., Kakugo, M., Macromolecules, 1991. **24**: p. 1724.
118. Mirabella, F.M., Jr., J. Appl. Polym. Sci. Appl. Polym. Symp., 1993. **52**: p. 145.
119. Mirabella, F.M., Jr., J. Appl. Polym. Sci. Appl. Polym. Symp., 1992. **51**: p. 117.
120. Usami, T., Gotoh, Y., Umemoto, H., Takayama, S., J. Appl. Polym. Sci. Appl. Polym. Symp., 1993. **52**: p. 145.
121. Monrabal, B., *Encyclopedia of Analytical Chemistry*. Vol. 9. 2000, Chichester: John Wiley and Sons Ltd. p. 8074.
122. Soares, J.B.P., Anantawaraskul, S., J. Polym. Sci., Part B: Polym. Phys., 2005. **43**: p. 1557.
123. Nieto, J., Oswald, T., Blanco, F., Soares, J.B.P., Monrabal, B., J. Polym. Sci., Part B: Polym. Phys., 2001. **39**: p. 1616.
124. Anantawaraskul, S., Soares, J.B.P., Wood-Adams, P.M., Monrabal, B., Polymer, 2003. **44**: p. 2393.
125. Sarzotti, D.M., Soares, J.B.P., Penlidis, A., J. Polym. Sci., Part B: Polym. Phys., 2000. **40**: p. 2595.
126. Brüll, R., Pasch, H., Raubenheimer, H.G., Sanderson, R., Van Reenen, A.J., Wahner, U.M., Macromol. Chem. Phys., 2001. **202**: p. 1281.
127. Bruaseth, I., Soares, J.B.P., Rytter, E., Polymer, 2004. **45**: p. 7853.
128. Holtrup, W., Macromol. Chem., 1977. **178**: p. 2335.
129. Vilaplana, F., Morera-Escrich, V., Hierro-Navarro, P., Monrabal, B., Ribes-Greus, A., J. Appl. Polym. Sci., 2004. **94**: p. 1803.
130. Kotera, A., *Polymer Fractionation*, Ed. M.J.R. Cantow. 1967, New York: Academic Press. Chapter B1.

CHAPTER 3

An Investigation of Commercial Propylene/1-Pentene Copolymers

3.1 INTRODUCTION

Polypropylene and its copolymers are some of the major commodity polymers on the market today. A variety of different α-olefins are produced in the Sasol Synthol process, when coal is converted to ethylene, propylene and higher olefins.

It is well known that copolymerization of propylene with α-olefins decreases the glass transition temperature and introduces irregularities into the polymer backbone. These irregularities not only affect the macroscopic properties, like toughness or transparency, but also the microscopic ones. There are many references in literature [1-9] concerning the investigation of the crystallinity and morphology of propylene/ethylene or propylene/1-butene copolymers because of their great industrial importance.

Propylene/1-pentene copolymers are, however, a new family of random copolymers now being commercially prepared in South Africa [10, 11]. They have high impact strength, good tensile properties, excellent optical properties, good rheological properties and a large pool of processing possibilities. These commercial propylene/1-pentene copolymers are being prepared with stereospecific heterogeneous Ziegler-Natta catalytic systems. Typically, these catalyst systems contain multiple active sites, hence the copolymers that are produced have varying degrees of stereoregularity and CCD.

In order to understand the unique properties of these commercial propylene/1-pentene copolymers on a molecular level, the need for a thorough investigation of the relationship between the chemical structure and properties of these copolymers was therefore identified. This led to the research carried out in this project.

Sasol Polymers initially provided six totally different propylene/1-pentene copolymers. These six Group 1 copolymers (A - F) were used to carry out some preliminary studies on propylene/1-pentene copolymers. They were investigated with the goal to set up a "molecular toolbox" which was then to be used to investigate a second group of copolymers, namely the Group 2 copolymers (G - J). The Group 2 copolymers were all synthesized with the same Ziegler-Natta catalyst system, but with different donor:catalyst (Si:Ti) ratios, and had different comonomer contents.

Characterization of these original copolymers (A - J) was carried out using ^{13}C-NMR, HT-GPC, CRYSTAF, DSC and WAXD analyses. Additional positron annihilation lifetime spectroscopy (PALS) analysis was also carried out on the copolymers from Group 1.

3.2 EXPERIMENTAL

3.2.1 Commercial propylene/1-pentene copolymers

Sasol Polymers provided two groups, Group 1 and Group 2, of commercial propylene/1-pentene copolymers for this project. The first group, Group 1, consisted of six copolymers (A - F) differing with respect to the catalyst system used for polymerization, MFI values, comonomer content and nucleation. The details of the Group 1 copolymers, as supplied by Sasol Polymers, are summarized in Table 3.1.

Table 3.1 Details of Group 1 copolymers received from Sasol Polymers

Sample	Catalyst used	MFI	1-Pentene content (mol% from FTIR)	Nucleation
A	Catalyst 1	1.70	5.10	Nucleated
B	Catalyst 1	1.40	5.11	Nucleated
C	Catalyst 2	30.0	4.32	Nucleated
D	Catalyst 1	1.58	5.10	Non-nucleated
E	Catalyst 1	1.25	3.62	Nucleated
F	Catalyst 2	1.36	2.24	Nucleated

There are only two variables for the Group 2 copolymers. The copolymers were chosen from batches produced with the same ZN catalyst system, but with specifically different 1-pentene contents. Group 2 copolymers were, however, also synthesized with a catalyst system consisting of different donor:catalyst ratios. These are summarized in Table 3.2, together with the other information received from Sasol Polymers. These two differences made it possible to investigate the influence of the 1-pentene content and the donor:catalyst ratio on the make-up of these commercial propylene/1-pentene copolymers.

Table 3.2 Details of Group 2 copolymers received from Sasol Polymers

Sample	Si:Ti ratio	1-Pentene content (mol% from NMR)
G	2.2	1.13
H	2.9	1.99
I	6.8	2.23
J	10.0	1.86

3.2.2 ^{13}C-NMR

For the high-temperature ^{13}C-NMR analysis of Group 1 copolymers spectra were recorded on a 600 MHz Varian ^{Unity}*Inova* spectrometer equipped with an Oxford magnet (14.09 T) on a 5 mm (15N-31P) broadband probe.

Parameters used were as follows: acquisition time of 1.8 sec, recycle delay of 15 sec, 90° pulse angle and full decoupling. Resolution and accuracy were improved by zero-filling the data once before performing the Fourier transformation. Baseline correction was applied in order to further enhance the accuracy and repeatability of the integrals measured for selected peaks in the spectra. Samples (~ 60 mg) for ^{13}C-NMR analysis were dissolved in 1,1,2,2,-tetrachloroethane-d_2 (d_2-TCE) using the following procedure: 0.3 ml of the deuterated solvent was added to ~ 60 mg of the polymer. The polymer was then melted inside the NMR-tube in the presence of the solvent by carefully heating the tube with a heat-gun. The rest of the 0.6 ml solvent was added and the sample was slowly heated further in order to homogenize the solution. The analyses of these samples were executed at 120°C.

For the ^{13}C-NMR analysis of Group 2 copolymers, samples (~ 60 mg) were dissolved in 0.6 ml deuterated tetrachloroethane (d_2-TCE) (6 wt-%). First, the solvent was purged with nitrogen for 2 hours prior to preparing the sample for analysis. To 60 mg of the polymer was added 0.3 ml of the deuterated solvent. The polymer was melted in the NMR tube in the presence of the solvent by carefully heating the tube with a heat-gun. The rest of the solvent was added and the tube sealed with Teflon® tape. The sample was placed in a ventilated oven to homogenize at 140 °C for approximately 2 hours. Quantitative ^{13}C NMR experiments were performed at 150 MHz on a 5 mm PFG switchable/broadband probe (^{1}H -^{19}F, ^{15}N - ^{31}P) on a Varian $^{\text{UNITY}}$*INOVA* 600 MHz spectrometer at 130°C. 90° pulse widths of approximately 6 μsec and delay times between pulses of 15 sec were used with an acquisition time of 1.8 sec. The number of scans was set to 2400, but a signal-to-noise parameter was set to 5000. Thus, either 2400 scans were acquired or the acquisition was stopped after the required signal-to-noise was reached.

Resolution and accuracy were improved by zero-filling the data once before performing the Fourier transformation. Baseline correction was also applied in order to further enhance the accuracy and repeatability of the integrals measured for selected peaks in the spectra.

The percentage of 1-pentene content of all the commercial propylene/1-pentene random copolymers were calculated by means of integration. During calculation of the comonomer content, only the backbone carbon atoms are taken into account. The formula used for the calculation of the percentage of 1-pentene in the various comonomers is the following [12]:

$$\% \text{ 1-Pentene} = [2C_{\alpha} / (C_{\alpha} + C_{br} + C_{p1} + C_{p2})] \times 100$$

C_{α} and C_{br} represent the integrals of the α-carbon and the branch-carbon in the backbone of the 1-pentene, respectively, and C_{p1} and C_{p2} represent the integrals of the two propylene carbons forming part of the backbone of the copolymer.

The determination of the tacticity of these commercial propylene/1-pentene random copolymers was unfortunately not possible. Due to the overlap of the resonance signal of one of the methylene peaks (C_a in Figure 3.1) in the 1-pentene side-chain and the *mrrr* steric pentad signal of the propylene methyl (C_b in Figure 3.1) peak, the contribution of the *mrrr* pentad cannot be measured directly. Literature [13] describes an estimation method for the determination of the tacticity of these copolymers based on the subtraction of the integrated signal area of a 1-pentene methylene carbon measured in a different spectral region from the total integrated signal area of the original 1-pentene methylene and *mrrr* steric pentads. These tacticity values will unfortunately only be estimates and not a true resemblance.

The determination of the tacticity becomes even more complex at higher comonomer contents, where the methylene 1-pentene resonance signal overlaps both *mrrr* and *mrrm* pentads.

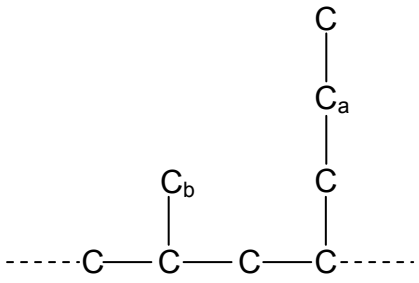

Figure 3.1 A representation of the structure of a propylene/1-pentene copolymer

3.2.3 HT-GPC

Molecular weights of the samples were determined using a PL-GPC 220 high temperature chromatograph (Polymer Laboratories) packed with three Polymer Laboratories PL-gel mixed B columns (polystyrene/divinylbenzene copolymer, particle size 10 μm, length/I.D.: 300*7.5 mm) and a PL-gel 10 μm guard (50*7.5 mm), at a flow rate of 1 ml/min (corrected using BHT as flow rate marker). The analyses were carried out at 160°C in 1,2,4,-trichlorobenzene (TCB) stabilized with 0.0125% (w/v) of 2,6-di-tert-butyl-4-methylphenol. The molecular weight and molecular weight distributions were obtained from this. The sample concentration was 2mg/ml. Differential refractive index was used for detection and molecular weights were calculated relative to a calibration with monodisperse polystyrene standards.

3.2.4 CRYSTAF

For CRYSTAF analysis of the different samples, a Hewlett Packard 6890 II oven was used for the crystallization temperature program. Crystallization of polymers was carried out in 5 stainless steel reactors, of 60 ml capacity each, in which dissolution and filtration takes place automatically. Each of these reactors is also fitted with a stirrer. A dual wave length, optoelectronic infrared detector together with a heated flow-through micro cell was used to measure the polymer concentration in solution at each sampling

step during the crystallization. The microcell operates at 150°C and uses 3.5 μ as the measuring wavelength. Samples of 10 mg were dissolved in TCB (commercial grade) at a concentration of 0.1% w/v. The samples were stabilized at 110°C for one hour after dissolving them at 140°C. Crystallization then took place at a rate of 0.10°C/min, until the temperature reached 30°C.

3.2.5 DSC

Thermal analysis was carried out on the original Group 1 and Group 2 copolymers before slow cooling and after slow cooling. The calorimetric measurements of these samples were performed with a TA Instruments Q100 RCS DSC system. Indium metal was used for the calibration of the instrument according to standard procedures. The analyses were carried out in nitrogen atmosphere. About 4 mg of sample was sealed in an aluminium sample pan for these analyses

The samples were first subjected to a heating ramp up to 220 °C and kept isothermally at that temperature for 5 min in order to remove any thermal history. The cooling cycle for crystallization then followed, with the subsequent heating scan being recorded for analysis. Both the cooling cycle and the final heating cycle were carried out at a standard rate of 10 °C/min. For the slow-cooled samples, however, both the heating stages as well as the cooling stage were carried out at the standard rate of 10 °C/min and the data for all three stages were collected for analysis purposes.

3.2.6 WAXD

The samples to be analyzed by WAXD were slow cooled before analysis. These samples were hot-pressed at 230 °C into 100-μm thick films. They were then cut into circles with a diameter of 15 mm, and individually placed into glass pans. Three pans were fitted simultaneously into a 350-ml stainless-steel Parr autoclave. The autoclave was fitted with a seal ring and connected to a vacuum pump. An oil bath equipped with a temperature

controller acted as controlled heating mantle for the autoclave. The films were then melted at 180°C under vacuum and subsequently slow cooled at a rate of 2°C/h, from 180°C to room temperature.

WAXD analysis of the examined samples was performed at room temperature with a Bruker AXS D8 ADVANCE diffractometer coupled to a source of filtered CuK_α radiation. The scans were performed within the range of 2θ = 9 - 36°, with a sampling width of 0.05° and a scanning rate of 28°/min.

3.2.7 Positron annihilation lifetime spectroscopy

The positron lifetime measurements were carried out using a fast-fast coincidence system [14] with a time resolution of 260 ps (full width at half maximum, FWHM, of a Gaussian resolution function) and a channel width of 50 ps. Two identical samples of 1.5-mm thickness were sandwiched around a 1 x 10^6 Bq positron source (^{22}Na), which was prepared by evaporating carrier-free ^{22}NaCl solution on an aluminium foil. Measurements were carried out at room temperature.

For the decomposition of the lifetime spectra *s(t)* the conventional analysis in terms of a weighted sum of discrete exponentials [14] were used

$$s(t) = \Sigma(I_i / \tau_i)\exp(-t / \tau_i) \qquad \Sigma I_i = 1$$

where τ_i denotes the mean (characteristic) lifetime of the positron state *i*, and I_i is the relative intensity of the corresponding lifetime component. After subtraction of the source components and the background, the parameters of the lifetime spectra are obtained from a non-linear least squares fitting of s(t), convoluted with the Gaussian resolution function, to the experimental spectra, using the routine PATFIT. Three exponential components were needed to obtain a good fit.

All the samples were re-processed and annealed prior to analysis.

3.3 RESULTS AND DISCUSSION

3.3.1 ^{13}C-NMR

^{13}C-NMR analyses were carried out on all the commercial propylene/1-pentene random copolymers. Figure 3.2 and Table 3.3 show the ^{13}C-NMR results of the Group 1 copolymers.

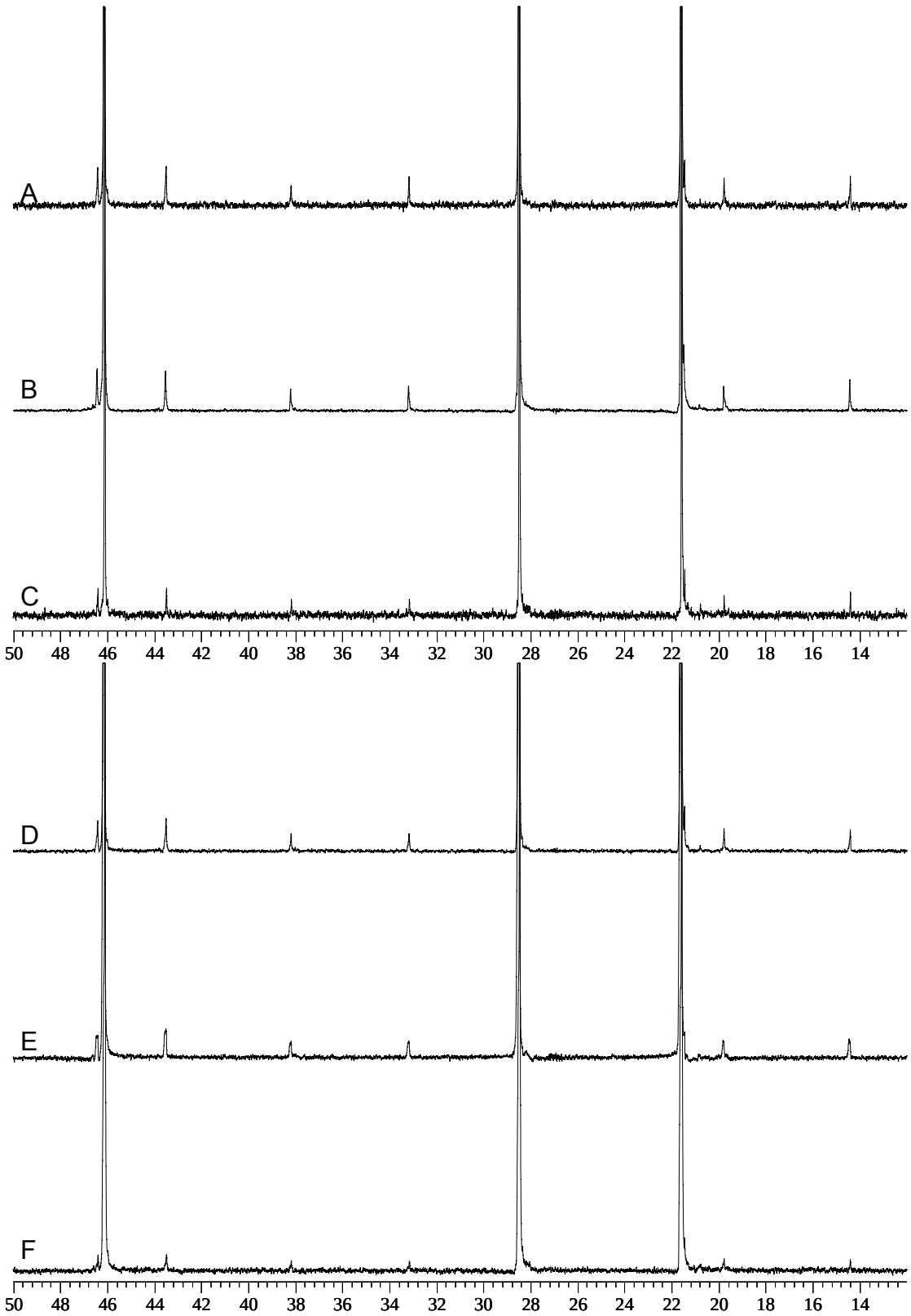

Figure 3.2 **^{13}C-NMR spectra of Group 1 propylene/1-pentene copolymers**

Table 3.3 Comonomer content of the Group 1 propylene/1pentene copolymers according to FTIR and NMR

Sample	1-Pentene content (mol % from FTIR)	1-Pentene content (mol % from NMR)
A	5.10	3.41
B	5.11	3.09
C	4.32	2.09
D	5.10	3.50
E	3.62	2.03
F	2.24	1.21

In Table 3.3 the comonomer content values of the Group 1 copolymers, as determined by FTIR and by ^{13}C-NMR analysis, are compared. FTIR analysis shows that Polymers A, B and D have approximately the same 1-pentene contents, which are also the highest of the the six copolymers, followed by Polymer C and Polymer E and Polymer F have the lowest comonomer content. Analysis by ^{13}C-NMR and by FTIR shows the same trend of a decrease in comonomer content for Polymers C, E and F, which also has the lowest 1-pentene content of the six copolymers of Group 1. The three copolymers with the highest comonomer content (determined by ^{13}C-NMR analysis) are, with respect to the calculation of the 1-pentene content, more differentiated. In this case Polymer D shows the highest comonomer content followed by Polymer A and then Polymer B.

Figure 3.3 and Table 3.4 show the ^{13}C-NMR results of the Group 2 copolymers. We already know that there is an increase in the donor:catalyst ratio from Polymer G to Polymer J. Table 3.4 shows that the comonomer content increases in the following order: Polymer G, J, H and then I. We can therefore conclude that the trend in donor:catalyst ratio of the ZN catalyst system used to produce these copolymers does not correspond with the 1-pentene content of the copolymers. The possibility therefore exists to identify which of the two factors has the dominating effect on certain properties (e.g. degree of crystallinity, melting temperature, crystallization temperature and percentage of γ-phase crystal) of the copolymers. It is unclear whether or not the 1-pentene content in the feed was kept constant during polymerization. It

is therefore not clear whether the 1-pentene content is due to the Si:Ti ratio or not.

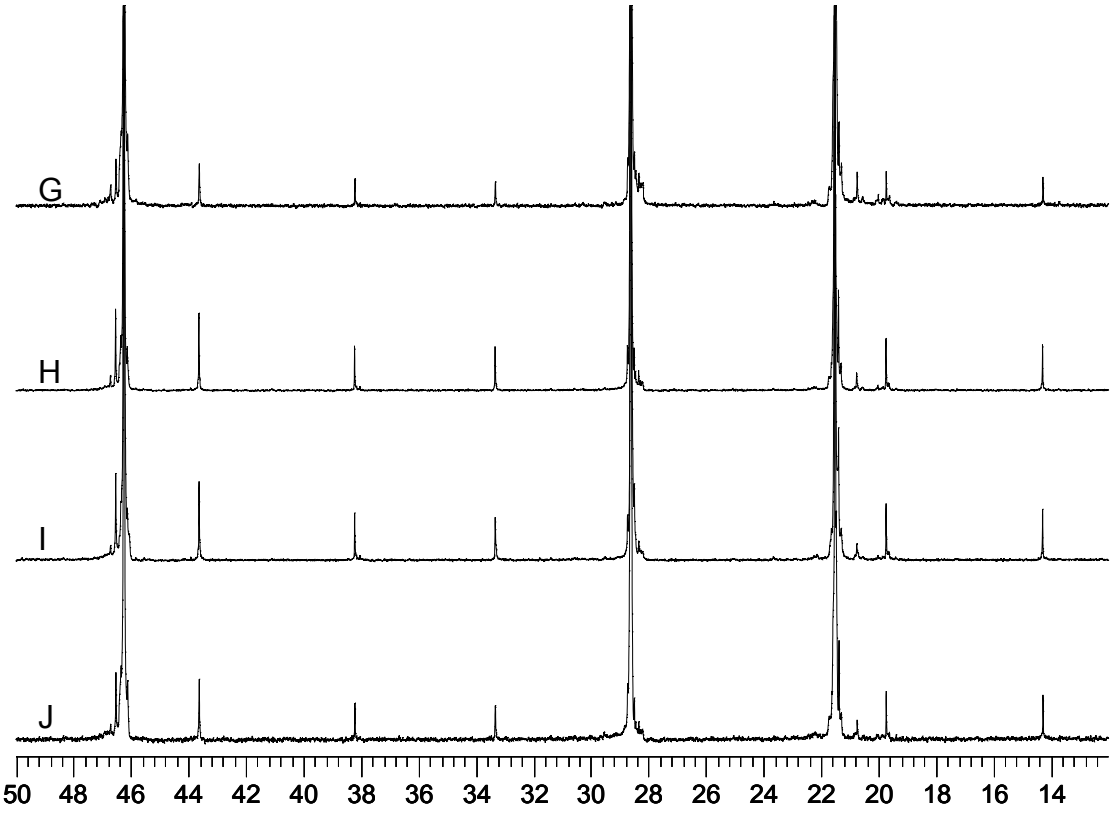

Figure 3.3 ^{13}C-NMR spectra of Group 2 propylene/1-pentene copolymers

Table 3.4 Comonomer content of the Group 2 copolymers

Sample	1-Pentene content (mol% from NMR)
G	1.13
H	1.99
I	2.23
J	1.86

It was already mentioned in Section 3.2.2 that it is not possible to calculate the true tacticity values of these propylene/1-pentene copolymers. An estimation may however be made by having a closer look at the methyl pentad region. Figure 3.4 shows the ^{13}C-NMR spectra of the propylene methyl region (20.0 – 23.0 ppm) of the Group 2 copolymers. The spectra are

arranged from the top to the bottom according to the increase in 1-pentene content of Polymers G - J. According to the increase in intensity of the shoulder peak on the right hand side of the *mmmm* pentad (21.5 ppm) it seems as if there is a decrease in tacticity with the increase in 1-pentene content, as expected.

There appears to be little correlation between the Si:Ti ratios and the apparent tacticities; which was supposedly to be expected. It is clear that the polymer with the highest Si:Ti ratio (10.0) has the second highest apparent tacticity, but Polymer I (Si:Ti = 6.8) has the lowest apparent tacticity.

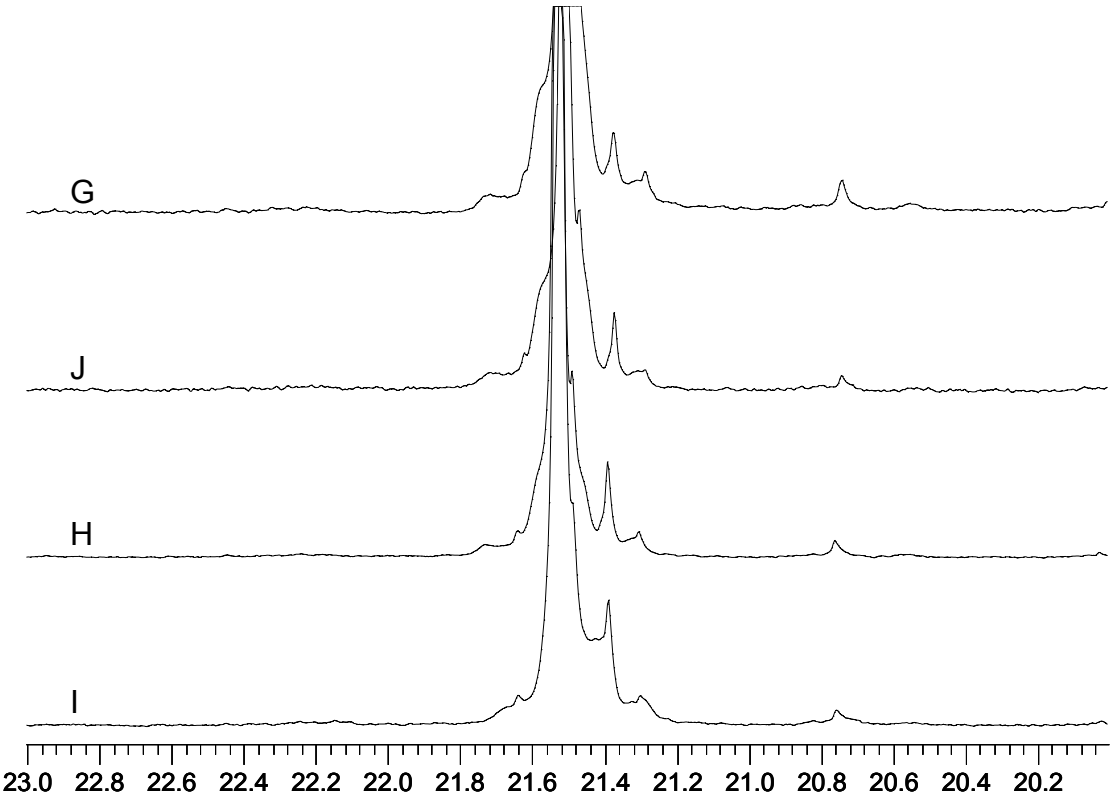

Figure 3.4 ^{13}C-NMR spectra of the propylene methyl region of the Group 2 propylene/1-pentene copolymers

3.3.2 HT-GPC

Table 3.5 shows the molecular weight and polydispersity results as determined by HT-GPC as well as the corresponding MFI values as supplied by Sasol Polymers.

The polydispersity values of the copolymers are relatively high. This was expected, due to the heterogeneous ZN catalysts used to produce these copolymers. The molecular weight values as well as the polydispersity values of the copolymers of Group 1 are all in the same range, except the values for Polymer C. Polymers C and F were produced by the same ZN catalyst system but Polymer C contains approximately twice the amount of comonomer than Polymer F. It is obvious that the high MFI copolymer (Polymer C) has a much lower molecular weight, as expected. Interestingly enough, the polydispersity of Polymer C is lower than that of the other materials. It is unclear whether this material was vis-broken.

Table 3.5 HT-GPC results of Polymers A - F

Sample	MFI	M_n (g/mol)	M_w (g/mol)	PD
A	1.70	78 000	567 000	7.09
B	1.40	84 200	562 900	6.69
C	30.0	54 000	208 800	3.86
D	1.58	83 400	592 000	7.10
E	1.25	80 200	557 000	6.94
F	1.36	82 600	584 100	7.07

Table 3.6 shows the molecular weight and polydispersity values of the Group 2 copolymers as well as the donor:catalyst ratio values of the ZN catalyst system with which these copolymers were produced.

Table 3.6 HT-GPC results of Polymers G - J

Sample	Si:Ti ratio	M_n (g/mol)	M_w (g/mol)	PD
G	2.2	72 200	305 800	4.23
H	2.9	79 100	343 300	4.34
I	6.8	93 500	299 600	3.21
J	10.0	96 700	337 700	3.49

Table 3.6 shows that the polydispersity values of the Group 2 copolymers are very similar, ranging from 3.21 to 4.34. The polydispersities are in general lower than those of the Group 1 copolymers, but are still relatively high due to the heterogeneous character of the ZN catalyst system with which these commercial copolymers were produced. The M_n values of the copolymers increase with an increase in the donor:catalyst ratio, which can be expected, according to literature [15]. The polydispersity values are also 25% lower for polymers produced by a higher (Si:Ti > 6) ratio. This indicates that active sites with more uniform activity are formed. While the Si:Ti ratio seems to have little effect on the tacticity (Figure 3.4) it does appear to have an effect on the polydispersity.

3.3.3 Thermal analysis

Figure 3.5 shows the crystallization curves of Polymers A - F as determined by CRYSTAF analysis. Table 3.7 tabulates the thermal analysis results received from CRYSTAF and DSC analyses as well as the comonomer content of the various copolymers as determined by ^{13}C-NMR. The copolymers and their results are arranged from the top to the bottom in Table 3.7 according to the decrease in their comonomer contents

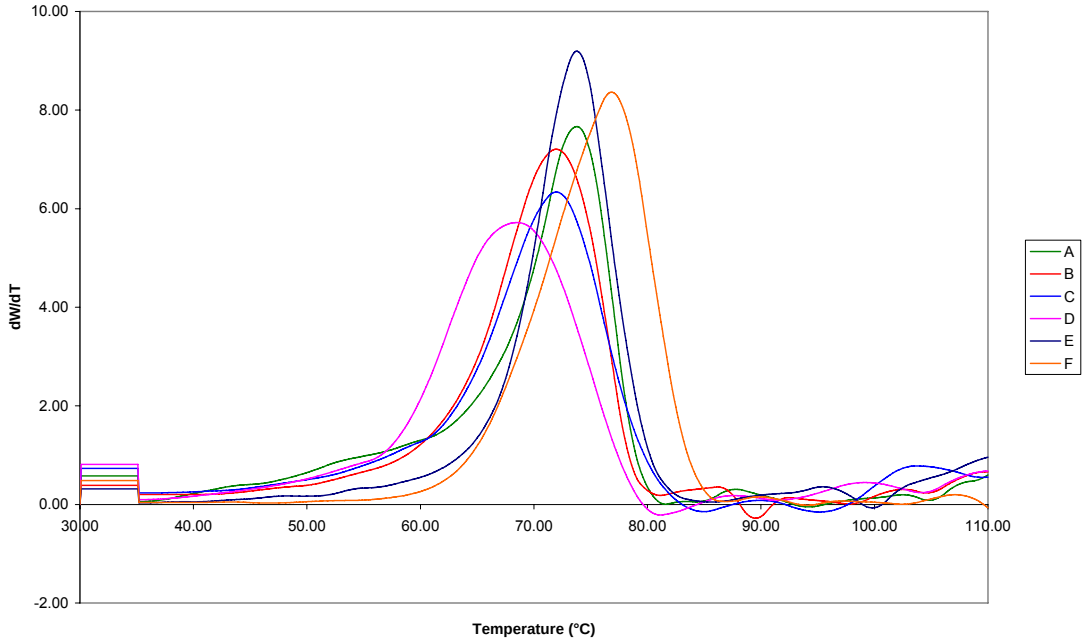

Figure 3.5 Spectra of the CRYSTAF analysis of Group 1 copolymers

From Figure 3.5 and Table 3.7 it is clear that Polymer D with the highest 1-pentene content has the lowest T_c and, on the other hand, Polymer F with the lowest 1-pentene content shows the highest T_c. Polymers B and C show the same T_c values during CRYSTAF analysis as do Polymers A and E. The copolymers were therefore further examined by means of DSC analysis in order to obtain more detail. The percentages of soluble fraction (from the CRYSTAF results in Table 3.7) of the copolymers range from 1.6 to 4.1, which are relatively low.

Table 3.7 Thermal analysis data of Group 1 copolymers

Sample	1-Pentene content (mol % from NMR)	T_c (CRYSTAF) (°C)	Soluble fraction (CRYSTAF) (%)	T_c (DSC) (°C)	Crystallinity (DSC) (%)	T_m (DSC) (°C)
D	3.50	63.3	4.1	97.44	59.28	138.9
A	3.41	68.6	2.9	101.68	72.92	142.66
B	3.09	66.8	1.9	117.72	66.27	145.51
C	2.09	66.8	3.7	119.39	66.17	147.22
E	2.03	68.6	1.6	120.12	68.95	148.26
F	1.21	71.6	2.4	123.75	79.57	154.23

An estimate of the degree of crystallinity of the commercial propylene/1-pentene copolymers can be obtained using the following formula [16]:

$$\% \text{ Crystallinity} = \Delta H_m / \Delta H \text{ (100\% crystallized PP)} \times 100$$

where ΔH_m is the experimental melt enthalpy obtained from the DSC melting thermogram and ΔH (100% crystallized PP) = 209 J/g [17].

According to the DSC results in Table 3.7 an increase in T_c and T_m can be seen as the comonomer content decreases. Except for Polymer A, we also see a general increase in the percentage of crystallinity, calculated using the method described above. According to the initial information, Polymers A, B and D should be virtually identical. They were produced by the same catalyst, have the same MFI, and, according to FTIR, have the same 1-pentene content. Yet, these materials appear to be significantly different. The T_c (CRYSTAF) varies, and, the T_c (DSC) varies even more significantly. In the latter case, the values for Polymers D and A are around 100°C (97.44°C and 101.68°C), while Polymer B has a crystallization temperature of 117.72°C. This is significantly different.

The ^{13}C-NMR results indicate that the FTIR values for the 1-pentene content may be misleading, and that the values are different; varying from 3.50 mol %(D) to 3.09 mol %(B). The question remains: is this variation (0.41 mol %) enough to change the crystallization and melting properties this much? This is illustrated by the relatively small increase in T_c (DSC) from Polymer B to Polymer E (made by the same catalyst) of only 2.40°C, with a change of 1.06 mol % in comonomer content. The only other and more probable factor should be due to the absence of a nucleating agent in Polymer D.

Figure 3.6 illustrates the graphs of the original samples of Group 2 and Table 3.8 represents a summary of the thermal analysis results from CRYSTAF and DSC analysis. Again we find that the copolymer containing the highest amount of 1-pentene (Polymer I) has the lowest T_c (CRYSTAF) and Polymer G with the lowest comonomer content shows the highest T_c

(CRYSTAF). According to Figure 3.6 and Table 3.8 the peak crystallization temperatures (T_c) of Polymers J and H are very similar. This can be ascribed to the fact that the comonomer content of these two polymers does not differ by much (0.13 mol %). Despite this small difference, we still find a decrease in the T_c from the CRYSTAF analysis with an increase in the 1-pentene content of the copolymers, as expected. Another conclusion from the CRYSTAF results is that the percentages of soluble fraction are very low (1.3 - 1.6%), especially when we compare these results with those of the Group 1 copolymers (1.6 - 4.1%).

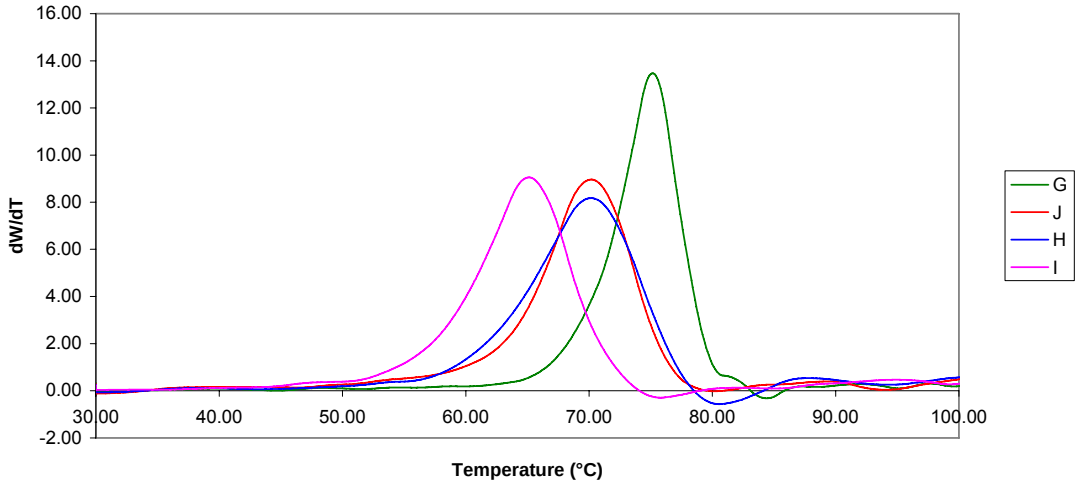

Figure 3.6 CRYSTAF curves of the four original Group 2 copolymers

In Table 3.8 the copolymers and their analysis results are arranged from top to bottom in the order of increasing comonomer content. The T_c values from DSC analysis are very similar for Polymers H and I. The T_c values from DSC analyses do however not give such a definite trend as in the case of the T_c values from CRYSTAF analysis. In fact, the crystallization temperatures for H and I are significantly higher than those of G and J, which seems independent of Si:Ti ratio or comonomer content.

The samples are allowed to crystallize from solution during CRYSTAF analysis and this allows more mobility for the chains to rearrange for crystallization than in the case of DSC analysis where crystallization takes place from the molten state. TREF may be an appropriate technique to use in order to make sense of the T_c values received from DSC analysis. The T_m

values of the Group 2 copolymers remain relatively constant, independent of a difference in comonomer content.

Table 3.8 Thermal analysis data of Group 2 copolymers

Sample	Si:Ti	1-Pentene content (mol % from NMR)	T_c (CRYSTAF) (°C)	Soluble fraction (CRYSTAF) (%)	T_c (DSC) (°C)	Crystallinity (%)	T_m (DSC) (°C)
G	2.2	1.13	75.1	1.6	110.41	67.94	151.82
J	10.0	1.86	70.2	1.5	106.52	54.88	149.60
H	2.8	1.99	70.2	1.3	120.97	68.28	151.12
I	6.8	2.23	65.1	1.2	121.16	64.64	149.84

According to DSC analysis there is furthermore a very significant decrease in the degree of crystallinity with an increase in the donor:catalyst ratio of the ZN catalyst system used to produce these copolymers. It is known from literature [18] that donors are used in order to improve the stereospecifity of $MgCl_2$-supported catalysts and thereby also the stereoregularity of the polymers they produce. From the results shown in Figure 3.6 and tabled in Table 3.8, it can be concluded that the donor:catalyst ratio has little or no effect on the crystallization and melting characteristics of the copolymers. Polymers H and I have similar T_c (DSC) and T_m yet the Si:Ti ratio is 2.8 for Polymer H and 6.8 for Polymer I (more than double). Variations in the CRYSTAF T_c values seem to indicate that crystallization is affected primarily by 1-pentene content, yet this is not as clearly reflected by the DSC data. It would appear, therefore, that properties are affected primarily by the amount, and possibly by the distribution of 1-pentene in the copolymer, rather than the Si:Ti ratio. It is, of course, quite possible that the Si:Ti ratio could influence the latter, i.e. the distribution of 1-pentene in the copolymer.

3.3.4 WAXD

The prevalent crystal phase of iPP is the monoclinic α-phase [19]. Under the following conditions however the growth of the γ-phase crystal is favoured:

- High pressure crystallization
- Isothermal crystallization at low super cooling
- Low molecular weight
- The presence of chain defects and stereodefects [1, 3, 20]
- Slow cooling [21]

A study by Turner-Jones [1] of copolymers of propylene with minor proportions of 1-butene and ethylene, made in the presence of the $TiCl_3/AlEt_2Cl$ catalyst, proved that such copolymers developed the γ-form crystallinity, mixed with the α-form on crystallization by slow cooling from temperatures near the melting point. He also reported that the proportion of γ-form increases with increasing comonomer content and ascribed this phenomenon to the interruptions in the isotactic polypropylene sequences caused by the comonomer units. The α-phase requires chain folding as the chains exit the crystalline regions for the growth of a crystal whereas the γ-phase does not need chain folding but is formed preferentially by short isotactic sequences [1, 21]. The more chains that are therefore excluded from the α-phase, the more γ-phase crystals will be formed [20]. Stereoirregularities in the 3_1helix also promote the formation of γ-phase crystals as they are also excluded from the forming crystals.

The results of Juhász and Belina [22] lead them to the conclusion that the 1-pentene comonomer is the highest α-olefin that can be included in the crystal phase. They reported that the γ-form increases with the comonomer content in propylene/1-pentene copolymers three times faster than in propylene/ethylene copolymers.

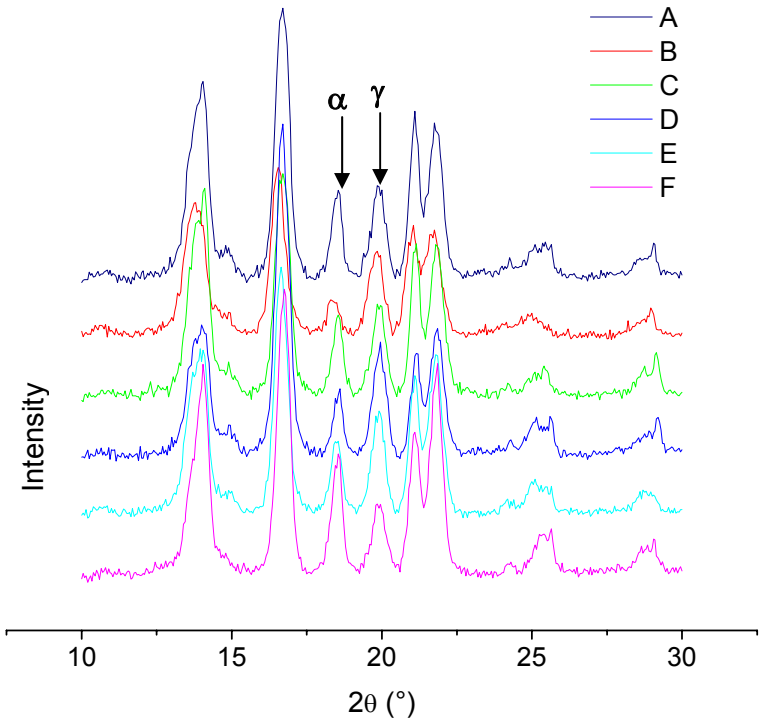

Figure 3.7 X-ray diffractograms for Polymers A - F

Figure 3.7 represents the spectra of the WAXD analysis of the Group 1 copolymers. The peaks of the α-phase as well as the γ-phase are clearly indicated in the crystal structure of Figure 3.7 at $2\theta \approx 18.6°$ and $2\theta \approx 20.1°$. In Figure 3.7 it is clear that the WAXD results of Polymers B, D and E resulted in a predominant γ-phase, whereas Polymer F is the only one indicating a predominant α-phase. In previous studies [3, 6] the γ to α ratio was calculated simply from the relative intensities of the unique γ and α peaks. Although this ratio provides the correct limits of zero γ and α phase in the absence of the respective peaks, it does not necessarily give the correct ratios in the intermediate regime. Therefore, in the present work the overall intensities in the angular range 10 - 30° of both phases are determined by means of a WAXD pattern deconvolution procedure [1]. In this way the amorphous background is subtracted from the crystalline peaks with the aid of OriginLab software. The percentages of γ-phase crystal of the Group 1 samples were calculated in this way and are given in Table 3.9, in addition to

the comonomer content calculated from ^{13}C-NMR results, and the overall percentage crystallinity calculated from the DSC results of all the commercial copolymers.

Table 3.9 Comonomer content, percentage crystallinity and percentage of γ-phase crystals present in slow-cooled Polymers A - F

Sample	1-Pentene content (%)	Crystallinity (%)	γ-phase crystal (%)
D	3.50	59.28	67.65
A	3.41	72.92	53.88
B	3.09	66.27	71.20
C	2.09	66.17	52.81
E	2.03	68.95	59.02
F	1.21	79.57	39.40

The copolymers and corresponding results of Table 3.9 are arranged according to decreasing comonomer amount from the top to the bottom. According to theory [1, 19, 23] an increase in the γ-phase can be expected for an increase in the comonomer content. The WAXD results of Polymers A - F do however not follow this trend, maybe because of the many different variables in these copolymers. There may however also be other important factors playing a role here. The γ-phase is formed preferentially in the presence of short isotactic sequences [24]. It is notable that Polymers A and B should be quite similar, yet exhibit widely different γ-phase percentage. The non-nucleated Polymer D (similar in all other respects to Polymers A and B) has a high γ-phase, yet slightly lower than Polymer B, which has lower 1-pentene content. Polymers C and E have similar 1-pentene contents and crystallinities but have different γ-phase percentages. These two copolymers were, of course, made by different catalyst systems. Once again it appears as if there are differences in the way the 1-pentene is distributed in the copolymers. If the 1-pentene distribution is very much limited to the amorphous regions of the copolymer, then the low comonomer content in the crystalline areas could cause a lower γ-phase.

Figure 3.8 shows the WAXD spectra for the copolymers in Group 2. The spectra are arranged from the top to the bottom in the order of increasing 1-pentene content.

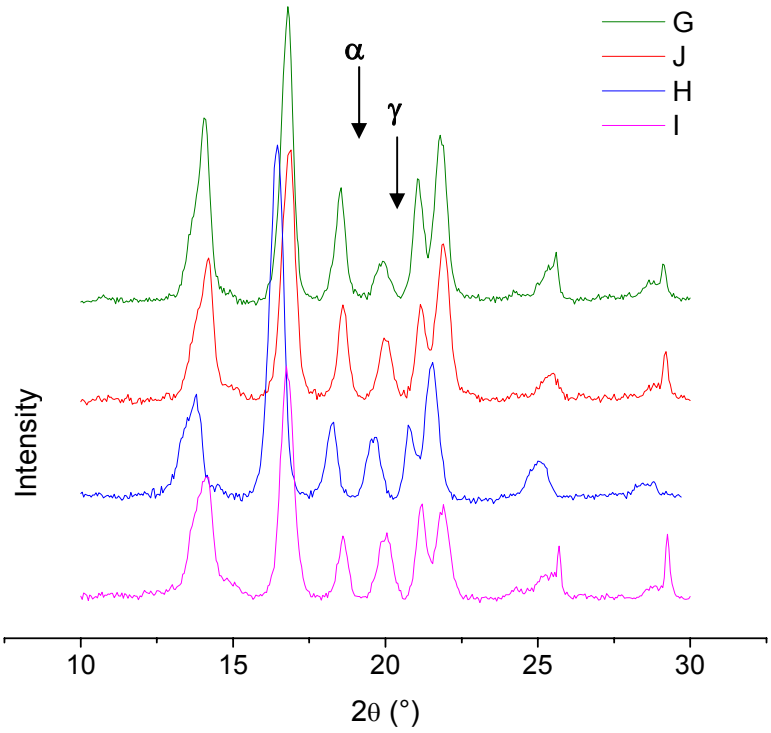

Figure 3.8 X-ray diffractograms for Polymers G - J

Table 3.10 shows the calculated percentage of γ-phase crystal calculated from WAXD analysis, the 1-pentene content calculated from ^{13}C-NMR analysis and the percentage crystallinity as calculated from the thermal analysis. The copolymers as well as corresponding results are arranged in the same way as in Figure 3.8.

Table 3.10 Comonomer content, percentage of crystallinity and percentage of γ-phase crystals present in slow-cooled samples of Group 2 copolymers

Polymer	1-Pentene content (%)	Crystallinity (%)	γ-phase crystal (%)
G	1.13	67.94	22.65
J	1.86	54.88	37.99
H	1.99	68.28	43.43
I	2.23	64.64	47.72

From the results in Figure 3.8 it can already be seen that there is a decrease in the ratio of α-:γ-phase intensities. The calculated values of the percentage γ-phase crystal in Table 3.10 further substantiates that an increase in 1-pentene content favours the growth of the γ-phase crystals, as described in literature [1, 19, 23]. This indicates that the copolymer composition is more uniform in these samples than in those of the Group 1 copolymers.

All of the slow-cooled samples which were analyzed by WAXD were also investigated by DSC. Figure 3.9 illustrates the DSC results of the first and second heating cycles of the slow-cooled Polymer E.

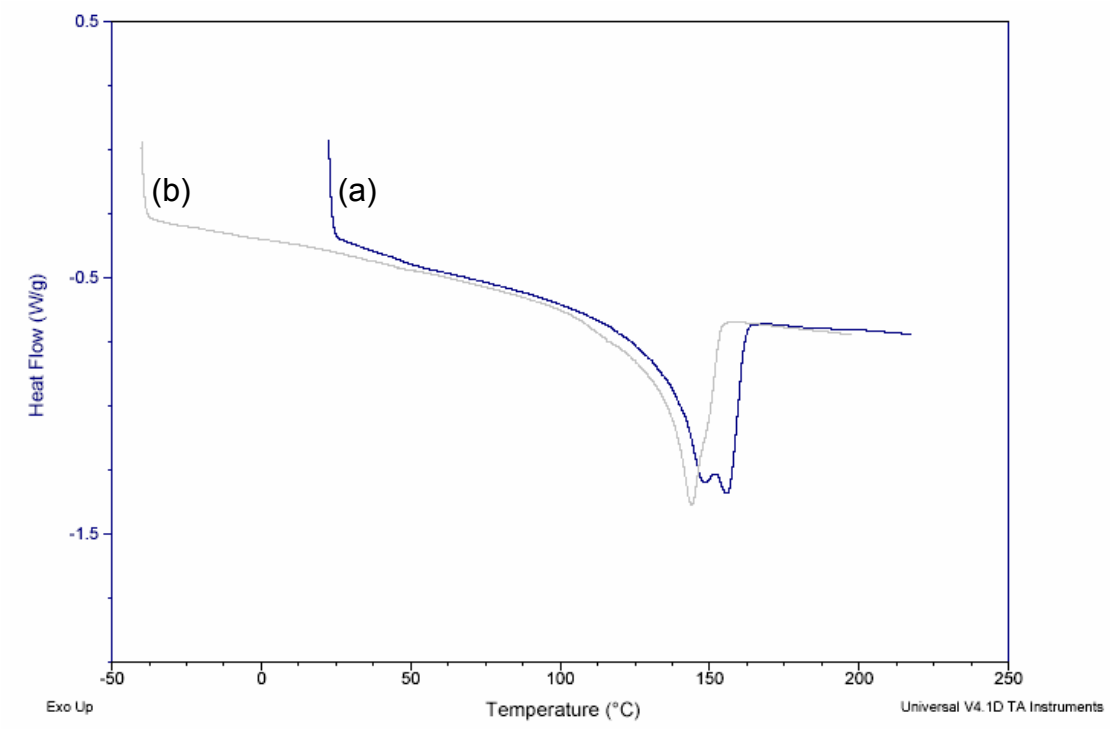

Figure 3.9 Melting thermograms of (a) the first and (b) the second heating cycles of the slow-cooled Polymer E

It is known from theory [25-27] that the γ-phase melts at a lower temperature than the α-phase. In Figure 3.9 a small shoulder can be seen to the left hand side of the main melting peak in the endotherm of the first heating cycle. The samples were isothermally maintained at 220°C for 5 min after the first heating cycle in order to remove the thermal history of the sample. The endotherm of the second heating cycle in Figure 3.9 therefore indicates a melting peak due to the α-phase crystals only. From Figure 3.9 it is also noticeable that the melting endotherm due to the α-phase is at a lower temperature during the second heating cycle than in the case of the first heating cycle. The reason for this is that the initial slow-cooling of the samples allows them to form thicker and more stable crystals which melt at higher temperatures than in the second heating cycle.

3.3.5 PALS

Positron annihilation is a well developed analytical technique for studying atomic and subnanometer-size voids in solids [28, 29]. Although the concept of free volume in polymers has been known for almost half of a century, only limited experimental data have been reported. Positron annihilation has however been developed to be probably the most successful technique for studying local free volumes in polymers [29-35].

In molecular materials, positrons annihilate either as free positrons or from a bound state called positronium (Ps) [29]. Ps appears either as a *para*-positronium (*p*-Ps, singlet spin state) or as an *ortho*-positronium (*o*-Ps, triplet spin state) with a relative formation probability of 1:3. In positron lifetime spectra of poly(α-olefins) four different lifetimes appear when analyzed with the routine MELT which assumes continuous lifetime distributions. The two lower peaks have mass centres at $\tau_1 \approx 160$ ps and $\tau_2 \approx 360$ ps. These lifetimes are well known and come from *p*-Ps self-annihilation and free positron (not Ps) annihilation [29, 31-35]. The longest lifetime, $\tau_4 = 2.2 - 3$ ns, is attributed to *o*-Ps annihilation from free-volume holes in the amorphous phase of the polymers. The medium lifetime time, $\tau_3 \sim 1$ ns, is attributed to *o*-Ps annihilation from the interstitial region of the crystalline phase [36].

Some preliminary PALS studies were carried out at the University of Missouri on the Group 1 polymers.

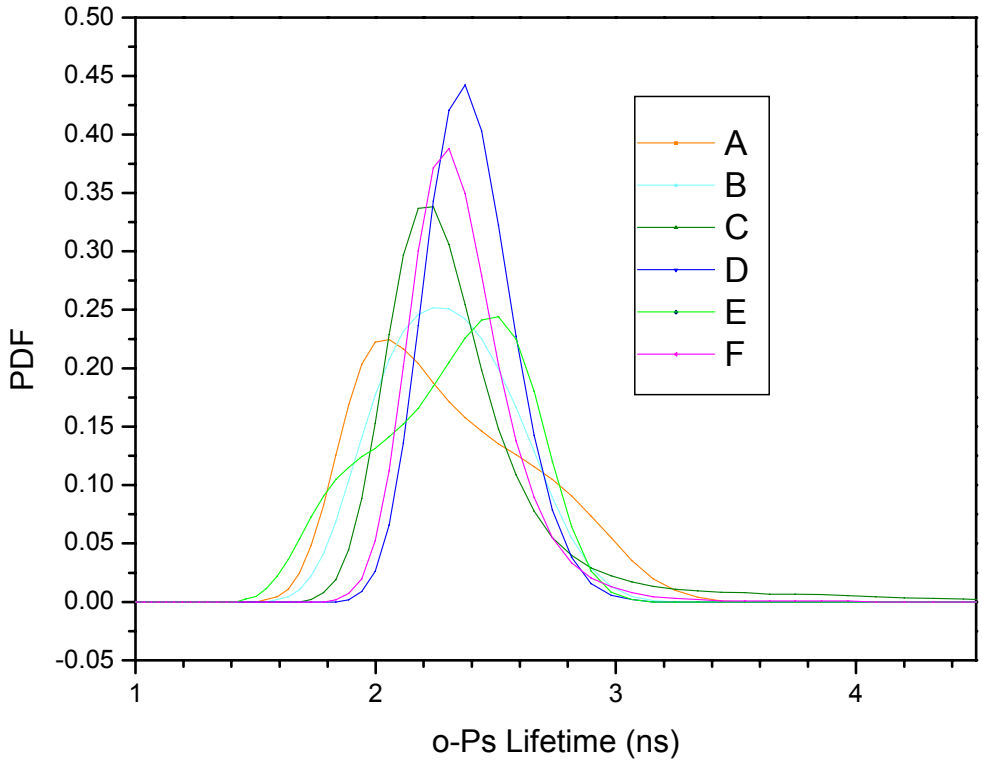

Figure 3.10 Graphs of *o*-Ps lifetime distribution of original commercial Polymers A - F

Figure 3.10 illustrates the *o*-Ps lifetime distributions of the commercial Polymers A - F. All the samples show a single peak, except for Polymers A and E which show a bimodal distribution. The bimodal peaks might be due to a better defined separation between the crystalline and the amorphous phases, represented by τ_3 and τ_4 respectively, of Polymers A and E than in the case of the other polymers. Another noticeable difference in the spectra in Figure 3.10 is the difference in peak width. The narrower the peak, the smaller is the transition between the crystalline and the amorphous phases.

3.4 CONCLUSIONS

Two different groups (Group 1 and 2) of commercial propylene/1-pentene random copolymers were investigated in this study. The copolymers

in Group 1 differed with respect to the Ziegler-Natta catalyst system used for the production of the copolymers, their 1-pentene content, MFI and nucleation. The Group 2 copolymers were all produced by the same Ziegler-Natta catalyst system differing only in donor:catalyst ratio and having different 1-pentene contents.

Due to the fact that Polymers A - F have so many different variables playing a role, it is not possible to investigate certain trends. It is however clear from the experimental results that the different analytical techniques used in this study reveal properties that may be attributed to certain of the different variables. In the case of the Group 2 copolymers it is however possible to investigate the influence of the 1-pentene content and the donor:catalyst ratio by looking at certain trends in the analysis results.

Calculations of the comonomer content of Polymers A - F from the ^{13}C-NMR analysis corresponded well with that from FTIR analysis. The 1-pentene content decreases in the following order: Polymer D, A, B, C, E and F. The ^{13}C-NMR analysis results of Polymers G - J shows that the comonomer content decreases in the following order: Polymer G, J, H and I. A decrease in tacticity is seen with this increase in 1-pentene content of the Group 2 copolymers. When comparing the comonomer contents of the two groups, it is furthermore clear that the 1-pentene content of Polymers A - F is in general (except for Polymer F) higher than that of the Group 2 copolymers.

The molecular weight analysis of Group 1 shows that the M_w and PD values of Polymer C are significantly lower than that of the rest of the copolymers of this group. Polymers C and F were produced by the same catalyst, but Polymer C contains approximately twice the amount of comonomer than that of Polymer F. The extremely high MFI obviously leads to a very low molecular weight, as expected. It is unclear from the results whether the much lower polydipersity of Polymer C is caused due to the material being vis-broken or not.

The HT-GPC results of Polymers G - J show a definite increase in the M_n values for the increase in donor:catalyst ratio, as expected according to literature. The polydispersities of both groups are relatively high due to the heterogeneous character of the Ziegler-Natta catalyst systems used for the production of these commercial propylene/1-pentene copolymers. The

polydispersities of Polymers G - J are however lower than those of the Group 1 copolymers which must be caused by the difference in catalyst systems used.

The thermal analysis results of Polymers A - F show in general an increase in T_c, T_m and percentage of crystallinity with an increase in the 1-pentene content, regardless of the catalyst used or the type of nucleation. The percentages of crystallinity of Polymers B and C are however very much the same values, although the 1-pentene content differs with 1 mol %. This may be explained in terms of the different catalysts used for the polymerization of these two copolymers. Furthermore Polymers A, B and D are supposed to be virtually identical according to their similar MFI values, comonomer contents and production by the same catalyst. Yet they show significant differences in thermal properties. The absence of a nucleating agent in Polymer D seems to influence the thermal properties in comparison with the nucleated Polymers A and B.

The CRYSTAF analysis results of Polymers G - J also show a decrease in T_c with the increase in comonomer content a in the case of the Group 1 copolymers. The T_m values are however more or less the same for all the Group 2 copolymers. The DSC results show a very significant decrease in the degree of crystallinity with an increase in the donor:catalyst ratio. From the thermal analysis results of the Group 2 copolymers it can be concluded that the Si:Ti ratio has little or no effect on the crystallization and melting properties of the copolymers and that these properties are rather primarily affected by the amount, and possibly the distribution of the 1-pentene in the copolymers. The possibility also exists that the 1-pentene distribution are influenced by the Si:Ti ratio.

The percentages of soluble fractions (as determined by CRYSTAF) of the Group 2 copolymers are noticeably lower than those of the Group 1 copolymers due to the influence of the different catalyst systems used.

According to literature an increase in γ-phase can be expected with an increase in the 1-pentene content. This trend is observed in the case of the Group 2 copolymers, but not in the case of the Group 1 copolymers. It may be due to different distribution patterns of the comonomer in the two groups.

If the 1-pentene is very much limited to the amorphous parts of the copolymer, then a lower γ-phase will be shown due to the low comonomer content in the crystalline areas. This is an indication that the 1-pentene must be more uniformly distributed in the Group 2 copolymers than in the Group 1 copolymers.

The *o*-positron lifetime distributions from the PALS analyses of Polymers A - F shows bimodal peaks for Polymers A and E and single peaks for the rest of the samples. The bimodal peaks indicate a better defined separation between the crystalline and amorphous phases in the copolymers. The narrowness of the *o*-positron lifetime distribution curves also differ for all the polymers, indicating a difference in the size of the transition between the crystalline and amorphous areas for the different polymers.

Throughout the analysis of the Group 1 copolymers it is clear that the different analytical techniques can be used to point out significant differences in the properties of these copolymers and thereby give an indication of how these differences relate to the original information supplied regarding the catalyst, MFI, nucleation and 1-pentene content of the various copolymers.

The same analytical techniques were therefore used in order to investigate the influence of the 1-pentene content and the donor:catalyst ratio on the series of Group 2 copolymers.

3.5 REFERENCES

1. Turner-Jones, A., Polymer, 1971. **12**: p. 487.
2. Avella, M., Martuscelli, E., Della Volpe, G., Segre, A., Rossi, E., Simonazzi, T., Makromol. Chem., 1986. **187**: p. 1927.
3. Mezghani, K., Phillips, P.J., Polymer, 1995. **36**: p. 2407.
4. Laihonen, S., Gedde, U.W., Werner, P.-E., Matinez-Salazar, J., Polymer, 1997. **38**: p. 361.
5. Laihonen, S., Gedde, U.W., Werner, P.-E., Westdahl, M., Jääskeläinen, P., Matinez-Salazar, J., Polymer, 1997. **38**: p. 371.
6. Zimmerman, H.J., J. Makromol. Sci. Phys., 1993. **B32**: p. 141.

7. Crispino, L., Matuscelli, E., Pracella, M., Makromol. Chem., 1980. **181**: p. 1747.
8. Guidetti, G.P., Busi, P., Giulianelli, I., Zanetti, R., Eur. Polym. J., 1983. **19**: p. 757.
9. Wilberg, G., Werner, P.-E., Gedde, U.W., Mater. Sci. Eng., 1993. **A173**: p. 173.
10. Tincul, I., Joubert, D.J., Potgieter, A.H. in *Polypropylene 99, 8th Annual World Congress*. 1999. Zürich.
11. Tincul, I., Potgieter, A.H. in *Polypropylene 96, 5th Annual World Congress*. 1996. Zürich.
12. Assumption, H., *Principle Scientist, Analytical Technology - NMR, Sasol Technology, R and D*. 2005: Sasolburg.
13. Sacchi, C.M., Forlini, F., Losio, S., Tritto, I., Wahner, U., Tincul, I., Joubert, D.J., Sadiku, E.R., Macromol. Chem. Phys., 2003. **204**: p. 1643.
14. Mogenson, O.E., *Positron Annihilation in Chemistry*. 1995, Berlin: Springer-Verlag. pp. 21, 29, 221.
15. Soga, K., Shiono, T., Doi, Y., Makromol. Chem., 1988. **189**: p. 1531.
16. Karger-Kocsis, J., Kallo, A., Shaftner, A., Bodor, G., Polymer, 1979. **20**: p. 37.
17. D'Orazio, L., Greco, R., Mancarella, C., Martuscelli, E., Ragosta, G., Silvestre, G., Polym. Eng. Sci., 1982. **22**: p. 536.
18. Morini, G., Albizzati, E, Balbontin, G., Mingozzi, I., 1996. **29**: p. 5770.
19. Foresta, T., Piccarolo, S., Goldbeck-Wood, G., Polymer, 2001. **42**: p. 1167.
20. Thomann, R., Semke, H., Maier, R.-D., Thoman, Y., Scherble, J., Mülhaupt, R., Kressler, J., Polymer, 2001. **42**: p. 4597.
21. Hosier, I.L., Alamo, R.G., Esteso, P., Isasi, J.R., Mandelkern, L., Macromolecules, 2003. **36**: p. 5623.
22. Juhász, P., Belina, K., J. Reinf. Plastics and Comp., 2001. **20**: p. 2.
23. De Rosa, C., Auriemma, F., Spera, C., Talarico, G., Gahleiter, M., Polymer, 2004. **45**: p. 5875.
24. De Rosa, C., Auriemma, F., Circelli, T., Waymouth, R.M., Macromolecules, 2002. **35**: p. 3622.

25. Busico, V., Corradini, P., De Rosa, C., Di Benedetto, E., Eur. Polym. J., 1985. **21**: p. 239.
26. Alamo, R.G., Kim., M.-H., Galante, M.J., Isasi, J.R., Mandelkern, L., Macromolecules, 1999. **32**: p. 4050.
27. Auriemma, F., De Rosa, C., Macromolecules, 2002. **35**: p. 9057.
28. Dupasquier, A., Mills, Jr. A.P., *Positron Spectroscopy of Solids.* 1995, Amsterdam: IOS Press.
29. Mogenson, O.E., *Positron Annihilation in Chemistry*. 1995, Berlin: Springer-Verlag.
30. Pethrick, R.A., Progr. Polym. Sci., 1997. **22**: p. 1.
31. Brandt, W., Berko, S., Walker, W.W., Phys. Rev., 1960. **15**: p. 1289.
32. Brandt, W., Fahs, J.H., Phys. Rev. B, 1970. **17**: p. 1425.
33. Tao, S.J., J. Chem. Phys., 1972. **56**: p. 5499.
34. Eldrup, M., Lightbody, D., Sherwood, J.N., Chem. Phys., 1981. **63**: p. 51.
35. Lightbody, D., Sherwood, J.N., Eldrup, M., Chem. Phys., 1985. **93**: p. 475.
36. Dlubek, G., Bamford, D., Henschke, O., Knorr, J., Alam, M.A., Arnold, M., Lüpke, Th., Polymer, 2001. **24**: p. 5381.

CHAPTER 4

Analysis of Solvent Extracts

4.1 INTRODUCTION

The formation of atactic polymer in commercial polymers is a very important concern to industry as this part of the polymer has a very important influence on the physical and optical properties of the polymers [1]. TREF is a well-known fractionation method used to study the make-up of polymers [2-6]. In order to investigate the atactic polymer, analysis of the low molecular weight TREF fraction is, however, not sufficient on its own. Solvent extractions must be used to compensate for this shortcoming. Various solvent extraction methods to isolate the atactic fractions of polypropylene have been reported. Natta [7] reported that fractions with low crystallinity and different melting points can be extracted using different *n*-alkane solvents. Polypropylene has been extracted by Nakajima *et al.* [8] with solvents having different boiling points and it was found that the respective extracts varied with regards to molecular weight and isotacticity. These results suggest that extraction with *n*-alkane solvents leads to tacticity and molecular weight fractionation. Successive extractions of polypropylene with *n*-alkane solvents with different boiling points also confirmed the occurrence of a difference in pentad tacticities of the respective fractions obtained. This, in itself, indicates fractionation based on tacticity [9-11].

In this study the commercial polymers of Group 1 (A - F) were initially extracted with hexane, heptane, xylene and decalin. The analysis results of the Group 1 extracts led to the extraction of the commercial copolymers of Group 2 (G - J) with only hexane, heptane and xylene. The analysis results of the Group 2 extracts then again led to a further, more detailed extraction method: successive extractions [12] of Group 2 copolymers were also carried out using the same three solvents (hexane, heptane and xylene).

The extracted fractions were analyzed mainly by ^{13}C-NMR and HT-GPC.

4.2 EXPERIMENTAL

4.2.1 Extractions of Group 1 Copolymers (A - F)

Group 1 (A - F) propylene/1-pentene copolymers were initially extracted using four different solvents. These solvents, hexane, heptane, xylene and decalin were chosen due to the fact that each of them was reportedly able to extract a different molecular fraction from the copolymers. For extractions with hexane and heptane, a standard Soxhlet method was used and for xylene and decalin, a solution-crystallization process was carried out. The boiling points of each of the solvents are given in Table 4.1.

Table 4.1 Boiling points of different extraction solvents used to extract propylene/1-pentene copolymers

Solvent	Boiling Point (°C)
Hexane	69
Heptane	98
Xylene	140
Decalin	190

The Soxhlet method involved the use of a Soxhlet-type extractor, connected to a 250-ml round bottom flask filled with 200 ml either hexane or heptane. A 28 x 80-mm-sized thimble containing approximately 8 g copolymer pellets covered with a layer of glass wool was fitted into the Soxhlet extractor. The extraction solvent was heated to boiling point and refluxed through the Soxhlet extractor for 8 hours. A reflux condenser was fitted on top of the Soxhlet extractor in order to prevent evaporation of the solvent. The thimble was left inside the fume hood to dry while the solvent was removed directly from the round bottom flask by means of a rotary evaporator in order to isolate the extract.

The content of the flask was weighed and then the sticky extract had to be scraped out. Upon using acetone during the scraping process, it was found that the heptane extract could be separated into an acetone soluble and insoluble fraction, whereas the hexane extract was totally soluble in acetone. These two heptane fractions (acetone soluble and acetone insoluble) were therefore kept apart and analyzed separately. These respective results confirmed the difference in extracts obtained with hexane and heptane.

The solution-crystallization method which was used for xylene and decalin extractions originated from the standard xylene-soluble method (ISO 6427, 1992) which is commonly used in industry to calculate the percentage of xylene-soluble fraction of a polymer. This method was slightly modified in order to suit this project. The interest did not particularly lie in the weight of the xylene soluble fraction, but rather in the composition of the fraction. The copolymer was dissolved in either xylene or decalin by stirring approximately 2.5 g of the specific copolymer in 250 ml xylene at boiling point in a 500-ml round bottom flask fitted with a reflux condenser, for 1 hour. Thereafter the solution was rapidly cooled down in an ice bath for 1 hour and then in a water bath for a further hour. The precipitated polymer was filtered off and the soluble fraction in the filtrate was isolated directly from the round bottom flask by means of a rotary evaporator. Both the filtrate and the extract had a definite yellowish colour. In the case of the decalin extract (as with the heptane extract) the extract was separated into an acetone soluble and acetone insoluble fraction.

The extracts from all the extractions were dried overnight in the fume hood whereafter they were dried in a vacuum oven at 40°C for a further 8 hours. Extracts were analyzed with ^{13}C-NMR and HT-GPC.

4.2.2 Extractions of Group 2 Copolymers (G - J)

The analysis results of the Group 1 copolymer extracts led to extracting Group 2 (G - J) propylene/1-pentene copolymers with only hexane, heptane and xylene, and not decalin. The same procedures as with Group 1 were used except that the heptane extracts were not divided into soluble and insoluble fractions. They were combined as one fraction, a combination of acetone soluble and non-soluble material.

Again all the extracts were analyzed by means of ^{13}C-NMR and HT-GPC. The poor signal to noise ratio from the ^{13}C-NMR spectra of the Group 1 extracts made it impossible to have a clear view of the low intensity peaks. In order to achieve a better signal to noise ratio for the ^{13}C-NMR spectra of the Group 2 extracts a higher pulse (> 4000) was used. According to the analysis results (Section 4.3) this improvement was still clearly not sufficient for a thorough investigation into the composition of the extracts. Another problem was the fact that when using pellets in the Soxhlet extraction process, no quantitative conclusions could be made. In this process only the surface of the pellets were exposed to the solvent and therefore extracted. It has been reported [13] that grinding the pellets before extraction could solve this problem, but this could lead to a change in molecular weight and degradation.

4.2.3 Successive Extractions of Group 2 Copolymers (G - J)

In order to further separate the low molecular weight material of the copolymers of Group 2, further successive extractions were carried out on them. The successive extraction process that was used is demonstrated in Figure 4.1.

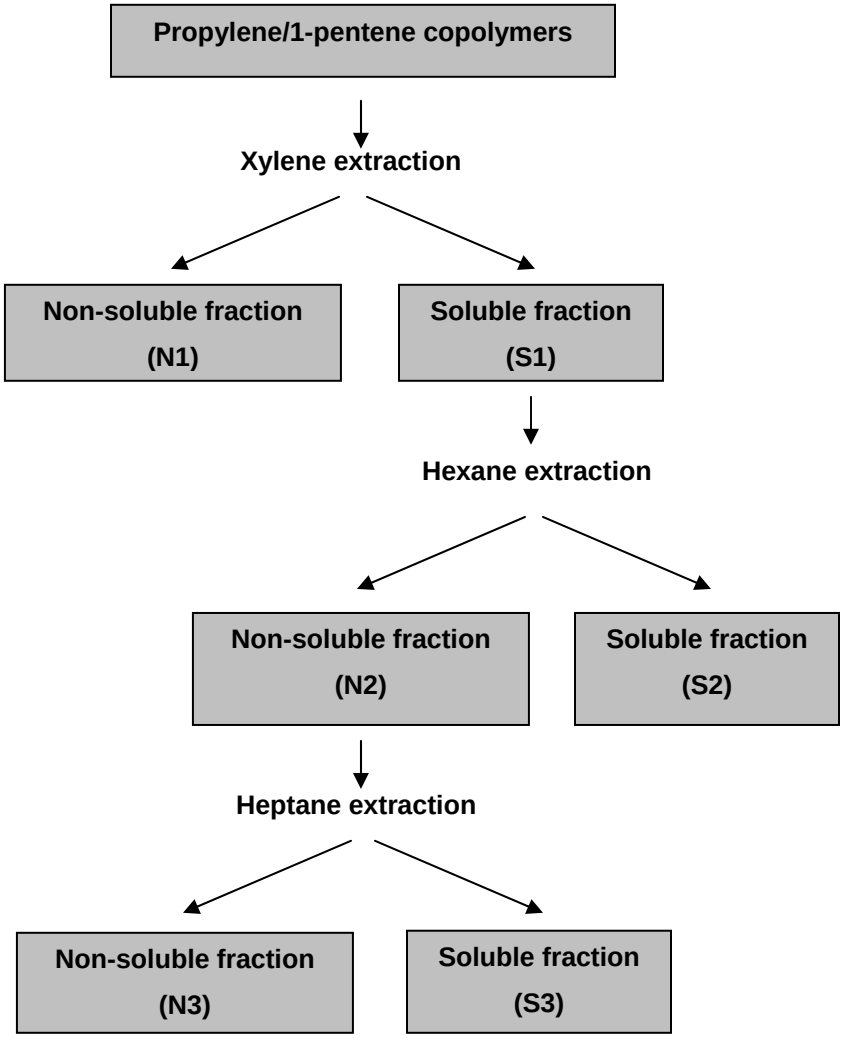

Figure 4.1 Scheme of successive fractionation of propylene/1-pentene copolymers with xylene, hexane and heptane

The propylene/1-pentene copolymers were extracted with xylene during the first step by means of the solution-crystallization method, as described in Section 4.2.1. After the isolation of the xylene soluble fraction (S1), it was then extracted further with hexane using the Soxhlet method, also described in Section 4.2.1. This step separated the xylene soluble fraction into a hexane soluble fraction (S2) and a hexane non-soluble fraction (N2). The N2 fraction was kept inside the thimble and during the last step of the successive extraction process it was extracted with heptane. HT-GPC and ^{13}C-NMR analyses were

carried out on fractions N1, S1, S2, N3 and S3. DSC and WAXD analyses were also carried out on fraction N1 in order to compare the properties of the xylene non-soluble material with that of the original copolymers.

4.2.4 Quantitative analysis

In a separate experiment the industrial xylene-soluble method was used in order to carry out a quantitative evaluation on the Group 1 and 2 copolymers. The most important difference between this standard industrial procedure and the method used for this project is that the experiment is done quantitatively. The % xylene-solubles (XL) was then determined by the use of the following equation:

$$XL = [(M3 - M2) \times 500 \times 100] / [M1 \times V]$$

XL: % xylene-solubles
M1: mass of pellets
M2: empty round bottom flask
M3: round bottom flask with sample
V: aliquot part of sample

4.2.5 ^{13}C-NMR analysis

For the ^{13}C-NMR analysis of Group 1 copolymer extracts, broadband proton decoupled ^{13}C synthesis were conducted at 5.42 MHz, using a Varian VXR 300 NMR spectrometer. A pulse angle of 45° and a relatively short repetition time of 0.82 seconds were used together with accumulating less than 3 000 transients for each sample. The number of transients were increased to above 4 000 at a later stage in order to improve the sensitivity of the collected data. Resolution and accuracy were improved by zero-filling the data once before performing the Fourier transformation. Baseline correction was also

applied in order to further enhance the accuracy and repeatability of the integrals measured for selected peaks in the spectra. Samples (~ 60 mg) were dissolved at 120°C in a mixture of 1,2,4-trichlorobenzene and benzene-d_6 (9:1 volume ratio). The analyses of these samples were executed at 120°C.

For the high temperature ^{13}C-NMR analyses of Group 2 copolymers the spectra of the successive extracts were recorded on a 600 MHz Varian ^{Unity}*Inova* by the same method as described earlier in Section 3.2.2. The analyses of these samples were done at 100°C.

4.2.6 HT-GPC analysis

HT-GPC analyses for the samples were carried out using the same method as described in Section 3.2.

4.2.7 DSC analysis

Thermal analysis by DSC was carried out on the xylene non-soluble (XNS) material which remained after extracting the original Group 1 and 2 copolymers with xylene as well as on the XNS material after slow cooling. The calorimetric measurements of these samples were performed with a TA Instruments Q100 RCS DSC system in the same way as described in Section 3.2.5.

The original polymers as well as XNS samples were first subjected to a heating ramp up to 220°C and kept isothermally at that temperature for 5 min in order to remove any thermal history. The cooling cycle for crystallization then followed, with the subsequent heating scan being recorded for analysis. Both the cooling cycle and the last heating cycle were carried out at a standard rate of 10°C/min. For the slow cooled samples, however, both the heating stages as well as the cooling stage were carried out at the standard rate of 10°C/min and the data for all three stages were collected for analysis purposes.

4.2.8 WAXD analysis

The samples to be analyzed by WAXD were prepared and analyzed in the same way as described in Section 3.2.6.

4.2.9 Positron annihilation lifetime spectroscopy

PALS analysis was carried out on the XNS fractions of Polymers A - F. The preparation of the samples as well as the analysis method were the same as described in Section 3.2.7.

4.3 RESULTS AND DISCUSSION

4.3.1 Group 1 (A - F)

4.3.1.1 Quantitative analysis

Quantitative analyses were carried out on Group 1 copolymers in order to determine the percentage of xylene-solubles in each copolymer. Extractions for these analyses were carried out only once in order to have a rough estimate of the amount of material being extracted with from these copolymers.

Table 4.2 shows the percentages of xylene-solubles for the Group 1 copolymers as well as their molecular weights, polydispersities, comonomer contents and detail about the catalysts used for production. The % XL values of the Group 1 copolymers vary between 1.8 - 7.2% which are in general quite low.

Polymers A - D have higher percentages of xylene-solubles compared to those of Polymers E and F. Polymer C has the highest % XL which may be due to the fact that the M_w and PD of this copolymer are significantly lower than that of the rest of the Group 1 copolymers. When comparing Polymers A and B,

which were produced with the same catalyst system and have more or less the same M_w's, it is clear that the lower PD of Polymer B might be the reason for the lower % XL for Polymer B. In the case of Polymers D and F, they have more or less the same M_w and PD values. The lower % XL for Polymer F must therefore result from the different catalyst used to produce Polymer F. From the above it is therefore clear that the M_w, PD and type of catalyst used to produce the polymer must play a definite role in the percentage of xylene-solubles of a specific polymer. This is in keeping with the findings of the initial analyses of the original materials (Section 3.3.2).

Table 4.2 Percentage of xylene-solubles in Polymers A - F

Sample	Catalyst used	M_w (g/mol)	PD	XL (%)	1-Pentene content (mol %)
A	1	567 000	7.09	5.48	3.41
B	1	562 900	6.69	4.58	3.09
C	2	208 800	3.86	7.12	2.09
D	1	592 000	7.10	3.44	3.50
E	1	557 000	6.94	2.01	2.03
F	2	584 100	7.07	1.88	1.21

There appears to be the same relationship between the 1-pentene content and the % XL as well; with the exception being sample C, where the molecular weight seems to the overriding factor. If this value is ignored, then the only copolymer that falls outside of the trend is Polymer D. This material seems to have much lower extractable than should be the case when looking at 1-pentene content. The question arises here whether this could be due to the absence of nucleating agents.

4.3.1.2 ^{13}C-NMR

The ^{13}C-NMR results of the extracts of Group 1 copolymers are shown in Figures 4.2 - 4.5 and Figures 4.7 - 4.11. Figures 4.2 - 4.4 show the ^{13}C-NMR spectra of the extracts due to the different solvents used for extracting Polymer C, whereas Figures 4.5 - 4.10 compare the results for a specific solvent used in extracting the six copolymers (A - F), respectively. From Figures 4.2 - 4.4 it is clear that the differences in the spectra confirm the difference in extracts obtained with the various solvents.

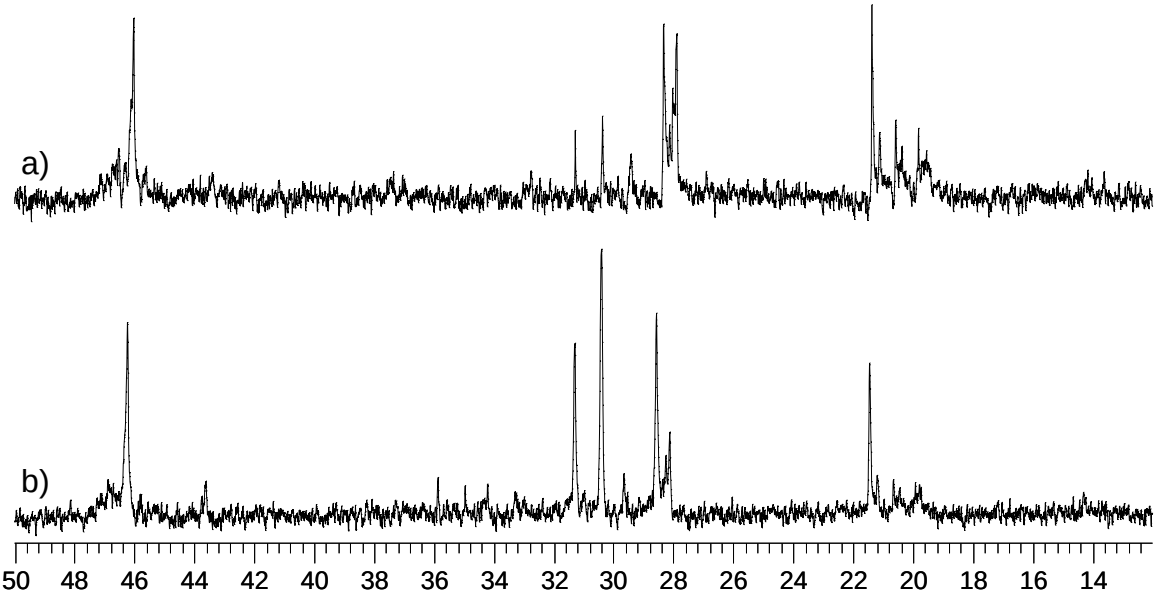

Figure 4.2 a) Hexane extract and b) xylene extract of Polymer C

Figure 4.2 compares the ^{13}C-NMR spectra of the a) hexane extract and b) xylene extract of Polymer C. The three major peaks appearing in the spectra represent the carbons of propylene: the methine carbon at 28.5 ppm, the methyl carbon at 21.4 ppm and the methylene carbon at 46.4 ppm. When taking a close look at the resonance signal of the methyl carbon ($\delta \approx 21.4$ ppm) from the propylene, the high-intensity shoulder peaks (19.2 - 21.3 ppm) are due to

stereoirregularities and indicate a highly atactic fraction. This is confirmed by the many shoulder peaks on the methylene resonance ($\delta \approx 46.4$ ppm) as well. The spectra of the xylene and the hexane extracts look very much alike for most of the spectra except for a few “extra” smaller resonances appearing in the spectrum of the xylene extract as well as a difference in intensities of the similar peaks in the two spectra. The intensity of the shoulder peaks on the methyl carbon is higher for the hexane extract than for the xylene extract. This indicates that the hexane extract consists of more atactic material than the xylene extract. The methine resonance ($\delta \approx 28.5$ ppm) in the hexane extract also has a shoulder peak on the right hand side ($\delta \approx 28.1$ ppm), with extremely high intensity, compared to that of the same shoulder peak in the case of the xylene extract. This confirms the much lower tacticity of the hexane extract. It is therefore clear that xylene and hexane extract atactic material, but xylene extracts a more complex fraction than hexane does. The three significant peaks appearing between 29 and 32 ppm (Figure 4.3) and other smaller ones in the spectra will be discussed at a later stage.

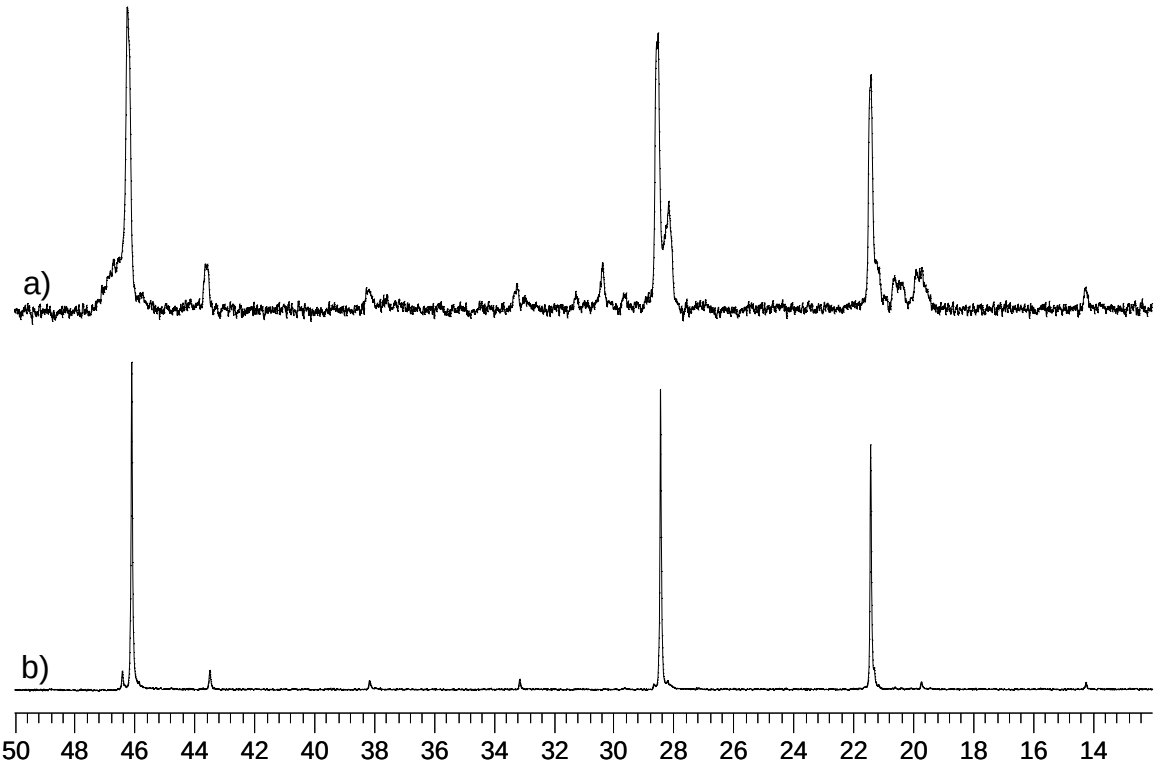

Figure 4.3 a) Heptane extract (acetone soluble) and b) heptane extract (acetone non-soluble) of Polymer C

Figure 4.3 shows the ^{13}C-NMR spectra of the heptane extract of Polymer C which was separated into a) an acetone soluble fraction and b) an acetone non-soluble fraction. The fraction from a) has a very low tacticity when compared to the highly isotactic fraction from b) which is not soluble in acetone. The fact that the whole of the hexane extract was soluble in acetone and the heptane extract only partly dissolved in acetone not only indicates that fractions with different molecular structures are extracted by the two solvents, but suggests that hexane extracts atactic material only and heptane is able to extract some atactic material as well as some isotactic fraction. This suggestion was confirmed at a later stage (Section 4.3.3).

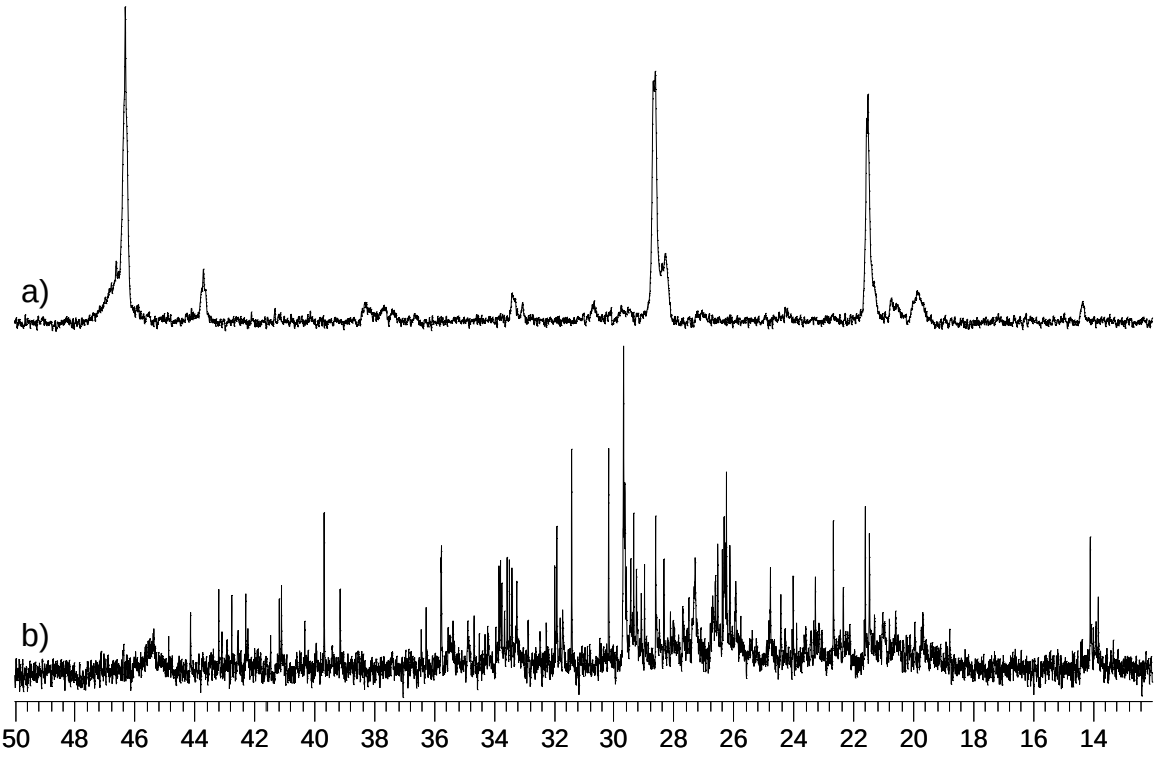

Figure 4.4 a) Decalin extract (acetone non-soluble) and b) decalin extract (acetone soluble) of Polymer C

Figure 4.4 shows the decalin extract of Polymer C after separation into two fractions: a) acetone non-soluble and b) acetone soluble. According to the spectra the two fractions from the decalin extract differ greatly in their molecular composition. In the ^{13}C-NMR spectrum of the non-soluble fraction we can clearly distinguish the different peaks from the propylene carbons as well as those from the 1-pentene carbons. Shoulder peaks on the methyl peak indicate stereoirregularities. The spectrum of the acetone soluble sample however looks extremely complex. Decalin has a very high boiling point (190°C) and the variety of peaks from the spectrum in Figure 4.4 b) might be due to products arising from degradation of the copolymers at such a high temperature, but this is very unlikely. The question therefore arises whether we fully understand the way the material dissolves and crystallizes in decalin. It appears that these questions regarding the solution and crystallization mechanism in decalin may well be the

cause of a flaw in the experimental method. The result can be seen in the complex spectrum in Figure 4.4 b). Similar complex spectra were also seen for the decalin extracts of all the other copolymers. Due to this uncertainty and the difficult process involved in removing all the decalin from the extract no further studies or analyses were carried out with decalin as extraction solvent. Xylene, hexane and heptane were found to be sufficient as extraction solvents.

Table 4.3 shows the different percentages of comonomer content of the original commercial copolymers from Group 1 as well as of the xylene non-soluble (XNS) fractions of the Group 1 copolymers.

Table 4.3 Comonomer contents of the original Polymers A - F and of their XNS fractions

Sample	1-Pentene content (mol% from NMR)	1-Pentene content of XNS fraction (mol% from NMR)
A	3.41	2.40
B	3.09	3.13
C	2.09	2.71
D	3.50	2.70
E	2.03	2.04
F	1.21	1.51

Polymers A and D had the highest 1-pentene content before xylene extraction and both of these polymers lost a significant amount of 1-pentene after extraction. The xylene extracts of these two copolymers must therefore have contained a relatively large quantity of comonomer. The comonomer contents of Polymers B and E remained almost the same, which indicates that the extracts had roughly the same amount of 1-pentene incorporated into the XS fractions. The 1-pentene content of Polymers C and F however increased after extraction with xylene which means that the XS fractions must have contained very little or no comonomer.

This is a clear indication that the difference between two seemingly similar copolymers (Polymers A and B) with regard to the xylene solubles must lie in the distribution of the 1-pentene in the copolymer. On the other hand, Polymer D, which is similar to Polymer A, except for the absence of a nucleating agent, has lower extracts appearing to lose a significant amount of 1-pentene in the extractable fraction.

It is clear from these results that most of the 1-pentene in the higher comonomer content material must be located in the amorphous and low M_w fraction. This implies that these samples do not have a uniform CCD. The results therefore show that the lower the initial 1-pentene content is, the more uniformly must the 1-pentene distribution be in order to see this increase after extraction of the low molecular weight material. Polymers C and F were produced by a different catalyst than the rest of the Group 1 copolymers and this may also have played a role in the non-uniform CCD of these two polymers.

The ^{13}C-NMR spectrum in Figure 4.5 represents the methyl region of the propylene methyl resonance of the xylene extract of Polymer A between 19 and 22 ppm. The methyl resonance of the xylene extract is split into various major peaks, which correspond to the steric pentads from Figure 4.6. One of the 1-pentene methylene carbon peaks appears at 19.7 ppm, but cannot be seen from the spectrum in Figure 4.5 due to overlapping with the *mrrr* pentad resonance of the propylene methyl carbon.

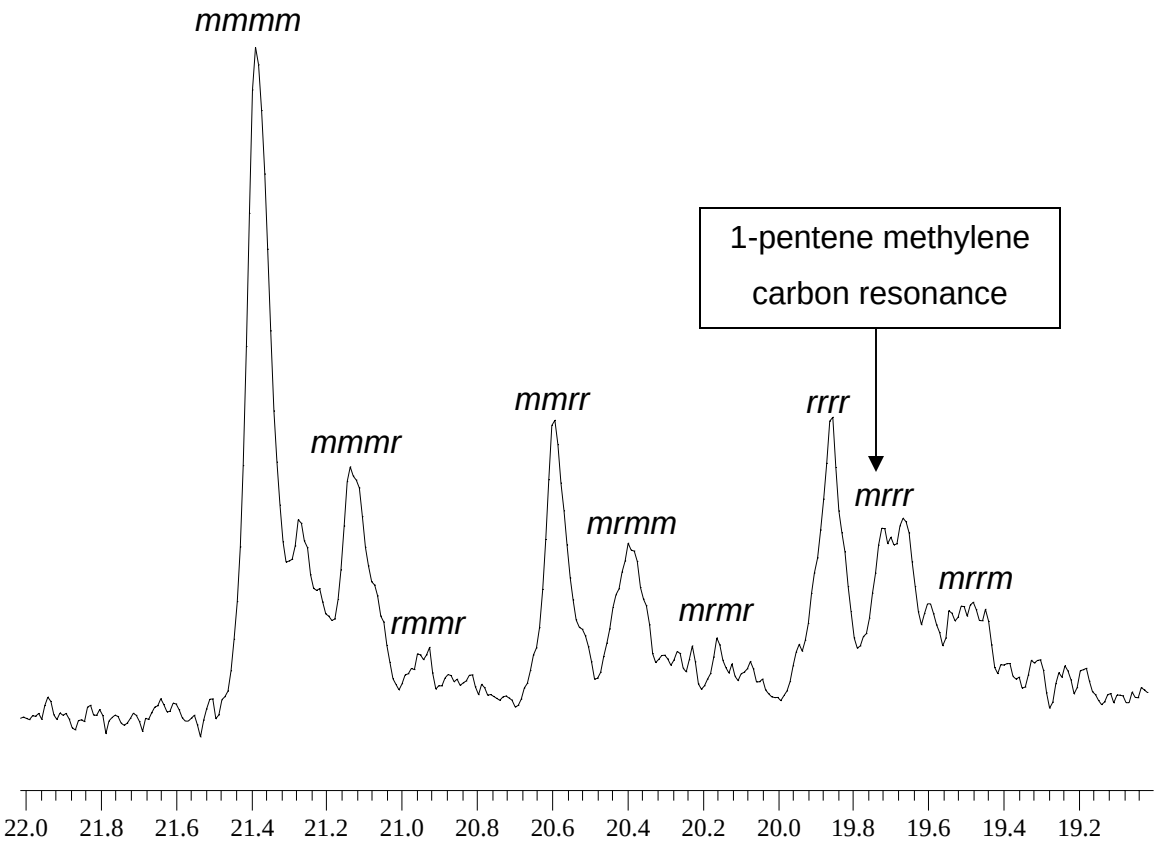

Figure 4.5 Methyl region of xylene extract of Polymer G

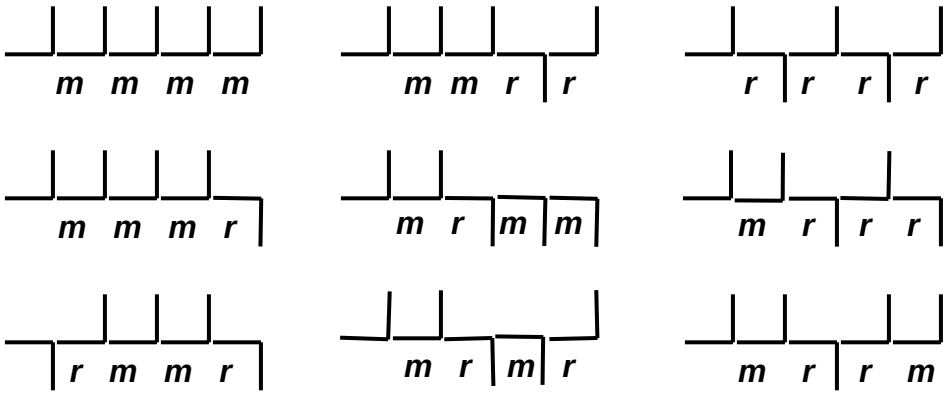

Figure 4. 6 Steric pentads of the methyl region

Figure 4.7 shows the comparisons between the ^{13}C-NMR spectra of the xylene extracts of Polymers A - F. From these spectra it is clear that there are some propylene resonance peaks (a) with stereoirregularities (b) visible in all the spectra. From the difference in intensities of the shoulder peaks of the methyl and methine resonances it can be concluded that the tacticities of these samples differed. The xylene extract of Polymer F had the lowest tacticity by far, followed by that of Polymer E, followed by the others. It is however difficult to distinguish between the degree of tacticity of the other extracts without carrying out any qualitative calculations. As explained in Section 3.2.2 the qualitative calculation of the percentage of tacticity is however not possible due to the overlapping of one of the 1-pentene peaks with one of the stereoirregular pentads from the methyl peak. It must be pointed out that tacticity does not necessarily correspond directly with the 1-pentene content. The amount of extracts of Polymer F is quite low (1.88%) and seems to be comprised mainly of atactic PP. Very little copolymer seems to be present.

Peaks appearing at (d) - (f) will be discussed at a later stage.

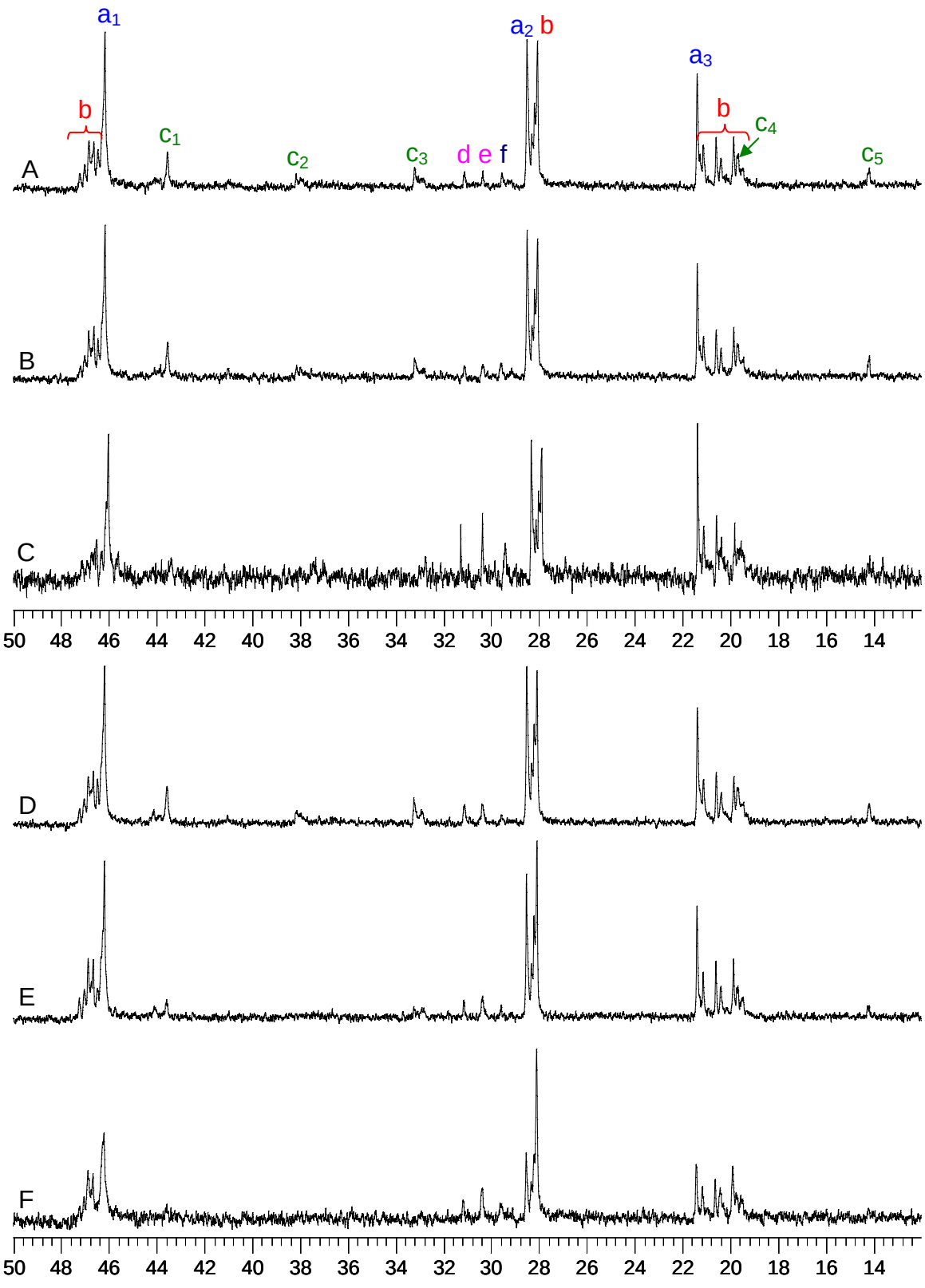

Figure 4.7 ^{13}C-NMR spectra of xylene extracts of Polymers A - F

Figure 4.8 shows the ^{13}C-NMR spectra of the xylene extract of Polymer A as well as of the original random copolymer (Polymer A). The dashed arrow indicates the position of the 1-pentene peak which overlaps with the *mmmr* pentad of the propylene methyl resonance.

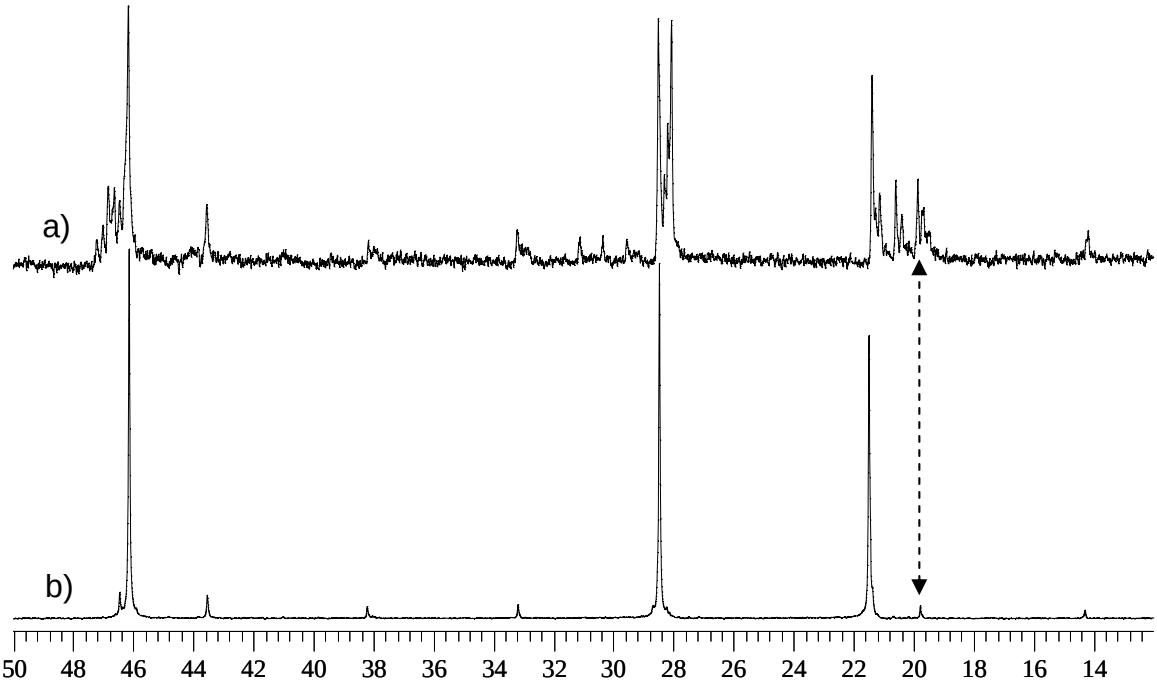

Figure 4.8 ^{13}C-NMR spectra of a) the xylene extract of Polymer A and b) the original commercial Polymer A

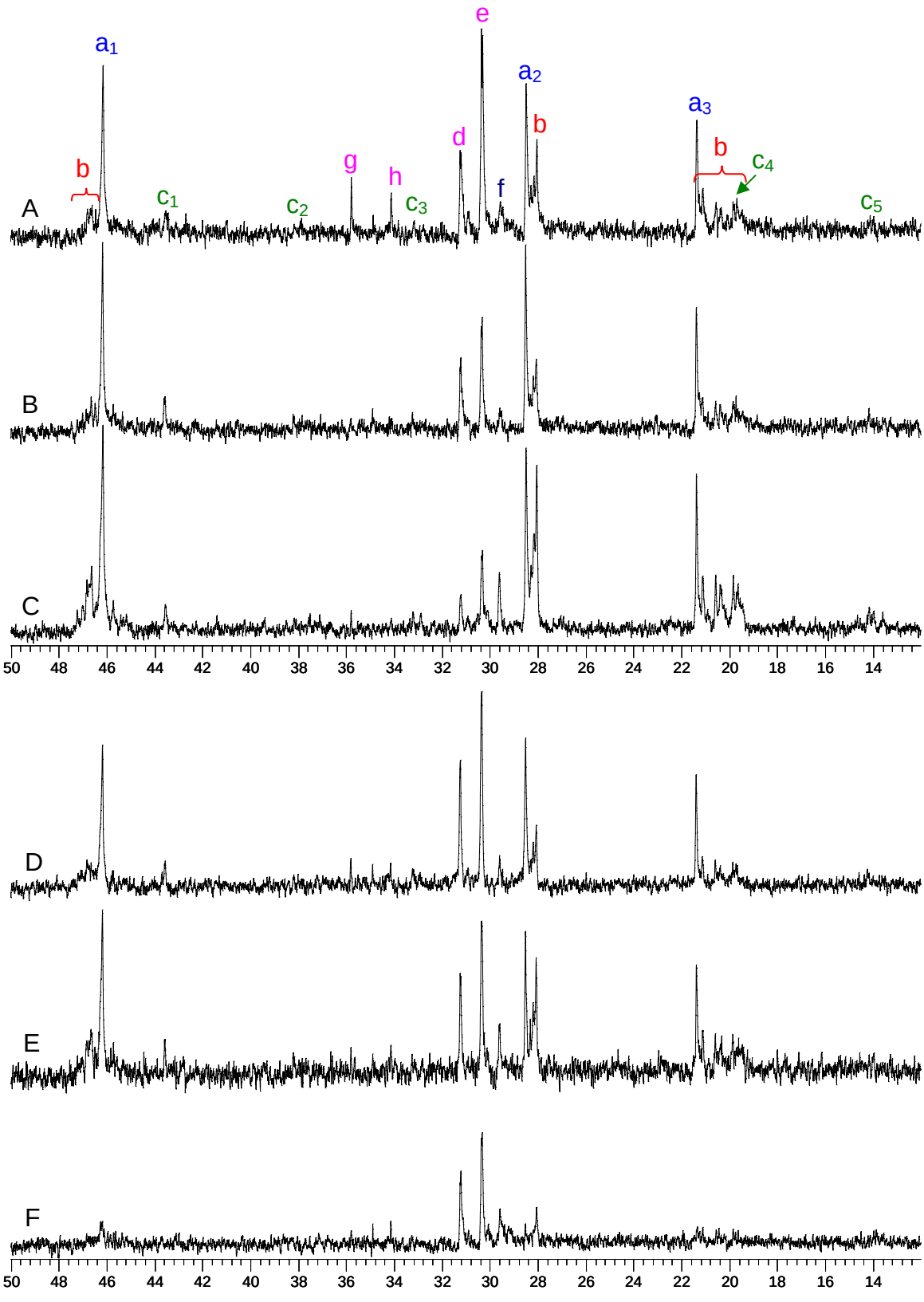

Figure 4.9 ^{13}C-NMR spectra of hexane extracts of Polymers A - F

Figure 4.9 shows the ^{13}C-NMR results of the hexane extracts of Polymers A - F. As with the spectra in Figure 4.7 the following are clear: the main propylene peaks indicated by (a), with their stereoirregular sequences (b), as well as the 1-pentene peaks indicated by (c). The exception is the hexane extract of Polymer F where the propylene peaks are only barely visible. All the 1-pentene peaks in the various spectra of the hexane extracts are unfortunately not very clearly visible due to the noisy baseline. By looking at the methine peaks of the extracts together with the intensities of their shoulder peaks, in order to compare the tacticities of the samples, we can conclude that the extract of Polymer F has the lowest tacticity, followed by the extracts of Polymers C and E, and then Polymer A, with the extracts of Polymers B and D having the highest tacticity.

The three peaks indicated as (d) - (f) were also present in the spectra of the xylene extracts (Figure 4.7). Their intensities here in the spectra of the hexane extracts were however much higher. Two additional peaks, (g) and (h), which did not show up in the spectra of the xylene extracts, are now visible in the spectra of the hexane extracts.

Most heterogeneous ZN catalysts are highly regioselective in propene insertion and the ^{13}C-NMR spectra of these polymers usually give no evidence of regioerrors, which means that their concentration is below 0.1 mol% [14]. The chance of peaks appearing due to 2,1- or 3,1-misinsertions can therefore be ruled out. According to literature [15-19] when H_2 is used as transfer agent, as in the case with the commercial copolymers studied, mostly propyl, *iso*-butyl and butyl end groups are detected by ^{13}C-NMR. The amount of butyl end groups also often exceeds that of the *iso*-butyl ones. In addition, there may also be some 1-pentene end groups in the propylene/1-pentene copolymers.

This information as well as ^{13}C-NMR predictions, using ACD labs software, is used in order to identify the peaks appearing at (d) - (h). Figure 4.10 illustrates the assignment of the peaks of the propylene/1-pentene copolymer chains with the various possible end groups, as discussed above. The peak indicated by (f) is to be due to the two branching carbons in the main chain on both the sides of the 1-pentene side chain. Peaks appearing at (d) and (e) are

caused mainly by *n*-propyl end groups. The peak appearing at (e) however shows a much higher intensity than the one appearing at (d). This is because one side of the polymer chain will always contain a standard *n*-propyl end group and the branching carbon thereof appears with the same resonance as that at (e). The increased intensity of the peak at (e) is further also be attributed by the branching carbon of an *iso*-pentyl end group. The two peaks at (g) and (h) are assigned to one of the carbons in the standard *n*-propyl end group and one of the carbons in the *n*-propyl end group on the other side of the chain respectively, as illustrated in Figure 4.10.

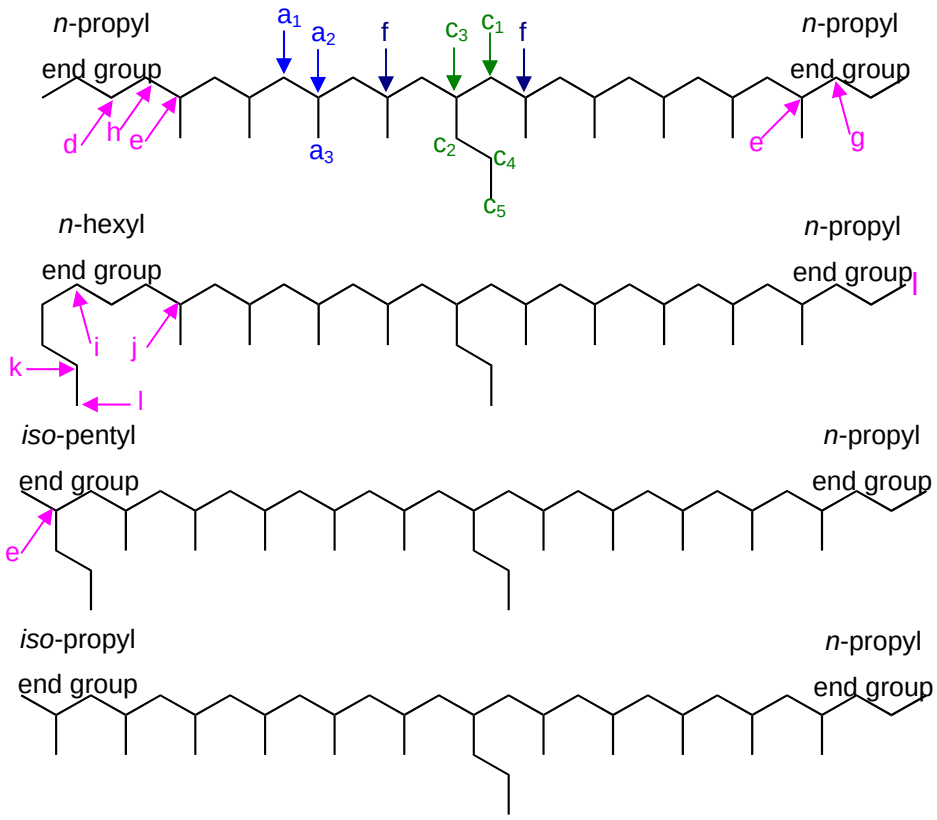

Figure 4.10 Illustration of propylene/1-pentene copolymers with possible end groups

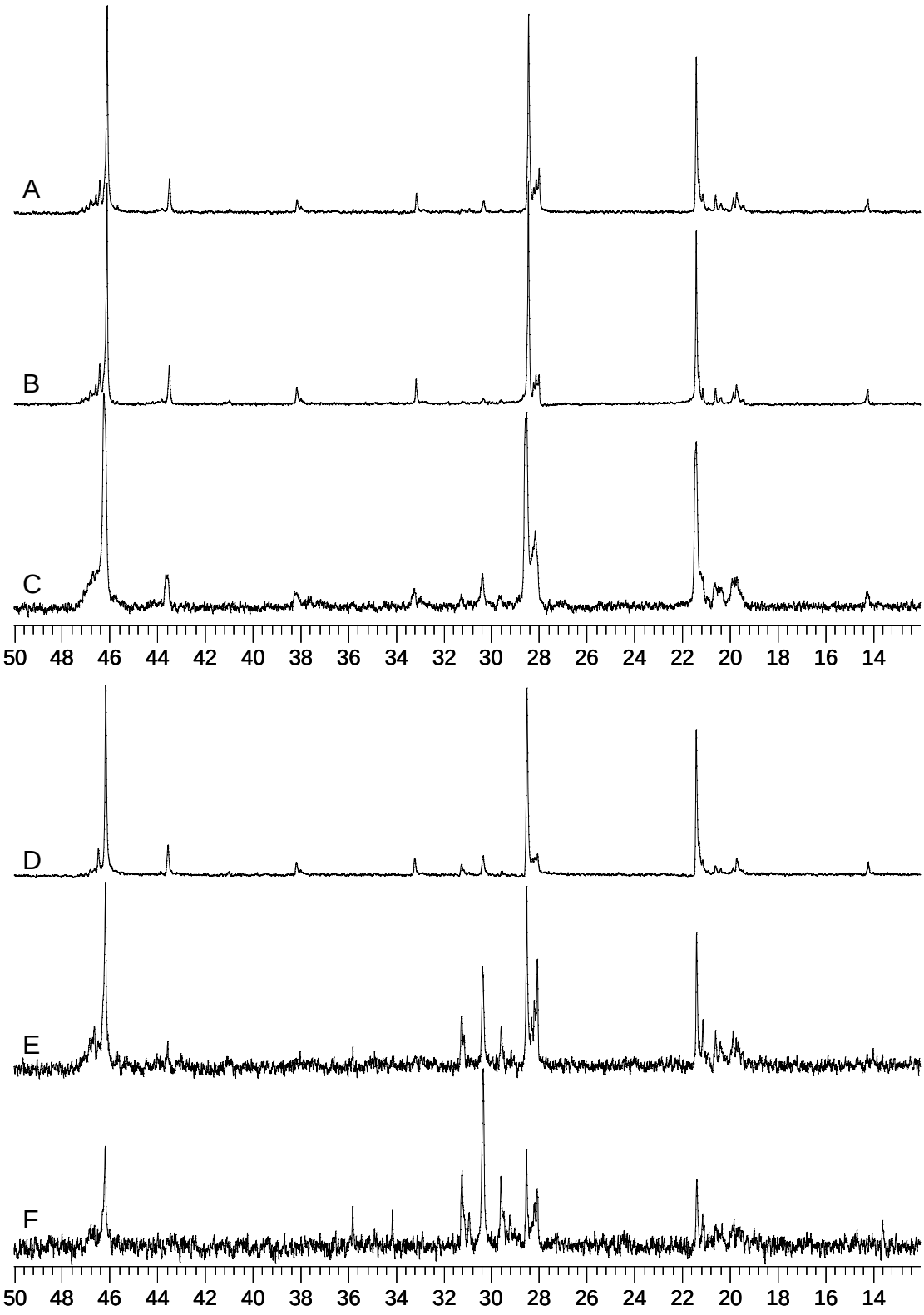

Figure 4.11 ^{13}C-NMR spectra of heptane extracts (acetone soluble fractions) of Polymers A - F

Figure 4.11 shows the spectra of the acetone soluble fractions of the heptane extracts of Polymers A - F. These spectra clearly show the propylene resonance peaks with their stereoirregular sequences as with the xylene and hexane extracts. The 1-pentene peaks are also clearly visible except in the spectrum of the extract of Polymer F. This is due to low comonomer content in this sample as well as a noisy baseline. The three minor peaks which appeared, due to end groups, in the spectra of the xylene and hexane extracts (d) - (f) are visible to some extent in all the spectra of the samples. In the spectra of the extracts of Polymers A, B, C and D, the intensity of these peaks is very low, but the peak arising at (e) can clearly be seen. This peak represents the resonances of two or more carbons (branching carbons in *iso*-pentyl, *n*-propyl standard end group or *n*-propyl end group on the other side of the chain) as discussed earlier. The intensities of the three peaks appearing at (d) - (f) are very high for extracts of Polymers E and F. End group peaks appearing at (g) and (h) can also be recognized in these two spectra. The end groups must therefore be present in very high concentrations in the extracts of Polymers E and F compared to the other four copolymers, which predict a low M_w for these extracts. The spectra of these six samples also indicate that the heptane extracts of Polymers E and F have much lower tacticity than Polymers A, B, C and D.

4.3.1.3 HT-GPC

Figure 4.12 illustrates the different HT-GPC curves of the various solvent extracts of Polymer C. The curves were normalized before overlapping. The heptane extract, which was insoluble in acetone, was the only sample to show a single, smooth curve. This indicates that the material consists of material with the same type of molecular structure, possibly low molecular weight isotactic chains. The other samples (xylene, heptane soluble and hexane extracts) showed three overlapping peaks appearing, (a), (b) and (c), all showing different intensities for the various extracts. Peak (a) in the curve of the xylene extract

shows higher intensity compared to the two smaller peaks on the right hand side. Peak (a) appears at almost the same retention time as that of the heptane (acetone insoluble) extract and it is therefore to be expected that the xylene extract consists of mainly the same type of material as the heptane (acetone insoluble) extract. A shift in the peak marked by (a) can also be observed for the various extract curves. The peak appearing at (c) shows highest intensity in the hexane extract curve and the lowest for the xylene extract curve.

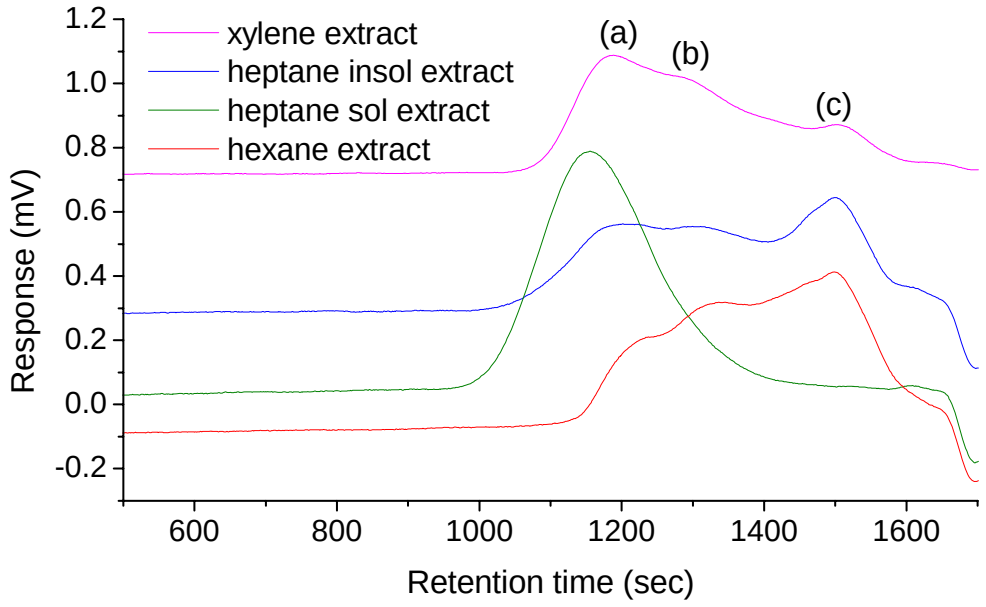

Figure 4.12 Normalized HT-GPC curves of solvent extracts of Polymer C

Table 4.4 shows the molecular weight and polydispersity results of all the material extracted by the different solvents from the Group 1 copolymers.

Table 4.4 HT-GPC results of the different extracts of Polymers A - F

Sample	M_n (g/mol)	M_w (g/mol)	PD
Xylene extracts			
A	5 800	37 700	6.49
B	-	-	-
C	3 100	34 900	11.1
D	4 700	53 400	11.4
E	3 100	53 200	17.2
F	1 600	32 100	19.8
Hexane extracts			
A	4 300	20 500	4.82
B	3 200	15 300	4.77
C	1 200	10 900	8.9
D	3 600	16 500	4.5
E	900	10 300	11.2
F	900	6 700	7.8
Heptane extracts (acetone non-sol)			
A	30 800	148 900	4.84
B	32 900	183 300	5.56
C	30 000	115 500	3.9
D	31 400	128 400	4.1
E	29 900	169 600	5.7
F	1 000	4 800	4.7
Heptane extracts (acetone soluble)			
A	6 700	53 700	8.01
B	5 900	50 800	8.65
C	4 200	41 900	10.1
D	7 400	83 100	11.2
E	2 900	22 500	7.8
F	700	7 600	10.6

Figure 4.13 shows a visual three dimensional presentation of the HT-GPC results of the extracts of Polymers A - F.

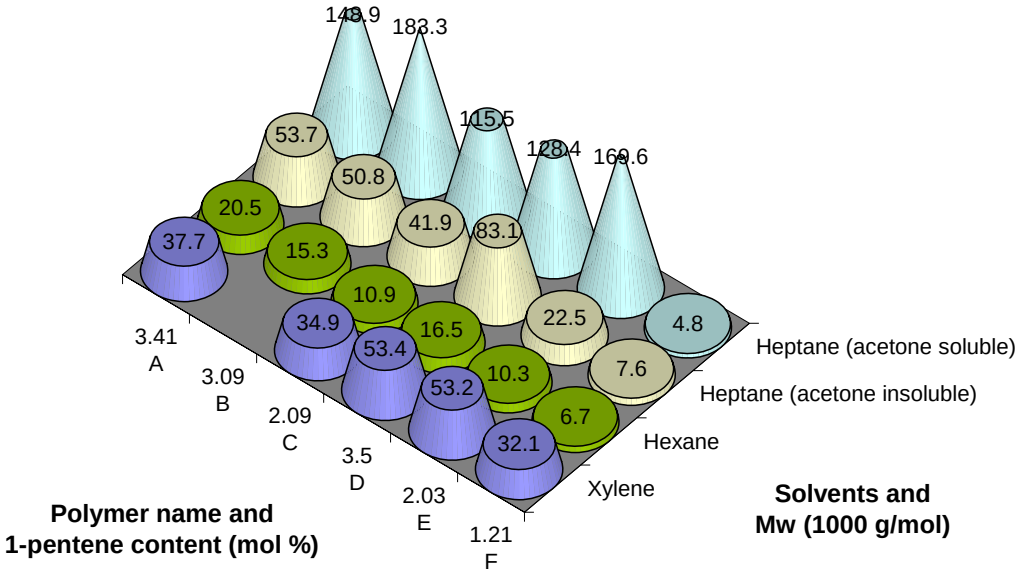

Figure 4.13 Visual representation of the M_w results of the different extracts of Polymers A - F

The polydispersities and molecular weights of the xylene extracts are much higher than those of the hexane extracts. The relatively low molecular weights of the hexane extracts appear to be typical of atactic fractions. It is also interesting to note that copolymer F has by far the highest polydispersity of the xylene extracts and copolymer E for the hexane extracts. This is the result of a very heterogeneous atactic fraction. Polymer F again has the lowest molecular weight by far for all the extracts. This extract therefore must consist of a variety of very short chains. These results correspond very well with those seen in the various NMR spectra discussed in the previous section. The high polydispersity of the xylene extracts reflects that of a more complex material than any of the other solvent extracts. This may be due to a combination of atactic material as well as a variety of different low and higher molecular weight isotactic chains.

The polydispersities of the acetone soluble fractions from the heptane extracts are all much higher than those for the acetone non-soluble fractions.

The molecular weights are however generally much higher for the non-soluble fractions. This information strengthens the suggestion that heptane extracts atactic material (acetone soluble fraction) as well as low molecular weight isotactic material (acetone non-soluble fraction).

Table 4.5 shows the molecular weight and polydispersity results of the copolymers from Group 1 as well as of their XNS fractions.

Table 4.5 HT-GPC results of Polymers A - F before and after extraction with xylene

Sample	M_n (g/mol)	XNS M_n (g/mol)	M_w (g/mol)	XNS M_w (g/mol)	PD	XNS PD
A	74 500	162 300	596 200	881 400	8.01	5.43
B	78 000	168 100	626 500	958 000	8.03	5.70
C	54 000	102 600	208 800	373 600	3.86	3.64
D	78 800	142 400	584 400	853 500	7.41	5.99
E	80 200	161 900	557 000	909 100	6.94	5.62
F	82 600	137 900	584 100	944 000	7.07	6.84

There is a large increase in the molecular weight of all the samples after extraction with xylene. This result seems not to make sense when reasoning that the largest molecules cannot increase in size. The M_w values are however averages. Xylene removes a significant amount of low molecular weight material from the commercial copolymers during these extractions. When this low molecular weight material is removed, there is a change in the average calculated value. This change is towards a higher M_w value since the effect of the low M_w material is removed from the calculation. The much smaller polydispersities of the copolymers after xylene extraction also implies that the XNS fractions have a more homogeneous chain distribution due to the removal of heterogeneous chains of low molecular weight material.

4.3.1.4 Thermal analysis

Table 4.6 shows the thermal analysis results acquired by DSC of the original copolymers of Group 1 as well as of their high molecular weight XNS fractions. The table also shows the comonomer contents for the various commercial copolymers and their XNS fractions as determined by ^{13}C-NMR analysis. Polymers A and D experience a significant decrease in the average percentage of 1-pentene content after extraction with xylene. As discussed earlier in Section 4.3.1.2 this is due to the non-uniform CCD's of these copolymers. This leads to a slight increase in the T_c of both polymers as well as a somewhat greater increase in the T_m values, as expected. An increase in the percentage of crystallinity after extraction with xylene is also expected, as happened in the case of Polymers B - E. There is however a slight decrease in the crystallinity percentage for Polymers A and F. This indicates that some of the material extracted by xylene is crystallizable.

Table 4.6 DSC results of Group 1 copolymers and their XNS fractions

Sample	1-pent (mol%)	XNS 1-pent (mol%)	T_c (°C)	XNS T_c (°C)	T_m (°C)	XNS T_m (°C)	Crystal-linity (%)	XNS Crystal-linity (%)
A	3.41	2.40	101.68	103.00	142.66	145.93	72.92	66.41
B	3.09	3.13	117.72	102.24	145.51	142.90	66.27	69.90
C	2.09	2.71	119.39	103.00	147.22	145.01	66.17	68.66
D	3.50	2.70	97.44	99.06	138.90	142.18	59.28	69.62
E	2.03	2.04	120.12	103.45	148.26	146.11	68.95	72.34
F	1.21	1.51	123.75	109.52	154.23	152.97	79.57	77.85

Calculations from the ^{13}C-NMR analysis data of Polymers B, C and F indicate an increase in 1-pentene content after extraction with xylene. These three copolymers show a large decrease in their T_c values with their increase in comonomer content and removal of the xylene soluble fraction, as expected. The also expected decrease in T_m for these three samples is however much smaller. Although an increase in comonomer content would generally lead to a

decrease in the percentage of crystallinity, there is an increase in the crystallinity percentage of Polymers B and C and a small decrease in the case of Polymer F. The increase is due to the removal of an amorphous or less crystallizable fraction of the copolymers by extracting with xylene. In the case of Polymer F the effect of an increase in 1-pentene content overrules that of the removal of the XS fraction and that causes a slight decrease in percentage of crystallinity.

In the case of Polymer E, where the percentage of comonomer content remains constant after xylene extraction, an increase in the crystallinity percentage due to the removal of the amorphous fraction is seen. Polymer E also shows a large decrease in the T_c and small increase in T_m after extraction with xylene.

4.3.1.5 WAXD

Figure 4.14 and Table 4.6 show the WAXD spectra of the Group 1 copolymers after extraction with xylene, melt pressed and slow cooled.

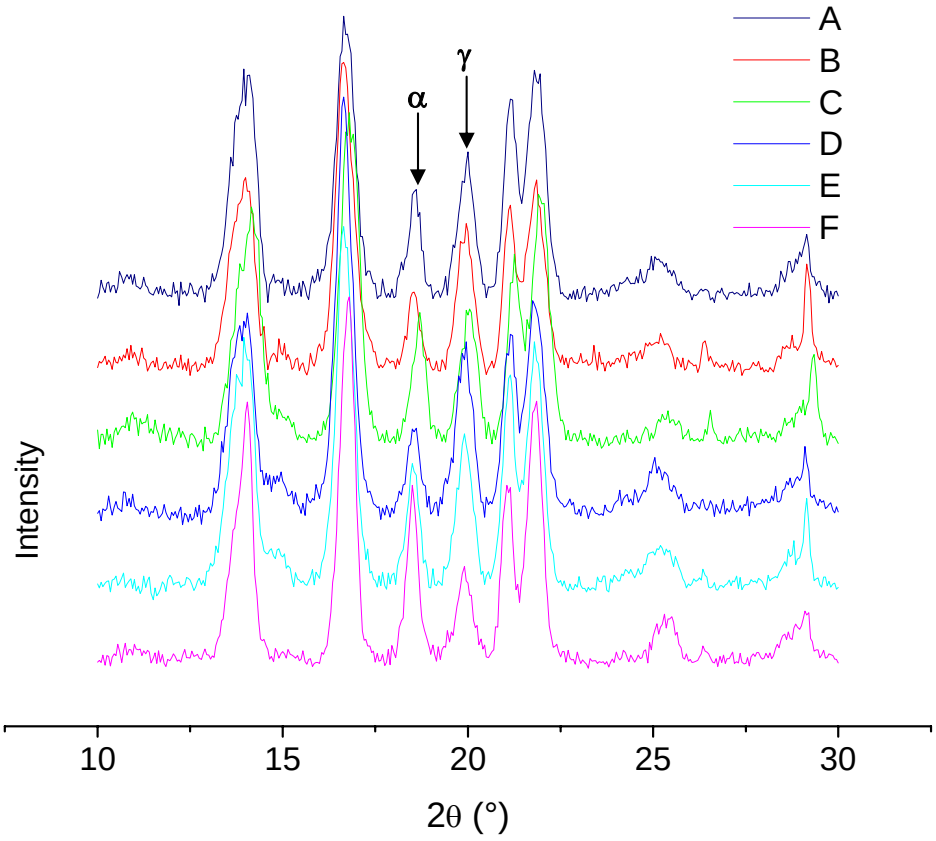

Figure 4.14 X-ray diffractograms of XNS fractions of the Group 1 copolymers

The peaks of the α-phase as well as the γ-phase are indicated in Figure 4.13 at $2\theta \approx 18.6°$ and $2\theta \approx 20.1°$ respectively. The WAXD results of Polymers A, B, D and E result in a predominant γ-phase, whereas Polymer F is the only one indicating a predominant α-phase. This is not totally unexpected, as the 1-pentene content of Polymer F is much lower than the other copolymers.

Table 4.7 Comonomer content, percentage crystallinity and amount of γ-phase crystals present in slow-cooled XNS samples

XNS	XNS 1-pentene content (mol %)	Original 1-pentene content (mol %)	XNS Crystallinity (%)	XNS γ-phase crystal (%)	Original γ-phase crystal (%)
A	2.40	3.41	66.41	56.01	53.88
B	3.13	3.09	69.90	62.61	71.20
C	2.71	2.09	68.66	51.66	52.81
D	2.70	3.50	69.62	51.39	67.65
E	2.04	2.03	72.34	55.48	59.02
F	1.51	1.21	77.85	34.65	39.40

In the last two columns of Table 4.7 the percentages of γ-phase are compared for the copolymers of Group 1 before and after the extraction with xylene. The percentage of γ-phase generally decreases after the extraction with xylene. As in the case with the original copolymers before extraction with xylene, the expected trend of an increase in the percentage of γ-phase with an increase in 1-pentene content is once again not observed. The same reasons therefore may apply as those discussed in Section 3.3.4.

According to these results it is possible that the extractables play a role in the way these materials crystallize. It is known that growth of the γ-phase is favoured by short isotactic sequences and previous results from this study already pointed out the presence of some low M_w isotactic material in the xylene extracts.

4.3.1.6 Positron annihilation lifetime spectroscopy

Preliminary PALS studies were carried out on the six original copolymers from Group 1 and the same six copolymers after extracting them with xylene. Positron annihilation spectroscopy results resemble the true free volume of a polymer and therefore the comparison between the original polymers and those after xylene extraction shows interesting detail.

A short introduction to PALS, as well as the results of the original Group 1 copolymers, were given earlier in Section 3.3.5. In this section the PALS results of the Polymers A - F will be compared with those of their XNS fractions.

Figure 4.15 illustrates the difference in fractional free volume of Polymers A - F before and after extraction with xylene. The fractional free volume is directly related to the mechanical properties of a polymer. This important parameter can be thought of as the product of the average hole size and the hole concentration. The fractional free volume, f_v, is therefore calculated using the following equation [20]

$$f_v = CI_3\langle v_f(\tau_3)\rangle$$

where $\langle v_f(\tau_3)\rangle$ (in $Å^3$) is the mean hole volume assuming a spherical cavity and C is an empirical scaling constant that reflects the probability of o-Ps formation that does not depend on the free volume and is usually determined from specific pressure-volume-temperatures (PVT) measurements above and below glass transition temperature (T_g).

Figure 4.15 indicates a significant increase in the fractional free volume for all the polymers after extraction with xylene. The difference in fractional free volume is to be the largest for Polymers E and F.

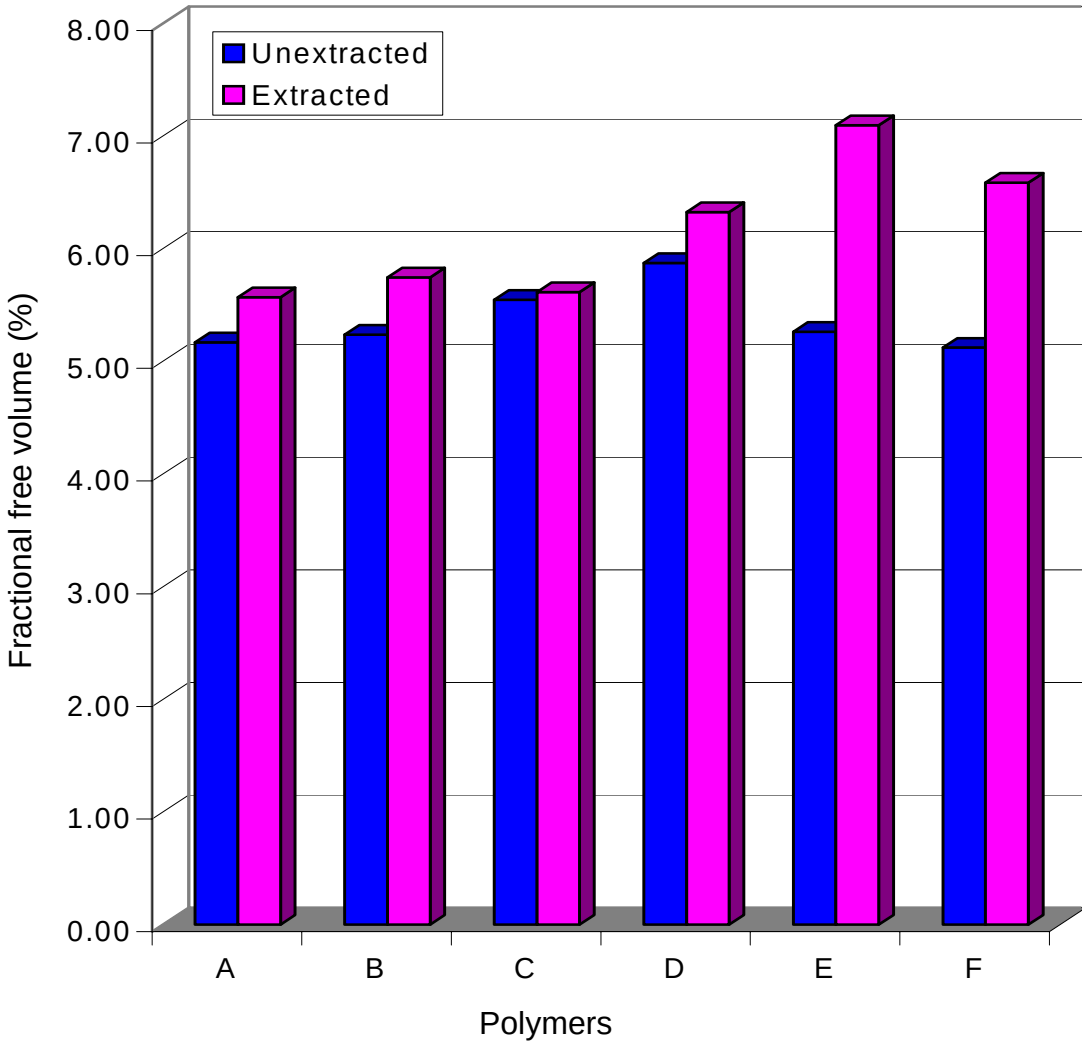

Figure 4.15 Fractional free volume of the original Polymers A - F compared to that of their XNS fractions

Figures 4.16 to 4.20 illustrate comparisons of the probability distribution functions of five of the polymers from Group 1 with their respective XNS fractions.

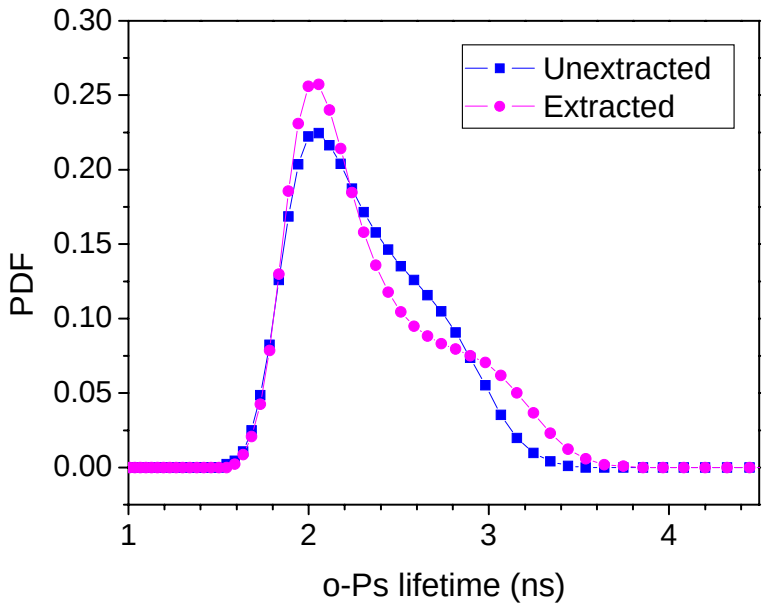

Figure 4.16 Probability distribution function vs. the *o*-Ps lifetime of Polymer A before and after xylene extraction

In Figure 4.16 Polymer A shows a bimodal probability distribution function before and after extraction with xylene. The separation between the first and second peaks for the unextracted copolymer is however not as well defined as in the case of the extracted one. According to the explanation in Section 3.3.5 we can assume that the first peak represents τ_3 (the crystalline fraction) and the second peak τ_4 (the amorphous fraction). The transition between the two peaks then represents an interstitial state which is half crystalline, half amorphous. The better separation between the crystalline and the amorphous peaks of the XNS fraction must then be due to the removal of the interstitial phase (or part thereof) during the xylene extraction. From the curves it seems as if the left hand side peak becomes narrower after extraction and therefore τ_3 becomes more defined. The right hand side peak shifts towards a higher *o*-Ps lifetime value and the value of τ_4 therefore increases.

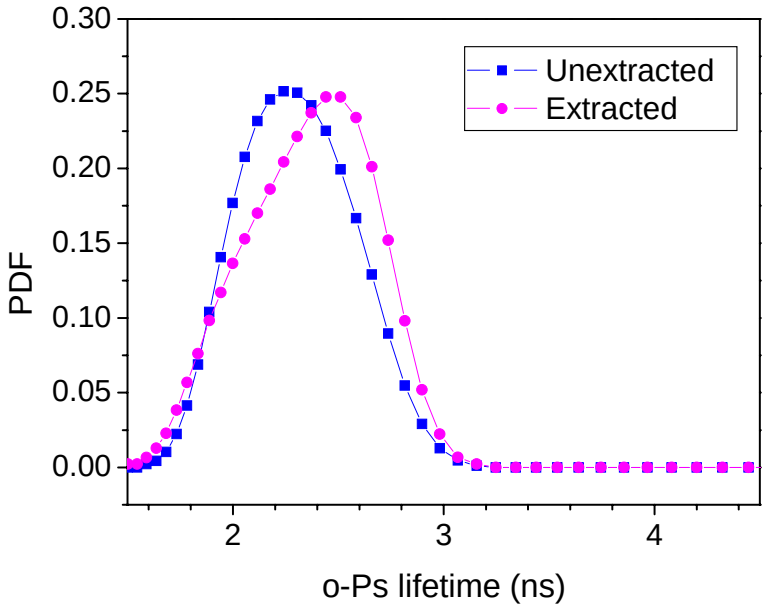

Figure 4.17 Probability distribution function vs. the *o*-Ps lifetime of Polymer B before and after xylene extraction

Figure 4.17 shows the difference in probability distribution for Polymer B and its XNS fraction. The unextracted copolymer shows a somewhat broad single peak which represents an overlap of the *o*-Ps lifetimes of the crystalline, amorphous and interstitial phases. After extraction with xylene there is a bimodal peak with a somewhat indistinct transition between the crystalline and amorphous phase appearing. The *o*-Ps lifetime of τ_4 also shifts to a higher value after extraction, as in the case of Polymer A.

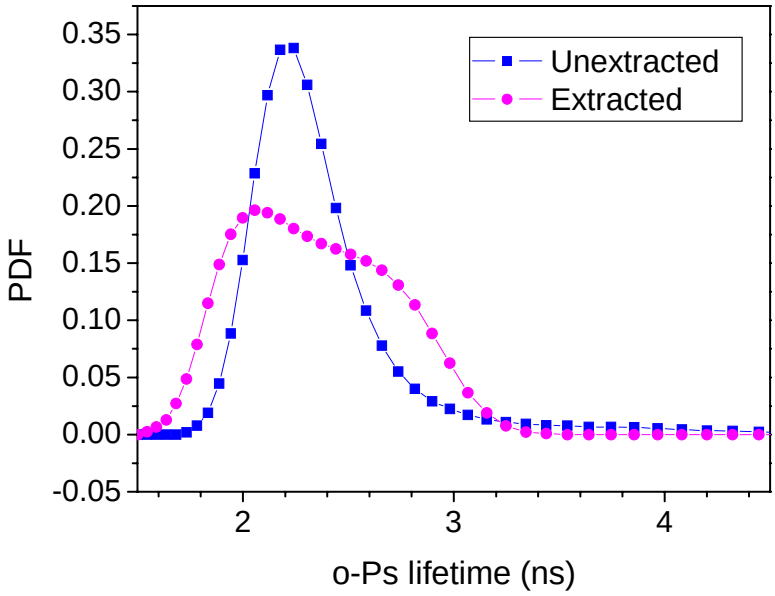

Figure 4.18 Probability distribution function vs. the *o*-Ps lifetime of Polymer C before and after xylene extraction

Figure 4.18 shows the difference in the probability distribution function of Polymer C before and after extraction with xylene. The graph shows a single peak with a tail to the right hand side which indicates that the *o*-Ps lifetime curves of the three morphology states, crystalline, amorphous and interstitial, overlap to such an extent that the difference cannot be seen, except for the tail which might indicate the appearance of τ_4. The XNS fraction is represented by a bimodal peak which clearly indicates the difference between τ_3 and τ_4. The bimodal peak therefore appears due to the removal of some low molecular weight fraction by extraction with xylene. This low molecular weight fraction must therefore contain a mixture of amorphous and crystalline material.

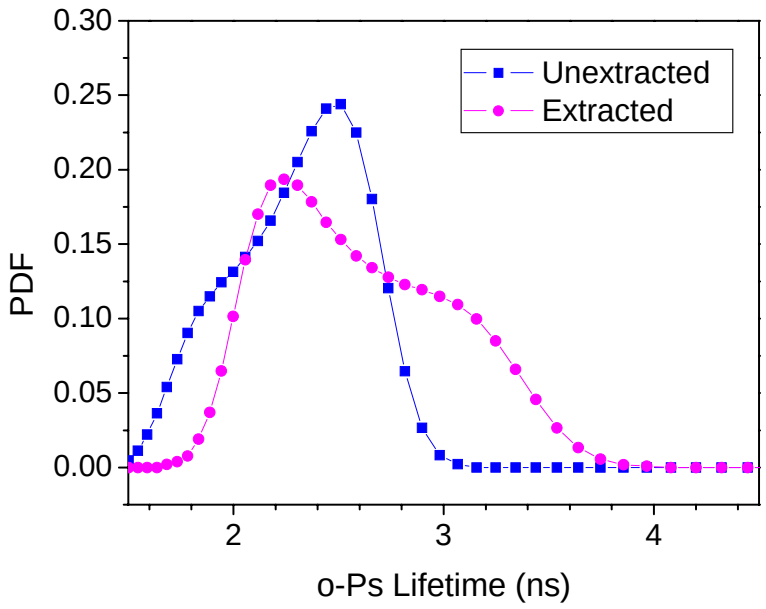

Figure 4.19 Probability distribution function vs. the *o*-Ps lifetime of Polymer E before and after xylene extraction

Figure 4.19 shows the probability distribution function of Polymer E and its XNS fraction. Here a crystalline and amorphous fraction for both the samples can be distinguished. The separation between the two phases is however better defined for the XNS fraction due to the removal of the interstitial phase through xylene extraction. There is also a clear increase in the *o*-Ps lifetime of both τ_3 and τ_4.

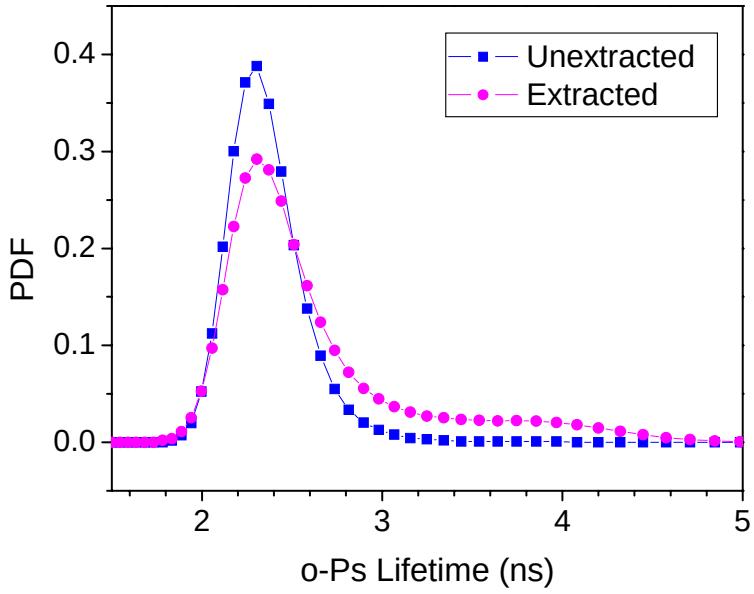

Figure 4.20 Probability distribution function vs. the *o*-Ps lifetime of Polymer F before and after xylene extraction

Figure 4.20 illustrates the difference in probability distribution for Polymer F before and after extraction with xylene. Both samples produced a single peak,but the XNS fraction shows a significant tail on the right hand side. This may mean that the copolymer consists of a high degree of crystalline material even before extraction. The amorphous fraction in both these samples must then be very small and the composition of the extract not significant enough to reveal a clear defined amorphous phase.

It is also worth noting that the propylene/1-pentene copolymers used in this study have the τ_3 value larger (~ 2 ns) than that of the poly(α-olefin) series measured by Dlubek *et al* [21]; They measured τ_3 ~ 1 ns. The crystalline/intersititial area of the former copolymers therefore reveals a longer lifetime than that of the poly(α-olefin) series. The measured τ_4 values for the Sasol copolymers correspond with that of the poly(α-olefin) series of Dlubek *et al.* The unique τ_3 value which was measured for the Sasol propylene/1-pentene

copolymers leads to a very significant and different result than reported for any other poly-olefin lifetime study to date.

4.3.2 Group 2 (G - J)

4.3.2.1 Quantitative analysis

Quantitative analyses were carried out on Polymers G - J in order to determine the percentage of xylene-solubles in each copolymer. Extractions for these analyses were carried out only once in order to have a rough estimation of the amount of material being extracted from these copolymers.

Table 4. 8 Percentage of xylene-solubles in Polymers G - J

Sample	M_w (g/mol)	PD	XL (%)
G	305 800	4.23	3.20
H	343 300	4.34	2.48
I	299 600	3.21	2.37
J	337 700	3.49	3.92

Table 4.8 shows the molecular weight results and the percentages of xylene-soluble material of Polymers G - J. The percentage of xylene-soluble material is generally lower for the Group 2 copolymers than for the Group 1 copolymers. The percentage of xylene-soluble material does not differ much for Polymers G - J. During the quantitative analysis of the Group 1 copolymers the conclusion was made that the percentage of xylene-soluble material is influenced by the M_w and PD values of the copolymer. The M_w and PD values of Polymers G - J are all in the same range and this is then the reason for the little difference in the percentage of xylene-soluble material of these copolymers. There also

seems to be little or no comparison between the 1-pentene content of the original copolymer and the percentage of extracts.

4.3.2.2 ^{13}C-NMR

Table 4.9 represents the percentage of 1-pentene contents of the original commercial Polymers G - J, and of their respective XNS fractions as well as the percentage change in the comonomer content. According to the data the comonomer content of all the polymers is a little lower after extraction with xylene, except for Polymer H where the comonomer content decreases significantly after extraction and Polymer I where the comonomer content stays relatively the same. Xylene therefore extracts material from the copolymers containing some 1-pentene.

The above indicates that the distribution of 1-pentene remains constant for the materials made by a catalyst with a high Si:Ti ratio, but that there appears to be (percentage wise) a bigger change in the copolymers produced by a low Si:Ti ratio.

Table 4.9 Comonomer contents of the original Polymers G - J and of their XNS fractions

Sample	1-Pentene content (mol% from NMR)	1-Pentene content of XNS fraction (mol% from NMR)	Change in 1-pentene content (%)
G	1.13	0.92	18.58
H	1.99	1.18	40.70
I	2.23	2.29	-2.69
J	1.86	1.75	5.91

The ^{13}C-NMR spectra of the original commercial Polymer G, the XNS fraction of Polymer G and the xylene-soluble (XS) fraction of Polymer G are compared in Figure 4.21. According to Figure 4.21 (a) and (b) the comonomer

content clearly decreased after extracting the copolymer with xylene, which corresponds with the results calculated in Table 4.9. Hence the XS fraction of the copolymers must contain some 1-pentene. The 1-pentene peaks of the XS sample are not very clearly visible in the NMR spectrum of Figure 4.21 (c). The relatively noisy baseline may be hiding the 1-pentene peaks. The figure also shows that, by extracting with xylene, the polymer is separated into a highly isotactic fraction (b) and a predonimantly atactic fraction (c). The low intensity of the methyl peak compared to the adjacent pentads in the XS fraction confirms the low tacticity of the xylene extract.

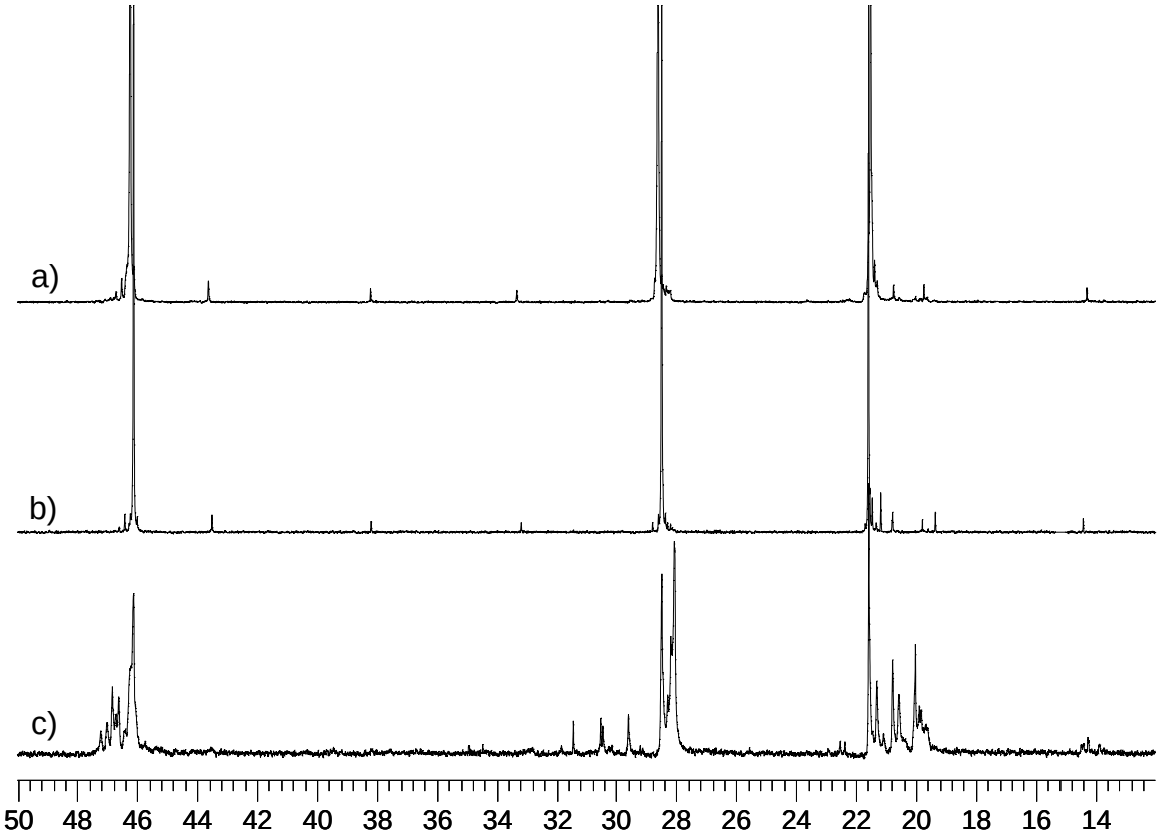

Figure 4.21 ^{13}C-NMR of a) original Polymer G, b) Polymer G after extraction with xylene and c) xylene extract of Polymer G

Figure 4.22 compares the ^{13}C-NMR spectra of the xylene extracts of the copolymers of Group 2. The methyl resonance of the xylene extracts is split into various major peaks, which correspond to the steric pentads shown in Figure 4.6.

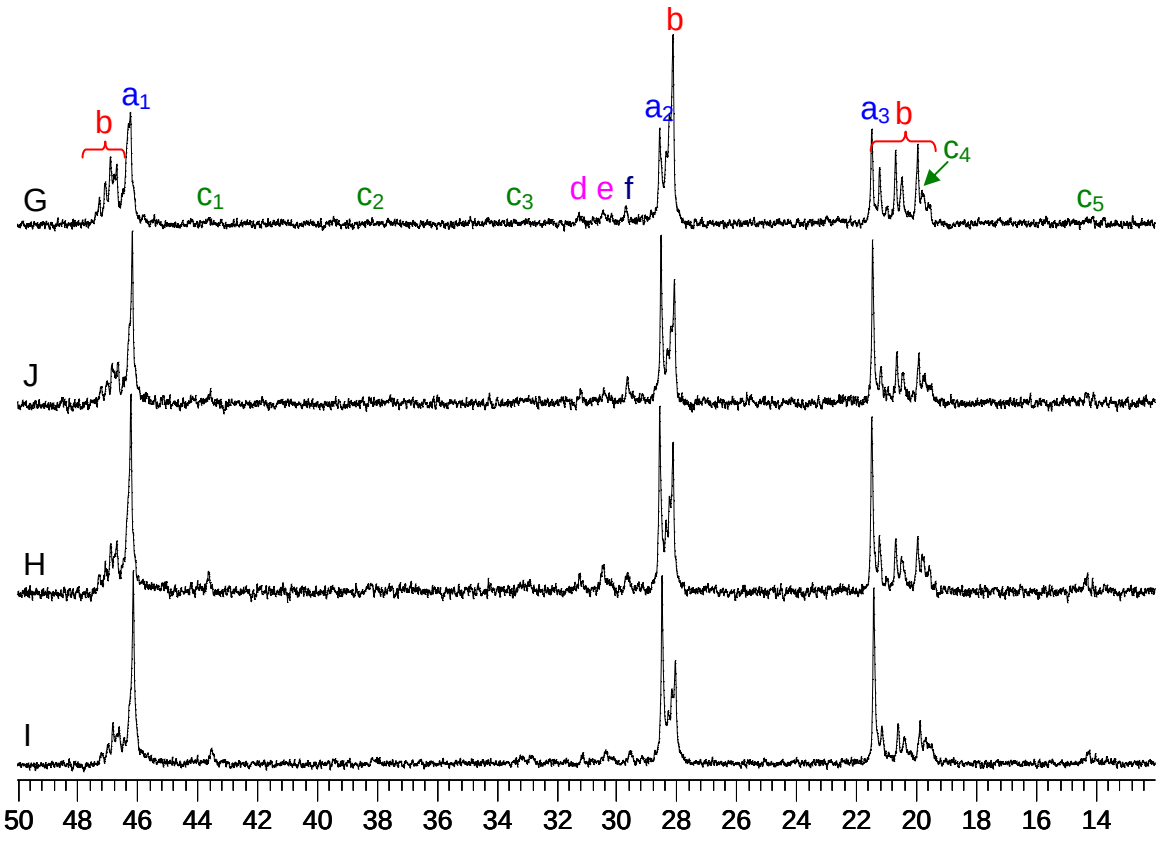

Figure 4.22 ^{13}C-NMR of xylene extracts of Polymers G - J

In Figure 4.22 the ^{13}C-NMR spectra of Polymers G - J are arranged from top to bottom in the order of increasing 1-pentene content of the original copolymers. The relative intensities of the methyl peaks compared to those of the neighbouring pentads indicate an increase in tacticity of the xylene extracts with an increase in 1-pentene content of the original copolymers. This trend is confirmed by the increase in ratio of the intensity of the methine peak to its shoulder peak. The extract from Polymer G also clearly has a very low tacticity compared to other samples.

This trend is rather interesting; although it must be pointed out that the isotacticities are still very low. The isotacticity of the xylene extracts (amorphous and low tacticity high M_w material) appears higher with more 1-pentene in the original copolymers. This means there is a higher amount of "medium" tacticity high M_w polypropylene present in the copolymers with the higher comonomer content. There is, however, no relationship between the microstructure of the xylene extracts and the Si:Ti ratio.

As in the ^{13}C-NMR spectra of the Group 1 xylene extracts (Figure 4.7) the three peaks on the left hand side of the propylene methine peak are present. As explained earlier in Section 4.3.1.1 the peak indicated by (f) is to be due to the two branching carbons in the main chain on both the sides of the 1-pentene side chain. Peaks appearing at (d) and (e) are caused mainly by *n*-propyl end groups. The peak appearing at (e) is attributed to the branching carbon of the standard *n*-propyl end group as well as an *iso*-pentyl end group.

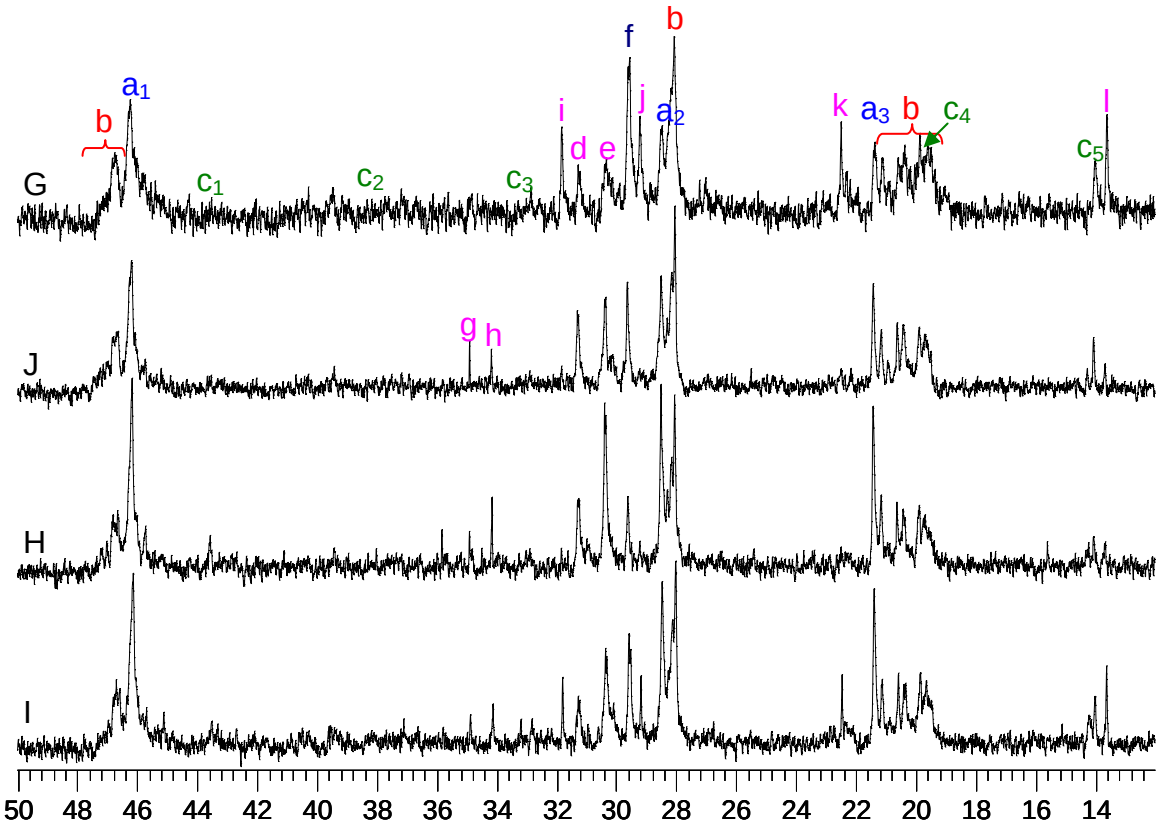

Figure 4.23 ^{13}C-NMR of hexane extracts of Polymers G - J

Figure 4.23 compares the ^{13}C-NMR spectra of the hexane extracts of the copolymers of Group 2. The spectra in Figure 4.23 are again arranged from top to bottom in the order of increasing 1-pentene content of the original copolymers. The same trend as in the case of the xylene extracts is seen: an increase in the tacticity of the extracts with an increase in comonomer content of the original copolymers. The intensities of the branching carbon and the other carbon peaks between 29 - 32 ppm, representing end groups, are much higher in the spectra of the hexane extracts than in the spectra of the xylene extracts. This indicates a lower molecular weight and higher 1-pentene content for the hexane extracts.

The tacticities of the hexane extracts are all much lower than in the case of the xylene extracts. This indicates that hexane extracts mainly atactic material, probably due to the temperature of the boiling solvent. It therefore

confirms that hexane extracts only atactic material and xylene extracts all atactic material as well as a certain amount of low molecular weight isotactic material, which causes the ^{13}C-NMR spectra of the xylene extracts to reveal a higher tacticity than the hexane extracts. The suggestion that hexane extracts only atactic material corresponds well with the fact that the entire hexane extract is soluble in acetone. It then also makes sense that because of the fact that the spectra in Figure 4.23 originate from pure atactic material so many smaller secondary peaks are visible in these spectra than in the case of the xylene extracts.

Peaks indicated as (a) - (h) in the spectra of Figure 4.23 have already been identified during the discussion of the xylene and hexane extracts of the Group 1 copolymers. These peaks were all identified as indicative of the existence of a high concentration of end groups, for instance the standard *n*-propyl, *iso*-pentyl, or *n*-propyl end groups on the other end of the chain. There are however three extra peaks (i), (j) and (k) appearing in the spectra of Polymers G and I as well as a peak (l) appearing in the spectra of all the hexane extracts. The peak appearing at (l) however, has a much higher intensity in the spectra of the hexane extracts of Polymers G and I than in the other copolymers in Group 1. According to the NMR predictions, using ACD labs software, the peaks appearing at (i) - (l) are caused by the presence of *n*-hexyl end groups as shown in Figure 4.10. The peak at (l) is also attributed to by the standard *n*-propyl end group and therefore present in all four spectra. The higher intensity of the peak at (l) in the two spectra of the hexane extracts of Polymers G and I is then caused by an overlapping of the resonance of the methyl carbon in the *n*-hexyl end group with the methyl carbon in the standard *n*-propyl end group.

Figure 4.24 shows the ^{13}C-NMR analysis results of the heptane extracts of the Group 2 copolymers. Once again, the spectra in Figure 4.24 are arranged from top to bottom in the order of increasing 1-pentene content of the original copolymers. In the case of the heptane extracts there is however no trend for the tacticity of the various extracts as with the xylene and hexane extracts of these copolymers with regard to the 1-pentene content of the original copolymers. As a

matter of fact, the four spectra do not even look alike, as in the case with the xylene and hexane extracts. The spectra of extracts of Polymers G and H seem to contain very little atactic material compared to that of I and J, with the extract of Polymer J showing the lowest tacticity. This is significant, as Polymers G and H were produced with the lowest Si:Ti ratios, with J and I having Si:Ti ratios of 10 and 6.8 respectively.

With propylene homopolymers, extracts are directly related to the isotacticity index of the material, and can be varied by varying the Si:Ti ratio, but it appears that in the case of copolymers this is not the case, and that the distribution of 1-pentene plays a major role.

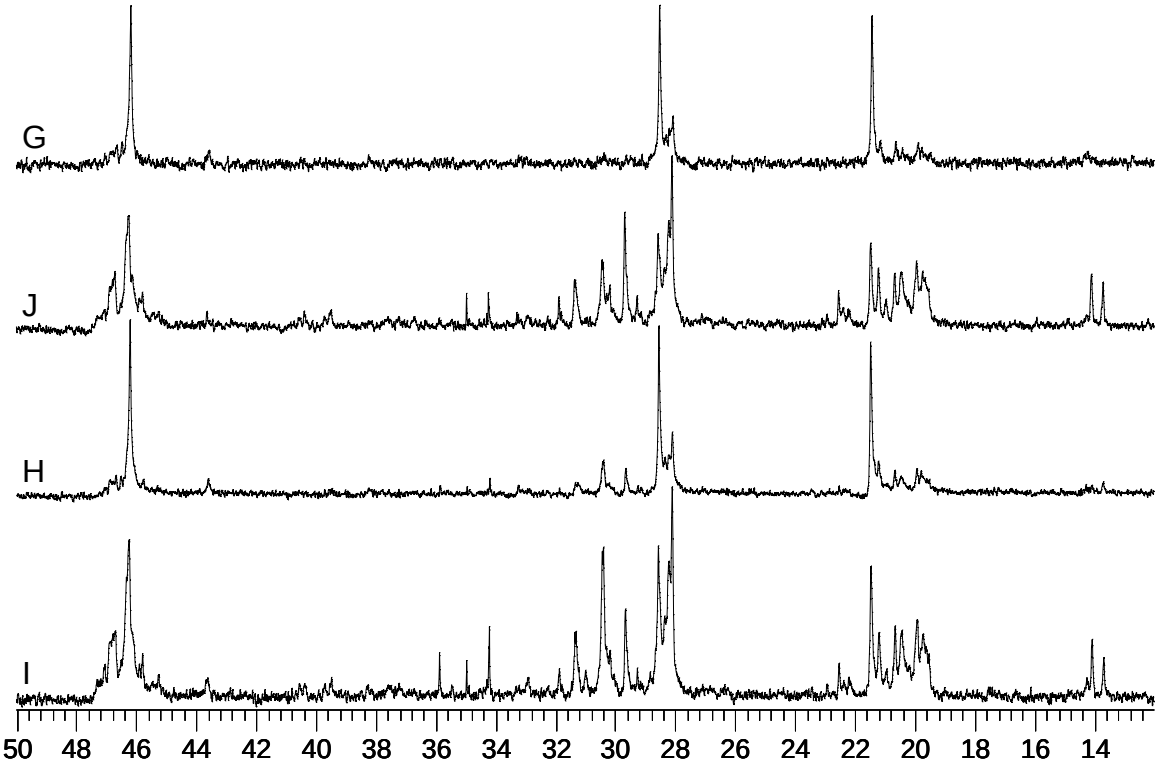

Figure 4.24 ^{13}C-NMR of heptane extracts of Polymers G - J

No resonances due to end group carbons are visible in the spectra of the heptane extracts of Polymers G and H. The concentration of the end groups

must therefore be very low in these extracts compared to those of Polymers I and J. In the spectra of the heptane extracts of Polymers I and J in Figure 4.24 the resonances appearing due to standard *n*-propyl end groups, *n*-propyl end groups on the other end of the chain, *iso*-pentyl and *n*-hexyl end groups are identified.

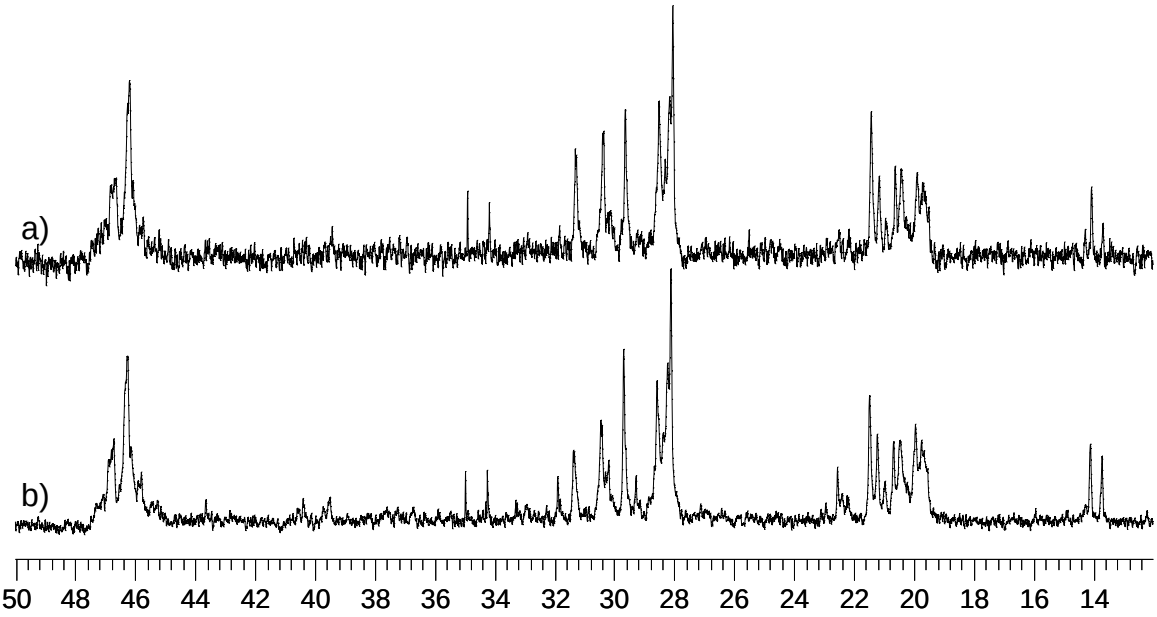

Figure 4.25 ^{13}C-NMR of a) hexane extract and b) heptane extract of Polymer J

The results from Figure 4.23 were investigated further by directly comparing them with the spectra in Figure 4.24. The spectra of Polymers G and H differ significantly, which corresponds with the fact that different solvents extract different molecular structures. However, the ^{13}C-NMR spectra of hexane and heptane extracts of Polymers I and J look almost the same. In Figure 4.25 the same resonances occur in both spectra and only the intensities of some of them differ slightly. The similarity between the spectra, coupled with the fact that more material was obtained by heptane extraction, prompted a more complete investigation of the composition of the extracts. Hence the method of successive extractions as described in Section 4.3.3 was introduced.

4.3.2.3 HT-GPC

Figure 4.26 represents the HT-GPC curves of the heptane, hexane and xylene extracts of Polymer G after normalization. As in the case of the Group 1 copolymers, there are mainly three peaks appearing for the xylene-extract curve and a single peak for the heptane-extract curve. The heptane peak overlaps with a peak in the hexane- and xylene-extract curves. The intensity of this peak however decreases for the hexane extract and is the lowest in the case of the heptane extract. In the curve of the hexane extract there is a lower molecular weight peak overlapping with that of the higher molecular weight peak. These two overlapping peaks also appear with a lower intensity in the xylene extract curve. The curve of the xylene however shows another even lower molecular weight peak appearing.

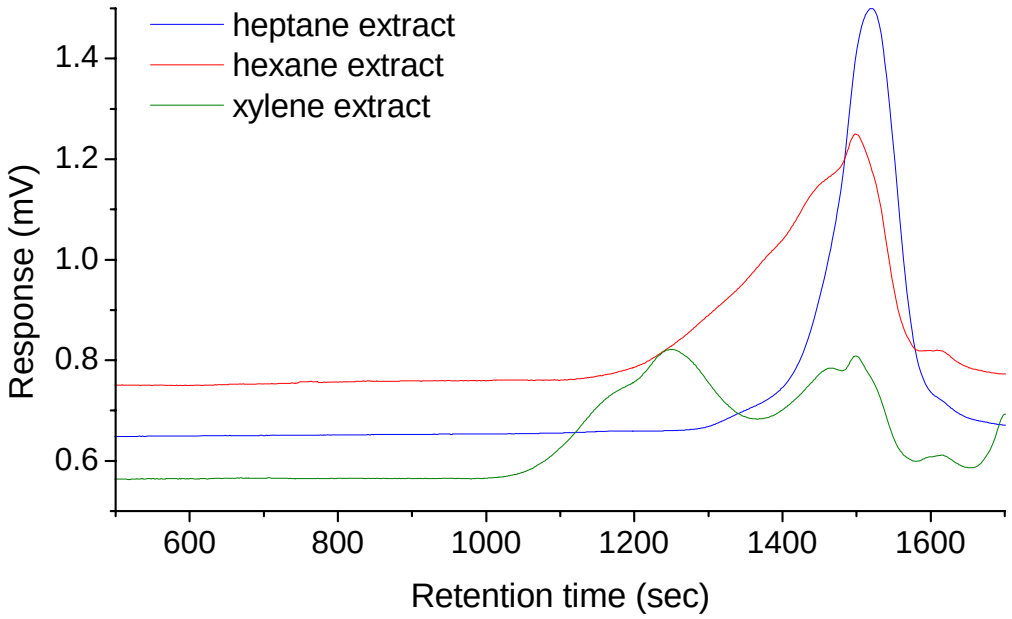

Figure 4.26 Normalized HT-GPC curves of solvent extracts of Polymer G

Table 4.10 presents the HT-GPC data of the solvent extracts of the Group 2 copolymers. The hexane extracts show the lowest molecular weights and PD

values and the xylene extracts the highest values. It must however be considered that the HT-GPC curves of the hexane and xylene extracts show more than one peak and these values are therefore not comparable for the different solvents.

Table 4.10 HT-GPC results of the different extracts of Polymers G - J

Sample	M_n (g/mol)	M_w (g/mol)	PD
Xylene extracts			
G	1 400	44 300	32.82
J	1 600	80 500	50.47
H	900	67 200	72.61
I	1 400	78 400	54.70
Hexane extracts			
G	400	900	2.13
J	500	900	1.99
H	600	3 300	5.40
I	500	3 200	5.90
Heptane extracts			
G	800	5 400	7.00
J	500	1 000	2.11
H	700	4 700	6.65
I	1 500	13 300	8.71

Figure 4.27 shows a visual three dimensional representation of the HT-GPC results of the extracts of Polymers G - J.

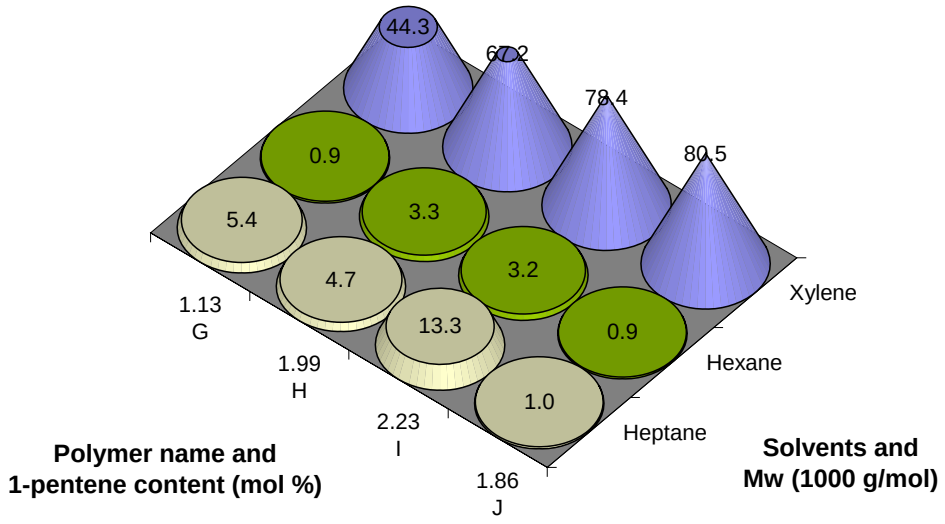

Figure 4.27 Visual representation of the M_w results of the different extracts of Polymers G - J

Table 4.11 compares the HT-GPC results of the Group 2 copolymers before and after extraction with xylene. The most important difference in the molecular weight results of these copolymers is the significant increase in M_w after extraction with xylene. It is therefore clear that some low molecular weight material is removed by the extraction with xylene. The polydispersities of the XNS fractions of the Group 2 copolymers however increase, which is in contrast with the decrease in the case of the Group 1 copolymers (Section 4.3.1.3). As these are a completely different set of materials, it is not possible to directly compare the two groups of materials.

Table 4.11 HT-GPC results of Polymers G - J before and after extraction with xylene

Sample	M_n (g/mol)	XNS M_n (g/mol)	M_w (g/mol)	XNS M_w (g/mol)	PD	XNS PD
G	72 200	77 900	305 800	339 200	4.23	4.36
J	96 700	80 200	337 700	355 500	3.49	4.43
H	79 100	74 400	343 300	368 400	4.34	4.95
I	93 500	90 600	299 600	324 800	3.21	3.59

4.3.2.4 Thermal analysis

DSC analyses were carried out on the Group 2 copolymers before and after extraction with xylene. The thermal analysis results of the XNS samples are compared to those of the original Polymers G - J in Table 4.12. The table also shows the comonomer contents for the various commercial copolymers and their XNS fractions as determined by ^{13}C-NMR analysis.

Table 4.12 DSC results of Group 2 copolymers and their XNS fractions

Sample	1-pent (mol%)	XNS 1-pent (mol%)	T_c (°C)	XNS T_c (°C)	T_m (°C)	XNS T_m (°C)	Crystal-linity (%)	XNS Crystal-linity (%)
G	1.13	0.92	110.41	110.24	151.82	151.44	67.94	66.36
H	1.99	1.18	120.97	107.72	151.12	147.14	68.28	62.39
I	2.23	2.29	121.16	105.16	149.84	144.45	64.64	56.36
J	1.86	1.75	106.52	106.57	149.60	148.11	54.88	59.19

Table 4.12 reveals a decrease in T_c, T_m and crystallinity after the low molecular weight material was removed by extraction with xylene for Polymers H and I. Most of the copolymers, except Polymer I, show a decrease in 1-pentene content after extraction with xylene. This decrease in the amount of chain interruptions creates the expectation of an increase in the T_m, T_c and crystallinity

of the relevant copolymers. In the case of Polymers H and I, there are significant changes in T_c as well as T_m, and a decrease in crystallinity. Yet while with Polymer H, where there is a sharp decrease in the 1-pentene content, I is largely unchanged. It is therefore expected that some other factors to play a role in the value decrease of these thermal parameters after xylene extraction.

Of interest here is that where there is a limited amount of 1-pentene (Polymer G), and a similar amount of 1-pentene in both the unextracted and extracted material (which indicates a homogeneous distribution) there is no significant difference in T_c and T_m.

There is, however a very small decrease in the T_c, T_m and crystallinity of Polymer G after extraction with xylene. There is a bigger decrease in the same parameters for Polymer H and an even bigger decrease for Polymer I. Polymer J then falls outside this trend. The trend for Polymers G, H and I may be related to the increase in Si:Ti ratio in the original copolymers. It then seems that the thermal properties are no longer influenced in a decreasing way after extraction with xylene when the Si:Ti ratio reaches the highest value for the four copolymers (10).

4.3.2.5 WAXD

Figure 4.28 illustrates the X-ray diffraction profiles of the Group 2 XNS samples slow cooled from the melt at a rate of 2°C/h. According to De Rosa *et al.* [22] the samples of iPP crystallize from the melt in a mixture of crystals of the α and γ forms. This phenomenon also occurs in the low-comonomer-content propylene/1-pentene copolymers used in the present study. The 1-pentene in this study acts as a defect in the crystal structure and hence the amount of γ-phase crystals will increase relative to the amount of 1-pentene included [23, 24]. The α and γ forms present very similar X-ray diffraction profiles, the main difference being the position of the third strong diffraction peak, which occurs at $2\theta = 18.6°$ in the α form [25] and at $2\theta = 20.1°$ in the γ form [26, 27].

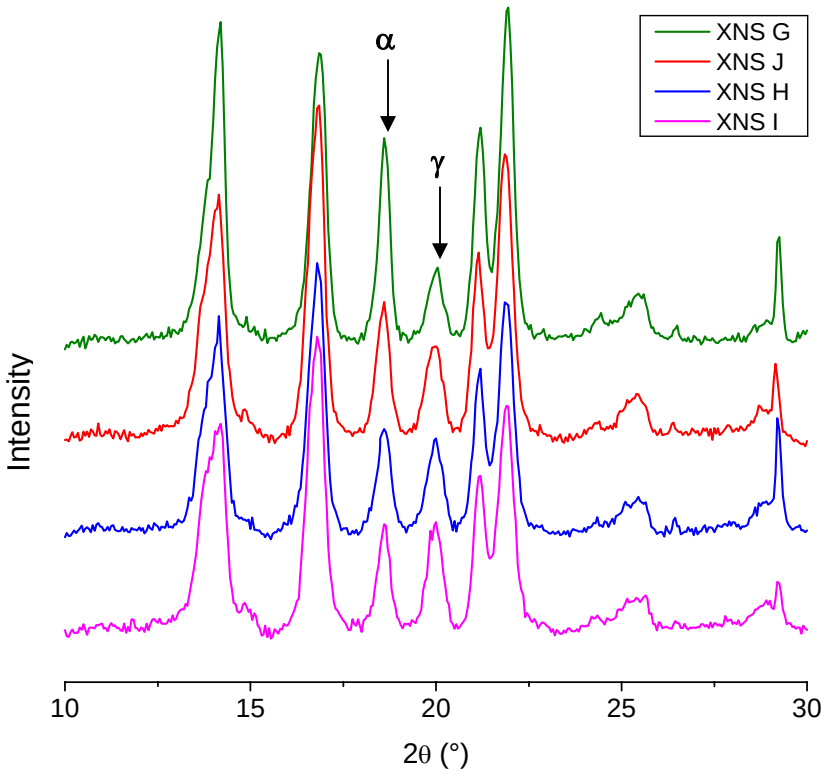

Figure 4.28 X-ray diffractograms of the Group 2 XNS copolymers (slow-cooled)

The peaks of the α-phase as well as the γ-phase are clearly indicated in the crystal structure of Figure 4.26 at $2\theta \approx 18.6°$ and $2\theta \approx 20.1°$ respectively. The percentage of γ-phase crystal of the XNS samples was calculated in the same way as described in Section 3.3.4. The percentages of γ-phase crystal are given in Table 4.13 together with the comonomer content for these samples calculated from the ^{13}C-NMR results, the percentage of crystallinity calculated from the DSC results and the percentage of γ-phase crystal of the original copolymers before extraction.

Table 4.13 Comonomer content and amount of γ-phase crystals present in slow-cooled XNS samples of Polymers G - J

Sample	Original 1-pentene content (mol %)	XNS 1-pentene content (mol %)	γ-phase crystal (%)	XNS γ-phase crystal (%)	Crystallinity (%)	XNS crystallinity (%)
G	1.13	0.92	22.65	22.86	67.94	60.91
J	1.86	1.75	37.99	41.28	54.88	55.50
H	1.99	1.18	43.43	47.06	68.28	56.36
I	2.23	2.29	47.72	52.18	64.64	52.68

According to previous studies [24, 27, 28] there should be an increase in the γ-phase for an increase in comonomer content. According to the calculations from Table 4.13 this is not the case with Polymers G, H and I. This must be due to the fact that the high molecular weight of the XNS fractions of Polymers G, H and I has a greater effect than the 1-pentene content. The γ-phase is preferentially formed in the presence of short isotactic [22] sequences and the high molecular weight of the sample may then inhibit the growth of the γ-phase.

The data in Table 4.13 also indicates a decrease in overall percentage of crystallinity of the slow-cooled XNS fractions with an increase in the 1-pentene content, as expected. There is also, generally, an increase in the γ-phase after extraction. This must be due to the removal of chains with limited or no crystallizability.

4.3.3 Successive extractions (G - J)

Successive extractions were carried out on the copolymers of Group 2 in order to get a more qualitative molecular structure analysis than from the extractions discussed in Section 4.3.2. Figure 4.29 shows the ^{13}C-NMR spectra of selected fractions of the successive fractionation of copolymer I. From these results and the HT-GPC results from Table 4.14 and Figure 4.30 it is now clear that xylene extracts a combination of atactic and isotactic material with a very

high polydispersity. When extracting the xylene soluble fraction (S1) further with hexane, according to the ^{13}C-NMR spectra of S2, this fraction was separated into an atactic fraction (S2) and an isotactic fraction (N2). This hexane insoluble fraction (N2) was then extracted with heptane and, according to the HT-GPC results from Table 4.14, separated into a very low molecular weight (S3) and a higher molecular weight isotactic fraction (N3).

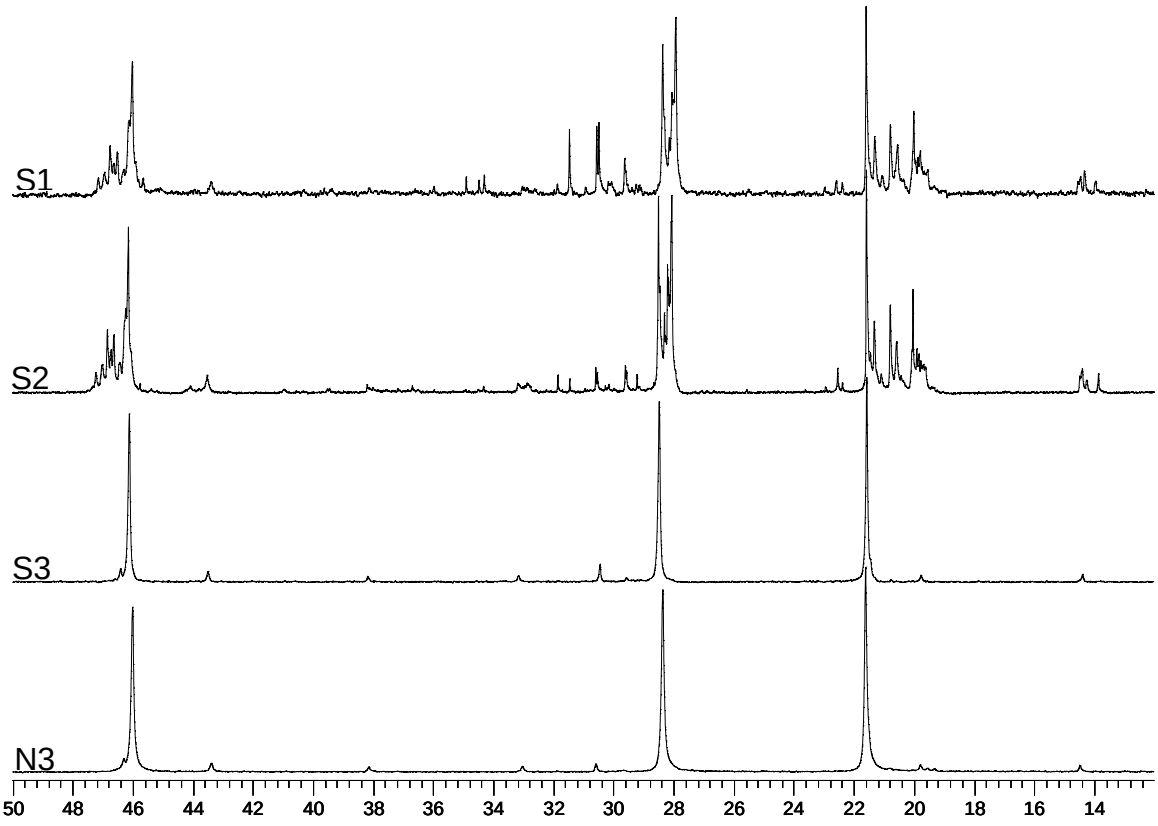

Figure 4.29 ^{13}C-NMR results of selected fractions from the successive fractionation of Polymer I

Table 4.14 Molecular weight and polydispersity results of selected fractions from successive fractionation of Polymer I

Fraction	M_n (g/mol)	M_w (g/mol)	PD
S1	1 500	34 100	22.66
S2	2 100	38 200	18.17
S3	62 700	154 900	2.47
N3	129 300	296 800	2.29

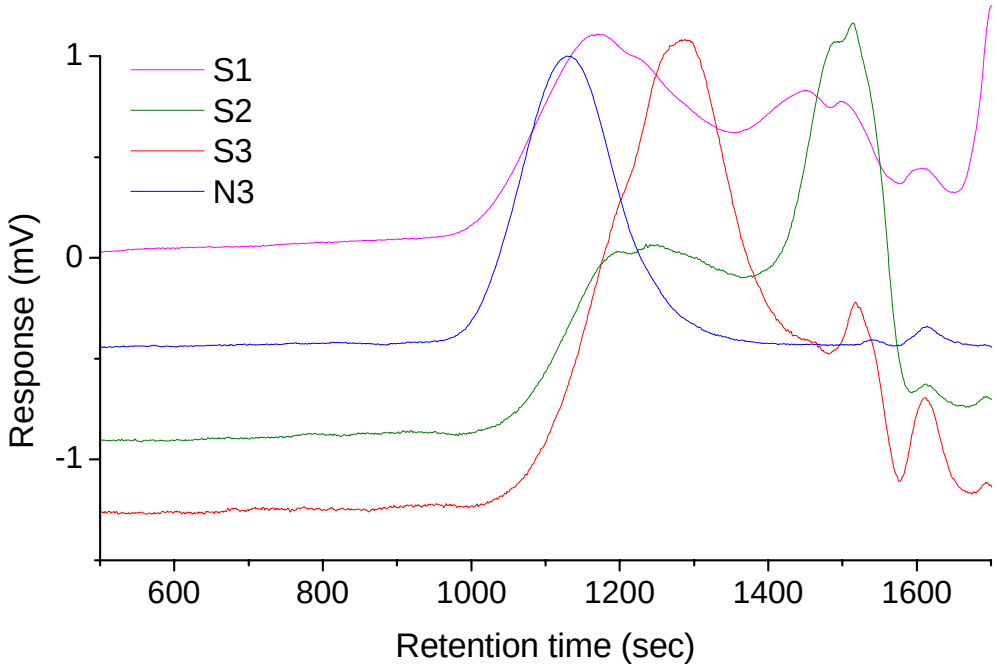

Figure 4.30 Normalized HT-GPC curves of extracts resulting from the successive extraction of Polymer I

The high polydispersity of fraction S2, and therefore also N1, is due to the complexity of the composition of the fraction. Figure 4.30 shows the HT-GPC curves of fractions S1, S2, S3 and N3. According to this figure the high polydispersity of S1 and S2 are caused by an overlapping of multiple peaks. These multiple peaks reflect the atactic character of these extracts. The curve of sample N3 is the only one that reveals a single peak, and this is due to the pure isotactic character of the extract. The successive extraction process eventually leads to the separation of the xylene extract into the three fractions, S2, S3 and N3 and the curves in Figure 4.30 correspond well with this. The curves of samples S2, S3 and N3, nicely add up to that of the xylene extract (S1).

When taking a closer look at the ^{13}C-NMR of the hexane soluble sample (S2) (Figure 4.31) it is seen that the sample consists of highly atactic propylene/1-pentene copolymer chains indicated by the stereodefects labeled by

(c), adjacent to propylene peaks labeled by (a) in Figure 4.31. Except for the 1-pentene peaks (b), the smaller peaks in the spectrum are mainly designated by a variety of end groups. The peaks labeled by (d) - (l) were already identified in Section 4.3.2.1 and hence only a summary thereof is given here:

(d) – *n*-propyl end group

(e) – standard *n*-propyl, *iso*-pentyl or *n*-propyl end group on the other end of the chain

(f) – branching carbons on both sides of 1-pentene side chain

(g) – standard *n*-propyl end group

(h) – *n*-propyl end group on the other end of the chain

(i) – *n*-hexyl end group

(j) – *n*-hexyl end group

(k) – *n*-hexyl end group

(l) – *n*-hexyl or standard *n*-propyl end group

The multiple small peaks adjacent to the 1-pentene peaks in the spectrum are caused by the clustering of 1-pentene side chains in the polymer main chain.

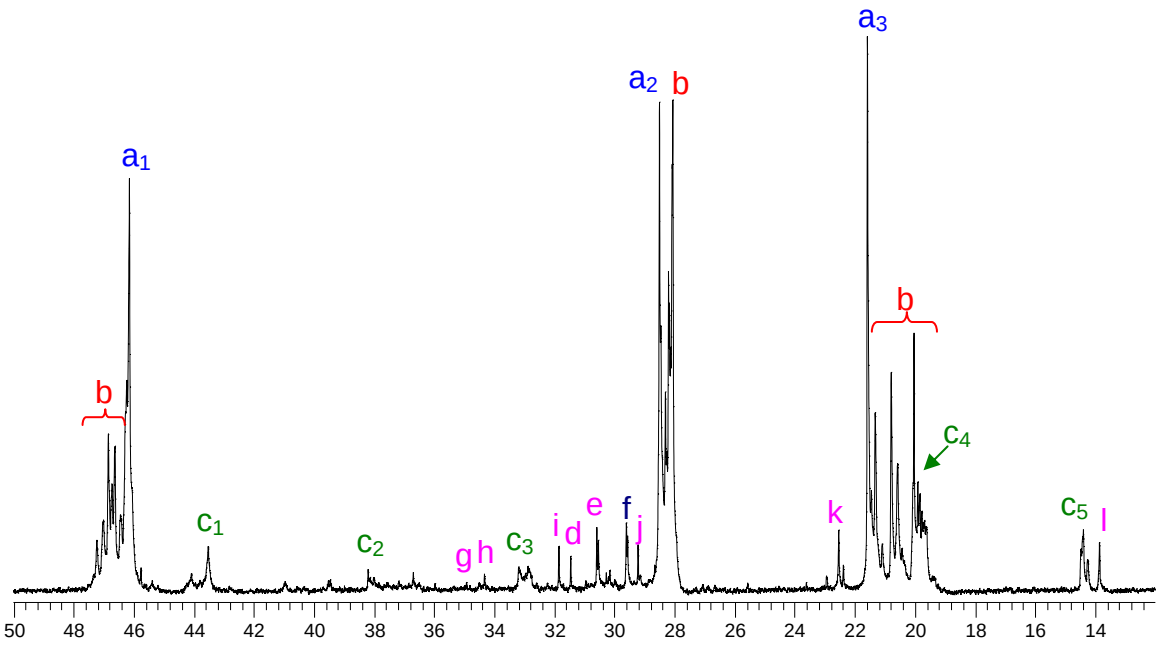

Figure 4.31 ^{13}C-NMR of the hexane soluble sample (S2) of Polymer I

Having already discussed the comparison of the xylene extracts of Polymers G - J in Section 4.3.2.1, the comparison of the hexane soluble fractions (S2) of the Group 2 copolymers as extracted with our successive extraction process will now be addressed. Figure 4.32 illustrates the ^{13}C-NMR spectra of these S2 fractions.

The extract of Polymer J clearly has the lowest tacticity, followed by that of Polymer G, then Polymer H and then Polymer I with the highest tacticity hexane soluble fraction. All the previously identified peaks (a) - (l) are present in all these spectra, but with different intensities. The spectrum of the Polymer H hexane extract shows a very high intensity for the branched carbon peak. This indicates that the extract contains a high amount of 1-pentene and this correlates with the significant decrease in 1-pentene content of the original copolymer after extraction (from 1.99 mol % to 1.18 mol %).

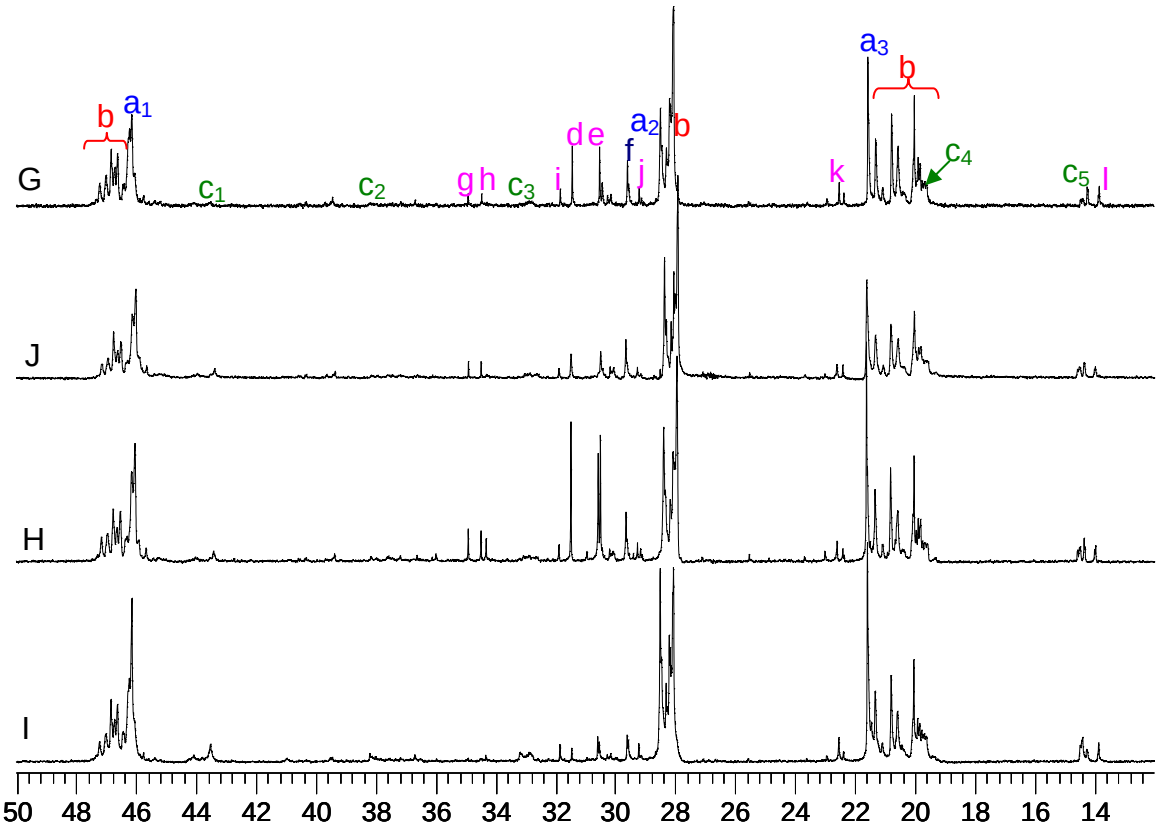

Figure 4.32 ^{13}C-NMR of hexane extracts from successive extractions of Polymers G - J

Figure 4.33 shows the ^{13}C-NMR spectra of the heptane soluble extracts of Polymers G - J isolated by the successive extractions. The sample from Polymer J clearly has the lowest tacticity, followed by that of Polymer G, then Polymer H and that of Polymer I showing the highest tacticity. Peaks (e) and (i) in the extract of Polymer G can also be identified. The presence of these two peaks was previously identified as due to standard *n*-propyl or *n*-propyl at the other end of the chain or *iso*-pentyl end groups and *n*-hexyl end groups respectively (Section 4.3.1.2). The ^{13}C-NMR spectrum of the extract from Polymer J clearly indicates the strong presence of *n*-hexyl end groups. The extract of Polymer H also shows the presence of *n*-hexyl end groups, but to a much lesser extent than that of Polymer J. The extract of Polymer I only shows an indication of peak (e) for end groups, which indicates the standard n-propyl, butyl or propyl end groups.

No relationship between the tacticity of the successive hexane extracts and the donor:catalyst ratios can be seen. There is however a relationship between the intensities of the end group peaks and the Si:Ti ratio. The intensities of the end group peaks are significantly higher for Polymers G and H with the lower Si:Ti ratios (2.2 and 2.8 respectively) than for Polymers I and J with the higher Si:Ti ratios (6.8 and 10.0 respectively). The higher end group intensities indicate lower molecular weight fractions for the extracts of Polymers G and H. The lower Si:Ti ratios therefore leads to lower molecular weight successive hexane extracts and therefore shorter atactic chains.

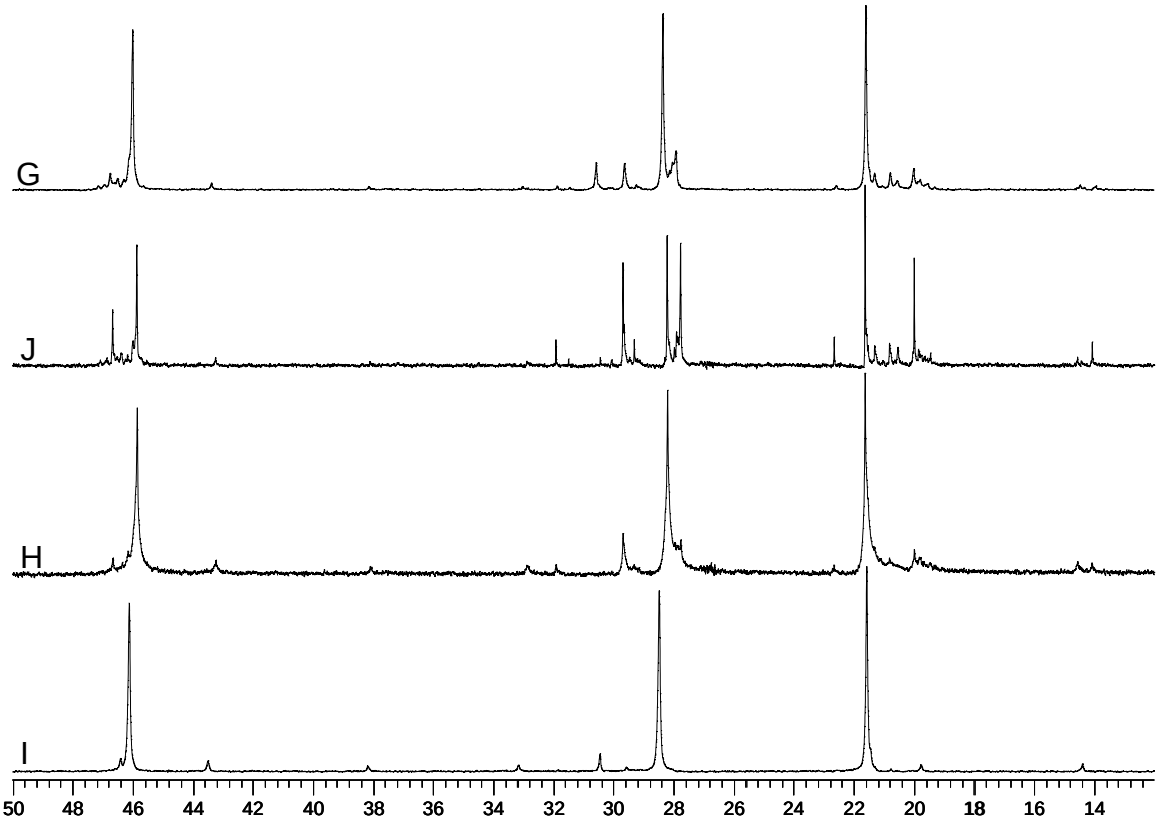

Figure 4.33 ^{13}C-NMR of heptane extracts (S3) from successive extractions of Polymers G - J

Figure 4.34 shows the ^{13}C-NMR spectra of the heptane insoluble extracts that remain after the successive extraction of the Group 2 copolymers. The spectra of these residue samples all indicate that they consist of highly isotactic material which corresponds with the low polydispersities given in Table 4.15. No relationship between the microstructure of the heptane insoluble successive extracts and the Si:Ti ratio can be seen.

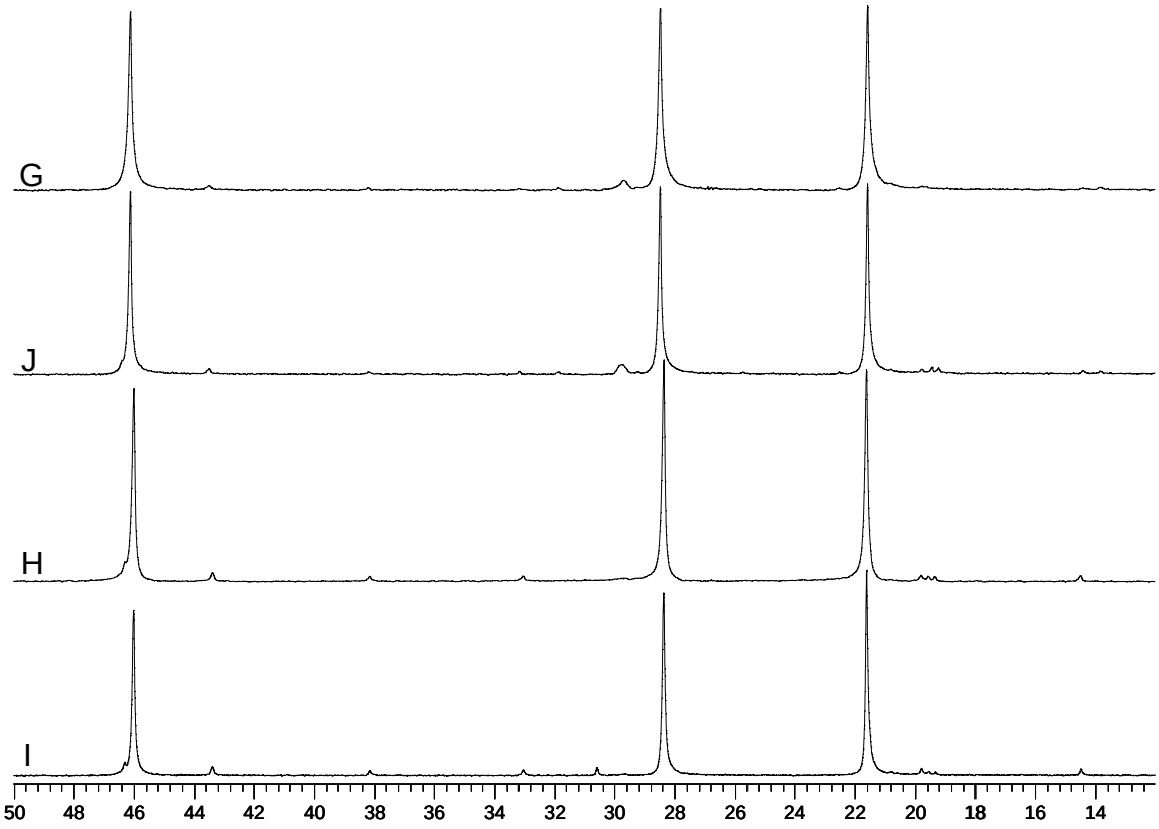

Figure 4.34 ^{13}C-NMR of the residue (N3) after successive extractions of Polymers G - J

Table 4.14 shows the HT-GPC results of the successively extracted samples of Polymers G - J.

Table 4.15 HT-GPC results of the various extracts of Polymers G - J extracted successively

Sample	M_n (g/mol)	M_w (g/mol)	PD
Xylene extracts			
G	1 700	77 400	44.58
H	2 300	113 700	50.21
I	2 100	26 400	
J	1 300	67 500	53.83
Hexane extracts			
G	1 900	27 100	13.94
H	1 100	33 600	31.27
I	2 100	38 200	18.17
J	1000	34 300	35.18
Heptane extracts			
G	4 100	37 300	9.16
H	45 100	143 300	3.17
I	62 700	154 900	2.47
J			
Residue			
G	98 100	285 600	2.91
H	133 800	450 000	3.36
I	129 300	296 800	2.29
J	129 900	381 300	2.93

4.4 CONCLUSIONS

During the qualitative analysis of the Goup 1 copolymers it became clear that the percentage of xylene-solubles are influenced by the M_w and PD values of the copolymers as well as by the type of catalyst used for the production of the copolymers. When ignoring Polymer C with the extremely high MFI, it also seems as if there is a relationship between the 1-pentene content and the percentage XL, except for the non-nucleated copolymer which led to a higher percentage XL than expected.

The Group 1 copolymers were extracted with decalin, xylene, heptane and hexane. NMR analysis of the decalin extract produced a very complex and noisy spectrum. The explanation for these complex spectra is the possibility of a lack

in the understanding of the recrystallization mechanism of these extracts and therefore a flawed experimental extraction method for decalin.

During comparison of the Group 1 comonomer content before and after extraction with xylene, it became clear that the copolymers with the lowest original 1-pentene content have a much more uniform distribution of the comonomer in the copolymer than those with the higher 1-pentene content. Surely the type of catalyst with which the copolymers were produced also plays a role in the CCD of these copolymers. The comonomer content results before and after extraction with xylene also indicated that seemingly similar copolymers with regard to their 1-pentene content differ in 1-pentene distribution. The absence of nucleating agent furthermore led to a significant amount of 1-pentene lost in the xylene extract.

End group analysis of the propylene/1-pentene copolymer extracts makes it possible to identify the dominant end groups present in the extracts. It is also possible from the ^{13}C-NMR spectra of these copolymers to get an idea of the molecular weight of the extracts.

The molecular weight results from the HT-GPC analyses confirm the tacticity interpretations from the ^{13}C-NMR spectra of the extracts, which were made purely by investigating the shoulder peaks of the propylene carbon resonances.

From the thermal analysis of the XNS fractions of Group 1 compared to that of the original Group 1 copolymers a definite decrease in the percentage of crystallinity is seen after extraction. This leads to the conclusion that xylene must extract a certain amount of crystallizable material together with the low molecular weight amorphous material.

WAXD analysis of the Group 1 copolymers and compared to their respective XNS fractions did not show the general expected trend of an increase of the percentage of γ-phase crystal with an increase in the 1-pentene content due to the fact that the 1-pentene content is not the only variable present in these copolymers. The extracts must play a definite role in the way the material crystallizes seeing that an increase in comonomer content after xylene extraction

of a specific copolymer leads to a decrease in the percentage of γ-phase crystal and the other way around when the 1-pentene content decreases after extraction. It is known that low molecular weight material is favoured for the growth of γ-phase crystal. The growth of γ-phase crystal therefore requires short isotactic sequences which are, as mentioned earlier on, removed during the extraction with xylene.

PALS was used as an alternative analytical technique to investigate the Group 1 copolymers in order to see what type of information can be gathered through this novel technique. An increase in the fractional free volume as well as a better separation between the crystalline and the amorphous phase were observed after extracting the original copolymers with xylene. The improved separation therefore means that the interstitial phase (half crystalline, half amorphous) is being removed during xylene extraction. A very interesting observation from the PALS study is that the value of τ_3 is very unique (to date) for the propylene/1-pentene copolymers used in this study. This unique value is double in value of that reported in other poly-olefine lifetime studies.

An overall conclusion from the study of the Group 1 copolymer extracts is that the techniques used to study these extracts point out significant differences and this shows that the techniques can be used in a more systematic study. The same techniques (except for PALS) were therefore applied to the study of the Group 2 copolymer extracts.

The qualitative analysis study of the Group 2 copolymers showed much lower percentages of xylene-solubles. According to the conculsions made from the qualitative analysis of the Group 1 copolymers this is due to the different catalyst systems used for the production of the Group 2 copolymers which produced propylene/1-pentene copolymers with lower M_w and PD values than the Group 1 copolymers. Another very significant conclusion is that a high Si:Ti ratio leads to a constant 1-pentene distribution before and after xylene extraction, whereas a low Si:Ti ratio causes a bigger change (percentage wise) in the 1-pentene content.

The xylene extraction of Polymers G - J shows that xylene extracts material containing 1-pentene. The xylene extracts show an increase in isotacticity with an increase in the comonomer content of the original copolymers. This means that there is more “medium” tacticity high molecular weight polypropylene present in the higher 1-pentene content copolymers. No relationship between the microstructure of the xylene extracts and the Si:Ti ratios are visible.

^{13}C-NMR analysis of the hexane extracts show a higher intensity of the branching carbon peak of the 1-pentene and the end group peaks, which indicates lower molecular weight and higher 1-pentene content for the hexane extracts. The lower tacticities of the hexane extracts than the xylene extracts confirm that hexane extracts only atactic material and xylene extracts atactic as well as low molecular weight isotactic material. The complete solubility of the hexane extracts in acetone corresponds well with the atactic character thereof.

The hexane extracts show a higher 1-pentene branching carbon intensity for the lower Si:Ti ratio copolymers, whereas the heptane extracts show a higher 1-pentene branching carbon intensity for the higher Si:Ti copolymers. The heptane extracts also show very little atactic material present for the lower Si:Ti ratios.

Certain end group peaks appearing in the spectra of the Group 2 extracts do not appear in that of the Group 1 extracts. The “additional” end groups observed for the Group 2 copolymers are *n*-hexyl end groups which are due to termination after 1-pentene following a 1,2-insertion.

The molecular weight of the XNS material of Polymers G - J is greater than for the original copolymers showing that the chemical composition significantly affects the chain size in solution.

From the ^{13}C-NMR analysis of the XNS fractions of Group 2 it is found that when the original copolymer and the XNS fraction thereof has a low 1-pentene content (~ 1 mol %) (which indicates a homogeneous distribution), there is no difference in the T_c and T_m after extraction with xylene. The amount of decrease in the T_c, T_m and crystallinity values after extraction with xylene increases with an

increase of the Si:Ti ratio up to a certain value (6.8) whereafter the influence of the donor:catalyst ratio is decreasing the thermal parameter values.

The WAXD results of the Group 2 copolymers show a decrease in the percentage of crystallinity of the slow-cooled XNS fractions with an increase in 1-pentene content. It also shows a general increase in γ-phase after extraction with xylene due to removal of chains with limited crystallinity.

Some of the hexane and heptane extracts of the Group 2 copolymers look similar with minor differences. This led to the introduction of the successive extraction method in order to investigate the composition of the extracts in a more thorough way. The successive extraction study confirms that xylene extracts a combination of atactic and isotactic material with a very high polydispersity. The successive extraction study also shows that the hexane extracts from this process consists of low molecular weight material with a wide variety of end groups which can be identified and compared with ^{13}C-NMR analysis. The hexane extracts from the successive extraction study also showed a higher 1-pentene branching carbon intensity for the lower Si:Ti ratio copolymers as seen with the hexane extracts from the normal extraction process.

4.5 REFERENCES

1. Kakugo, M., Miyatake, T., Naito, Y., Mizunuma, K., Macromolecules, 1987. **21**: p. 314.
2. Wild, L., Ryle, T., Knobeloch D., Peat, I., J. Polym. Sci., Polym. Phys. Ed., 1982. **20**: p. 441.
3. Wild, L., Trends Polym. Sci., 1993. **1**: p. 50.
4. Xu, J., Feng, L., Yang, S., Yang, Y., Kong, X., Eur. Polym. J., 1998. **34**: p. 431.
5. Lodefier, P., Daoust, D., Jonas, A.M., Legras, R., Macromol. Symp., 1999. **148**: p. 59.
6. Lodefier, P., Jonas, A.M., Legras, R., Macromolecules, 1999. **32**: p. 7135.
7. Natta, G., J. Polym. Sci., 1959. **34**: p. 531.

8. Nakajima, A., Fujiwara, H., Bull. Chem. Soc. Jpn., 1964. **34**: p. 909.
9. Doi, Y., Suzuki, E., Keii, T., Makromol. Chem., Rapid Commun., 1981. **2**: p. 293.
10. Pavan, A., Provassoli, A., Moraglio, G., Zambelli, A., Makromol. Chem., 1977. **178**: p. 1099.
11. Wolfsgruber, C., Zannoni, G., Rigamonti, E., Zambelli, A., Makromol. Chem., 1975. **176**: p. 2765.
12. Kawamura, H., Hayashi, T., Inoue, Y., Chûjô, R., Macromolecules, 1989. **22**: p. 2181.
13. Paukkeri, R., Polymer, 1994. **35**(8): p. 1673.
14. Busico, V., Cipullo R., Prog. Polym. Sci., 2001. **26**: p. 443.
15. Hayashi, T., Inoue, Y., Chujo, R., Asakura, T., Macromolecules, 1988. **21**: p. 2675.
16. Busico, V., Cipullo R., Corradini, P., Makromol. Chem., 1993. **194**: p. 1079.
17. Chadwick, J.C., Miedema, A., Sudmeijer, O., Macromol. Chem. Phys., 1994. **195**: p. 167.
18. Chadwick, J.C., Morini, G., Albizzati, E., Balbontin, G., Mingozzi, I., Christofori, A., Macromol. Chem. Phys., 1996. **197**: p. 2501.
19. Chadwick, J.C., Morini, G., Balbontin, G., Busico, V., Talarico, G., Sudmeijer, O., ACS Symp. Ser., 2000. **749**: p. 50.
20. Mallon, P.E., *Application to Polymers in Principles and Applications of Positron and Positronium Chemistry*. Principles and Applications of Positron and Positronium Chemistry, ed. Y.C. Jean, Mallon, P.E., Schrader, D.M. 2003, Singapore: World Scientific.
21. Dlubek, G., Bamford, D., Henschke, O., Knorr, J., Alam, M.A., Arnold, M., Lüpke, Th., Polymer, 2001. **42**: p. 5381.
22. De Rosa, C., Auriemma, F., Circelli, T., Waymouth, R.M., Macromolecules, 2002. **35**: p. 3622.
23. Hosier, I.L., Alamo, R.G., Esteso, P., Isasi, J.R., & Mandelkern, L., Macromolecules, 2003. **36**: p. 5623.

24. Turner-Jones, A., Polymer, 1971. **12**: p. 487.
25. Natta, G., Corradini, P., Nuovo Cimento Suppl., 1960. **15**: p. 40.
26. Del Duca, D., & Moore, E.P, Jr., *Polypropylene Handbook*, ed. J. E.P. Moore. 2002, Munich: Hanser. p. 237.
27. Busico, V., Corradini, P., De Rosa, C., & Di Benedetto, E., Eur. Polym. J., 1985. **21**: p. 239-244.
28. Foresta, T., Piccarolo, S., & Goldbeck-Wood, G., Polymer, 2001. **42**: p. 1167.

CHAPTER 5

Temperature Rising Elution Fractionation

5.1 INTRODUCTION

The commercial propylene/1-pentene copolymers analyzed in this study were prepared with stereospecific heterogeneous ZN catalytic systems containing multiple active sites and therefore producing copolymers with a varying degree of stereoregularity. It is very difficult to determine the structure of the highly reactive sites and various methods have been tried out with PP homopolymers in order to do so [1-3]. The only quantitative method for determining the distribution of stereodefects of PP [4] consists of the fractionation of the polymer using temperature rising elution fractionation (TREF) [4-10] where after the individual fractions are analyzed. TREF separates crystallizable polymers based on crystallinity. It is a two-step procedure starting with the slow cooling of the dissolved polymer to room temperature onto a support. The most easily crystallizable chains are the first to form thermodynamically stable crystals and segregate by crystallizing onto the support. When the temperature is lowered the second most crystallizable chains forms a second crystal layer on top of the first crystallites. More layers are formed in the same way. This leads to an onion-ring like structure. During the second step of TREF, these layers are then “peeled off” with an eluting solvent at increasing temperature.

All the commercial propylene/1-pentene copolymers were fractionated at least once by TREF. The copolymers of Group 2 were fractionated more than once with each attempt having different analysis outcomes. During the first attempt the copolymers of Groups 1 and 2 were fractionated into seven fractions at predetermined elution temperatures. These fractions were large enough in order to carry out a variety of analyses on them, including ^{13}C-NMR, HT-GPC, CRYSTAF and DSC. The second attempt of TREF separated the copolymers of

Group 2 into 23 fractions which were used to carry out weight fraction analysis of the copolymers. Polymers G and I were fractionated a third time into 15 fractions each which were used to compare the effect 1-pentene on the corresponding fractions of these two copolymers.

5.2 EXPERIMENTAL

5.2.1 TREF set-up

An in-house built TREF apparatus [11] was used to fractionate the commercial propylene/1-pentene copolymer pellets. This fractionation method is illustrated in Figure 5.1 and consists of two steps, the first of which is a very slow cooling process and the second an elution step.

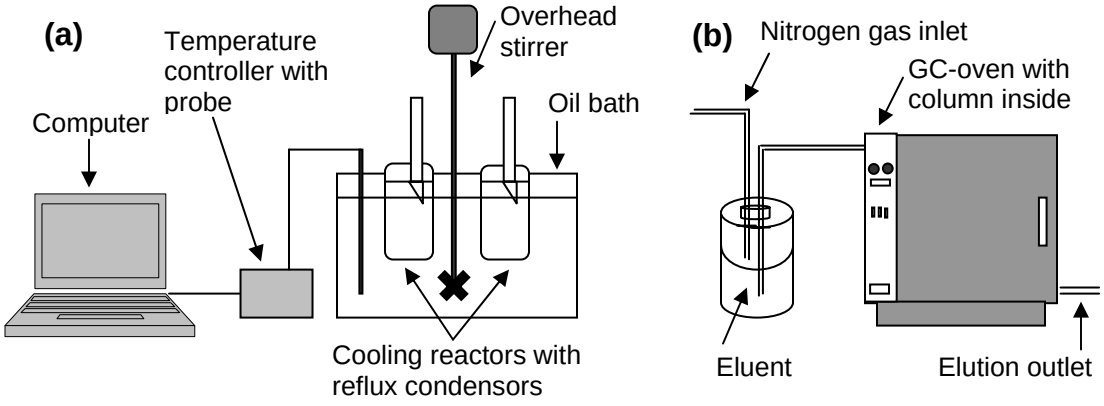

Figure 5.1 Representation of TREF system with a) the slow crystallization set-up and b) the solution set-up

The copolymer (3 g) plus Irganox 1010 stabilizer (2% w/w) were first dissolved in 300 ml xylene at 130°C in a round bottom flask. The solution was then very quickly transferred into a glass reactor which was situated in a large oil bath which had been preheated by a computerized temperature controller to the same temperature. The glass reactor was equipped with a mechanical stirrer as well as a reflux condenser. Another three different polymer samples were

dissolved in the same way and also placed in the large oil bath as explained. In this way four different batches of polymer could be cooled down at once and this saved much time during this most time consuming first step of TREF. 400 ml white quartz sand (50 - 70 mesh) was used as inert support for each solution. The sand was preheated to 130°C in order to prevent premature crystallization. The sand level had to be at least the same height as that of the solvent in order to prevent some polymer from crystallizing in solution and not on the support. The entire oil bath was then cooled at a rate of 1°C/90 min from 130°C to room temperature (~ 20 °C). This step took six days to complete.

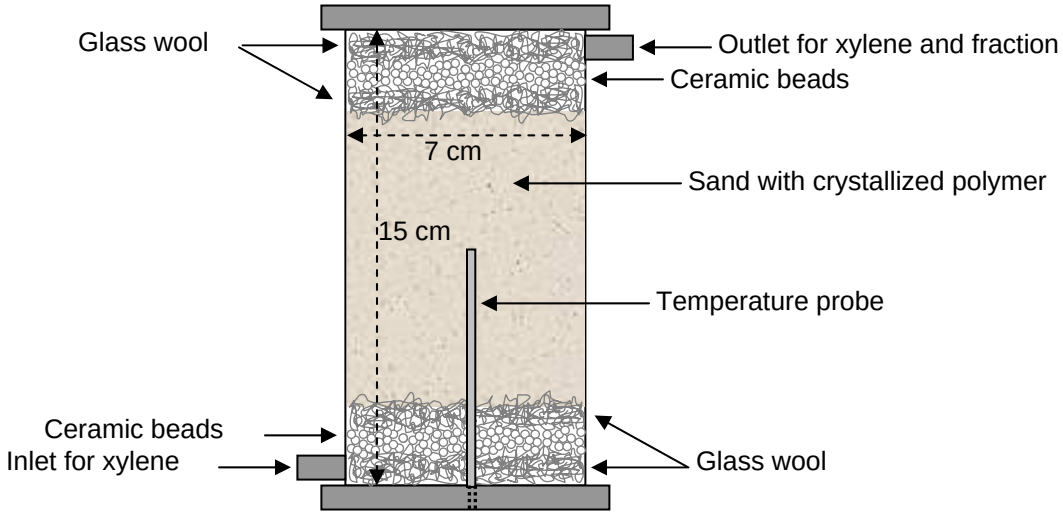

Figure 5.2 Packed stainless steel elution column

The elution process followed the cooling step. The xylene was decanted from the sand and therefore formed part of the lowest temperature fraction (25°C). The sand onto which the copolymer was crystallized was then packed into a stainless steel column as demonstrated in Figure 5.2. The layers of glass wool and ceramic beads at the top and bottom of the column were used to prevent preferential solvent channeling by breaking up the solvent flow. The column was sealed and connected inside a temperature controlled gas chromatography (GC) oven with a xylene inlet and -outlet. The column was also equipped with a temperature probe which measured the direct temperature in the

centre of the packed column. In this way we could monitor the exact fractionation temperature for each eluted fraction. The xylene inlet of the column was connected to a solvent reservoir which was under positive nitrogen pressure. The solvent flow was controlled by the nitrogen pressure at 4 ml/min and 200 ml xylene was used per fraction. The outlet pipe from the column was covered with a heating tape set to 130°C in order to prevent deposition of the fractions onto the cold pipe during the collection of the fractions and thereby causing clogging of precipitated polymer. The temperature of the oven was kept at the specific elution temperature until the temperature inside the column and the GC oven reached the desired elution temperature before the elution took place. Fractions were taken at various temperatures depending on the number and size of the fractions needed for analysis. The xylene was removed from each fraction on a rotary evaporator. Fractions were then further isolated in a vacuum oven at 50°C in order to remove any excess xylene.

5.2.2 ^{13}C-NMR

For the high temperature ^{13}C-NMR analysis of the fractions of Polymer H, spectra were recorded on a 600 MHz Varian ^{Unity}*Inova* spectrometer, as described in Section 3.2.2. Calculation of the 1-pentene content of the various fractions were also based on the methods described in Section 3.2.2.

5.2.3 HT-GPC

HT-GPC analysis was carried out on the different fractions using the experimental procedure as described in Section 3.2.3.

5.2.4 CRYSTAF

The experimental procedure for the CRYSTAF analysis of the various fractions was already discussed in Section 3.2.4. Note must however be taken

that the negative values for the percentage of soluble fraction sometimes given by CRYSTAF can only be used for comparison reasons and are not the true values. The reason for this follows. TCB which was used as solvent in CRYSTAF analysis has a freezing point of 17°C and some of our fractions appeared to have a T_c of lower than 20°C. The CRYSTAF was therefore pushed to a lower limit of 15°C. This however causes problems with the baseline reading. The IR cell takes a transmission reading of the pure solvent before the start of crystallization, i.e. at the maximum temperature and again at the end of the analysis. This is to allow for changes in the solvent transmission during the run. The CRYSTAF averages these two readings to calculate the zero baseline of the crystalline curve. This, however, gives a faulty value in the case where the lower temperature is close to or lower than 17°C. Possible crystals of TCB may form under these conditions and lead to a distorted baseline curve. The only way to form meaningful curves is to manually choose only one reading for the baseline i.e. the start reading. This gives you sensible crystalline curves but it also means that if there are any changes in the TCB transmission during the run because of changes in viscosity at lower temperatures for example then this could lead to readings of the solute transmission at the end of the run being apparently negative. Therefore any reported negative soluble fraction must either be zero of slightly above zero.

5.2.5 DSC

DSC analyses were carried out on the different fractions using the experimental procedure as described in Section 3.2.7 (for the samples which have not been slow cooled).

5.3 RESULTS AND DISCUSSION

5.3.1 TREF analysis

Fractionations of Polymers G - J were carried out using our in-house built TREF system. We started out by fractionating the original Group 2 copolymers into seven different fractions, eluting at 25, 60, 75, 90, 120, 130, and 145°C. In this way we kept the weight of the fractions, except the 145°C fraction, relatively large (> 0.1 g) in order to make sure that each fraction was large enough for complete analysis. Figure 5.3 and Table 5.1 illustrates the TREF results for the various fractionation temperatures (T_fs) used during the first fractionation attempt of copolymer H. It is clear that the 25°C fraction makes out a large part (13.17%) of the original copolymer. The size of the fractions increased from the 60°C fraction to the largest fraction eluting at 120°C. Thereafter we found a decrease in the fraction size for the rest of the elution temperatures. A more accurate interpretation would however be to investigate the differential weight fraction to temperature ($W_i\%/\Delta T$) and accumulative weight fraction ($\Sigma W_i\%$) values rather than the individual fraction sizes. The reason for this being that when interpreting only the individual fraction sizes, the temperature range for the specific fractions is not taken into account.

We can therefore conclude that the 90°C fraction produced the highest mass of copolymer fraction when the temperature range for the various fractions is taken into consideration. According to the graph of the $W_i\%/\Delta T$ over the fractionation temperature in Figure 5.3 we find an increase in $W_i\%/\Delta T$ for the first three fractions collected after the 25°C fraction and then a decrease for the last three fractions. The mass of the fraction eluted at 145°C was very low and not nearly enough for complete analysis.

The recovery percentage for this specific TREF run was 99.02% and was always above 96% for the other runs. This type of recovery percentage values are considered very high. One possible explanation for the “lost” polymer is the entrapment of some lower molecular weight material between inert support and

the chains which crystallize easily at the high temperatures. These chains would be unable to elute while trapped below the chains still in crystalline form. Another possible factor is of course loss during the experimental handling of the sample.

Table 5.1 TREF fractionation data for the fractions of Polymer H (first fractionation attempt)

T_f (°C)	W_i (g)	W_i% (%)	ΣW_i% (%)	ΔT (°C)	W_i%/ΔT (%/°C)
25	0.39	13.17	13.17	25	0.53
60	0.12	4.00	17.16	35	0.11
75	0.24	7.92	25.09	15	0.53
90	0.84	28.30	53.38	15	1.89
120	1.07	35.87	89.25	30	1.20
130	0.29	9.67	98.91	10	0.97
145	0.03	1.09	100	15	0.07

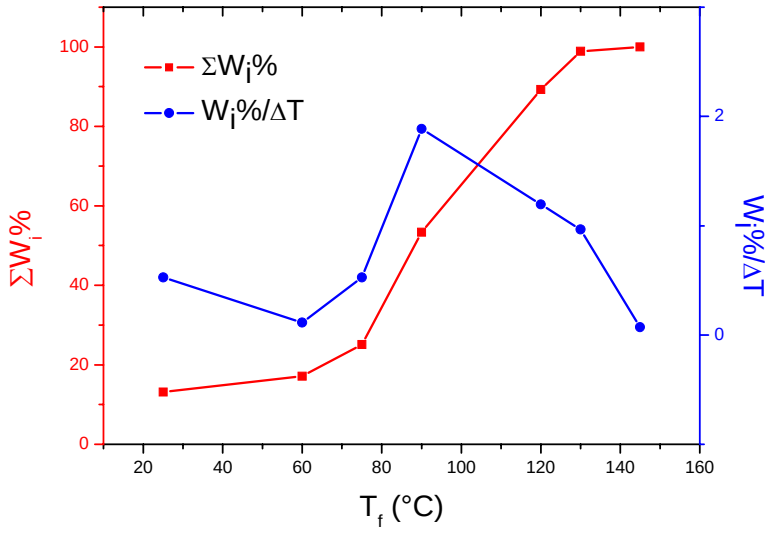

Figure 5.3 TREF results of the first fractionation of Polymer H

Although the size of these fractions was sufficient for a wide variety of analyses, it did not provide an accurate picture of the percentage of weight

distribution for the various fractions. This shortcoming was improved by increasing the amount of fractions taken during the elution step. Fractions were now taken every 5°C in order to give a much more reliable understanding of the molecular structure of the polymers. The TREF results of the refined fractionation method of copolymer H are shown in Table 5.2 and Figure 5.4. The lowest temperature fraction was no longer taken at 25°C, but at room temperature (RT) which differed for each run and was 19°C in this case. The RT and 25°C fractions added up to only 5.67% of the original polymer H. The main reason for this much lower value than in the case of the previous fractionation attempt (13.17%) is that the solvent level was higher than the sand level with the first TREF run. The copolymer which crystallized in the solvent above the sand level was therefore part of the lowest temperature fraction (25°). This did not happen in the second refined attempt. The sand and solvent levels were the same and all the crystallizable material crystallized on the inert sand support, therefore producing much more reliable results. The recovery percentage for this specific TREF run was 96.44%.

The RT fraction is relatively large compared to the following ten fractions up to the 75°C fraction. The reason for the size of this fraction then being the fact that it consists of a complex variety of different molecular chains, varying from low and high molecular weight atactic material to low molecular weight isotactic material. When comparing the quantity of the RT fraction with the extract from the standard xylene-soluble extraction (Section 4.3.2.1), it is found that the room temperature TREF fraction is ten times that of the XL fraction from the standard xylene-soluble extraction (in terms of weight percentage). This implicates that the quantity of extract strongly depends on the crystallization method. The first thirteen fractions following the RT fraction have very low $W_i\%/\Delta T$ values which increase gradually up to 0.66 for the 85°C fraction. The largest fractions are then found in the fractionation region from 90°C to 105°C, with the largest one eluted at 100°C. After the 100°C fraction there is a fast decrease in fraction size up to the 115°C fraction where after a more gradual decrease in the fraction size is followed.

Table 5.2 TREF fractionation data for the fractions of Polymer H (second fractionation attempt)

T_f (°C)	W_i (g)	W_i% (%)	ΣW_i% (%)	ΔT (°C)	W_i%/ΔT (%/°C)
19	0.16	5.42	5.42	19	0.29
25	0.01	0.24	5.67	6	0.04
30	0.01	0.17	5.84	5	0.03
35	0.01	0.17	6.01	5	0.03
40	0.01	0.18	6.19	5	0.04
45	0.01	0.21	6.39	5	0.04
50	0.01	0.26	6.66	5	0.05
55	0.01	0.34	7.00	5	0.07
60	0.01	0.44	7.44	5	0.09
65	0.02	0.66	8.11	5	0.13
70	0.03	1.15	9.25	5	0.23
75	0.04	1.48	10.74	5	0.30
80	0.06	2.07	12.80	5	0.41
85	0.10	3.32	16.12	5	0.66
90	0.20	6.73	22.86	5	1.35
95	0.73	25.23	48.09	5	5.05
100	0.99	34.11	82.20	5	6.82
105	0.36	12.43	94.63	5	2.49
110	0.10	3.31	97.93	5	0.66
115	0.03	0.98	98.91	5	0.20
120	0.01	0.39	99.30	5	0.08
125	0.01	0.41	99.71	5	0.08
130	0.01	0.29	100	5	0.06

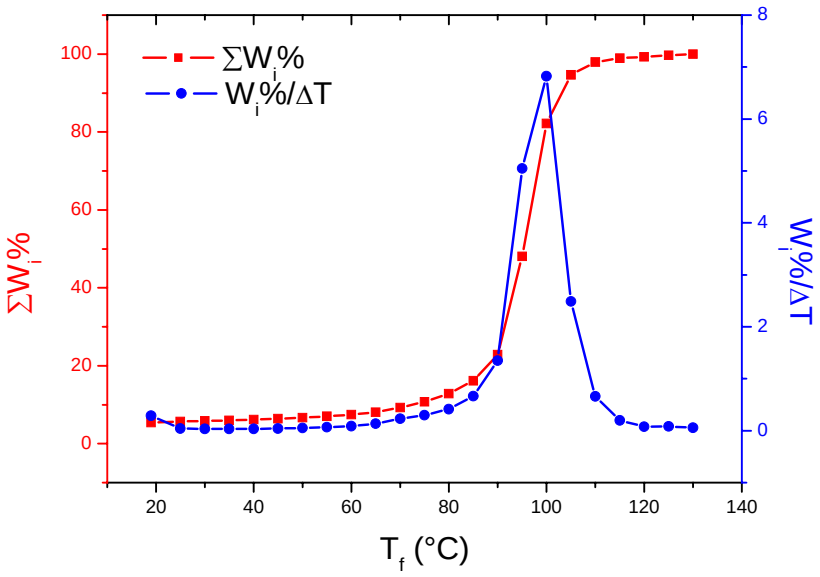

Figure 5.4 TREF results of the second fractionation of polymer H

From the graph in Figure 5.4 it is clear that when using smaller temperature intervals for the different fractions it reveals a much clearer and more refined picture of the molecular make-up of the copolymer. We therefore also fractionated the rest of the copolymers of Group 2 according to the predetermined temperatures used in the second TREF attempt of Polymer H in order to compare the weight fraction percentages of the different polymers. These comparisons are illustrated in Table 5.3 and Figures 5.5, 5.6 and 5.7.

From Table 5.3 we can see that the RT fractions of Polymers G and H were the largest by far and almost double of that eluted for Polymers I and J. This means that the copolymers of G and H contain a significant amount more of the xylene soluble low molecular weight material. This is significant in terms of the Si:Ti ratio; it appears to influence the percentage of xylene soluble material eluted during TREF.

Table 5.3 TREF fractionation data for the fractions of Polymers G - J (second fractionation attempt)

	G		J		H		I	
T_f (°C)	W_i% (%)	W_i%/ΔT (%/°C)	W_i% (%)	W_i%/ΔT (%/°C)	W_i% (%)	W_i%/ΔT (%/°C)	W_i% (%)	W_i%/ΔT (%/°C)
RT	4.60	0.24	2.67	0.14	5.42	0.29	2.61	0.14
25	0.42	0.07	0.23	0.04	0.24	0.04	0.36	0.06
30	0.39	0.08	0.17	0.03	0.17	0.03	0.08	0.02
35	0.29	0.06	0.20	0.04	0.17	0.03	0.12	0.02
40	0.30	0.06	0.21	0.04	0.18	0.04	0.16	0.03
45	0.35	0.07	0.22	0.04	0.21	0.04	0.20	0.04
50	0.36	0.08	0.24	0.05	0.26	0.05	0.22	0.04
55	0.42	0.08	0.31	0.06	0.34	0.07	0.28	0.06
60	0.53	0.11	0.39	0.08	0.44	0.09	0.29	0.06
65	0.85	0.17	0.62	0.12	0.66	0.13	0.40	0.08
70	1.63	0.33	0.59	0.12	1.15	0.23	0.39	0.08
75	2.93	0.59	1.04	0.21	1.48	0.30	0.69	0.14
80	1.87	0.37	1.97	0.39	2.07	0.41	1.33	0.27
85	2.49	0.50	2.45	0.49	3.32	0.66	3.01	0.60
90	6.15	1.23	4.52	0.90	6.73	1.35	5.61	1.12
95	8.14	1.63	16.59	3.32	25.23	5.05	34.74	6.95
100	25.20	5.04	37.93	7.59	34.11	6.82	33.86	6.77
105	22.07	4.41	19.20	3.84	12.43	2.49	10.88	2.18
110	12.88	2.58	8.17	1.63	3.31	0.66	2.50	0.50
115	6.38	1.28	1.37	0.27	0.98	0.20	0.65	0.13
120	1.04	0.21	0.33	0.07	0.39	0.08	0.51	0.10
125	0.37	0.07	0.23	0.05	0.41	0.08	0.48	0.10
130	0.35	0.07	0.35	0.07	0.29	0.06	0.64	0.13

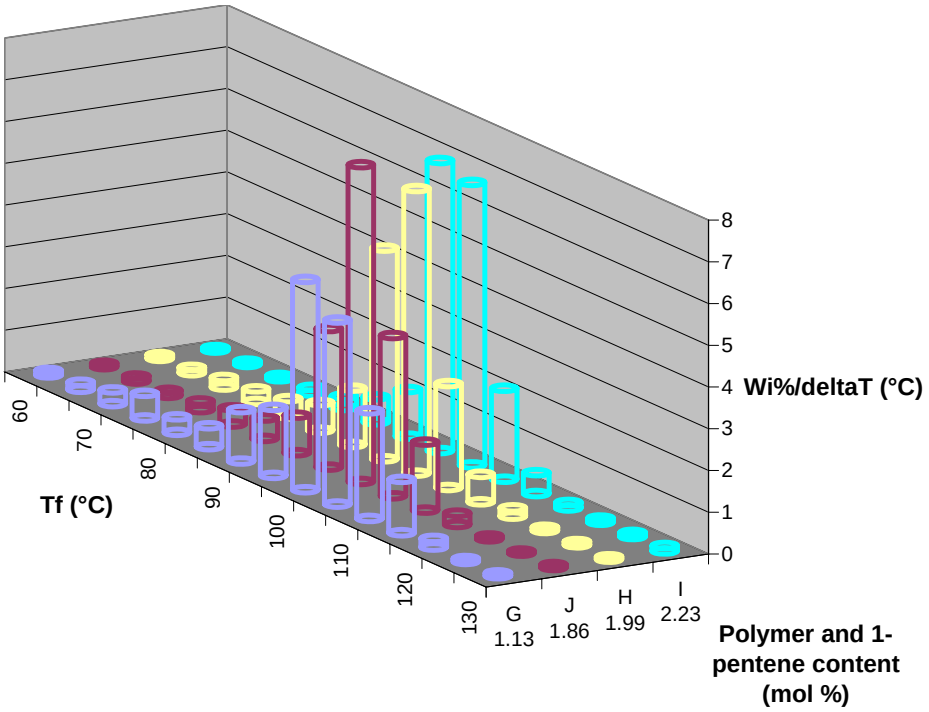

Figure 5.5 Three dimensional illustration of $W_i\%/\Delta T$ values of Polymers G - J for fractionation temperatures from 60°C to 130°C

Table 5.3 and Figure 5.5 also show that most of the material for all four polymers is eluted between 90°C and 110°C. Polymer J has the most defined peak elution temperature which is visible at 100°C. Polymer H also has a well defined peak elution temperature at 100°C, but not as well defined as in the case of Polymer J. Polymer G shows a broad peak temperature consisting of the two fractions eluted at 100°C and 105°C. Polymer I also shows a broad peak temperature, but in this case it consists of the fractions eluted at 95°C and 100°C.

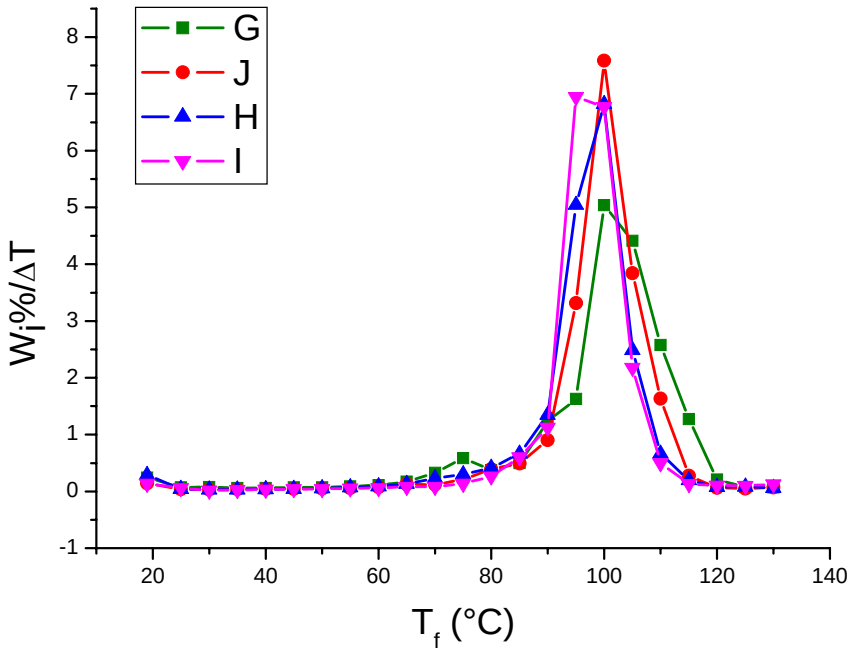

Figure 5. 6 Graphs for Polymers G - J of the derivatives of the weight fraction percentages vs the fractionation temperatures

The superimposed graphs from Figure 5.6 clearly indicate that the fractions become significantly larger only after 90°C. It is clear from the graphs that Polymer G has the broadest distribution of molecular species, followed by Polymer J, then Polymer H and Polymer I seems to have the narrowest distribution. In other words, the narrowness of these peaks increases with an increase in comonomer content of the copolymers. This indicates that a more homogeneous distribution of molecular species in the copolymer may be correlated to an increase in 1-pentene content. The distribution of molecular species in a copolymer is not simply a measure of the distribution of the comonomer throughout the copolymer, but it rather gives an indication of the degree of variation in the crystallizability of the copolymer chains. The crystallizability is again of course affected by the degree of 1-pentene inclusion as well as factors such as tacticity, molecular weight and rate of crystallization of the copolymer. The higher 1-pentene content might therefore be an indication of

more xylene soluble material present and then leaving more crystallizable material.

A further interesting observation is the significant increase in $W_i\%/\Delta T$ in the order G, J, H, I for the 95°C fraction and the decrease in $W_i\%/\Delta T$ in the same order for the fractions collected from 105°C to 115°C.

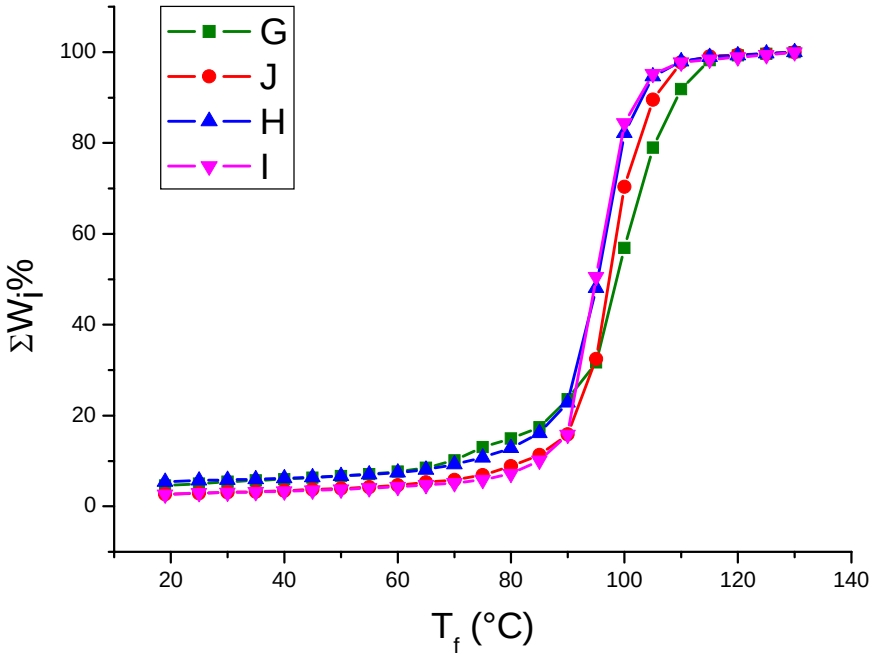

Figure 5.7 Graphs for Polymers G - J of the sum of the weight fraction percentages vs the fractionation temperatures

Figure 5.7 illustrates the accumulative weight fraction percentage vs the fractionation temperatures of Polymers G - J. We find the most significant increase in the graphs of Figure 5.6 for the fractions collected between 90°C and 110°C. For this range there is a definite increase in the sum of the weight fraction percentage as the 1-pentene content of the original copolymers increases, that's to say in the order G, J, H, I.

5.3.2 ^{13}C-NMR

In order to investigate the molecular structure of the different TREF fractions of the original copolymers with ^{13}C-NMR, sufficient weights of fractions were needed. We therefore used the fractions eluted by the first TREF attempt of copolymer H. These fractions were collected at 25°C, 60°C, 75°C, 90°C, 120°C, 130°C and 145°C. The 145°C fraction was unfortunately too small for ^{13}C-NMR analysis.

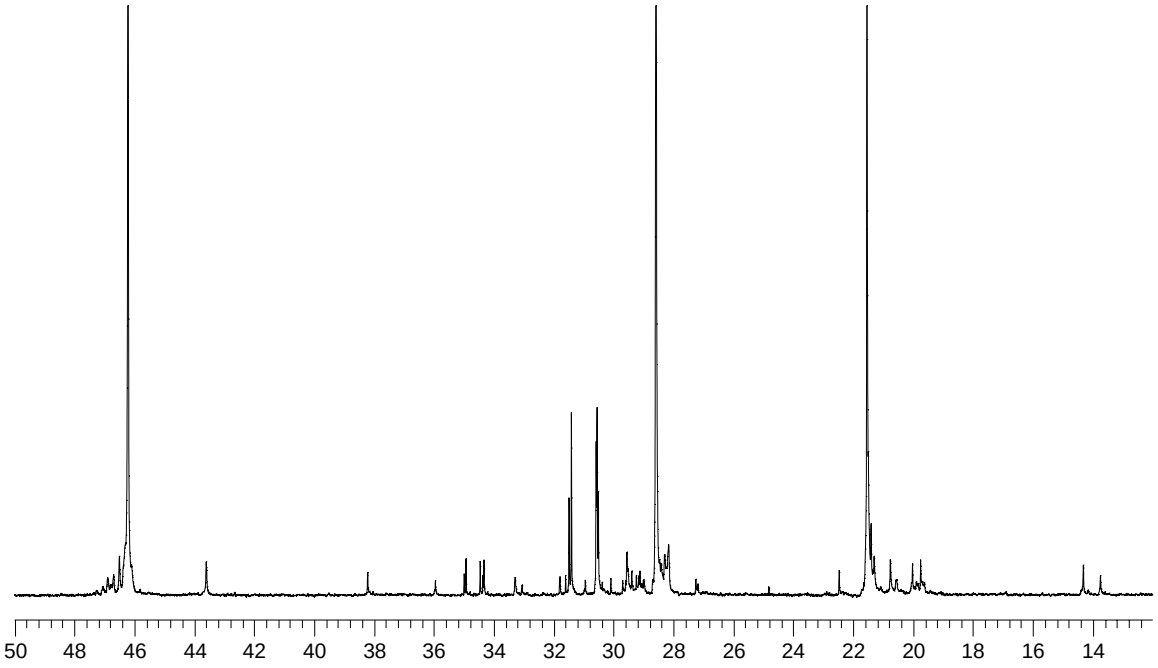

Figure 5.8 ^{13}C-NMR of the 25°C fraction from the first TREF attempt of Polymer H

As explained earlier, in the first fractionation attempt, the level of the solvent was higher than that of the sand during the cooling down step and some of the copolymer therefore crystallized in solution and not on the support. The ^{13}C-NMR spectrum in Figure 5.8 therefore represents the copolymer which crystallized in solution as well as the material soluble in xylene.

This ^{13}C-NMR spectrum shows the presence of a variety of end groups: the standard *n*-propyl, *n*-hexyl, *iso*-pentyl end groups and the *n*-propyl end group on the other side of the chain. The two high intensity peaks appearing between 30 - 32 ppm means that this RT fraction consists of low M_w material with a significant high concentration of *n*-propyl end groups.

Figure 5.9 illustrates the ^{13}C-NMR results of the various TREF fractions of Polymer H and Table 5.4 shows the different calculated comonomer contents for the specific fractions as well as the original commercial copolymer. According to Figure 5.9 and Table 5.4 there is a clear decrease in the 1-pentene content as the fractionation temperature is increased. The exception with relevance to the 1-pentene content is the 25°C fraction. The decrease in comonomer content with increasing T_f can be explained in terms of the comonomer reducing the ability of the chains to crystallize. The chains containing less comonomer would be able to crystallize at higher temperatures and therefore be eluted at higher temperatures. Chains containing the most of the 1-pentene would then, according to this explanation, be eluted at the lower temperatures. This trend in comonomer inclusion of the various fractions was observed for the fractionation of all our copolymers and corresponds with literature [5, 7, 12-14].

The reason for the exception in the trend with relevance to the 25°C fraction is because of the complexity of this XS-fraction, as also explained earlier with the xylene extractions, as well as the fact that it not only contains xylene soluble material but also some copolymer crystallized in solution. From the results in Table 5.4 we can conclude that most of the 1-pentene is included into the smaller, less significant weight fractions which were eluted at 90°C and below. According to the TREF weight fraction results these fractions make out less than 35% of the ΣW_i% of the original copolymers. The significant weight fractions ($T_f \geq 90$°C) from Figure 5.9 contain very low amounts of 1-pentene (< 1.5 mol %) compared to the average value for Polymer H (1.99 mol %).

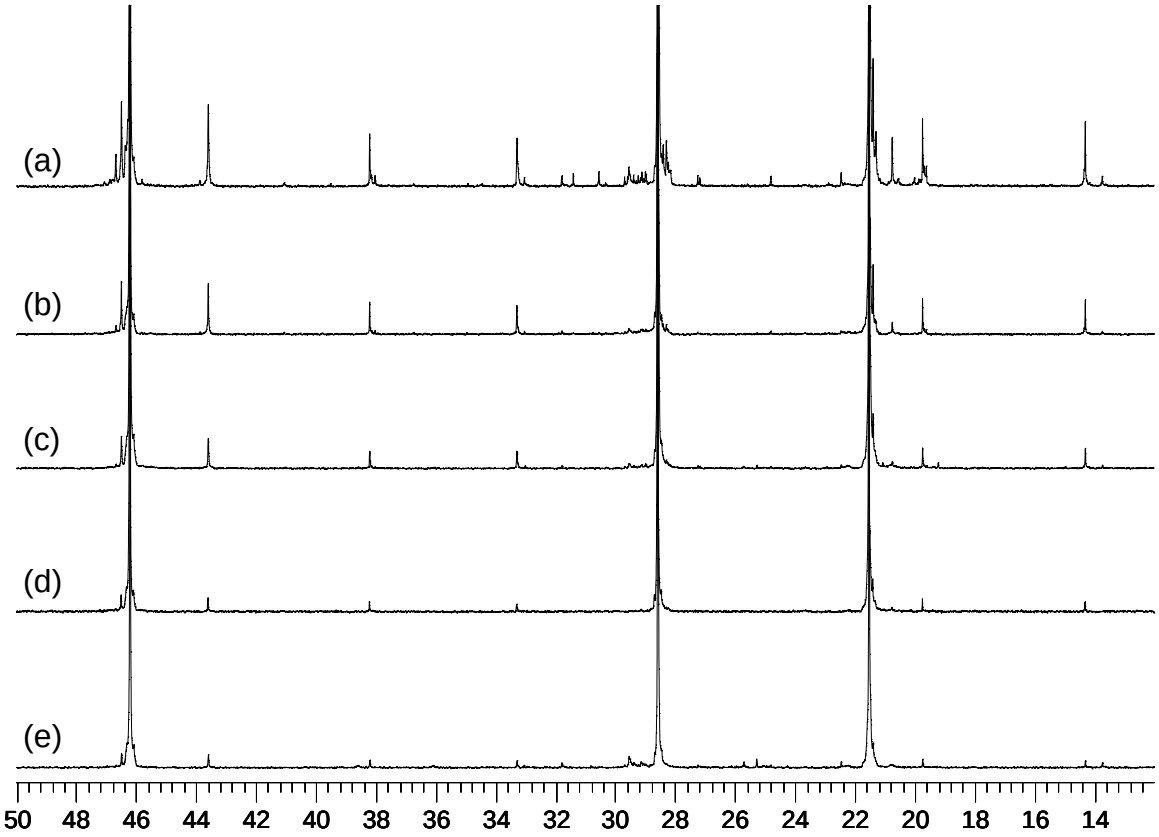

Figure 5.9 **^{13}C-NMR of the a) 60°C, b) 75°C, c) 90°C, d) 120°C and e) 130°C fractions of the first TREF attempt of Polymer H**

Table 5.4 **1-Pentene content (determined by ^{13}C-NMR) of the fractions of Polymer H**

T_f (°C)	1-Pentene content (mol %)
Original	1.99
25	1.45
60	3.48
75	2.32
90	1.35
120	0.67
130	0.66

When investigating the methyl regions of the fractions from Figure 5.9 more closely in Figure 5.10 it seems as if there is an increase in the tacticity for an increase in fractionation temperature. The increase in tacticity is seen in the decrease in intensity of the shoulder peaks of the *mmmm* pentad of the propylene methyl peak. The tacticity increases with an increase in the 1-pentene content of the fractions. Note that the tacticity increase is not necessarily due to the 1-pentene decrease as ^{13}C-NMR measures the number of stereochemical identical CH_3's in a chain. As discussed earlier it is unfortunately not possible to calculate the tacticities of these fractions due to the overlapping of the methylene peak in the 1-pentene side-chain with the *mrrr* steric pentad signal of the propylene methyl peak area.

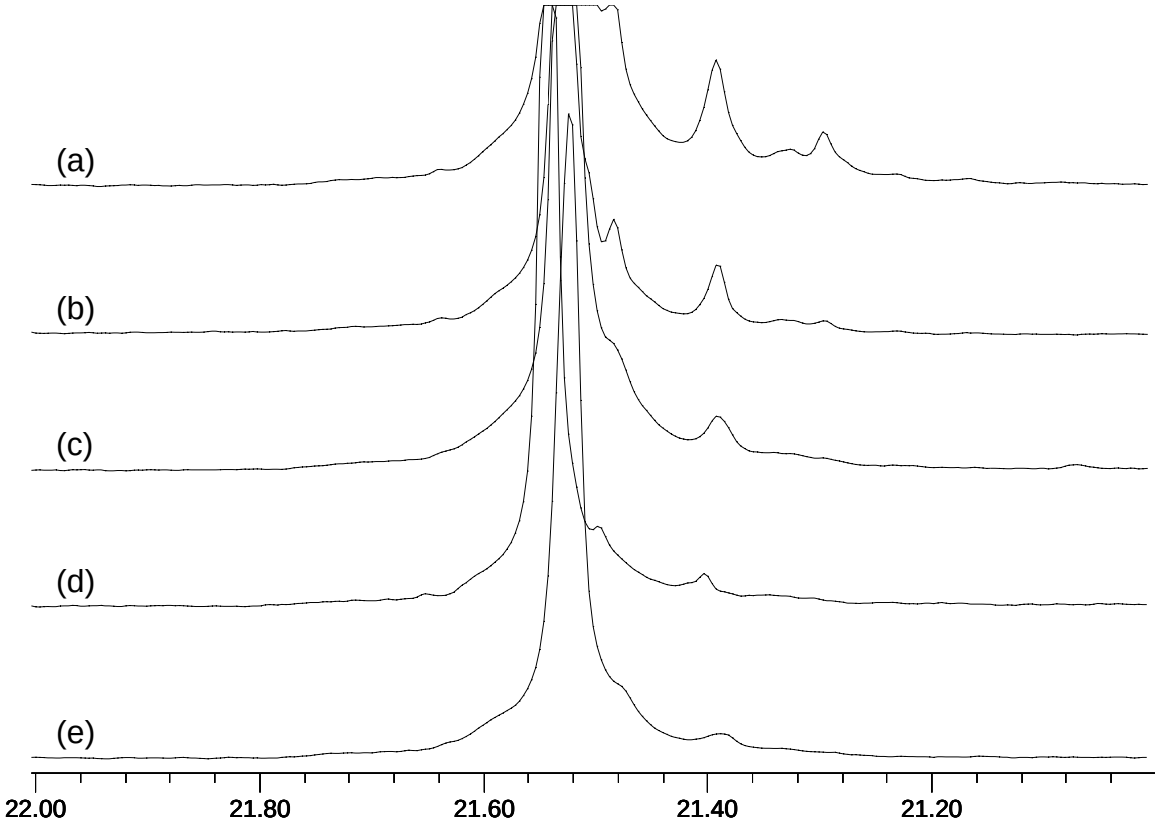

Figure 5.10 ^{13}C-NMR of the methyl region of the a) 60°C, b) 75°C, c) 90°C, d) 120°C and e) 130°C fractions of the first TREF attempt of Polymer H

A second ^{13}C-NMR analysis attempt of the fractionated material was carried out in order to compare the comonomer content distribution between two copolymers, Polymer G and Polymer I. These two copolymers were fractionated according to the more accurate procedure where there was no crystallizable material present in the room temperature fraction. Fractions were collected at room temperature, 60°C, 75°C, 90°C, 105°C and 130°C and the 1-pentene contents of these fractions were compared for the two copolymers.

Table 5.5 shows the weight fractions and comonomer contents (mol % and weight %) of the original Polymers G and I as well as their TREF fractions. Accurate integration of the relevant peaks in the ^{13}C-NMR spectra of the room temperature fractions was not possible due to overlapping of either end group peaks or branching carbon peaks of the 1-pentene side chain. The comonomer content detail of these fractions is therefore omitted.

Table 5.5 Weight fractions and 1-pentene content (mol % and weight %) of Polymers G and I and their TREF fractions

T_f (°C)	Polymer G: weight fraction (g)	Polymer G: 1-pentene content (mol %)	Polymer G: 1-pentene content (weight %)	Polymer I: weight fraction (g)	Polymer I: 1-pentene content (mol %)	Polymer I 1-pentene content (weight %)
Original	3.00	1.13	1.86	3.00	2.23	3.61
RT	0.15	-	-	0.19	-	-
60	0.06	1.02	1.70	0.12	3.38	5.51
75	0.10	1.64	2.70	0.29	4.64	7.49
90	0.36	2.27	3.72	0.79	2.86	4.69
105	1.76	1.37	2.26	1.37	1.50	2.47
130	0.53	0.09	0.00	0.18	0.00	0.00

Figures 5.11 and 5.12 illustrate the TREF and ^{13}C-NMR data given in Table 5.5. The bubbles in the figures represent the 1-pentene content (weight %) in the various fractions of the two copolymers. In both graphs it is clear that the most of the 1-pentene is distributed in the lower weight fractions ($<$ 0.8 g). Polymer G and I differ greatly in their Si:Ti ratios; Polymer G has a Si:Ti ratio of 2.2 and Polymer I of 6.8. According to Table 5.5 and Figures 5.11 and 5.12 this

difference has a definite influence on the distribution of the 1-pentene in the copolymers. In the case of Polymer G the 90°C fraction has the highest 1-pentene content, whereas for Polymer I the 75°C fraction has the highest 1-pentene content. Although Polymer I has almost double the 1-pentene weight % value of that for Polymer G, the weight % of the 105°C fraction has almost the same value. A very important conclusion from these results is that an increase in the donor:catalyst ratio does not affect the highest weight fraction significantly, but greatly affects the 1-pentene content of the lower weight fractions (< 0.80), which are also the lower fractionation temperature fractions ($\leq$90°C). A higher the Si:Ti ratio leads to a higher 1-pentene weight % in the lower weight fractions. More specifically, the 75°C fraction is affected the most when the Si:Ti ratio is increased.

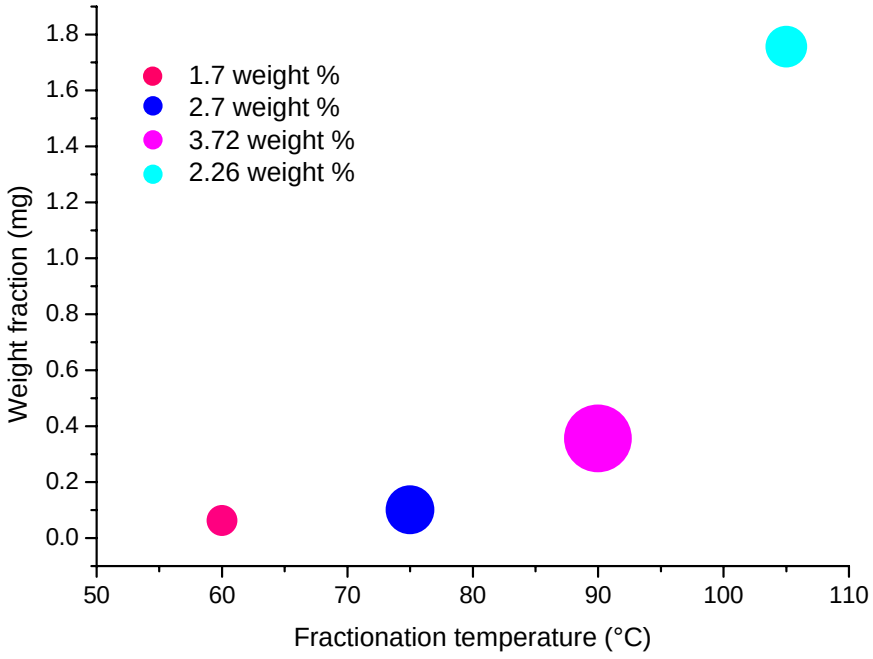

Figure 5.11 Illustration of 1-pentene (weight %) distribution in Polymer G

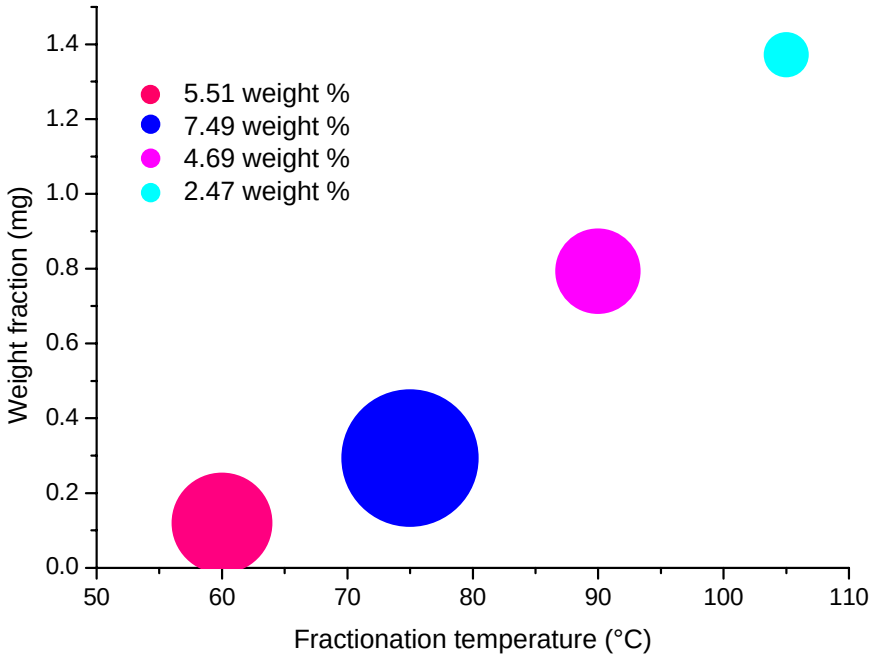

Figure 5.12 Illustration of 1-pentene (weight %) distribution in Polymer I

5.3.3 Thermal Analysis

Figures 5.13 and 5.18 show the CRYSTAF curves of the fractionated samples of Polymers G and I respectively. The fractionation of the material was carried out at RT, 50°C, 60°C and then every 5°C up to 115°C with a last fraction at 130°C (as described earlier in Section 5.2.1) and enough material was collected for each sample for CRYSTAF, DSC and HT-GPC analysis. The crystallization results of the 105°C fraction of Polymer G and the 110°C of Polymer I were left out due to experimental error. The CRYSTAF results of the RT and 50°C fractions are not included because these samples showed no crystallization properties during CRYSTAF analysis.

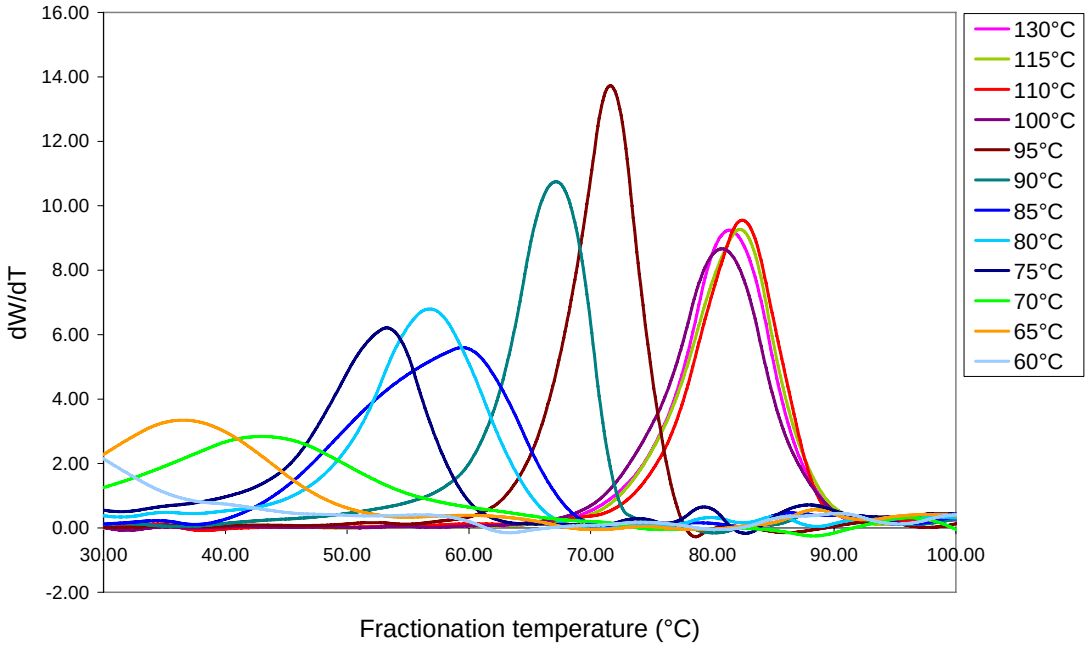

Figure 5.13 CRYSTAF spectra of TREF fractions of Polymer G

As indicated by Figure 5.13 and Table 5.6 there is a definite increase in the peak crystallization temperature of the fractions eluted from 60°C to 110°C. We know from the microstructure analysis that there is a decrease in the 1-pentene content and an increase in the tacticity with the increase in fractionation temperature. These microstructure properties must therefore lead to more easily crystallizable fractions as the fractionation temperature increases. This means that the less 1-pentene the fraction contains, the less difficult it is for the chains to crystallize, and thus the crystallization temperature increases. This result corresponds very well with both research carried out on the influence of the ethylene unit as comonomer on the crystallization behaviour of poly(propylene-*co*-ethylene)s [15] and the crystallization behaviour of fractions of a copolymer of propene and 1-hexane [16]. According to the mentioned publications the comonomer units act as defects in the chain structure and impede the crystallization of the chains.

The peak crystallization temperatures for the fractions from 100°C to 130°C are however more or less the same. It seems therefore that the microstructure and chain lengths of these fractions must differ very little.

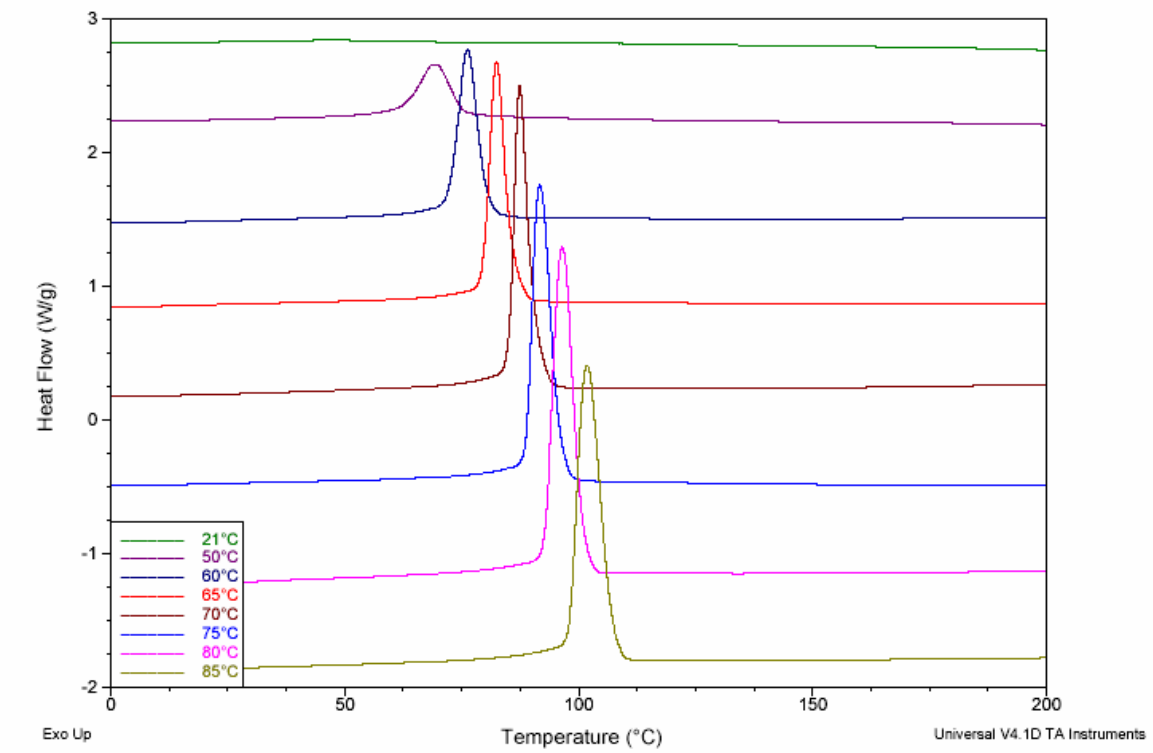

Figure 5.14 Waterfall graphs of the DSC crystallization thermograms of the first 8 fractions of Polymer G

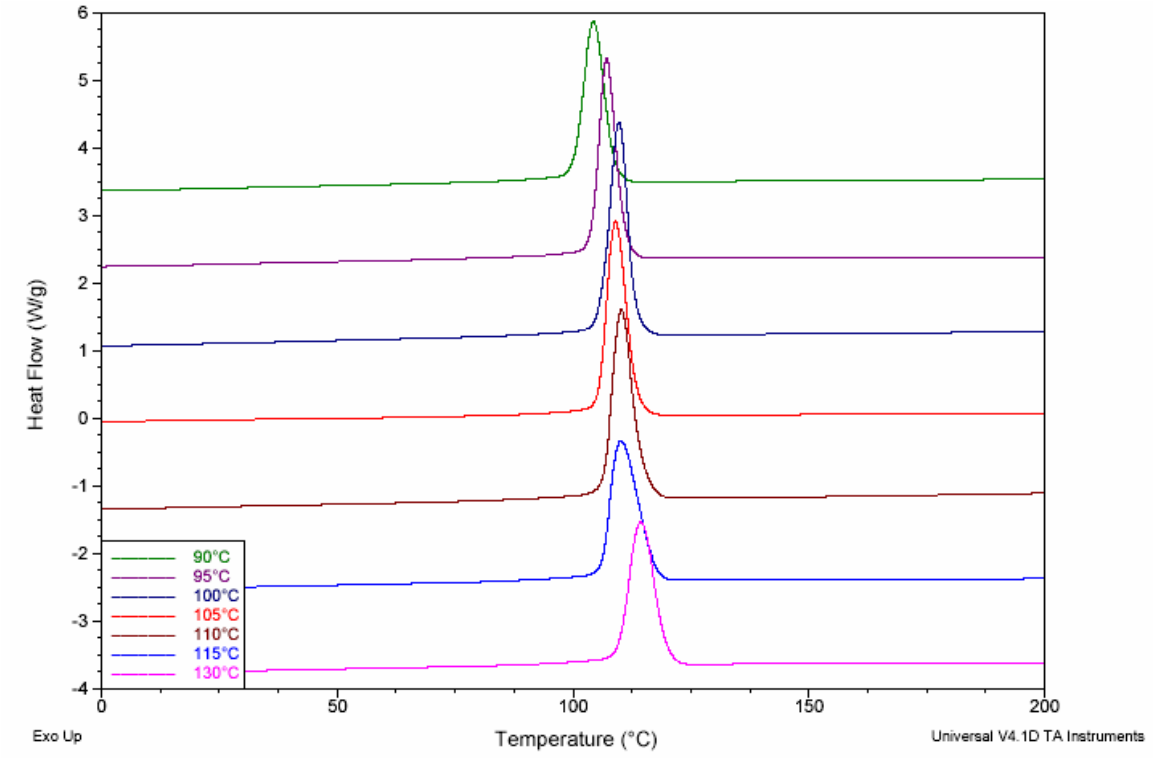

Figure 5.15 Waterfall graphs of the DSC crystallization thermograms of the last 7 fractions of Polymer G

Figures 5.14 and 5.15 illustrate the waterfall plots of the DSC crystallization thermograms for the fractions of copolymer G. (The graphs are offset in the y-direction.) The RT fraction shows no visible crystallization peak. In the ^{13}C-NMR analysis of Section 5.3.2 we've shown that this fraction consists of mainly atactic material and some low molecular weight isotactic material. The low tacticity and short chains of this fraction therefore leads to the non-crystallizabilty of this fraction. The fractions from 50°C to 100°C show an increase in peak crystallization temperature and an almost constant peak crystallization temperature for the fractions from 100°C to 115°C as in the case of the CRYSTAF results. According to Table 5.6, however, the peak crystallization temperatures from the CRYSTAF analyses are significantly lower than those from the DSC analyses. The CRYSTAF analysis takes place in solution and the chains therefore have much more mobility to rearrange and thus crystallize more

easily and at lower temperatures than in the case of the molten state of the sample used in DSC analysis.

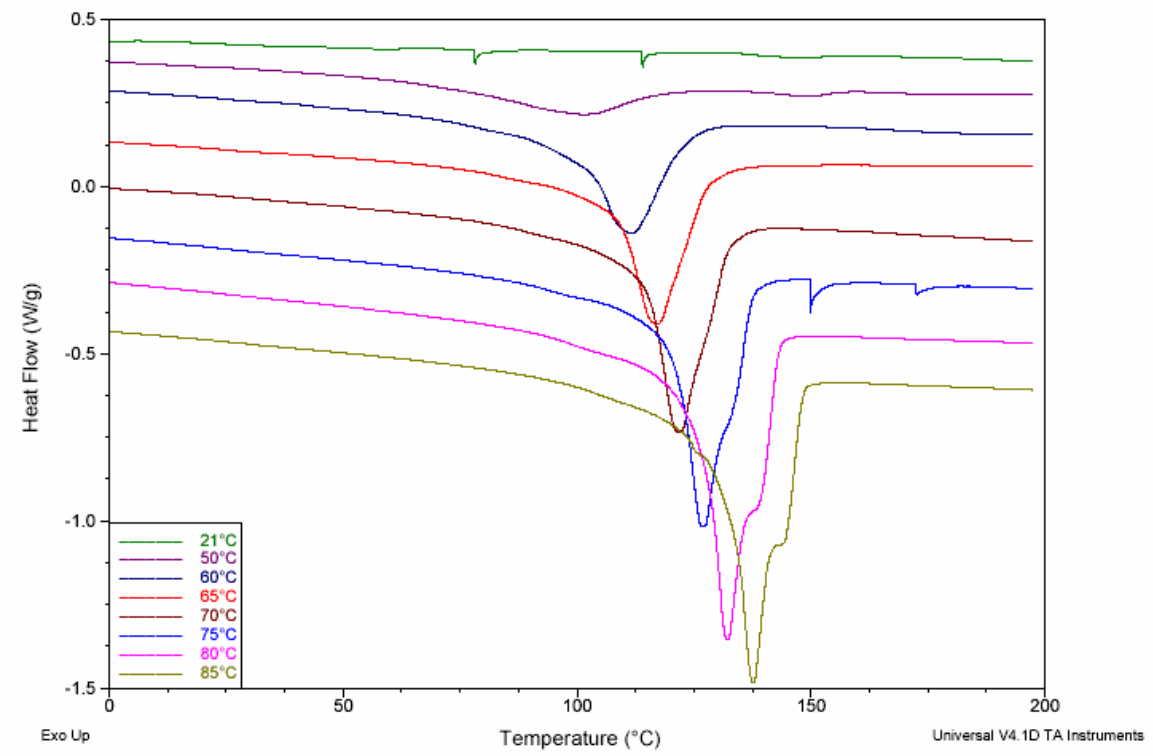

Figure 5.16 Waterfall graphs of the DSC melting thermograms of the first 8 fractions of Polymer G

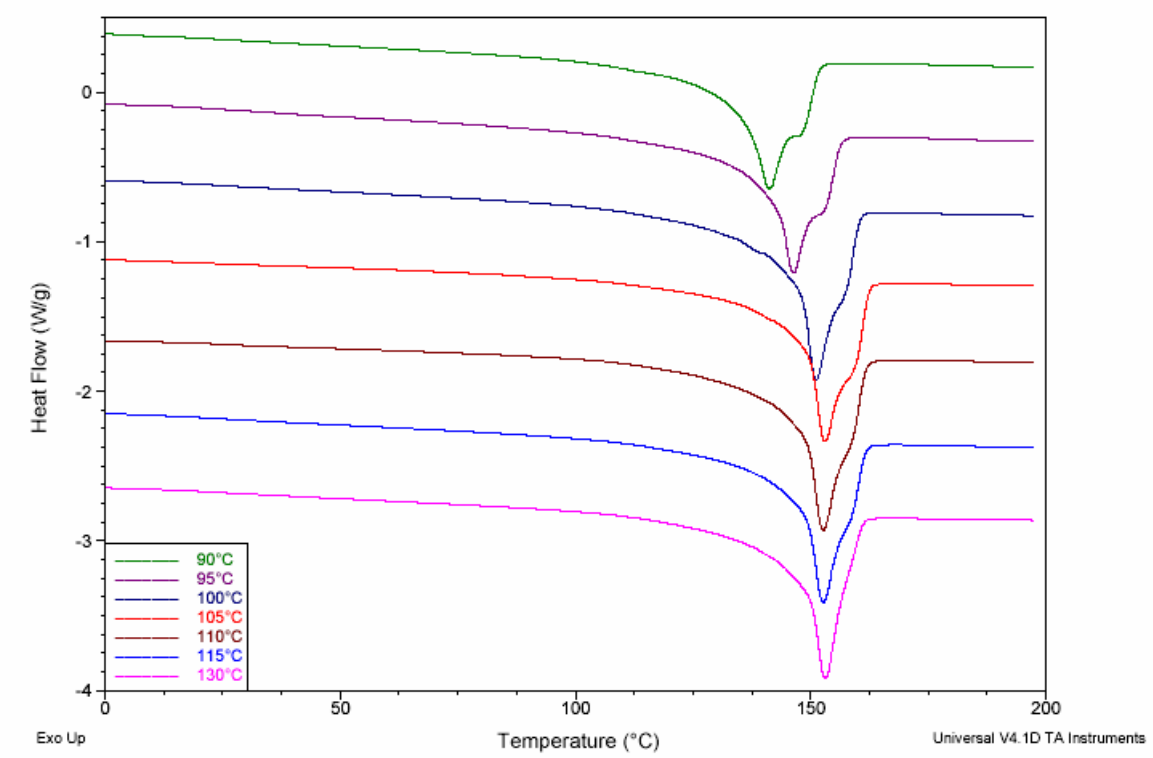

Figure 5.17 Waterfall graphs of the DSC melting thermograms of the last 7 fractions of Polymer G

Figures 5.16 and 5.17 illustrate the waterfall plots of the DSC melting thermograms for the fractions of copolymer G. (The graphs are offset in the y-direction.) Anomalies in Figure 5.16 are due to experimental errors and may be ignored. According to these figures as well as Table 5.6 there is a definite increase in the melting temperatures of the fractions with an increase in fractionation temperature. The RT fraction once again showed no detectable melting endotherm due to the low tacticity and low molecular weight of this fraction. The further fractions showed an increase in melting temperature up to the 105°C. Thereafter there was an almost constant melting temperature for the remainder of the fractions (105°C – 130°C). These almost similar melting and crystallization properties of the highest temperature fractions needed further investigation in order to explain this phenomenon.

Table 5.6 Summary of CRYSTAF and DSC data of the fractions of Polymer G

Fraction	T_c (CRYSTAF) (°C)	Soluble. Fract. (CRYSTAF) (%)	T_c (DSC) (°C)	Crystallinity (%)	T_m (DSC) (°C)
G (21°C)	N.D.	88.7	N.D.	N.D.	N.D.
G (50°C)	N.D.	76.8	69.01	10.01	99.65
G (60°C)	25.7	34.3	76.24	25.63	111.14
G (65°C)	36.5	21.1	82.41	29.95	117.03
G (70°C)	43	19.9	87.35	35.84	121.58
G (75°C)	53.2	6.9	91.69	31.81	127.01
G (80°C)	56.8	3.3	96.48	42.51	132.07
G (85°C)	59.4	0.9	101.79	45.20	137.52
G (90°C)	67.2	1	104.36	66.27	141.08
G (95°C)	71.6	0.2	107.11	71.63	146.24
G (100°C)	80.8	5.6	109.72	78.66	151.20
G (105°C)	-	-	109.04	49.47	152.96
G (110°C)	82.5	8	110.29	70.91	152.60
G (115°C)	82.3	9.5	110.14	72.97	152.67
G (130°C)	81.4	10.6	114.34	68.90	153.11

Table 5.6 gives a summary of the crystallization and melting data collected by CRYSTAF and DSC for the fractions of copolymer G. The high percentage of solubility for the RT and the 50°C fraction from the CRYSTAF analysis also explains why no clear peak crystallization temperature could be detected for these two fractions. The percentage of soluble fraction then decreases with an increase in fractionation temperature, up to the 95°C fraction. This corresponds with the fact that more material is able to crystallize due to the decrease in 1-pentene content. There seems to be a slight increase in the percentage of soluble fraction from the 100°C fraction to the 130°C fraction. One reason for this may be the presence of degraded material which is not able to crystallize due to their very low molecular weight. Another possibility is that some low molecular weight material may be entrapped between the inert support and the chains crystallizing at higher temperatures. There is also a general increase in the percentage of crystallinity of the fractions as the fractionation temperature is increased. The decreasing 1-pentene content causes less hindrance in the crystallinity.

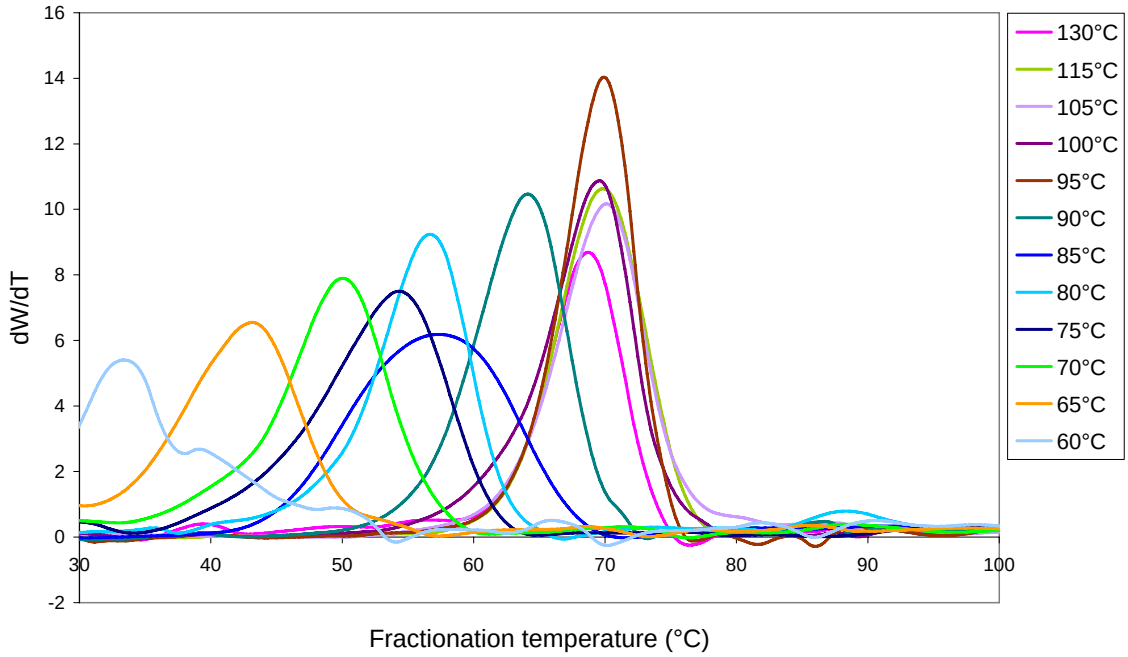

Figure 5.18 CRYSTAF spectra of TREF fractions of Polymer I

As with the fractions from copolymer G the same trend of an increase in peak crystallization temperature with the increase in fractionation temperature can be observed in Figure 5.18 and Table 5.7 in the case of copolymer I. This increase can be seen for the fractions collected between 60°C and 95°C. Thereafter we see almost a constant peak crystallization temperature for the rest of the fractions.

Table 5.7 shows the thermal data received from the CRYSTAF and DSC analyses of the fractions of Polymer I. The CRYSTAF results from Table 5.7 show that the percentage of soluble fraction of each of the first two fractions collected from the TREF of copolymer I is higher than 50%. Thereafter the soluble fraction decreases. There is a turning point at 100°C where after there is an increase in the percentage of soluble fraction for the remainder of the fractions.

From the DSC results there is a general increase in the crystallization temperature for the fractions from 50°C to 110°C where after the T_c starts to decrease. We can see the same trend for the melting temperatures, but the

decrease already starts after the 105°C fraction. The crystallinity also increases with an increase in fractionation temperature and starts to decrease after the 100°C fraction. The increase in these temperature parameters with the increasing fractionation temperature, is due to a decrease in the comonomer content. The decreasing trend for the last few fractions might be due to copolymer starting to degrade at the high temperatures or entrapment of low molecular weight material between the inert support and chains crystallizing at high temperatures, as in the case of Polymer G.

Table 5.7 Summary of CRYSTAF and DSC data of the fractions of Polymer I

Fraction	T_c (CRYSTAF) (°C)	Soluble. Fract. (CRYSTAF) (%)	T_c (DSC) (°C)	Crystallinity (%)	T_m (DSC) (°C)
I (21°C)	N.D.	50.8	N.D.	N.D.	N.D.
I (50°C)	N.D.	65.5	77.14	18.79	101.05
I (60°C)	33.4	14.1	93.78	29.46	116.35
I (65°C)	43.2	6.2	99.25	31.99	123.16
I (70°C)	50	2.3	103.81	46.71	127.10
I (75°C)	54.3	0.4	106.33	55.07	132.42
I (80°C)	56.7	-0.8	108.57	60.33	136.01
I (85°C)	57.3	-1.2	108.07	62.06	138.23
I (90°C)	64.1	-0.6	105.58	63.30	141.87
I (95°C)	69.9	-1.1	108.36	68.76	146.09
I (100°C)	69.6	-3.6	108.94	72.97	149.07
I (105°C)	70.1	1	111.22	70.62	149.67
I (110°C)	-	-	112.98	57.13	149.56
I (115°C)	69.8	1.8	110.62	48.66	148.13
I (130°C)	68.7	25.4	101.82	25.77	138.56

Figure 5.19 compares the peak melting temperatures of the fractions of copolymer G with those of the fractions of copolymer I. For the fractions from 50°C to 90°C we can clearly see that the peak melting temperatures are higher for copolymer I. The fractions eluted at 95°C have almost the same peak melting temperatures and thereafter we see the higher peak melting temperatures for the fractions of copolymer G.

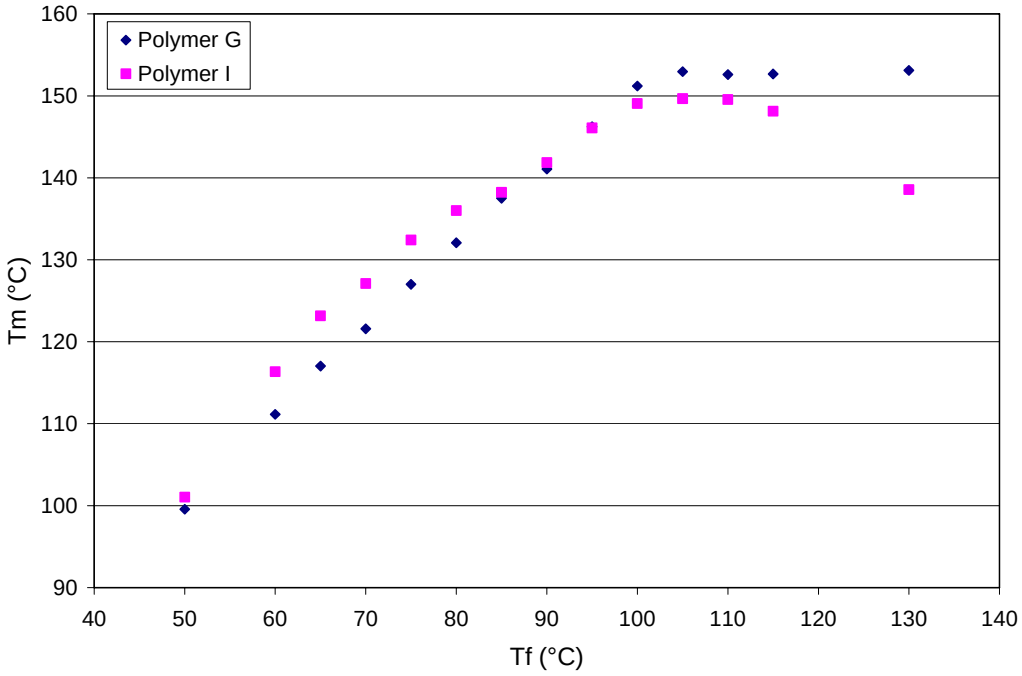

Figure 5.19 DSC peak melting temperatures of TREF fractions of copolymers G and I

Figure 5.20 illustrates a comparison between the peak crystallization temperatures of the various fractions of Polymers G and I. We can see that the fractions of Polymer I show much higher T_c values for fractionation temperatures up to 85°C. There after the fractions of the two copolymers show very much the same T_c values, except for the 130° C fraction for which Polymer G shows the highest T_c.

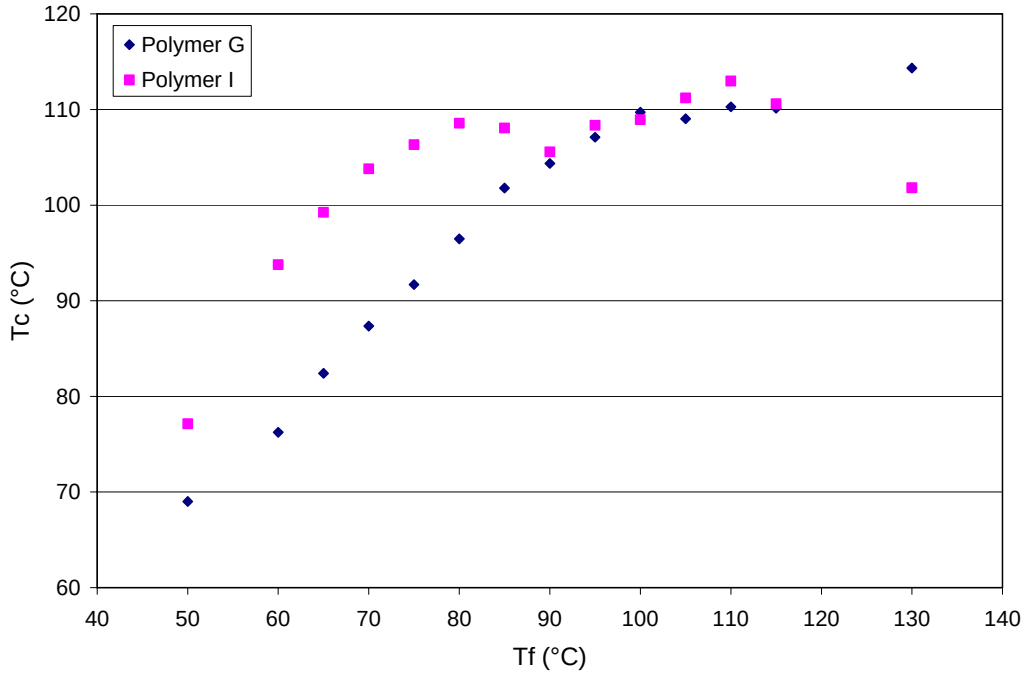

Figure 5.20 DSC peak crystallization temperatures of TREF fractions of copolymers G and I

One reason for these major differences between the peak crystallization and melting temperatures of the fractions of copolymers G and I eluted at low temperatures (≤ 90°C) is related to the distribution of the comonomer in the two copolymers. According to the ^{13}C-NMR results from Section 4.3.2 the higher Si:Ti ratio of Polymer I (6.8) leads to a significant increase in 1-pentene weight % in the lower fractionation temperature fractions (≤ 90°C) compared to Polymer G with the lower Si:Ti ratio (2.2). The fractions with higher 1-pentene content than other fractions eluted at the same temperature therefore have higher crystallization temperatures and lower melting points. Another important influence of the Si:Ti ratio from the thermal results is the much higher percentage of CRYSTAF soluble fractions for the fractions of Polymer G which has a lower Si:Ti ratio (2.2) than Polymer I (6.8).

Figures 5.21 and 5.22 shows contour maps of the CRYSTAF crystallization temperatures of the fractionated material of Polymers G and I

respectively. From these illustrations it is clear that the crystallization properties of these two copolymers differ significantly due to the influence of different Si:Ti ratios in the copolymers.

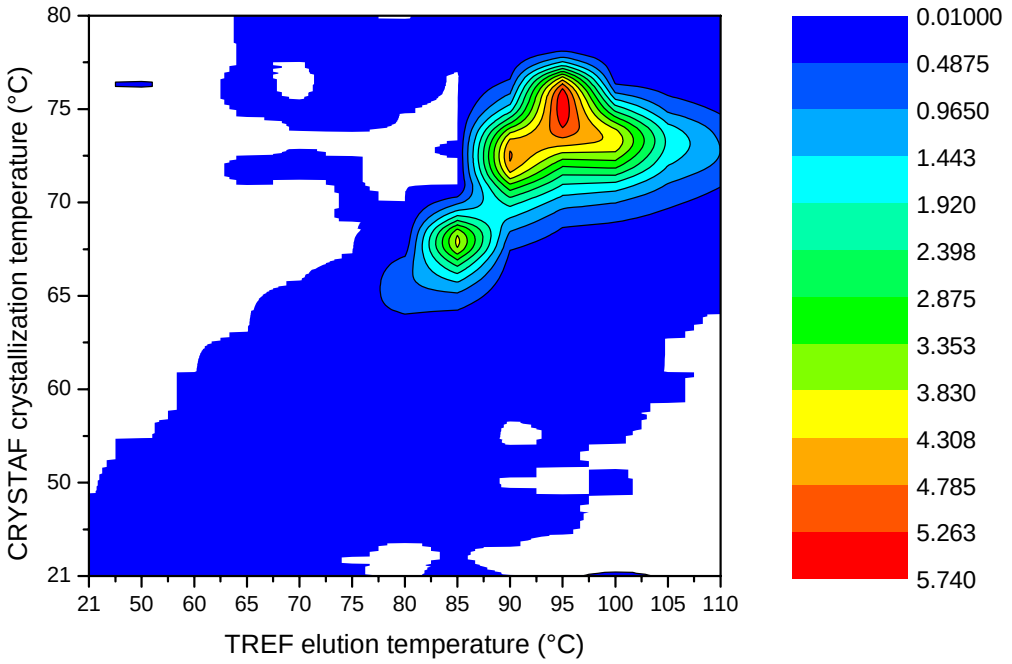

Figure 5.21 Contour map of CRYSTAF T_c of TREF fractions of Polymer G

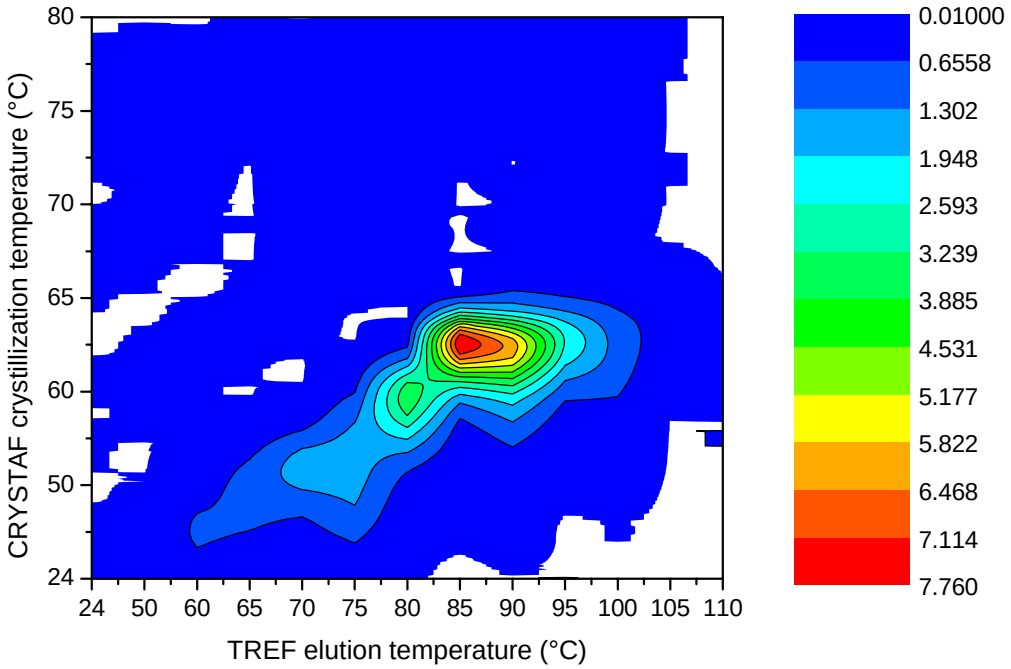

Figure 5. 22 Contour map of CRYSTAF T_c of TREF fractions of Polymer I

5.3.4 HT-GPC

Table 5.8 contains the molecular weights as well as polydispersities of the various fractions of Polymers G and I produced by the third fractionation attempt. We see a general increase in the molecular weight for the fractions collected from 50°C to 100°C for Polymer G and 50°C to 95°C for Polymer I. Thereafter the molecular weight decreases. The opposite trend is observed for the polydispersities of the fractions. The polydispersity values generally decrease from the 50°C fraction to the 115°C fraction for Polymer G and from the 50°C fraction to the 110°C fraction for Polymer I where after it shows an increase. It therefore indicates a generally broader distribution of the lower molecular weight material in the lower fractionation temperature fractions. On the other hand we find that the higher molecular weight fractions, which are eluted around 100°C,

are narrowly distributed. The decrease in molecular weight for the highest temperature fractions as well as the increase in the PD values for the last fraction or two collected confirm that TREF fractionation is not accomplished on the basis of molecular weight.

Table 5.8 HT-GPC data of fractionated material from copolymers G and I

	G			I		
T_f (°C)	***Mn (g/mol)***	***Mw (g/mol)***	***PD***	***Mn (g/mol)***	***Mw (g/mol)***	***PD***
R.T.	27 100	106 400	3.9	1 200	25 000	21.6
50	8 900	81 100	9.1	14 400	89 600	6.2
60	-	-	-	30 400	128 400	4.2
65	-	-	-	32 800	134 500	4.1
70	-	-	-	52 500	177 400	3.4
75	25 200	111 800	4.4	48 600	179 500	3.7
80	27 200	108 500	4	75 900	240 400	3.2
85	38 900	141 800	3.6	84 400	288 100	3.4
90	39 100	130 000	3.3	106 200	330 300	3.1
95	66 200	230 600	3.5	131 700	368 300	2.8
100	98 400	330 600	3.4	69 000	185 000	2.7
105	110 900	319 800	2.9	105 000	303 700	2.9
110	51 800	142 600	2.8	65 700	159 500	2.4
115	42 900	110 700	2.6	100 200	283 300	2.8
130	72 900	193 400	2.7	-	-	-

The lower molecular weights and higher PD values may also be due to an initial nucleation effect by the inert sand support at the high crystallization temperatures. This effect could possibly cause that some of the copolymer may crystallize at higher temperatures than expected due to the availability of a surface on which to crystallize and thereby lowering the surface energy needed for crystallization.

Another reason for the lower molecular weights and higher PD values may also be due to degradation of the copolymers. The fractions eluted at the highest temperatures must then degrade despite the effect of the stabilizer and due to their exposure to the high temperatures for longer periodes of time than the

material eluted at lower temperatures. The effect of the stabilizer makes this however less likely to happen. Entrapment of low molecular weight material between the inert support and chains crystallizing at high temperatures are a another possible reason for the decrease in molecular weights and increase in PD values.

When comparing the HT-GPC results of the fractions of the two copolymers it is found that the fractions of Polymer G have in general lower molecular weights than those of Polymer I, more specifically the lower fractionation temperature fractions (from 50°C to 95°C). The PD values for Polymer G are in general higher than those of Polymer I for fractions eluted from 50°C to 100°C. This is very significant with regard to the donor:catalyst ratio. The conclusion is made that a higher Si:Ti ratio (6.8 compared to 2.2) leads to significant higher (in most cases more than twofold) molecular weight and lower polydispersity values for the lower fractionation temperature (< 100°C) fractions.

5.4 CONCLUSIONS

TREF can be effectively used to fractionate propylene/1-pentene copolymers into any amount of fractions desired, depending on the minimum weight of the fractions needed for the necessary analyses.

TREF gave a good recovery percentage of above 96%. Some material may be “lost” during the experimental handling of the copolymer. Another possible reason for the “lost” sample is that some low molecular weight material becomes entrapped between the inert support and the chains which crystallize at high temperatures.

The difference in weight percentage of the room temperature TREF fraction and the fraction extracted by the standard xylene-soluble method implicates that the percentage of extractable material is dependent on the crystallization method.

The weight fraction results show that Polymers G and H have significantly higher weight percentage fractions for the room temperature fraction than

Polymers I and J. This is significant with regard to the donor:catalyst ratio, because Polymers G and H have much lower Si:Ti ratios (2.2 and 2.8 respectively) than Polymers I and J (6.8 and 10.0 respectively) and the conclusion therefore is that the Si:Ti ratio appears to have an influence on the percentage of xylene soluble material during TREF.

The width of the peaks of derivative of weight fraction percentage versus the fractionation temperature decreases with an increase in the comonomer content of Polymers G - J, indicating a more homogeneous distribution of molecular species with an increase in the comonomer content. The higher 1-pentene content may therefore be an indication of more xylene soluble material, leaving more crystallizable material.

The ^{13}C-NMR spectrum of the room temperature TREF fraction (using xylene as solvent) corresponds well, as would be expected, with that of the XS fraction (Section 4.3.2.2). The high concentration of peaks representing the presence of end groups indicates that the fraction consists mainly of low molecular weight material.

The NMR results show a decrease in the 1-pentene content with an increase in the fractionation temperature. The 1-pentene reduces the ability of the chains to crystallize and therefore chains with less comonomer are able to crystallize at higher temperatures.

The less significant fractions, which make out almost 35% of the original polymer, contain most of the 1-pentene. The most significant fractions ($T_f \geq$ 90°C) contain less than 1.5% 1-pentene.

An increase in the tacticity of the fractions is found as the fractionation temperature is increased. This also goes along with a decrease in comonomer content, but this is not due to the decrease in 1-pentene content. These microstructure properties must therefore lead to more crystallizable fractions as the T_f increases. Comonomer units act as chain defects impeding the crystallization of the chains.

Thermal investigation of the fractions shows an increase in T_c, T_m and percentage crystallinity up to a certain fraction (~ 100°C) where after it

decreases. The opposite was observed for the percentage of soluble fraction during CRYSTAF analysis. The decrease in T_c, T_m and percentage crystallinity and increase in percentage of soluble fraction after a certain temperature may be due to low molecular weight material entrapped between the inert support and the chains crystallizing at high temperatures or due to low molecular weight material which comes from degradation of the copolymer at the high temperatures.

The difference in T_m and T_c values of the corresponding fractions of different copolymers can be ascribed to a difference in 1-pentene distribution within the different copolymers.

The M_w values increase with an increase in fractionation temperature and decrease after ~ 100°C. This confirms the presence of lower molecular weight material in the higher temperature fractions causing the decrease in T_c, T_m and percentage of crystallinity and increase in percentage of soluble fraction after ~ 100°C.

The affect of the Si:Ti ratio on the microstructure, thermal properties and molecular weight can be clearly seen in the results from this chapter. According to the ^{13}C-NMR analyses of the fractions of two copolymers with significantly different Si:Ti ratios, an increase in the Si:Ti ratio leads to an increase in the 1-pentene content for the lower weight fractions which are also eluted at the lower temperatures. The highest weight fraction does not change much with regard to the 1-pentene content when the Si:Ti ratio changes. The increased amount of 1-pentene in the lower weight fraction then again leads to increased crystallization and decreased melting temperatures for these fractions. The higher weight fractions stay relatively unchanged with regard to the thermal properties due to their almost similar comonomer contents. A higher Si:Ti ratio also leads to lower percentage of CRYSTAF soluble fractions for the TREF fractions.

According to the HT-GPC results the Si:Ti ratio also affects the molecular weights and polydispersities of the various fractions. A higher Si:Ti ratio leads to a significant increase in the Mw and decrease in the PD values for the lower

weight fractions. The higher weight fractions do not seem to be influenced by change in the Si:Ti ratio.

5.5 REFERENCES

1. Boero, M., Parrinello, M., Hüffer, S., Weiss, H., J. Am. Chem. Soc., 2000. **122**: p. 501.
2. Cavallo, L., Guerra, G., Corradini, P., J. Am. Chem. Soc., 1998. **120**: p. 2428.
3. Virkkunen, V., Pietilä, L.-O., Sundholm, F., Polymer, 2003. **44**: p. 3133.
4. Virkkunen, V., Laari, P., Pitkänen, P., Sundholm, F., Polymer, 2004. **45**: p. 3091.
5. Xu, J., Feng, L., Eur. Polym. J., 2000. **36**: p. 867.
6. Xu, J., Fu, Z., Fan, Z., Feng, L., Eur. Polym. J., 2002. **38**: p. 1739.
7. Soares, J.B.P., Hamielec, A. E., Polymer, 1995. **36**: p. 1639.
8. Wild, L., Adv. Polym. Sci., 1990. **98**: p. 1.
9. Kioka, M., Makio, H., Mizuno, A., Kashiwa, N., Polymer, 1994. **35**: p. 580.
10. Xu, J., Feng, L., Yang, S., Yang, Y., Kong, X., Eur. Polym. J., 1998. **34**: p. 431.
11. Rabie, A.J., *Blends with low-density polyethylene (LDPE) and plastomers*, in *Department of Polymer Science and Chemistry*, *MSc thesis.* 2004, University of Stellenbosch: Stellenbosch.
12. Ananatawaraskul, S., Soares, J.B.P., Wood-Adams, P.M., Monrabal, B., Polymer, 2003. **44**: p. 2393.
13. Sarzotti, D.M., Soares, J.B.P., Pendilis, A.2002, J. Polym. Sci., Part B: Pol. Phys., 2002. **40**: p. 2595.
14. Glockner, G., J. Appl. Polym. Sci., Appl. Polym Symp., 1990. **45**: p. 1.
15. Wang, S., Yang, D., Polymer, 2004. **45**: p. 7711.
16. Pérez, E., Benavente, R., Bello, A., Perena, J.M., Zucchi, D., Sacchi, M.C., Polymer, 1997. **38**: p. 5411.

CHAPTER 6

Preparative Solution Fractionation

6.1 INTRODUCTION

Several well developed fractionation methods have been discussed in the previous chapters. One of the oldest methods of separating semi-crystalline polymers into a highly isotactic fraction and a low molecular weight, mainly atactic fraction is by carrying out solvent extractions of the specific polymer [1]. This method, however, has the limitation that the highly crystalline fraction of the polymer cannot be fractionated using solvent extractions. This fraction usually comprises more than 95% of commercial polymers and therefore is not entirely sufficient for fractionation analysis of semi-crystalline polymers.

TREF can be used as either an analytical or preparative technique. The two methods are compared in Table 6.1. TREF has been extremely well developed as a fractionation method since the mid 1960s [2]. Today it is widely used in order to analyze semi-crystalline polymers (especially polyolefins and their copolymers) by separation of the molecular species according to crystallizabilities. The most important advantage of the preparative technique is that fractions may be chosen to be large enough so that the necessary analyses can be carried out, by predetermining specific elution temperatures. The most import disadvantage of both the analytical as well as preparative TREF procedures is the considerable amount of time taken up by the cooling crystallization step.

Table 6.1 Differences between analytical and preparative TREF

Analytical TREF	**Preparative TREF**
A continuous process.	Fractions are collected at predetermined temperatures.
Online molecular structure analysis by means of a calibration curve.	Offline molecular structure analysis by additional analysis techniques.
Technique requires smaller columns and smaller fraction sizes.	Technique requires larger columns and larger fraction sizes.
Faster procedure but generates less information about the microstructure.	Time-consuming procedure but can generate detailed information about microstructure.

CRYSTAF has been reported to overcome this disadvantage of TREF. The technique has been developed as an alternative for TREF to obtain the CCD of polyolefins. Dissolved polymer chains are allowed to precipitate in a single step in solution at different temperatures according to their crystallizabilities. CRYSTAF has been shown to provide similar results to TREF but in shorter times and with a simplified apparatus [3-5]. The technique has therefore become a standard means of analysis in many laboratories, especially in the polyolefin industry. This technique, however, is connected to an online analysis system and the fractions can therefore not be used for further analysis, like NMR or DSC.

Two preparative CRYSTAF techniques have been described in literature. The first of these can however be better described as a preparative TREF or even better solution TREF technique [6]. The temperature program consists of dissolving the polymer in xylene at high temperature, equilibrating the solution for 90 min and then slow cooling (0.10°C/min) the solution to room temperature. Thereafter the crystallized polymer is heated stepwise to predetermined fractionation temperatures, at which each dissolved polymer fraction is isolated every time before the temperature is increased in order to collect the next fraction. Although the technique requires less time than

conventional TREF for the cooling step, because it takes place in solution, it still takes at least 16 hours before the first fraction can be collected.

The second reported preparative CRYSTAF technique has a solvent/non-solvent approach which allows for the fractionation of polymers based on molecular weight [7]. An increasing content of non-solvent is added to the polymer solution and this leads to a controlled precipitation of the initial polymer in different fractions of increasing molecular weight. This preparative method does not offer analytical information about the composition or morphology of polymers by itself. Other analytical techniques must be used to fully characterize their chemical and structural properties. The fractions collected with this technique can, however, not be compared to those collected by conventional TREF and CRYSTAF due to the different separation systems (molecular weight and crystallizability respectively).

It is therefore clear that the need exists for a fractionation method that is based on the crystallizability of different polymer chains and that is not as time consuming as the methods discussed above. This need further includes a simple preparative method that separates fractions of significant size for further analysis, blending, etc. A preparative solution fractionation (SF) was therefore developed in this research project and the development as well as application thereof will be discussed in the rest of the chapter.

6.2 EXPERIMENTAL

6.2.1 SF experimental set-up

This single-step fractionation technique is based on the principle of dissolving the polymer in a high-boiling solvent and then crystallizing the fractions in solution by decreasing the temperature to the predetermined fractionation temperatures. The experimental setup consists of two glass columns inside a 5-l glass beaker, which is filled with silicon oil and equipped with a temperature controller, as illustrated in Figure 6.1.

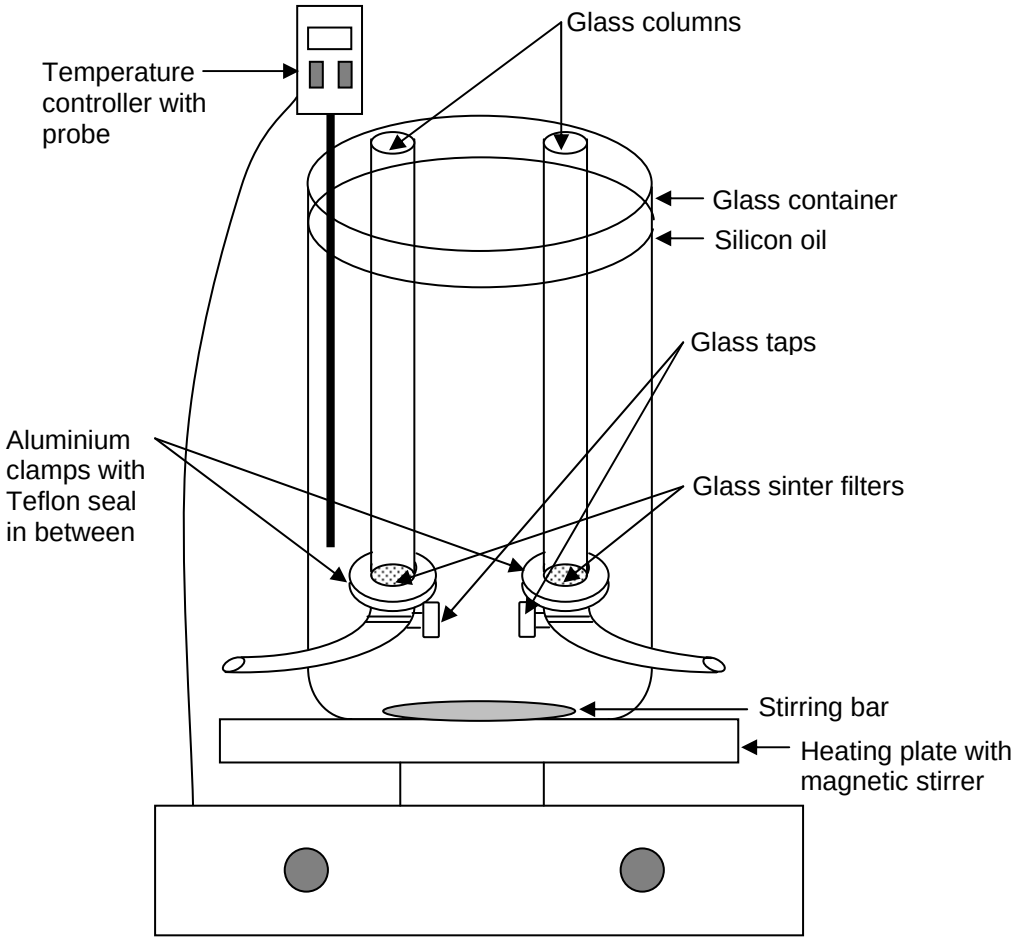

Figure 6.1 Illustration of experimental set-up for preparative SF

The oil beaker is preheated to 130°C and covered on the outside with aluminum foil in order to prevent heat loss. One gram of polymer is dissolved separately in 65 ml trichlorobenzene, after which the solution is decanted into one of the glass columns. After one hour the temperature is lowered to the first predetermined temperature and kept there for 6 hours. During this time the first fraction crystallizes completely from solution. The polymer still in solution is then separated from the first fraction by adding nitrogen pressure to the column. The solution is pushed through a suitable filter at the bottom of the column and exits through a tap leading to the outside of the column where it is collected into a beaker. This solution is decanted into the second column where it is kept at 130° for an hour, ensuring that all polymer is completely dissolved. The temperature is then lowered to the second predetermined temperature and again kept there for 6 hours, before the same method is

used to separate the solution from the second fraction. The third fraction now crystallizes in the beaker at room temperature. The fourth fraction is the one that remains in solution at room temperature.

Note must be taken that this technique was carried out roughly in order to determine whether the concept was effective. No improvements or refinements were carried out and therefore suggestions for the improvement of this technique will be discussed at the end of the chapter.

All the commercial propylene/1-pentene copolymers (A - J) were fractionated by this method and then analyzed. These results were compared to those recorded using the TREF technique. The results of the fractionated material of Polymers A and G from all of the various analysis methods used are illustrated and discussed in order to show the consistency of the results for Group 1 and Group 2 copolymers.

6.2.2 ^{13}C-NMR

The same procedure was used with the Varian VXR 300 NMR spectrometer as described in Section 3.2.2 for the analysis of the Group 1 copolymers.

6.2.3 HT-GPC

The same procedure was used as described in Section 3.2.3.

6.2.4 CRYSTAF

The same procedure was used as described in Section 3.2.4.

6.2.5 DSC

The same procedure was used as described in Section 3.2.5.

6.3 RESULTS AND DISCUSSION

6.3.1 ^{13}C-NMR

Polymer A was separated into three fractions, namely RT, 75°C and 85°C. The RT fraction therefore consists of all the material that was able to crystallize below 75°C from solution in TCB. The 75°C fraction comprises all the polymer chains able to crystallize between 75 and 85°C and the 85°C fraction consists of material able to crystallize above 85°C from solution.

^{13}C-NMR was used in order to investigate the structural analysis as well as the comomomer content of these fractions separated by SF. Results are shown in Figure 6.2.

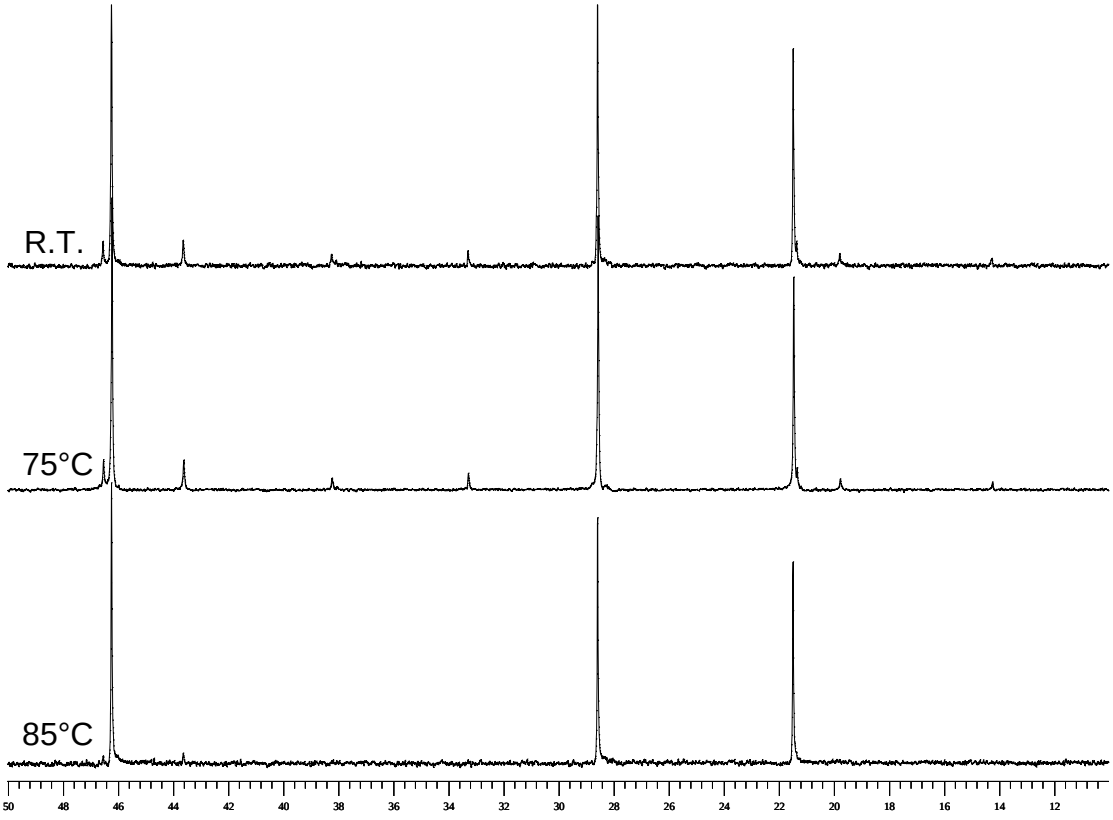

Figure 6.2 ^{13}C-NMR results of Polymer A fractionated by preparative SF

The ^{13}C-NMR results of the RT fraction can be taken into consideration when investigating the trend in 1-pentene content and tacticity for the fractions. This remark originates from the fact that the original polymer has a percentage XL of only 6.47% and therefore plays a rather minor role in this fraction consisting of polymer chains which crystallize in the wide temperature range of ~ 20 to 75°C.

According to Figure 6.2 there is a definite decrease in the 1-pentene content of the fractions with increasing the fractionation temperature during the preparative SF of Polymer A. This corresponds very well with the decrease in comonomer content with increasing the fractionation temperature from the TREF technique. The almost “invisible” 1-pentene peaks in the spectrum of the 85°C fraction make it impossible to calculate the comonomer content.

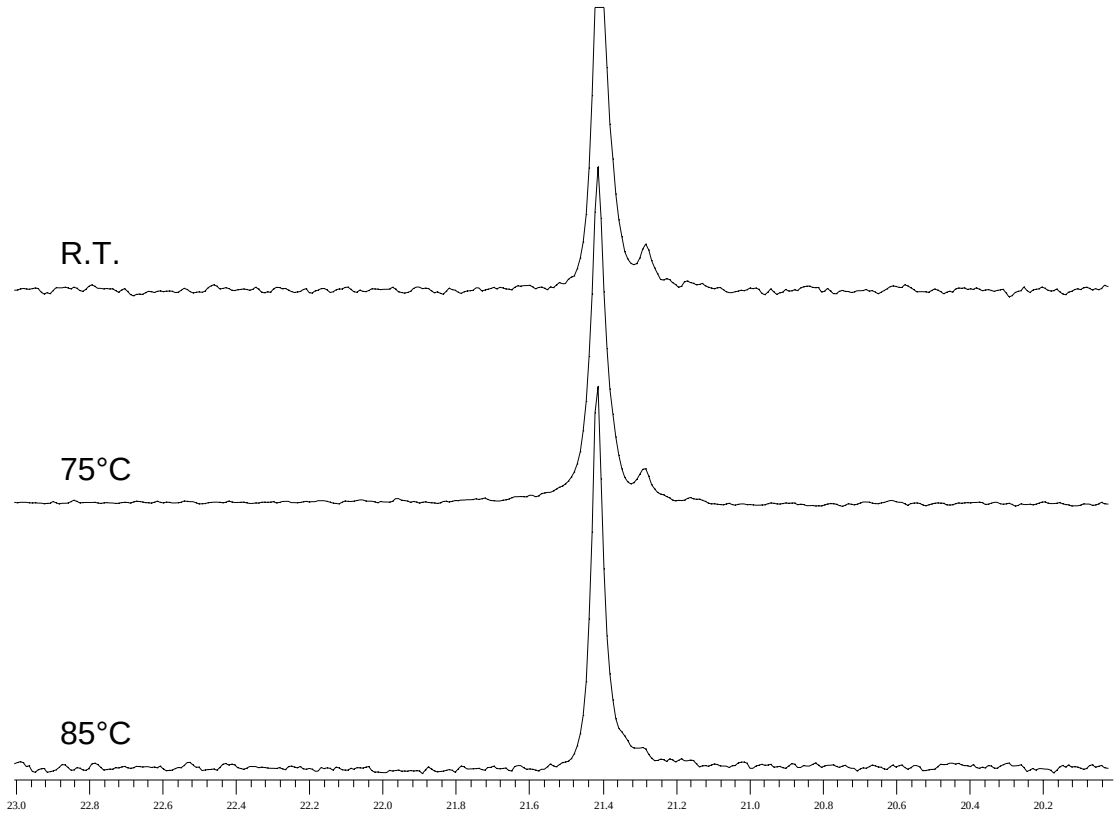

Figure 6.3 ^{13}C-NMR results of the methyl region of the fractions of Polymer A fractionated by preparative SF

Figure 6.3 shows a closer look at the methyl regions of the propylene in order to investigate the difference in tacticity for the various fractions. The shoulder peak of the methyl resonance, clearly visible in the RT fraction, decreases for the 75°C fraction and almost disappears in the 85°C fraction. This indicates an increase in tacticity for an increase in fractionation temperature.

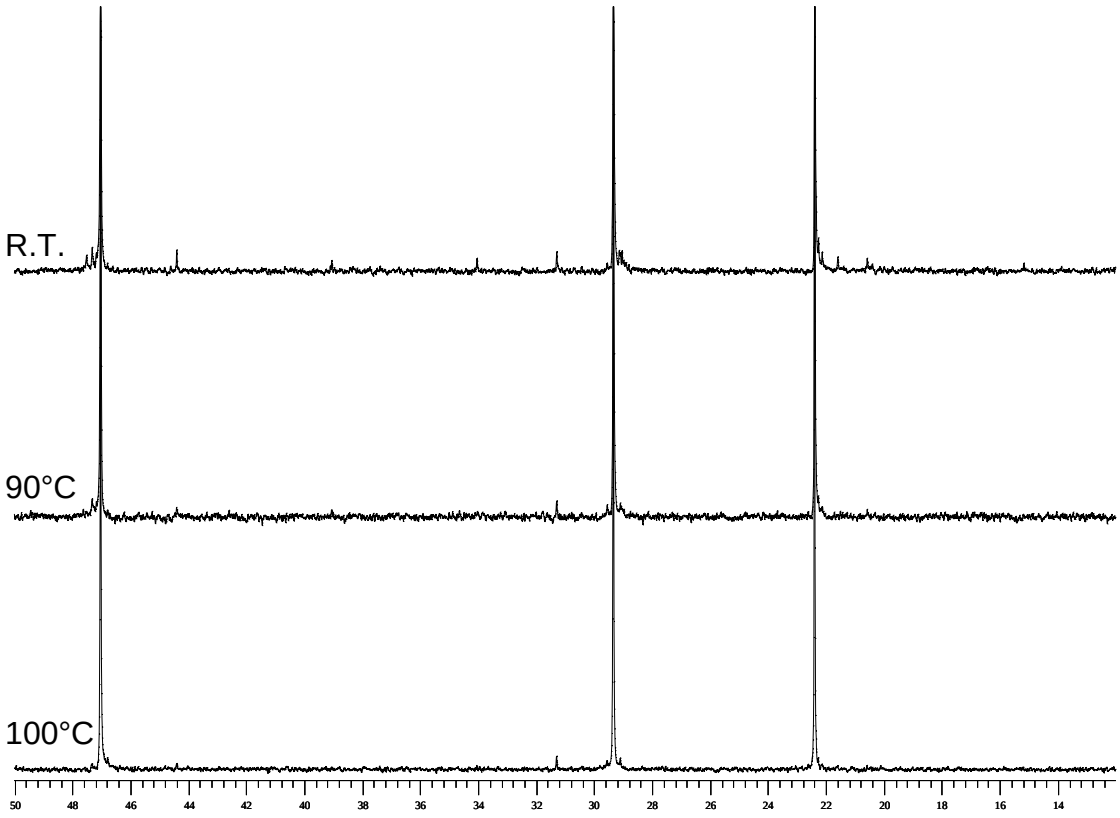

Figure 6.4 ^{13}C-NMR results of Polymer G fractionated by preparative SF

The ^{13}C-NMR results of the RT fraction can once again be taken into consideration when investigating the trend in 1-pentene content and tacticity for the fractions. An even lower XL (3.20%) was determined for this original copolymer and therefore the xylene soluble fraction plays a very insignificant role in this fraction consisting of polymer chains which crystallized in an even wider temperature range of ~ 20 to 90°C.

Figure 6.4 shows similar results for Group 2 copolymers as for the Group 1 copolymers. The 1-pentene content is so low for the 90 and 100°C fractions that it is impossible to calculate the content. There is however a definite decrease in 1-pentene content as the fractionation temperature increases.

Figure 6.5 shows the ^{13}C-NMR results of the methyl region of the fractions of Polymer G fractionated by preparative SF. It shows an increase in tacticity for the fractions when increasing the fractionation temperature. The shoulder peak on the methyl resonance decreases until it almost disappears for the 100°C fraction.

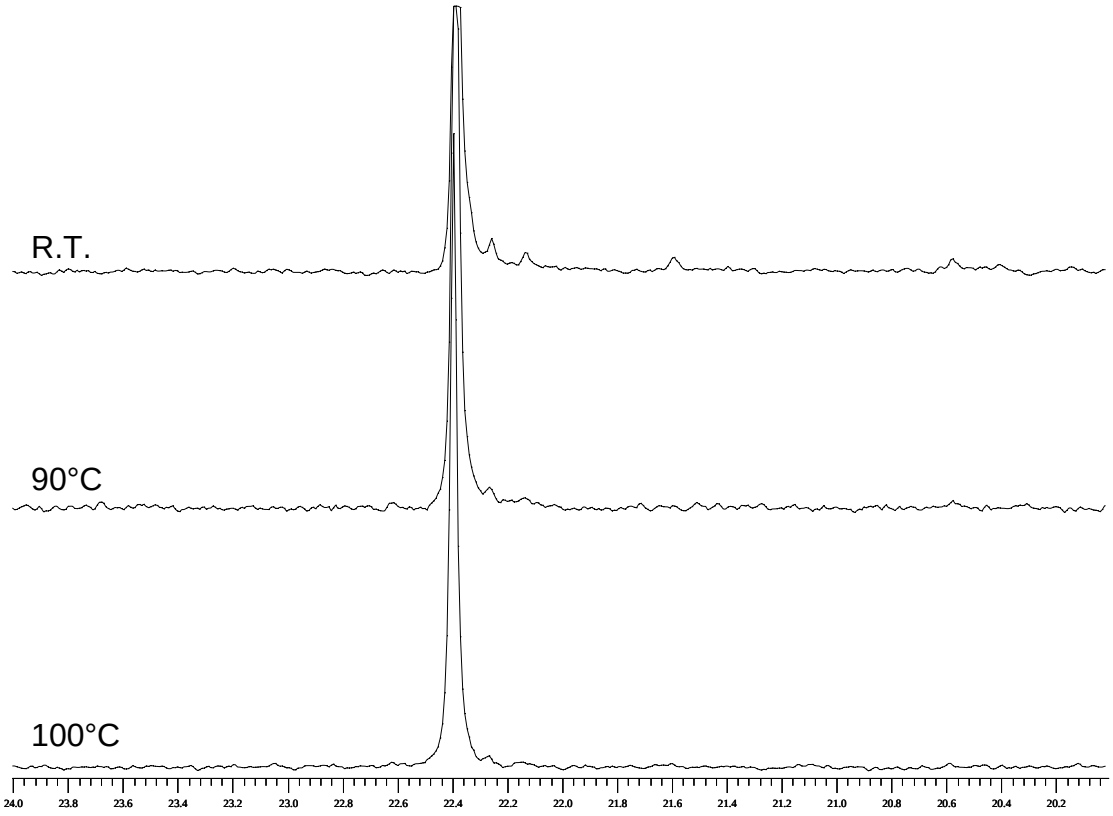

Figure 6.5 ^{13}C-NMR results of the methyl region of the fractions of Polymer G fractionated by preparative SF

6.3.2 HT-GPC

Table 6.2 shows the molecular weights and polydispersities of the original Polymer A as well as the three fractions isolated through preparative SF. It shows a definite increase in the number average molecular weight with an increase in the fractionation temperature. The two fractions of 75°C and 85°C also show similar polydispersities, which are much lower than that of the RT fraction. The higher PD of the RT fraction is definitely due to the fact that this fraction contains high and low molecular weight isotactic material as well as some atactic material.

Table 6.2 Molecular weight results from HT-GPC analysis of the SF of Polymer A

Fraction	M_n (°C)	M_w (°C)	PD
Original	78 000	567 000	7.09
RT	11 400	118 400	10.38
75°C	14 300	86 100	6.03
85°C	24 400	148 000	6.06

Table 6.3 gives the molecular weight and polydispersity results of the original Polymer G as well as the three fractions isolated through preparative SF. In this case we can see a definite increase in the molecular weights and a decrease in polydispersity with increasing fractionation temperature.

Table 6.3 Molecular weight results from HT-GPC analysis of the SF of Polymer G

Fraction	M_n (°C)	M_w (°C)	PD
Original	88 300	350 300	3.97
RT	25 400	106 100	4.17
90°C	64 500	171 900	2.66
100°C	78 400	192 200	2.45

Figure 6.6 shows the HT-GPC curves of the three fractions of Polymer G isolated by preparative SF at RT, 90°C and 100°C. There is a shift towards the higher molecular weight area on the x-axis as well as an increase in the narrowness of the peaks as the fractionation temperature is increased. The fraction consisting of crystallized material below 90°C results in a bimodal peak and not a single, sharp peak like the other two fractions. This bimodality indicates that the fraction consists of some lower molecular weight material (possibly isotactic and atactic) as well as some higher molecular weight chains.

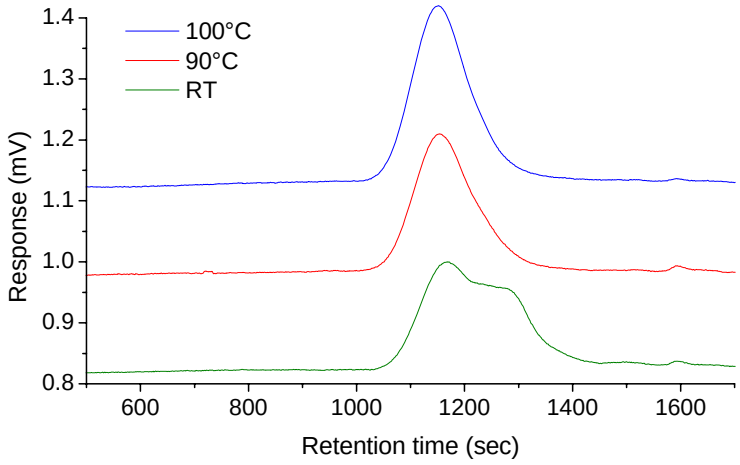

Figure 6.6 HT-GPC curves of the fractions of Polymer G isolated by SF

6.3.3 Thermal results

CRYSTAF and DSC analyses were carried out on all the samples fractionated by SF. The CRYSTAF results from this novel fractionation technique are shown in Figures 6.7 and 6.8 and Tables 6.4 and 6.5.

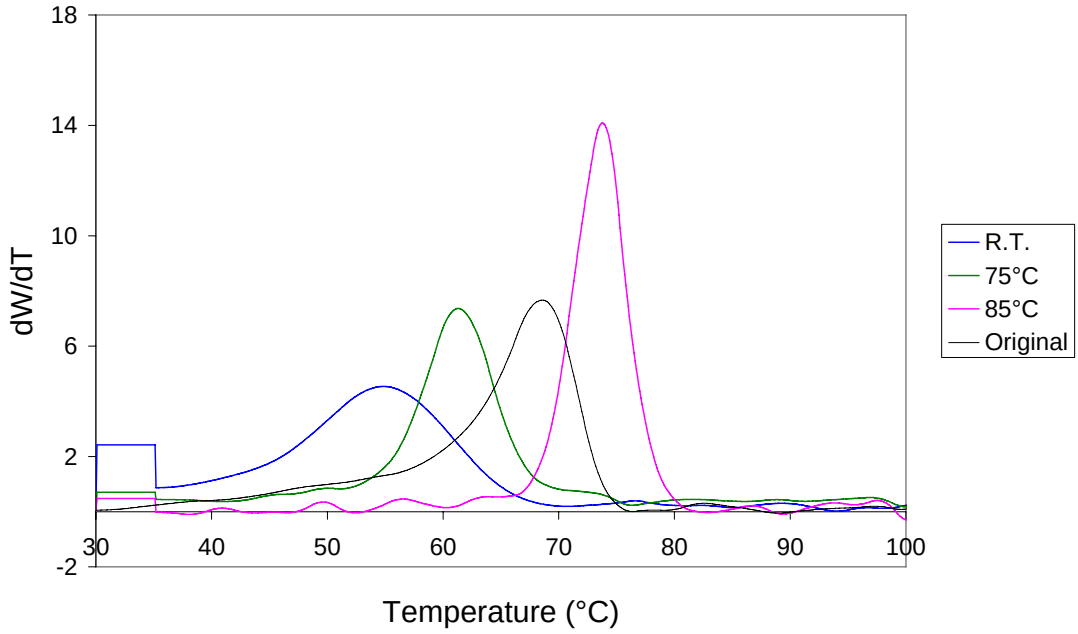

Figure 6.7 CRYSTAF spectra for the three fractions of polymer A resulting from solution fractionation

Table 6.4 DSC and CRYSTAF results from the SF of polymer A

Fraction	T_m (DSC) (°C)	Crystallinity (DSC) (%)	T_c (DSC) (°C)	T_c (CRYSTAF) (°C)	Sol. Frac. (CRYSTAF) (%)
Original	142.7	72.9	101.7	68.6	2.9
R.T.	126.3	21.2	83.6	49.6	12.1
75°C	132.5	18.8	92.6	56.1	3.5
85°C	141.0	39.3	102.0	68.6	2.4

Figure 6.7 shows a definite increase in T_c for an increase in fractionation temperature. From the CRYSTAF results in Table 6.4 the T_c values measured for the fractions isolated at 75 and 85°C are more or less 20°C lower than the crystallization fractionation temperature of these two fractions. For the T_c values measured by DSC for these two samples the crystallization temperatures are in this case about 20°C higher than their crystallization fractionation temperatures. We know that the T_c values from the CRYSTAF results are much lower than those from the DSC results, because the polymer chains in the CRYSTAF analysis are able to crystallize

much easier due to their increased mobility in the analysis solvent compared to the solid state in DSC analysis. It seems however that the fractions in our SF procedure isolated above RT crystallized at temperatures more or less in the middle of the T_c's resulting from DSC and CRYSTAF analyses.

CRYSTAF results further reveal a decrease in the percentage of soluble fraction. The RT fraction however already contains a relatively low amount of soluble fraction (12.1%), compared to that collected by TREF (> 85%). The reason for this is that the RT fraction in the case of SF is over a very wider temperature range (~ 20°C to 75°C, instead of up to 60°C) and it must also be taken into account that the polymer chains start to crystallize at lower temperatures because of their increased mobility in solution. This fraction therefore contains significantly more crystallizable material than in the case of the smaller TREF fractions.

According to the CRYSTAF and DSC results there is an increase in T_c with an increase in fractionation temperature. These results as well as the increase in T_m according to the DSC melting thermograms correspond very well with the trends found with TREF. As expected, the increases in T_c and T_m also correspond with the decrease in 1-pentene content as the fractionation temperature is increased.

Another interesting phenomenon from the CRYSTAF and DSC results is that the T_c values found from both analysis methods as well as the T_m from DSC analysis for the highest temperature (85°C) are very much the same as the corresponding crystallization or melting temperatures of the original polymer before fractionation, especially for the T_c found from the CRYSTAF analysis.

The low percentage of crystallinity (18 - 40%) calculated from the DSC melting enthalpy of the various fractions seems not to be a true reflection seeing that the percentage of crystallinity of the original polymer is 72.9%. The fractions of all Group 1 copolymers were not washed with acetone after isolation and do contain a small amount of TCB (according to the distinctive sweet smell). The reason for these low values might therefore be caused by the TCB trapped in the samples.

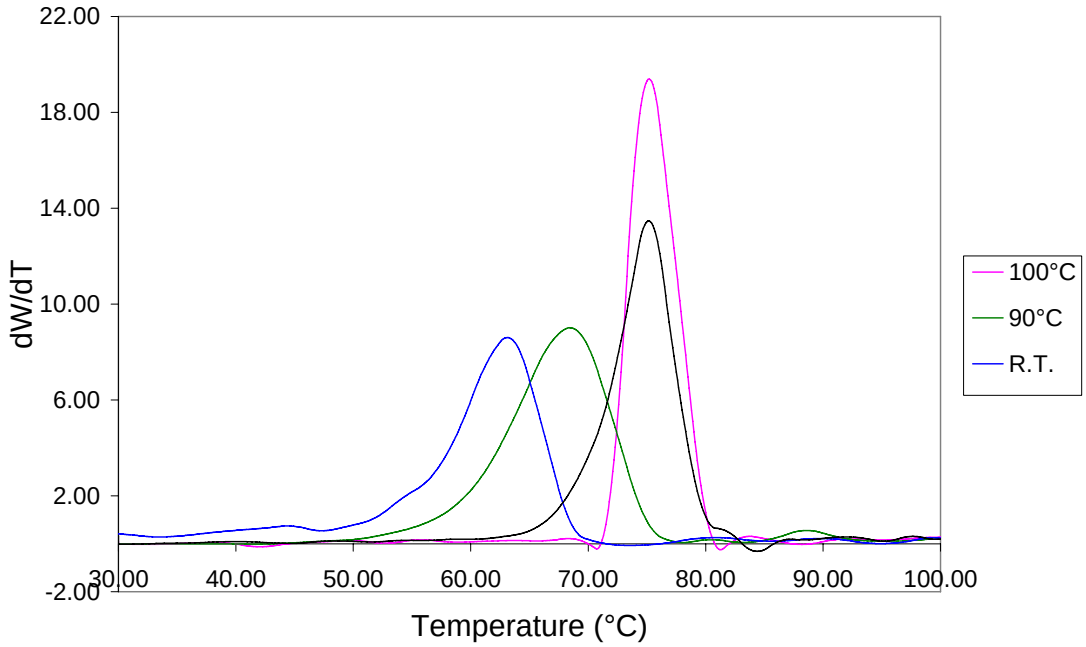

Figure 6.8 CRYSTAF spectra for the three fractions of Polymer G resulting from solution fractionation

Table 6.5 DSC and CRYSTAF results from the SF of Polymer G

Fraction	T_m (DSC) (°C)	Crystallinity (DSC) (%)	T_c (DSC) (°C)	T_c (CRYSTAF) (°C)	Sol. Frac. (CRYSTAF) (%)
Original	151.9	68.9	111.6	75.1	1.6
R.T.	139.6	57.7	102.3	63.1	3.5
90°C	150.3	76.0	113.2	68.4	0.2
100°C	155.3	86.5	115.0	75.2	0.5

According to Figure 6.8 and Table 6.5 the results of thermal analysis of the SF samples of Polymer G show similar trends as for Polymer A. The two higher temperature fractions were eluted at higher temperatures for Polymer G than for Polymer A. These temperatures were decided on in order to separate the original polymer into three fractions of more or less the same size in order to ensure enough polymer in each fraction for a complete analysis of the respective fractions. There is an even smaller percentage of soluble fraction (3.6%) for the RT fraction of Polymer G than for Polymer A.

This makes perfectly sense when taking into account that this fraction was taken over an even wider temperature range (~20 to 90°C, instead of up to 75°C) and the percentage of soluble fraction in the original Polymer G is almost half that of Polymer A. All the Group 2 copolymers were fractionated at higher temperatures than those of Group 1.

Again we see that according to CRYSTAF analysis the T_c of the original copolymer is very similar to that of the highest temperature (100°C) fraction. But in this case the T_c and T_m according to DSC analysis also do not correspond well with that of the original copolymer and the highest temperature fraction.

As in the case of Polymer A the trend of an increase in melting (according to DSC results) and crystallization (according to DSC and CRYSTAF results) temperatures for the increase in fractionation temperature of Polymer G is seen. Again these trends are expected and correspond to the decrease in comonomer content with an increase in fractionation temperatures calculated in the NMR results in Section 6.3.2.

According to the melting enthalpy calculations there is a significant increase in the percentage of crystallinity (from 58 to 87%) of the isolated fractions of G when the fractionation temperature is increased. The crystallinities of these samples are more reliable than in the case of Polymer A because the isolated fractions were thoroughly washed with acetone and do not contain any solvent residue trapped in the material. It therefore indicates that this fractionation technique is based on the separation of polymer chains due to their different crystallinities.

6.4 CONCLUSIONS

A preparative solution fractionation technique was developed and commercial propylene/1-pentene copolymers were fractionated according to this technique into four well separated fractions. The fractions were analyzed by ^{13}C-NMR, HT-GPC, CRYSTAF and DSC and the results compared very well with that of the analysis of the same copolymers fractionated by TREF (Chapter 5).

6.5 EXPERIMENTAL EVALUATION

The preparative SF technique has much potential as a fractionation method, especially for polyolefins and has many advantages over the current existing fractionation methods generally used:

- the method takes less time than TREF or CRYSTAF,
- because it is preparative the size and the number of fractions may be chosen according to the analysis requirements,
- the experimental set-up is simple, and
- the technique is inexpensive.

A few improvements in the experimental set-up and procedure may simplify this novel technique even more.

6.5.1 Automation

The experimental procedure used in this study is not very labour intensive but may be even more simplified if automated. Automation of the system will not only make the manual control of the temperature easier, but it will also make it possible to work with a consistent temperature program for different runs. In order to automate the different temperature settings needed at different time intervals a computerized temperature profiler may be connected to the heating system.

6.5.2 Heat loss

A 5-l glass container filled with silicon oil is used as heating mantle in the set-up used in this study. Aluminum foil is then wrapped around the outside of the glass container in order to prevent heat loss. This may be improved by replacing the aluminum foil with a type of electrical heating mantle which can provide heat and act as insulator. The mantle may then even be connected to the temperature controller in order to link up with the

automated temperature program. The top of the glass container also needs to be covered with an insulator to prevent heat loss.

Another option is to work in a temperature controlled oven, rather than a glass beaker. The only problem is that crystallization of the polymer can then not be monitored with the eye.

6.5.3 Number of fractions

The procedure used in this study can fractionate the polymer into three different fractions. If the isolation of the fraction which is soluble at room temperature in the specific solvent used is taken into account then, this number adds up to four. The number of fractions into which the polymer is separated may however be increased by increasing the number of columns connected inside the temperature-controlled heating system. A bigger container/mantle is therefore needed or another option is to duplicate the whole set-up.

6.5.4 Set-up design

The whole set-up may be converted from glass to steel, but again the crystallization process can then not be monitored with the eye. An important aspect of the columns is to seal them properly in order to handle pressure when nitrogen is used to push the solvent through and also to prevent leakage of the solvent to the outside of the column or to prevent leakage from the high temperature silicon to the inside of the column. The design of the column should therefore also be improved in order to prevent these problems.

6.5.5 Solvent

TCB is a high boiling solvent in which polyolefins dissolve readily. It is however not the ideal solvent due to the associated health hazards. Another

problem with this solvent is removing it from the fractions. The boiling point is too high in order to remove it under vacuum on a rotary evaporator. TCB was removed from the fractions by washing it out with acetone. It should be noted that when doing so for the lowest temperature crystallized fraction, there is some low molecular weight material which is soluble in the TCB and it will be removed together with the solvent. Xylene may be considered as an option for substituting TCB.

6.5.6 Glass sinter filters

The filter sometimes blocked. Although they could easily be replaced with new ones, a better filter system should also be investigated. Such filters must however be easily removable from the column. Another option may be to prevent blocking of the sinter filters by using a type of membrane filter on top of the glass filter. Polymer will then also not be trapped inside the glass filters.

6.6 REFERENCES

1. Natta, G., Mazzanti, G., Crespi, G., Moraglio, G., Chim. Ind., 1957. 39: p. 275.
2. Shirayama, K., Okada, T., Kita, S., J. Polym. Sci. A-2, 1965. 3: p. 907.
3. Monrabal, B., J. Appl. Polym. Sci., 1994. 52: p. 491.
4. Monrabal, B., Macromol. Symp., 1996. 110: p. 81.
5. Monrabal, B., *Encyclopedia of Analytical Chemistry*. Vol. 9. 2000, Chichester: John Wiley and Sons Ltd. 8074.
6. Bruaseth, I., Soares, J.B.P., Rytter, E., Polymer, 2004. 45: p. 7853.
7. Vilaplana, F., Morera-Escrich, V., Hierro-Navarro, P., Monrabal, B., Ribes-Greus, A., J. Appl. Polym. Sci., 2004. 94: p. 1803.

CHAPTER 7

Blends with Metallocene Catalyzed Copolymers

7.1 INTRODUCTION

Isotactic polypropylene has been blended with various elastomers to improve the mechanical properties such as impact strength at low temperature toughness. Ethylene-propylene rubber (EPR) [1-7], polyisobutylene [5] and styrene/ethylene-butene/styrene triblock copolymer [8] were widely used as the respective rubber components. The mechanical properties of these binary blends, however, are unsatisfactory because the blends are immiscible and/or incompatible. In the past, therefore, much attention was been focused on the improvement of the morphology of the binary blends of iPP with these elastomers.

As is well known, iPP and the ethylene-1-butene copolymers, namely linear low density polyethylene (LLDPE), are an incompatible polymer pair [9-15], whereas iPP and isotactic poly(1-butene) (PB1) are a compatible pair [16-22], although both LLDPE and PB1 are crystalline polymers.

Fortunately, recent development in catalysts and new synthetic techniques [23-28] has made it possible to prepare various ethylene-α-olefin random copolymers, such as ethylene-1-butene copolymers, covering nearly the entire composition range from LLDPE to PB1. Thus, a rubbery α-olefin copolymer, consisting of a chain with a number of short branches, can be prepared.

The commercial propylene/1-pentene copolymers have the advantage that the comonomer chain disruptions already improve the impact properties of the polymer. The influence of blending the commercial copolymers with some tailored propylene/1-pentene copolymers on the thermal and crystal properties however require investigation This chapter therefore describes a

preliminary survey of blends of Ziegler-Natta catalyzed commercial propylene/1-pentene random copolymers with a tailored metallocene catalyzed propylene/1-pentene copolymer with very low comonomer content (< 1 mol%). The blending was carried out in a *p*-xylene solution with a freeze-crystallization process in order to limit any changes in the composition and molecular weight of the original commercial copolymer to the minimum. Molecular weight, WAXD and thermal analyses were carried out on the blends as well as on the original copolymers used for blending. Unfortunately the samples quantities were not enough for optical and mechanical analysis.

7.2 EXPERIMENTAL

7.2.1 Materials and blend preparation

Polymer J was used as ZN catalyzed commercial propylene/1-pentene random copolymer. Parameters for this copolymer, as determined in Chapter 3, as well as the homogeneous metallocene catalyzed propylene/1-pentene copolymer (Polymer M) were the following:

Table 7.1 List of parameters for original copolymers used in blends

Parameter	Polymer J	Metallocene copolymer
1-Pentene content (^{13}C-NMR)	1.86%	< 1%
M_n (HT-GPC)	96 700 g/mol	18 300 g/mol
M_w (HT-GPC)	337 700 g/mol	72 200 g/mol
PD (HT-GPC)	3.49	3.95
T_c (CRYSTAF)	70.2°C	64.1°C
Soluble Fraction (CRYSTAF)	1.5%	5.6%
T_c (DSC)	106.52 °C	103.89°C
T_m (DSC)	149.60 °C	138.60°C
Crystallinity (DSC)	54.88 %	69.33%
Gamma phase (WAXD)	37.99%	-

The blends were prepared in four different ratios of metallocene catalyzed copolymer to Polymer J, namely: 10, 20, 30 and 40%. Neither one of the two well known, conventional blending methods, namely solution blending using xylene and melt blending were used. In the solution blending procedure, the blend is precipitated with methanol and then filtered. The low molecular weight material of the blend which is soluble in xylene will be separated from the blend during this process. The removal of the xylene soluble material from the blend is not desired in our process. During melt blending, the blending is often not very homogeneous, and if a screw extruder is used then the chains may break.

An alternative method, in which the above would not play a role was therefore selected. The method involved the use of solution blending with p-xylene as solvent. The two copolymers were dissolved in 250 ml of *p*-xylene in a 500-ml round bottom flask. The hot solution was then quenched in liquid nitrogen in order to crystallize on the biggest part of the round bottom flask. The *p*-xylene was then removed, under strong vacuum, from the cold crystallized blend, while the temperature of the system was allowed to return to room temperature. A minimum of 24 hours was required in order to remove

all the *p*-xylene. The blend remained in the flask in the form of a fine, fluffy powder.

7.2.2 HT-GPC

The same procedure was used as described in Section 3.2.3.

7.2.3 CRYSTAF

The same procedure was used as described in Section 3.2.4.

7.2.4 DSC

Thermal analysis was carried out on the blends before slow cooling and after slow cooling, using the same procedures as described in Section 3.2.5.

7.2.5 WAXD

The samples to be analyzed by WAXD were-slow cooled prior to analysis. These samples were hot-pressed at 230 °C into 100-μm thick films and then analyzed using the same procedure as described in Section 3.2.6.

7.3 RESULTS AND DISCUSSION

7.3.1 HT-GPC

Table 7.2 shows the HT-GPC results of the original copolymers used for the blends and the 10 - 40% blends.

Table 7.2 HT-GPC results of blends and Polymers J and M

Sample	M_n (g/mol)	M_w (g/mol)	PD
Polymer J	96 700	337 700	3.49
Polymer M	18 300	72 200	3.95
10% blend	80 600	337 700	4.19
20% blend	63 200	316 500	5.01
30% blend	54 000	272 900	5.06
40% blend	74 800	263 700	3.52

The molecular weight of Polymer J is much higher than that of Polymer M. The HT-GPC results of all the blends resulted in a single curve. In Table 7.2 there is an overall slight decrease in the molecular weight of the blends with an increase of the Polymer M content, as expected. The polydispersities of Polymers J and M are in a similar range (3.4 - 4.0). The blends, however, show increased PD values, except for the 40% blend which again shows a PD value in the same range as that of the original two copolymers.

The molecular weight of the ZN catalyzed copolymer is not affected significantly when low percentages (10% and 20%) of metallocene copolymer are used in the blends. It is only at a level of 30% metallocene copolymer in the blend that the M_w decreases significantly. The polydispersities are however affected by even the smallest amount of metallocene copolymer added to the blend. This is because of the more heterogeneous distribution of different chain lengths.

7.3.2 THERMAL ANALYSIS

Figure 7.1 shows the CRYSTAF curves of the blends as well as of Polymers J and M.

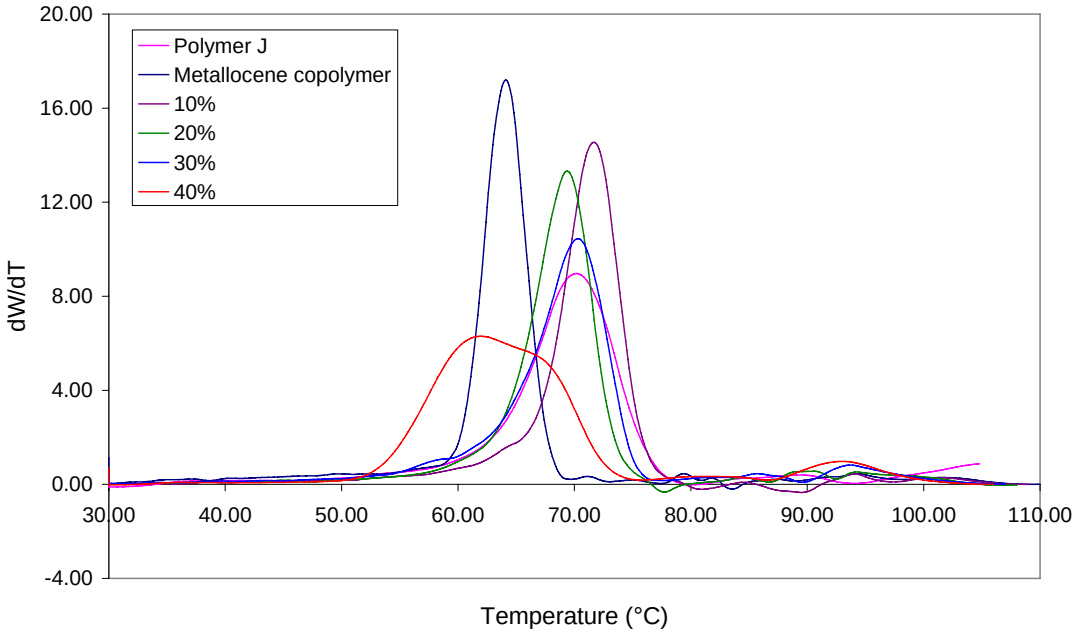

Figure 7.1 CRYSTAF curves of blends and original copolymers

Polymer M shows a much lower and narrower peak crystallization temperature curve than Polymer J. According to Figure 7.1 it can be seen that the curves of the 10 - 30% blends do not shift very much. It is only the 40% blend that shows a very broad, bimodal peak and shifts significantly to the lower temperatures.

Table 7.3 shows of a summary of the thermal data results of the CRYSTAF and DSC analysis of the blends as well as the original copolymers.

Table 7.3 Thermal results of blends and Polymers J and M

Sample	T_c CRYSTAF (°C)	Sol. Fraction (%)	T_c DSC (°C)	T_m DSC (°C)	Crystallinity DSC (%)
Polymer J	85.5	1.5	106.42	149.32	51.67
Polymer M	64.1	5.6	103.89	138.60	69.33
10% blend	71.7	2.4	106.95	148.72	69.04
20% blend	69.4	2.4	104.47	147.97	66.79
30% blend	70.3	2.5	104.81	147.60	53.88
40% blend	62.0	3.4	105.06	145.52	78.76

There is a notable difference in the CRYSTAF T_c of Polymers J and M, but only a relatively small difference in the DSC T_c. This clearly indicates that the molecular weight has an effect on crystallization in solution, but not in bulk.

According to the CRYSTAF results the T_c values of the 10 - 40% blends are all much lower than of Polymer J, when blended with Polymer M. The blends of 10 - 30% have, however, similar values, regardless of the content of Polymer M. Only when the content of Polymer M in the blend reaches 40%, a further significant decrease in the T_c can be seen, which is even lower than the T_c of Polymer M.

During CRYSTAF analysis the same trend is observed for the percentage of soluble fraction. Polymer J has a much lower percentage of soluble fraction than Polymer M. When Polymer J is blended with Polymer M, however, the percentage of soluble fraction increases due to the contribution of the higher soluble fraction content of Polymer M. The percentage of soluble fraction for the 10 - 30% fractions are however similar and for the 40% blend a further increase is seen.

The T_c values of the blends, according to DSC analysis, shows a general decrease from the T_c value of Polymer J when blended with Polymer M, which has a lower T_c.

The T_m of Polymer J is approximately 10°C higher than the T_m of Polymer M. A definite decrease in the T_m of Polymer J can therefore be expected when blended with Polymer M. The results in Table 7.3 however show only a slight decrease.

Table 7.3 shows a very significant affect on the crystallinity with blending the ZN copolymer with even the smallest amount (10%) of metallocene copolymer. A very important conclusion is that the metallocene copolymer definitely affects the crystallinity and therefore also the crystallization temperature of the ZN copolymer significantly without changing the melting temperature significantly.

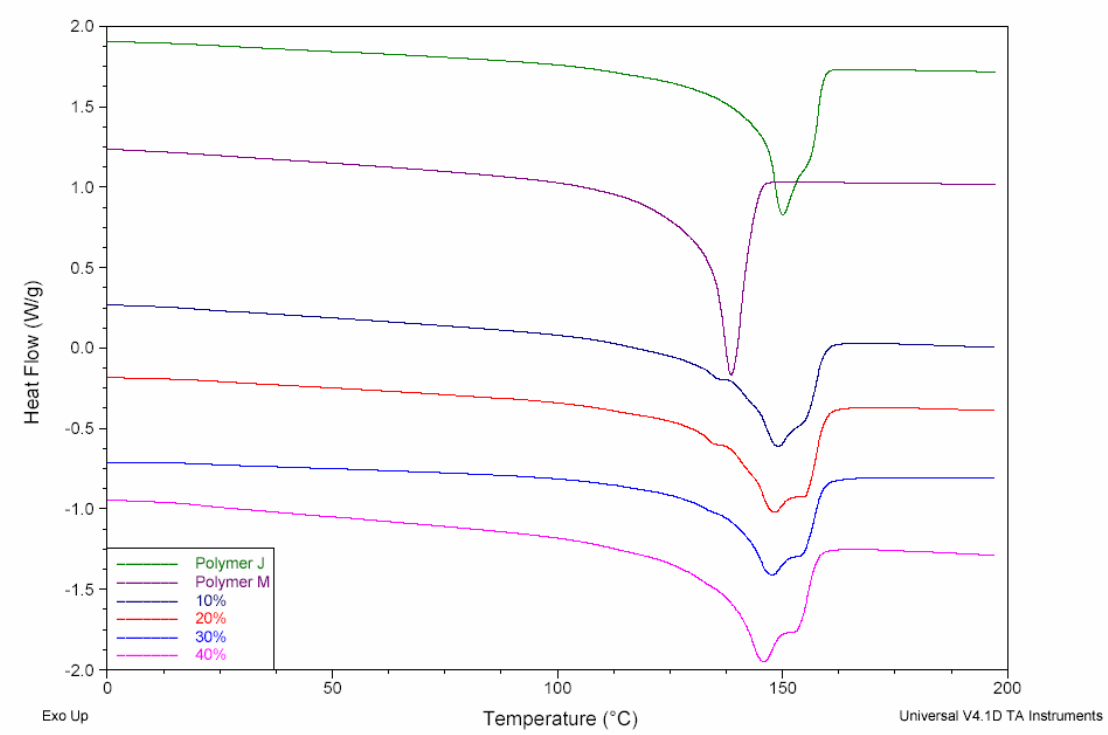

Figure 7.2 DSC melting thermograms of Polymers J and M and the 10 - 40% blends

Figure 7.2 shows the melting endotherms of the original copolymers used for blending and of the blends. The endotherms of the blends give an indication of very good co-crystallization, which is desired to give a homogeneous, compatible blend. It is only in the melting thermogram of the 40% blend that some separation between the two copolymers seems to be visible. The long lower temperature tails of the blends also show the existence of many small crystals which then starts melting before the bulk of the sample.

7.3.3 WAXD

Figure 7.3 shows the WAXD diffractograms of the blends of Polymers J and M. Table 7.4 shows the WAXD results of the blends and of Polymer J.

WAXD studies were unfortunately not carried out on Polymer M because of insufficient material.

The percentage of gamma phase crystal is higher for all the blends than for Polymer J. There is a general increase in the percentage of gamma phase from 43% to 50% for an increase in the content of Polymer M in the blend. The growth of γ-phase crystals is enhanced by the presence of short, crystallizable isotactic chains, which in the case of the blends from this study, are provided by the the metallocene catalyzed Polymer M. The significant increase in the γ-phase crystal content therefore means that the metallocene copolymer does not only affect the crystallinity of Polymer J significantly,but also the way the copolymer crystallizes. This important effect will therefore also definitely influence the optical properties of Polymer J.

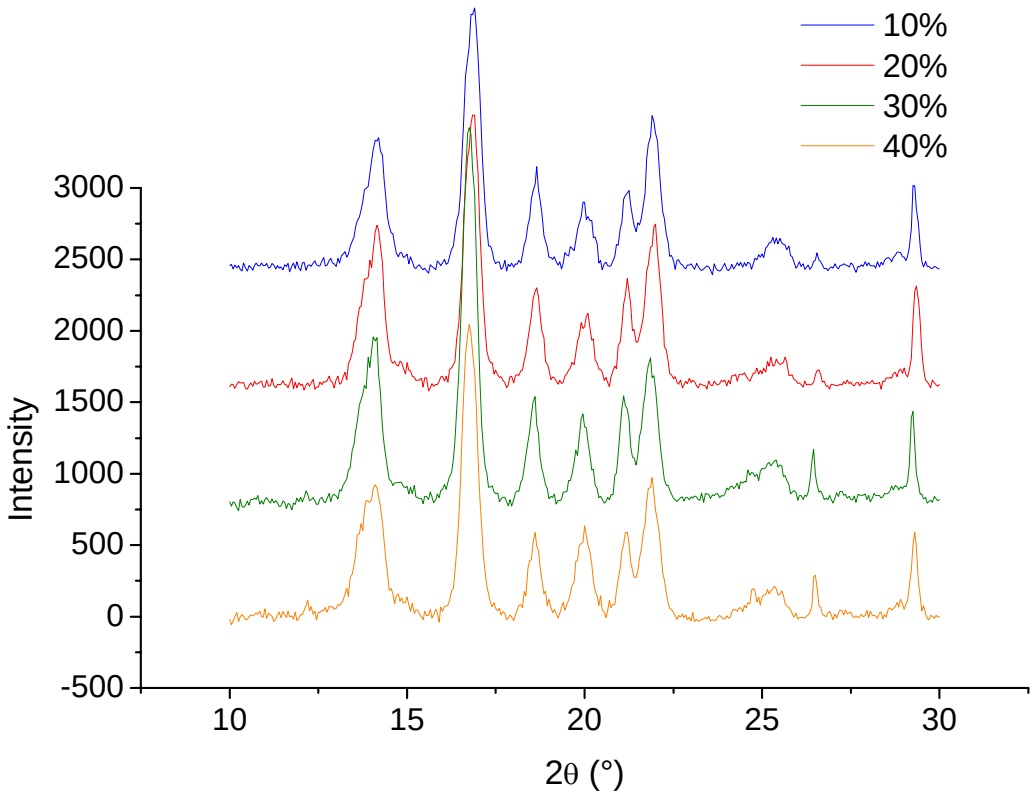

Figure 7.3 WAXD diffractograms of blends

Table 7.4 Gamma phase content of blends and Polymers J and M

Sample	γ-phase crystal (%)
Polymer J	37.99
Polymer M	-
10% blend	43.79
20% blend	38.10
30% blend	46.82
40% blend	50.09

All of the samples prepared for WAXD analysis were also analyzed with DSC. Figure 7.4 shows the first and second heating cycle thermograms of the 40% blend after slow-cooling.

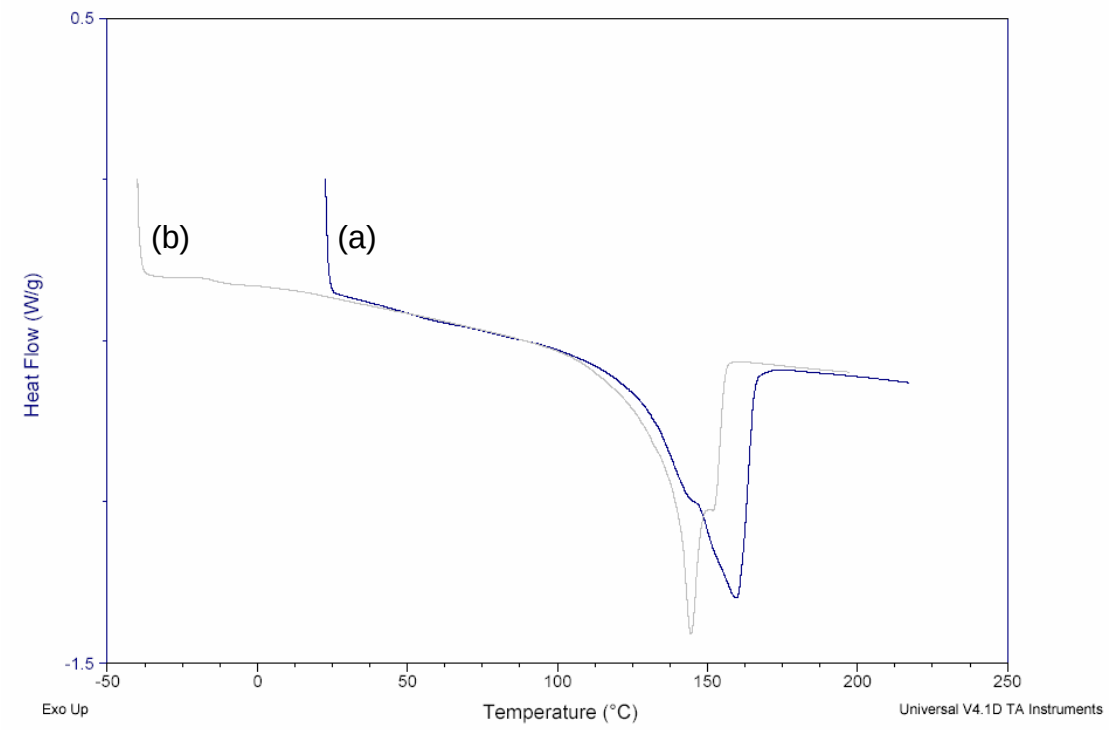

Figure 7.4 Melting thermograms of the slow cooled 40% blend for the (a) first and (b) second heating cycle

The results in Figure 7.4 correspond very well with the WAXD analyses results. According to a previous explanation (Section 3.3.4) the γ-phase melts

at a lower temperature than the α-phase. A small shoulder can be seen to the left hand side of the main melting peak in the endotherm of the first heating cycle. The samples were isothermally maintained at 220°C for 5 min after the first heating cycle to remove the thermal history of the sample. The endotherm of the second heating cycle in Figure 7.4 therefore indicates a melting peak due to the α-phase crystals only. From Figure 7.4 it is also noticeable that the melting endotherm, due to the α-phase, appears at a lower temperature during the second heating cycle than in the first heating cycle. The reason for this is that the initial slow-cooling of the samples allow them to form thicker and more stable crystals which melts at higher temperatures in the first heating cycle than in the second heating cycle.

7.4 CONCLUSIONS

A special freeze-crystallization solution blending procedure was used to blend two propylene/1-pentene copolymers: Polymer J (which was produced with a ZN catalyst) and Polymer M (which was produced with a metallocene catalyst). Molecular weight, thermal and WAXD analyses were carried out on the blends and the original copolymers.

The molecular weight, polydispersity, crystallization temperature and percentage of gamma phase crystal of the original ZN catalyzed copolymer were influenced by blending with the metallocene catalyzed copolymer, but the melting temperature did not show much change. The smallest amount of metallocene catalyzed copolymer therefore changes not only the crystallinity of the ZN catalyzed copolymer, but also the way the chains crystallize in the copolymer. The analyses of the blends showed excellent co-crystallization properties of the two copolymers. These two copolymers therefore form a very compatible blend and it may therefore be used to investigate mechanical and optical influences on the original ZN catalyzed copolymer.

An overall conclusion is that the possibility exists to choose a specific ZN catalyst system which will optimize the fraction which was mimicked by the metallocene catalyzed copolymer in the copolymerization process and in that

way change the crystallinity and way of crystallization in such a way that the optical properties can be improved.

7.5 REFERENCES

1. Dorazio, L., Greco, R., Martuscell, E., Ragosta, G., Polym. Eng. Sci., 1983. **23**: p. 489.
2. Galli, P., Danesi, S., Simonazzi, T., Polym. Eng. Sci., 1984. **24**: p. 544.
3. Greco, R., Mancarella, C., Martuscelli, E., Ragosta, G., Jinghya, Y., Polymer, 1987. **28**: p. 1929.
4. Karger-Kocsis, J., Kallo, A., Szafner, A., Bodor, G., Senyei, Z., Polymer, 1979. **20**: p. 37.
5. Matuscelli, E., Polym. Eng. Sci., 1984. **24**: p. 563.
6. Nomura, T., Nishio, T., Maeda, S., Kamei, E., J. Soc. Rheology. JPN., 1994. **22**: p. 165.
7. Onogi, S., Asada, T., Tanaka, A., J. Polym. Sci., A-2, 1969. **7**: p. 171.
8. Gupta, A.K., Purwar, S.N., J. Appl. Polym. Sci., 1986. **31**: p. 535.
9. Lejiv, M., Polym. Eng. Sci., 1988. **28**: p. 670.
10. Zhou, X., Polymer, 1993. **34**: p. 4710.
11. Dumoulin, M.M., Carreau, P.J., Polym. Eng. Sci., 1987. **27**: p. 4627.
12. Hill, M.J., Polymer, 1994. **35**: p. 3332.
13. Liu, Y., Truss, R.W., J. Polym. Sci., Polym. Phys., Ed., 1995. **33**: p. 813.
14. Flaris, V., Polym. Eng. Sci., 1995. **35**: p. 28.
15. Bains, M., Balke, S.T., Reck, D., Horn, J., Polym. Eng. Sci., 1994. **34**: p. 1260.
16. Siegmann, A., J. Appl. Polym. Sci., 1982. **27**: p. 1053.
17. Hsu, C.C., Geil, P.H., Polym. Eng. Sci., 1987. **27**: p. 1542.
18. Lee, M., Chen, S., J. Polym. Sci., Polym. Lett., Ed., 1987. **25**: p. 37.
19. Cham, P.M., Lee, T.H., Marand, H., Macromolecules, 1994. **27**: p. 4263.
20. Bartczak, Z., Galeski, A., Pracella, M., J. Appl. Polym. Sci., 1994. **54**: p. 1513.

21. Boiteux, G., Dalloz, J., Douillard, A., Guillet, J., Seytre, G., Eur. Polym. J., 1980. **16**: p. 489.
22. Piloz, A., Decroix, J.Y., May, J.F., Makromolekulare Chemie, 1976. **54**: p. 77.
23. Shinn, H., Kaminsky, W., Adv. Organomet. Chem., 1980. **18**: p. 99.
24. Ewen, J.A., J. Am. Chem. Soc., 1984. **106**: p. 6355.
25. Uozumi, T., Soga, K., Makromol. Chem., 1992. **193**: p. 823.
26. Heiland, K., Kaminsky, W.,, Makromol. Chem., 1992. **193**: p. 601.
27. Chen, J.C.W., Nozak, T., J. Polym. Sci., Polym. Chem., Ed., 1992. **30**: p. 227.
28. Sebanobish, K., Patel, P.M., Croft, B.A., Chum, S.P., Kao, C.I., J. Appl. Polym. Sci., 1994. **51**: p. 887.

CHAPTER 8

CONCLUSIONS

Commercial propylene/1-pentene random copolymers are very unique with regard to their properties. The study of these relatively novel commercial copolymers lead to a better understanding of the properties on molecular level by investigating the relationship between the chemical structure and properties of these materials.

The main objective of the investigation of the Group 1 copolymers was to identify appropriate analytical techniques which could then be used to investigate certain trends in the Group 2 copolymer series. The different analytical techniques used in this study revealed properties that may be attributed to certain of the different variables in the different copolymers of Group 1. One of the interesting conclusions from the investigation of the Group 1 copolymers was that the absence of a nucleating agent in the copolymer affected the thermal properties. From the thermal results of the Group 2 copolymers it appeared that the thermal properties are affected primarily by the amount, and possibly the distribution of the comonomer in the copolymer, rather than the Si:Ti ratio. WAXD analyses of the Group 2 copolymers confirmed that there must be a difference in the way the 1-pentene is distributed in the copolymers. TREF analysis was used to show the influence of the Si:Ti ratio on the distribution of the 1-pentene.

Positron annihilation lifetime spectroscopy (PALS) was used as an alternative investigation method for the propylene/1-pentene copolymers (Group 1) and their XNS fractions in order to determine what type of information this novel analytical method could generate and how the results correlated with those of previous PALS studies on poly-olefins. The narrowness of the *o*-positron lifetime distribution curves differed for all the copolymers, indicating a difference in the size of the transition between the crystalline and amorphous areas for the different polymers. The propylene/1-pentene copolymers from this study showed a very significant property with

regard to the τ_3 value (which is attributed to the crystalline fraction). The unique τ_3 value from this study is a very significant and different result than reported for any other poly-olefin lifetime study to date.

The influence of the donor:catalyst ratio on the make-up and the properties of the propylene/1-pentene was a continuous theme for this project. Quantitative analysis of the Group 2 copolymers showed little or no comparison between the 1-pentene content of the copolymer and the percentage of xylene-soluble fraction. Xylene extractions of the Group 2 copolymers however indicated that the distribution of 1-pentene remained constant after extraction with xylene for the copolymers produced by a catalyst with a high Si:Ti ratio, but there appeared to be a bigger change (percentage wise) in the polymer made by a low Si:Ti ratio.

During the ^{13}C-NMR analysis of the xylene and hexane solvent extracts an increase in the isotacticity with an increase in the 1-pentene content of the original copolymers became evident. In the heptane extracts there was however a relationship between the tacticity of the extracts and the Si:Ti ratios. In the case of polypropylene homopolymers, extracts are directly related to the isotacticity index of the material, and can be varied by varying the donor:catalyst ratio. The copolymers from this study showed that this is not the case for the propylene/1-pentene copolymers, and that the distribution of 1-pentene plays a major role in the tacticity of the extracts. The Si:Ti ratio did not seem to have an effect on the microstructure of the xylene extracts, but did affect the end group intensities of the hexane and heptane extracts. The intensity of the end group peaks also correlated well with the molecular weight of the various fractions.

Successive extractions were carried out in order to investigate the extracts more completely. Analysis of these extracts proved that xylene extracts atactic material as well as some crystallizable low molecular weight isotactic material, hexane extracts only atactic material and heptane extracts atactic material as well as some low molecular weight isotactic material, but lower in molecular weight than for the xylene extract. The Si:Ti ratios seemed to play a role only in the hexane extracts in this case.

Difference in the Si:Ti ratios led to difference in the distribution of the 1-pentene throughout the copolymers. A higher ratio lead to more 1-pentene distributed in the lower weight fractions, but did not change the 1-pentene content of the highest weight fractions significantly. The lower weight fractions with the higher 1-pentene content of two different original copolymers then showed higher crystallization temperatures, lower melting temperatures, higher percentage of crystallinity and lower percentage of CRYSTAF soluble fractions.

TREF analysis of the copolymers showed a significant difference between the weight percentage of the room temperature TREF fraction and the fraction extracted by the standard xylene-soluble method. This has the important implication that the percentage of extractable material is very much dependent on the crystallization method. Even the slightest difference or error in the method would make the technique useless for standard index measurement purposes. The TREF as well as the standard xylene-soluble method showed that the donor:catalyst ratio has a definite influence on the amount of low molecular weight xylene soluble material.

TREF analysis further showed a correlation between the 1-pentene content and the distribution of molecular species in the copolymers. Higher 1-pentene content led to a more homogeneous distribution of the molecular species. This distribution again gives an indication of the degree of variation in the crystallizability of the copolymer chains. Higher 1-pentene content may therefore indicate that there is more xylene soluble material present and therefore leaves more crystallisable material. The NMR results of the TREF fractions showed a decrease in the 1-pentene content with an increase in the fractionation temperature. The 1-pentene reduces the ability of the chains to crystallize and therefore chains with less comonomer are able to crystallize at higher temperatures. An increase in the tacticity of the fractions was also found as the fractionation temperature is increased.

Thermal investigation of the TREF fractions showed an increase in T_c, T_m and percentage crystallinity up to a certain fraction (~ 100°C) where after it decreased. The opposite was observed for the percentage of soluble fraction during CRYSTAF analysis. The decrease in T_c, T_m and percentage

crystallinity and increase in percentage of soluble fraction after a certain temperature is explained as to be due to low molecular weight material entrapped between the inert support and the chains crystallizing at high temperatures or less likely due to low molecular weight material which comes from degradation of the copolymer at the high temperatures.

A new fractionation technique, preparative solution fractionation (SF), was developed and evaluated during this study. The analysis results of the fractions collected by the SF technique compared very well with results from the TREF and CRYSTAF techniques.

The last part of the project consisted of a blending study which involved the blending of one of the commercial ZN catalyzed propylene/1-pentene copolymers with a tailored metallocene catalyst in different ratios. Excellent co-crystallization properties was achieved and the smallest amount of metallocene catalyzed copolymer showed a significant influence on the crystallinity and the way the chains crystallize without changing the melting and molecular weight properties much. The blending study therefore showed that the possibility exists to choose a specific ZN catalyst system which will optimize the fraction which was mimicked by the metallocene catalyzed copolymer in the copolymerization process and therefore change the optical properties of the copolymer.